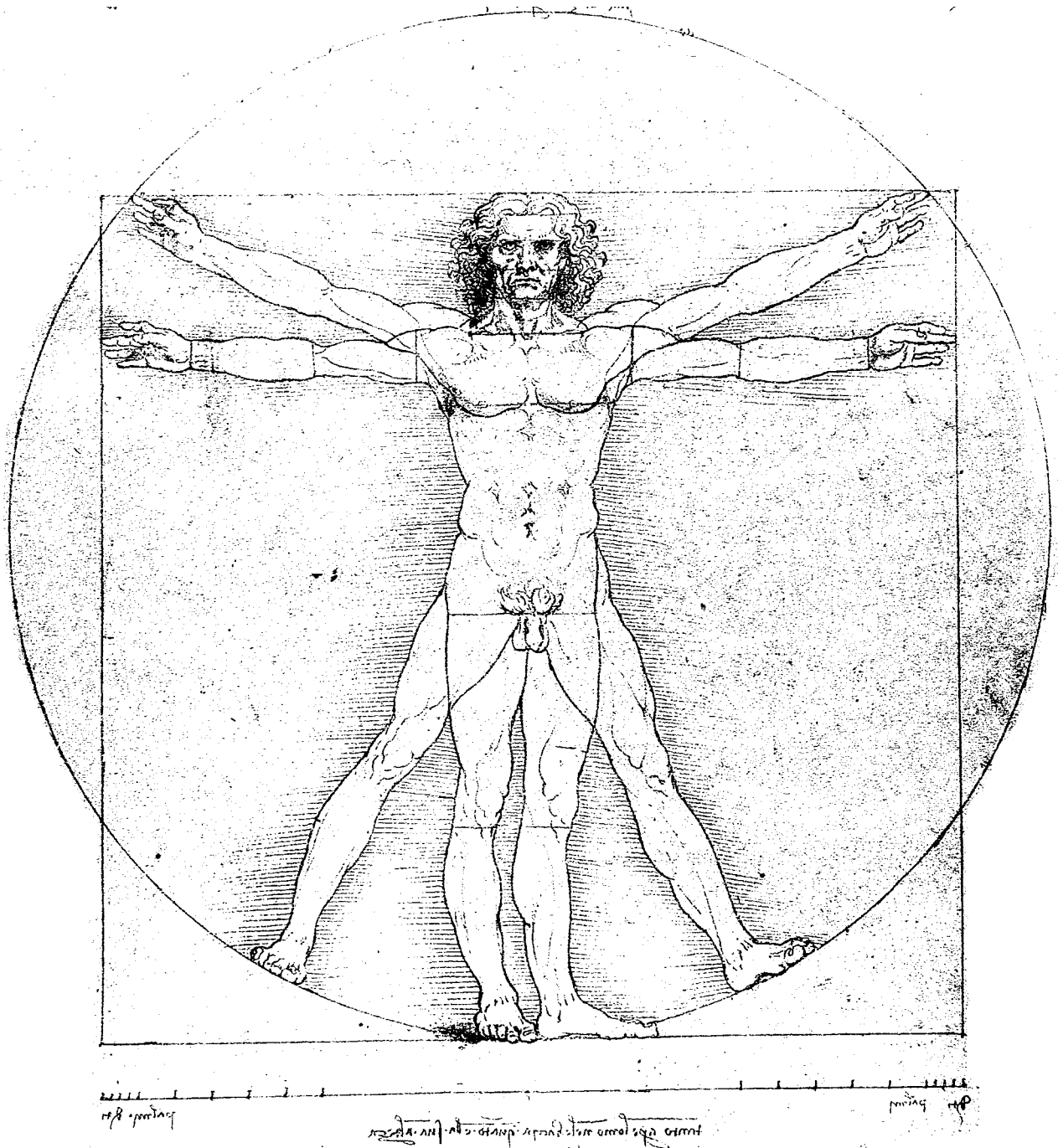


Sensory Systems

Physiology & Computer Simulations



March 25, 2013

On the 28th of April 2012 the contents of the English as well as German Wikibooks and Wikipedia projects were licensed under Creative Commons Attribution-ShareAlike 3.0 Unported license. An URI to this license is given in the list of figures on page 193. If this document is a derived work from the contents of one of these projects and the content was still licensed by the project under this license at the time of derivation this document has to be licensed under the same, a similar or a compatible license, as stated in section 4b of the license. The list of contributors is included in chapter Contributors on page 191. The licenses GPL, LGPL and GFDL are included in chapter Licenses on page 201, since this book and/or parts of it may or may not be licensed under one or more of these licenses, and thus require inclusion of these licenses. The licenses of the figures are given in the list of figures on page 193. This PDF was generated by the L^AT_EX typesetting software. The L^AT_EX source code is included as an attachment (`source.7z.txt`) in this PDF file. To extract the source from the PDF file, we recommend the use of <http://www.pdfplabs.com/tools/pdftk-the-pdf-toolkit/> utility or clicking the paper clip attachment symbol on the lower left of your PDF Viewer, selecting **Save Attachment**. After extracting it from the PDF file you have to rename it to `source.7z`. To uncompress the resulting archive we recommend the use of <http://www.7-zip.org/>. The L^AT_EX source itself was generated by a program written by Dirk Hünninger, which is freely available under an open source license from http://de.wikibooks.org/wiki/Benutzer:Dirk_Huenniger/wb2pdf. This distribution also contains a configured version of the `pdflatex` compiler with all necessary packages and fonts needed to compile the L^AT_EX source included in this PDF file.

Contents

1	Introduction	3
1.1	Keep it simple: Unicellular Creatures	3
1.2	Not so simple: Three-hundred-and-two Neurons	4
1.3	General principles of Sensory Systems	5
1.4	Transduction	5
1.5	Neurons	6
1.6	Principles of Information Processing in the Nervous System	8
2	Simulation of Neural Systems	9
2.1	Simulating Action Potentials	9
2.2	Simulating a Single Neuron with Positive Feedback	16
2.3	Simulating a Simple Neural System	18
2.4	References	21
3	Visual System	23
3.1	Introduction	23
3.2	Anatomy of the Visual System	27
3.3	Signal Processing	37
3.4	Retinal Implants	44
3.5	Other Visual Implants	52
3.6	Computer Simulation of the Visual System	54
3.7	References	65
4	Auditory System	67
4.1	Introduction	67
4.2	Anatomy of the Auditory System	68
4.3	Auditory Signal Processing	75
4.4	Human Speech	85
4.5	Cochlear Implants	91
4.6	Computer Simulations of the Auditory System	98
4.7	References	117
5	Vestibular System	119
5.1	Introduction	119
5.2	Anatomy of the Vestibular System	119
5.3	Signal Processing	124
5.4	Computer Simulation of the Vestibular System	130
5.5	References	139

6	Somatosensory System	141
6.1	Introduction	141
6.2	Sensory Organs	141
6.3	Sensory Organ Components	142
6.4	Proprioceptive Signal Processing	147
6.5	Modelling muscle spindles and afferent response	147
6.6	Internal models of limb dynamics	149
7	Olfactory System	151
7.1	Introduction	151
7.2	Sensory Organs	151
7.3	Sensory Organ Components	152
7.4	Signal Processing	154
7.5	References	157
8	Gustatory_System	159
8.1	Introduction	159
8.2	Sensory Organs	161
8.3	Transduction of Taste	163
8.4	Signal Processing	164
8.5	Taste and Other Senses	164
8.6	Taste disorders	165
9	Sensory Systems in Non-Primates	167
9.1	Octopus	167
9.2	Fish	173
9.3	Flies	177
9.4	Butterflies	180
9.5	References	181
10	Appendix	183
10.1	Spectrum	183
10.2	Colour Models	184
10.3	History of <i>Sensory Systems</i>	185
11	Sources	187
12	Authors	189
13	Contributors	191
	List of Figures	193
14	Licenses	201
14.1	GNU GENERAL PUBLIC LICENSE	201
14.2	GNU Free Documentation License	202
14.3	GNU Lesser General Public License	203

1 Introduction

In order to survive - at least on the species level - we continually need to make decisions:

- "Should I cross the road?"
- "Should I run away from the creature in front of me?"
- "Should I eat the thing in front of me?"
- "Or should I try to mate it?"

To help us to make the right decision, and make that decision quickly, we have developed an elaborate system: a sensory system to notice what's going on around us; and a nervous system to handle all that information. And this system is big. VERY big! Our nervous system contains about 10^{11} nerve cells (or *neurons*), and about 10-50 times as many supporting cells. These supporting cells, called *glia* cells, include *oligodendrocytes*, *Schwann cells*, and *astrocytes*. But do we really need all these cells?

1.1 Keep it simple: Unicellular Creatures

The answer is: "No!", we do not REALLY need that many cells in order to survive. Creatures existing of a single cell can be large, can respond to multiple stimuli, and can also be remarkably smart!



Figure 1 Xenophyophores are the largest known unicellular organisms, and can get up to 20 cm in diameter!

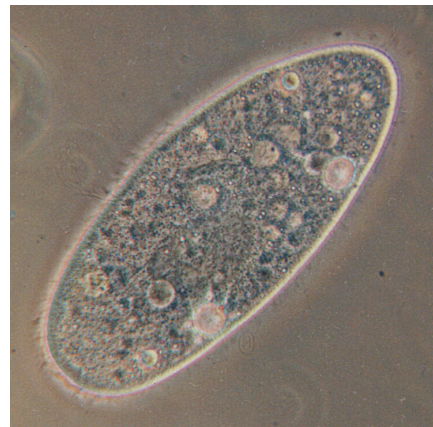


Figure 2 Paramecium, or "slipper animalcules", respond to light and touch.

We often think of cells as really small things. But *Xenophyophores* (see image) unicellular organisms that are found throughout the world's oceans, and can get as large as 20 centimetres in diameter.

And even with this single cell, those organisms can respond to a number of stimuli. For example look at a creature from the group *Paramecium*: the paramecium is a group of unicellular ciliate protozoa formerly known as *slipper animalcules*, from their slipper shape. (The corresponding word in German is *Pantoffeltierchen*.) Despite the fact that these creatures consist of only one cell, they are able to respond to different environmental stimuli, e.g. to light or to touch.

And such unicellular organisms can be amazingly smart: the plasmodium of the slime mould *Physarum polycephalum* is a large amoebalike cell consisting of a dendritic network of tube-like structures. This single cell creature manages to connect sources finding the shortest connections (Nakagaki et al. 2000), and can even build efficient, robust and optimized network structures that resemble the Tokyo underground system (Tero et al. 2010). In addition, it has somehow developed the ability to read its tracks and tell if its been in a place before or not: this way it can save energy and not forage through locations where effort has already been put (Reid et al. 2012).

On the one hand, the approach used by the paramecium cannot be too bad, as they have been around for a long time. On the other hand, a single cell mechanism cannot be as flexible and as accurate in its responses as a more refined version of creatures, which use a dedicated, specialized system just for the registration of the environment: a Sensory System.

1.2 Not so simple: Three-hundred-and-two Neurons

While humans have hundreds of millions of sensory nerve cells, and about 10^{11} nerve cells, other creatures get away with significantly less. A famous one is *Caenorhabditis elegans*, a nematode with a total of 302 neurons.

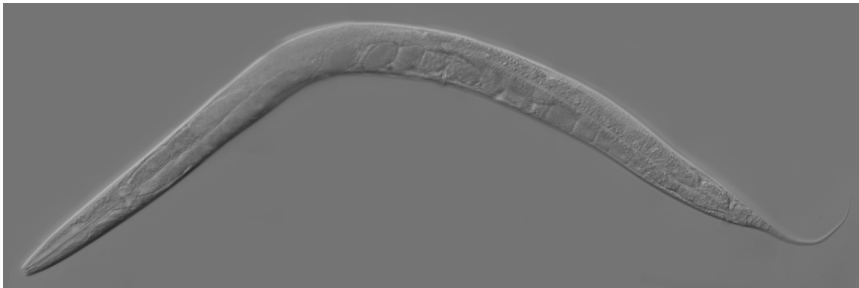


Figure 3 Crawling *C. elegans*, a hermaphrodite worm with exactly 302 neurons.

C. elegans is one of the simplest organisms with a nervous system, and it was the first multicellular organism to have its genome completely sequenced. (The sequence was published in 1998.) And not only do we know its complete genome, we also know the connectivity between all 302 of its neurons. In fact, the developmental fate of every single somatic cell (959 in the adult hermaphrodite; 1031 in the adult male) has been mapped out. We know, for example, that only 2 of the 302 neurons are responsible for chemotaxis (“movement guided by chemical cues”, i.e. essentially smelling). Nevertheless, there is still a lot of research conducted – also on its smelling - in order to understand how its nervous system works!

1.3 General principles of Sensory Systems

Based on the example of the visual system, the general principle underlying our neuro-sensory system can be described as below:

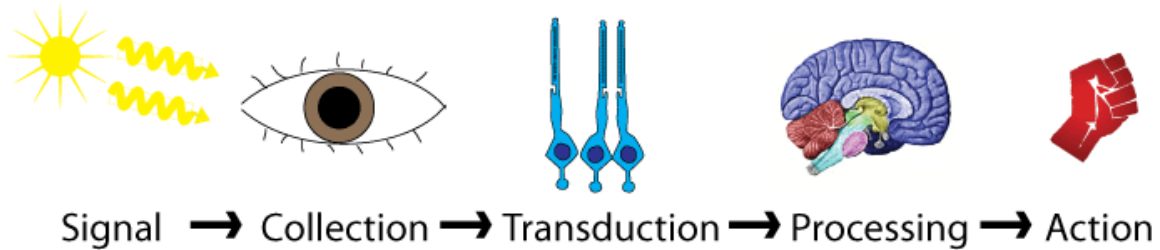


Figure 4 690

All sensory systems are based on

- a *Signal*, i.e. a physical stimulus, provides information about our surrounding.
- the *Collection* of this signal, e.g. by using an ear or the lens of an eye.
- the *Transduction* of this stimulus into a nerve signal.
- the *Processing* of this information by our nervous system.
- And the generation of a resulting *Action*.

While the underlying physiology restricts the maximum frequency of our nerve-cells to about 1 kHz, more than one-million times slower than modern computers, our nervous system still manages to perform stunningly difficult tasks with apparent ease. The trick: there are lots of nerve cells (about 10^{11}), and they are massively connected (one nerve cell can have up to 150'000 connections with other nerve cells).

1.4 Transduction

The role of our "senses" is to transduce relevant information from the world surrounding us into a type of signal that is understood by the next cells receiving that signal: the "Nervous System". (The sensory system is often regarded as part of the nervous system. Here I will try to keep these two apart, with the expression Sensory System referring to the stimulus transduction, and the Nervous System referring to the subsequent signal processing.) Note here that only relevant information is to be transduced by the sensory system! The task of our senses is NOT to show us everything that is happening around us. Instead, their task is to filter out the important bits of the signals around us: electromagnetic signals, chemical signals, and mechanical ones. Our Sensory Systems transduce those environmental variables that are (probably) important to us. And the Nervous System propagates them in such a way that the responses that we take help us to survive, and to pass on our genes.

1.4.1 Types of sensory transducers

1. Mechanical receptors

- Balance system (vestibular system)

- Hearing (auditory system)
 - Pressure:
 - Fast adaptation (Meissner's corpuscle, Pacinian corpuscle) ? movement
 - Slow adaptation (Merkel disks, Ruffini endings) ? shape Comment: these signals are transferred fast
 - Muscle spindles
 - Golgi organs: in the tendons
 - Joint-receptors
2. **Chemical receptors**
 - Smell (olfactory system)
 - Taste
 3. **Light-receptors** (visual system): here we have light-dark receptors (rods), and three different color receptors (cones)
 4. **Thermo-receptors**
 - Heat-sensors (maximum sensitivity at $\sim 45^{\circ}\text{C}$, signal temperatures $< 50^{\circ}\text{C}$)
 - Cold-sensors (maximum sensitivity at $\sim 25^{\circ}\text{C}$, signal temperatures $> 5^{\circ}\text{C}$)
 - Comment: The information processing of these signals is similar to those of visual color signals, and is based on differential activity of the two sensors; these signals are slow
 5. **Electro-receptors**: for example in the bill of the platypus
 6. **Magneto-receptors**
 7. **Pain receptors (nociceptors)**: pain receptors are also responsible for itching; these signals are passed on slowly.

1.5 Neurons

Now what distinguishes neurons from other cells in the human body, like liver cells or fat cells? Neurons are unique, in that they:

- can switch quickly between two states (which can also be done by muscle cells).
- That they can propagate this change into a specified direction and over longer distances (which cannot also be done by muscle cells).
- And that this state-change can be signalled effectively to other connected neurons.

While there are more than 50 distinctly different types of neurons, they all share the same structure:

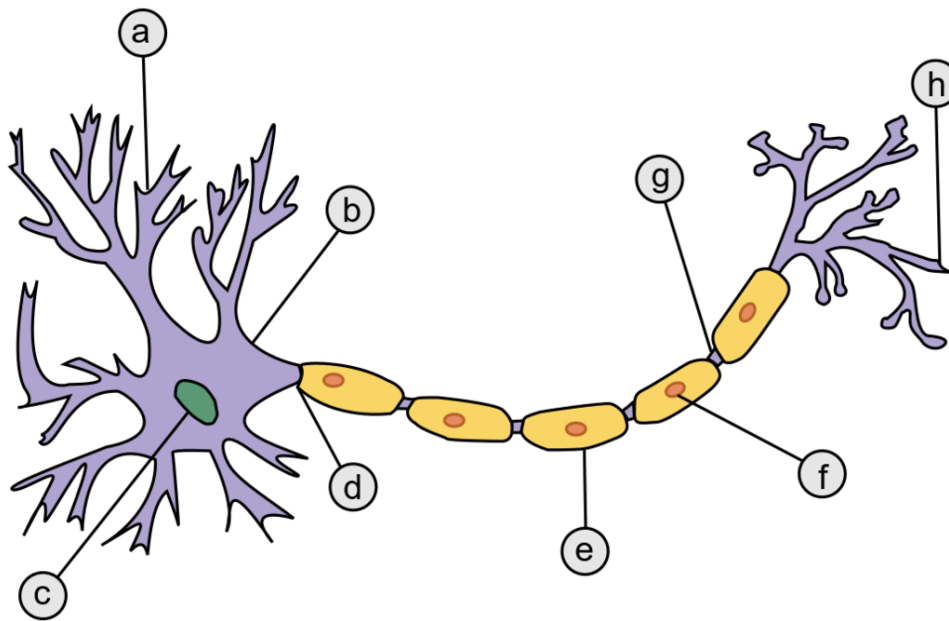


Figure 5 a) Dendrites, b) Soma, c) Nucleus, d) Axon hillock, e) Sheathed Axon, f) Myelin Cell, g) Node of Ranvier, h) Synapse

- An **input stage**, often called *dendrites*, as the input-area often spreads out like the branches of a tree. Input can come from sensory cells or from other neurons; it can come from a single cell (e.g. a bipolar cell in the retina receives input from a single cone), or from up to 150'000 other neurons (e.g. Purkinje cells in the Cerebellum); and it can be positive (excitatory) or negative (inhibitory).
- An **integrative stage**: the cell body does the household chores (generating the energy, cleaning up, generating the required chemical substances, etc), combines the incoming signals, and determines when to pass a signal on down the line.
- A **conductile stage**, the *axon*: once the cell body has decided to send out a signal, an action potential propagates along the axon, away from the cell body. An action potential is a quick change in the state of a neuron, which lasts for about 1 msec. Note that this defines a clear direction in the signal propagation, from the cell body, to the:
- **output Stage**: The output is provided by *synapses*, i.e. the points where a neuron contacts the next neuron down the line, most often by the emission of neurotransmitters (i.e. chemicals that affect other neurons) which then provide an input to the next neuron.

1.6 Principles of Information Processing in the Nervous System

1.6.1 Parallel processing

An important principle in the processing of neural signals is parallelism. Signals from different locations have different meaning. This feature, sometimes also referred to as line labeling, is used by the

- Auditory system - to signal frequency
- Olfactory system - to signal sweet or sour
- Visual system - to signal the location of a visual signal
- Vestibular system - to signal different orientations and movements

1.6.2 Population Coding

Sensory information is rarely based on the signal nerve. It is typically coded by different patterns of activity in a population of neurons. This principle can be found in all our sensory systems.

1.6.3 Learning

The structure of the connections between nerve cells is not static. Instead it can be modified, to incorporate experiences that we have made. Thereby nature walks a thin line:

- If we learn too slowly, we might not make it. One example is the "Eskimo curlew", an American bird which may be extinct by now. In the last century (and the one before), this bird was shot in large numbers. The mistake of the bird was: when some of them were shot, the others turned around, maybe to see what's up. So they were shot in turn - until the birds were essentially gone. The lesson: if you learn too slowly (i.e. to run away when all your mates are killed), your species might not make it.
- On the other hand, we must not learn too fast, either. For example, the monarch butterfly migrates. But it takes them so long to get from "start" to "finish", that the migration cannot be done by one butterfly alone. In other words, no single butterfly makes the whole journey. Nevertheless, the genetic disposition still tells the butterflies where to go, and when they are there. If they would learn any faster - they could never store the necessary information in their genes. In contrast to other cells in the human body, nerve cells are not re-generated in the human body.

2 Simulation of Neural Systems

2.1 Simulating Action Potentials

2.1.1 Action Potential

The "action potential" is the stereotypical voltage change that is used to propagate signals in the nervous system.

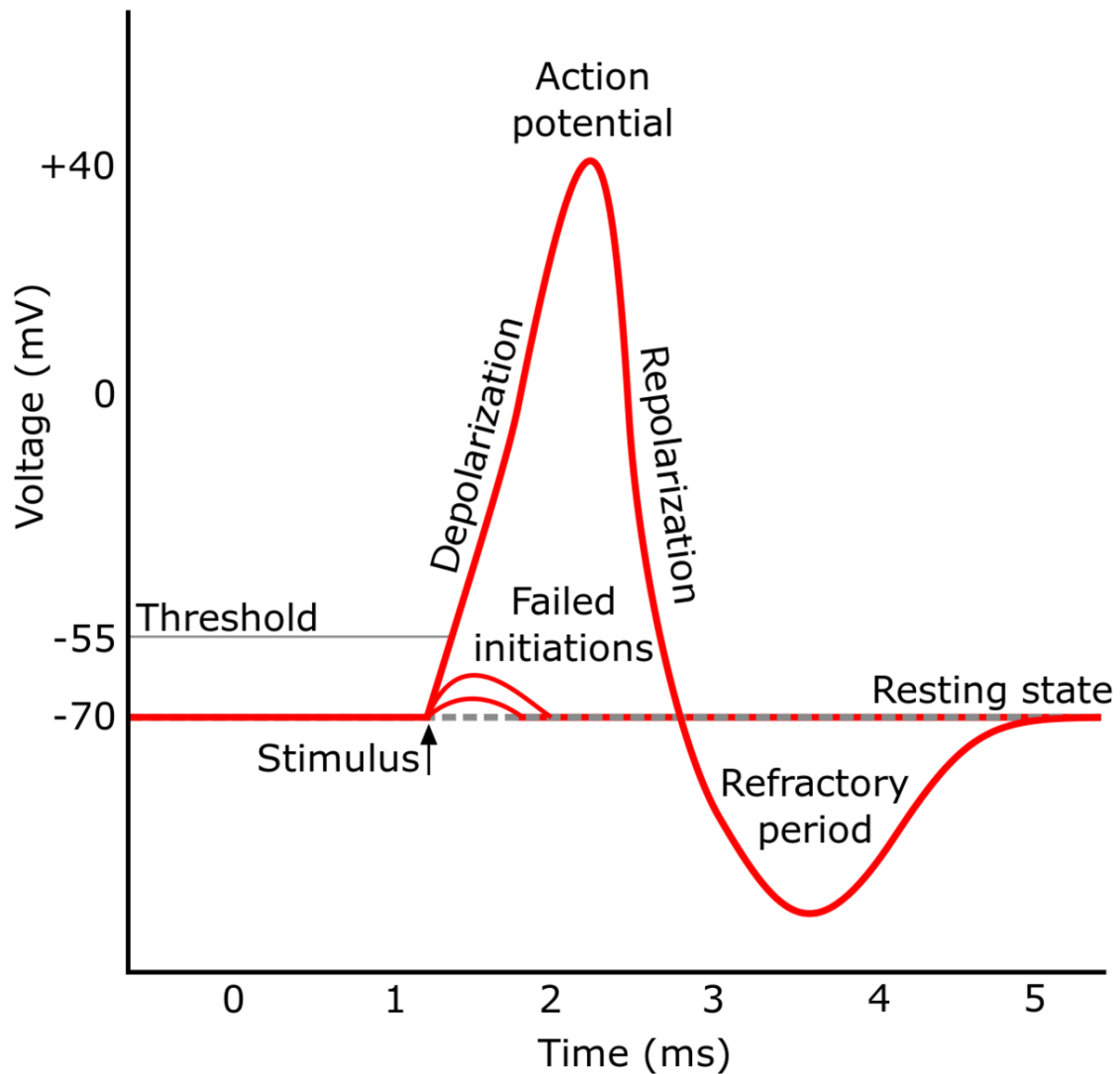


Figure 6 Action potential – Time dependence

With the mechanisms described below, an incoming stimulus (of any sort) can lead to a change in the voltage potential of a nerve cell. Up to a certain threshold, that's all there is to it ("Failed initiations" in Fig. 4). But when the Threshold of voltage-gated ion channels is reached, it comes to a feed-back reaction that almost immediately completely opens the Na⁺-ion channels ("Depolarization" below): This reaches a point where the permeability for Na⁺ (which is in the resting state is about 1% of the permeability of K⁺) is 20^{*}larger than that of K⁺. Together, the voltage rises from about -60mV to about +50mV. At that point internal reactions start to close (and block) the Na⁺ channels, and open the K⁺ channels to restore the equilibrium state. During this "Refractory period" of about 1 m, no depolarization can elicit an action potential. Only when the resting state is reached can new action potentials be triggered.

To simulate an action potential, we first have to define the different elements of the cell membrane, and how to describe them analytically.

2.1.2 Cell Membrane

The cell membrane is made up by a water-repelling, almost impermeable double-layer of proteins, the *cell membrane*. The real power in processing signals does not come from the cell membrane, but from ion channels that are embedded into that membrane. Ion channels are proteins which are embedded into the cell membrane, and which can selectively be opened for certain types of ions. (This selectivity is achieved by the geometrical arrangement of the amino acids which make up the ion channels.) In addition to the Na⁺ and K⁺ ions mentioned above, ions that are typically found in the nervous system are the cations Ca²⁺, Mg²⁺, and the anions Cl⁻.

States of ion channels

Ion channels can take on one of three states:

- Open (For example, an open Na-channel lets Na⁺ ions pass, but blocks all other types of ions).
- Closed, with the option to open up.
- Closed, unconditionally.

Resting state

The typical default situation – when nothing is happening - is characterized by K⁺ that are open, and the other channels closed. In that case two forces determine the cell voltage:

- The (chemical) concentration difference between the intra-cellular and extra-cellular concentration of K⁺, which is created by the continuous activity of the ion pumps described above.
- The (electrical) voltage difference between the inside and outside of the cell.

The equilibrium is defined by the Nernst-equation:

$$E_X = \frac{RT}{zF} \ln \frac{[X]_o}{[X]_i}$$

R ... gas-constant, T ... temperature, z ... ion-valence, F ... Faraday constant, $[X]_o/i$... ion concentration outside/ inside. At 25° C, RT/F is 25 mV, which leads to a resting voltage of

$$E_X = \frac{58mV}{z} \log \frac{[X]_o}{[X]_i}$$

With typical K⁺ concentration inside and outside of neurons, this yields $E_{K^+} = -75mV$. If the ion channels for K⁺, Na⁺ and Cl⁻ are considered simultaneously, the equilibrium situation is characterized by the Goldman-equation

$$V_m = \frac{RT}{F} \ln \frac{P_K[K^+]_o + P_{Na}[Na^+]_o + P_{Cl}[Cl^-]_i}{P_K[K^+]_i + P_{Na}[Na^+]_i + P_{Cl}[Cl^-]_o}$$

where Pi denotes the permeability of Ion "i", and I the concentration. Using typical ion concentration, the cell has in its resting state a negative polarity of about -60 mV.

Activation of Ion Channels

The nifty feature of the ion channels is the fact that their permeability can be changed by

- A mechanical stimulus (mechanically activated ion channels)
- A chemical stimulus (ligand activated ion channels)
- Or an by an external voltage (voltage gated ion channels)
- Occasionally ion channels directly connect two cells, in which case they are called gap junction channels.

Important

- Sensory systems are essentially based ion channels, which are activated by a mechanical stimulus (pressure, sound, movement), a chemical stimulus (taste, smell), or an electromagnetic stimulus (light), and produce a "neural signal", i.e. a voltage change in a nerve cell.
- Action potentials use voltage gated ion channels, to change the "state" of the neuron quickly and reliably.
- The communication between nerve cells predominantly uses ion channels that are activated by neurotransmitters, i.e. chemicals emitted at a synapse by the preceding neuron. This provides the maximum flexibility in the processing of neural signals.

Modeling a voltage dependent ion channel

Ohm's law relates the resistance of a resistor, R, to the current it passes, I, and the voltage drop across the resistor, V:

$$V = IR$$

or

$$I = gV$$

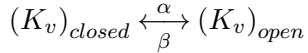
where $g = 1/R$ is the conductance of the resistor. If you now suppose that the conductance is directly proportional to the probability that the channel is in the open conformation, then this equation becomes

$$I = g_{\max} * n * V$$

where g_{max} is the maximum conductance of the channel, and n is the probability that the channel is in the open conformation.

Example: the K-channel

Voltage gated potassium channels (K_v) can be only open or closed. Let α be the rate the channel goes from closed to open, and β the rate the channel goes from open to closed



Since n is the probability that the channel is open, the probability that the channel is closed has to be $(1-n)$, since all channels are either open or closed. Changes in the conformation of the channel can therefore be described by the formula

$$\frac{dn}{dt} = (1-n)\alpha - n\beta = \alpha - (\alpha + \beta)n$$

Note that α and β are voltage dependent! With a technique called "voltage-clamping", Hodgkin and Huxley determine these rates in 1952, and they came up with something like

$$\alpha(V) = \frac{0.01 * (V+10)}{\exp\left(\frac{V+10}{10}\right) - 1}$$
$$\beta(V) = 0.125 * \exp\left(\frac{V}{80}\right)$$

If you only want to model a voltage-dependent potassium channel, these would be the equations to start from. (For voltage gated Na channels, the equations are a bit more difficult, since those channels have three possible conformations: open, closed, and inactive.)

2.1.3 Hodgkin Huxley equation

The feedback-loop of voltage-gated ion channels mentioned above made it difficult to determine their exact behaviour. In a first approximation, the shape of the action potential can be explained by analyzing the electrical circuit of a single axonal compartment of a neuron, consisting of the following components: 1) membrane capacitance, 2) Na channel, 3) K channel, 4) leakage current:

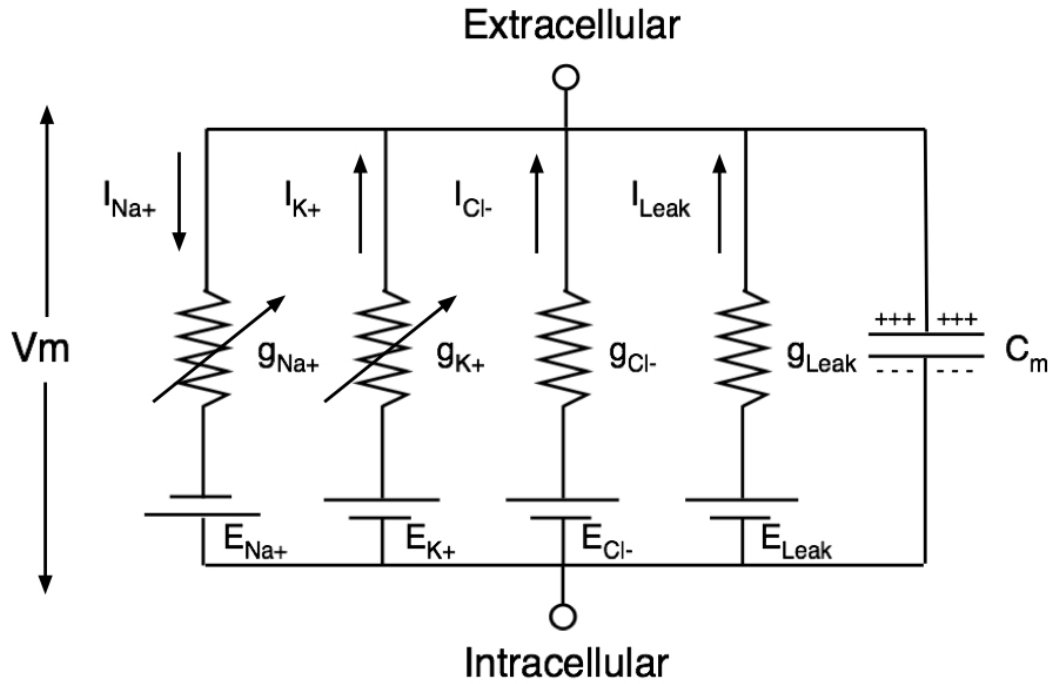


Figure 7 Circuit diagram of neuronal membrane based on Hodgkin and Huxley model.

The final equations in the original Hodgkin-Huxley model, where the currents in of chloride ions and other leakage currents were combined, were as follows:

$$C_m \frac{dV}{dt} = G_{Na} m^3 h (E_{Na} - V) + G_K n^4 (E_K - V) + G_m (V_{rest} - V) + I_{inj}(t)$$

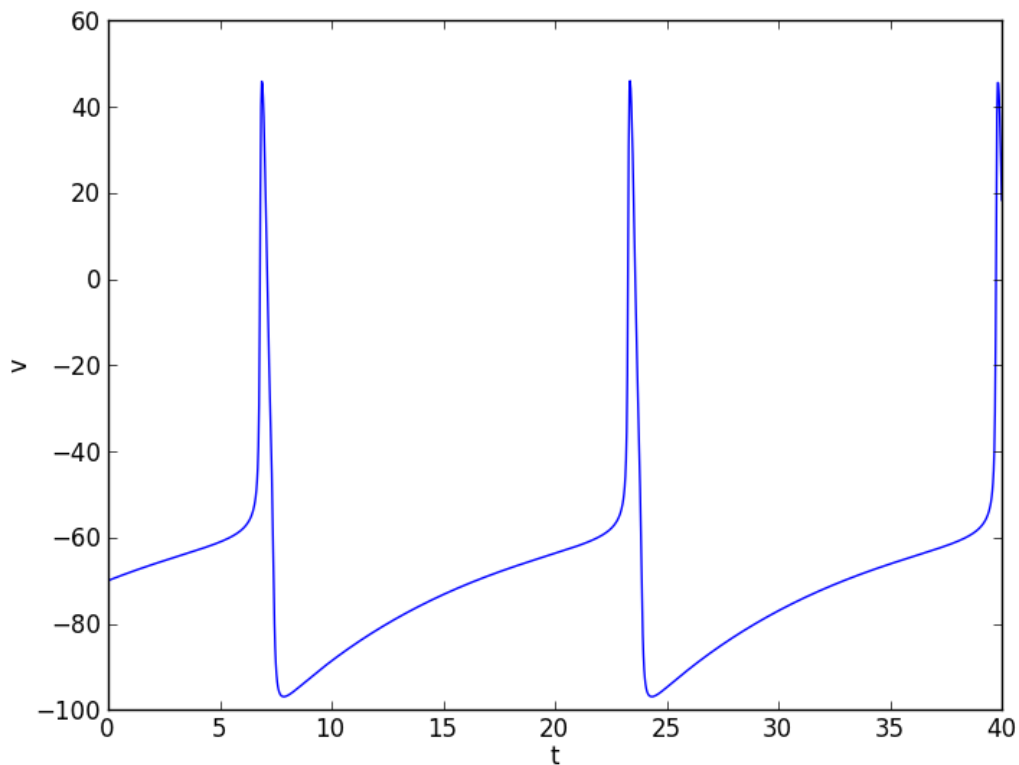


Figure 8 Spiking behavior of a Hodgkin-Huxley model.

where m , h , and n are time- and voltage dependent functions which describe the membrane-permeability. For example, for the K channels n obeys the equations described above, which were determined experimentally with voltage-clamping. These equations describe the shape and propagation of the action potential with high accuracy! The model can be solved easily with open source tools, e.g. the Python Dynamical Systems Toolbox *PyDSTools*. A simple solution file is available under ¹, and the output is shown below.

Links to full Hodgkin-Huxley model

- <http://itb.biologie.hu-berlin.de/~stemmler/sec1.html#SECTION00020000000000000000>
- <http://www.afodor.net/HHModel.htm>

¹ Hodgkin-Huxley Simulations [Python] ². . Retrieved

2.1.4 Modeling the Action Potential Generation: The Fitzhugh-Nagumo model

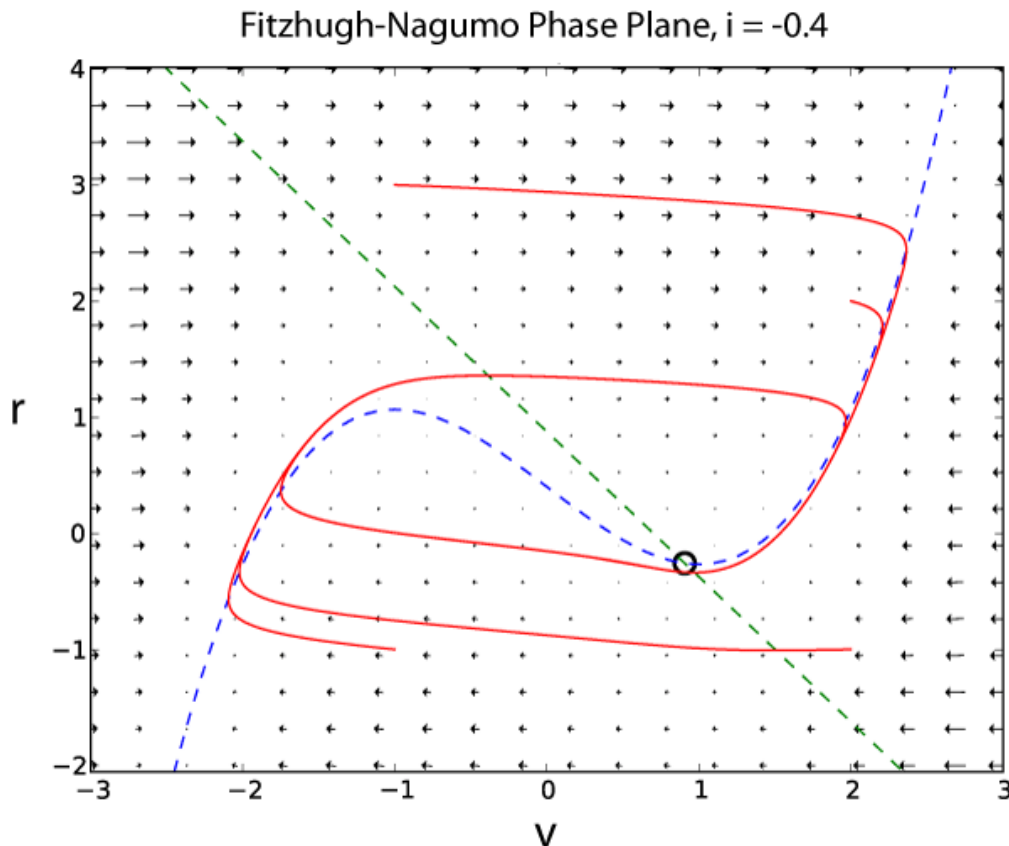


Figure 9 Phaseplane plot of the Fitzhugh-Nagumo model, with ($a=0.7$, $b=0.8$, $c=3.0$, $I=-0.4$). Solutions for four different starting conditions are shown. The dashed lines indicate the nullclines, and the "o" the fixed point of the model. $I=-0.2$ would be a stimulation below threshold, leading to a stationary state. And $I=-1.6$ would hyperpolarize the neuron, also leading to a different stationary state.

The Hodgkin-Huxley model has four dynamical variables: the voltage V , the probability that the K channel is open, $n(V)$, the probability that the Na channel is open given that it was closed previously, $m(V)$, and the probability that the Na channel is open given that it was inactive previously, $h(V)$. A simplified model of action potential generation in neurons is the Fitzhugh-Nagumo (FN) model. Unlike the Hodgkin-Huxley model, the FN model has only two dynamic variables, by combining the variables V and m into a single variable v , and combining the variables n and h into a single variable r

$$\frac{dv}{dt} = c\left(v - \frac{1}{3}v^3 + r + I\right)$$

$$\frac{dr}{dt} = -\frac{1}{c}(v - a + br)$$

I is an external current injected into the neuron. Since the FN model has only two dynamic variables, its full dynamics can be explored using phase plane methods (Sample solution in Python here ³)

2.2 Simulating a Single Neuron with Positive Feedback

The following two examples are taken from ⁵. This book provides a fantastic introduction into modeling simple neural systems, and gives a good understanding of the underlying information processing.

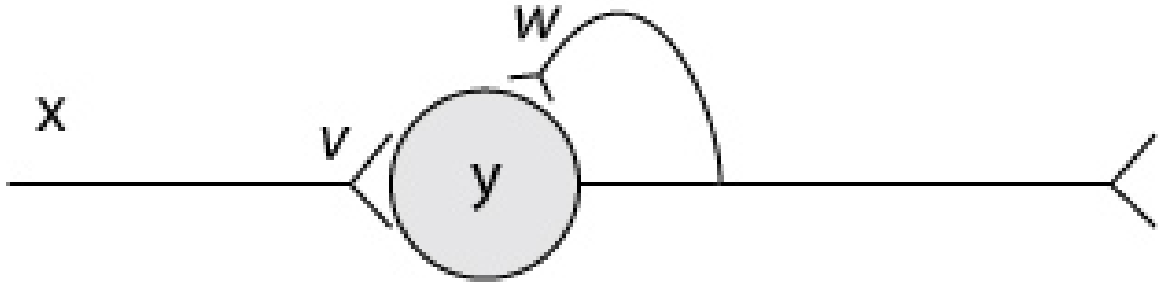


Figure 10 Simple neural system with feedback.

Let us first look at the response of a single neuron, with an input $x(t)$, and with feedback onto itself. The weight of the input is v , and the weight of the feedback w . The response $y(t)$ of the neuron is given by

$$y(t) = wy(t-1) + vx(t-1)$$

This shows how already very simple simulations can capture signal processing properties of real neurons.

³ Fitzhugh-Nagumo Model [Python] ⁴. . Retrieved

⁵ Tutorial on Neural systems Modeling ⁶. . Retrieved

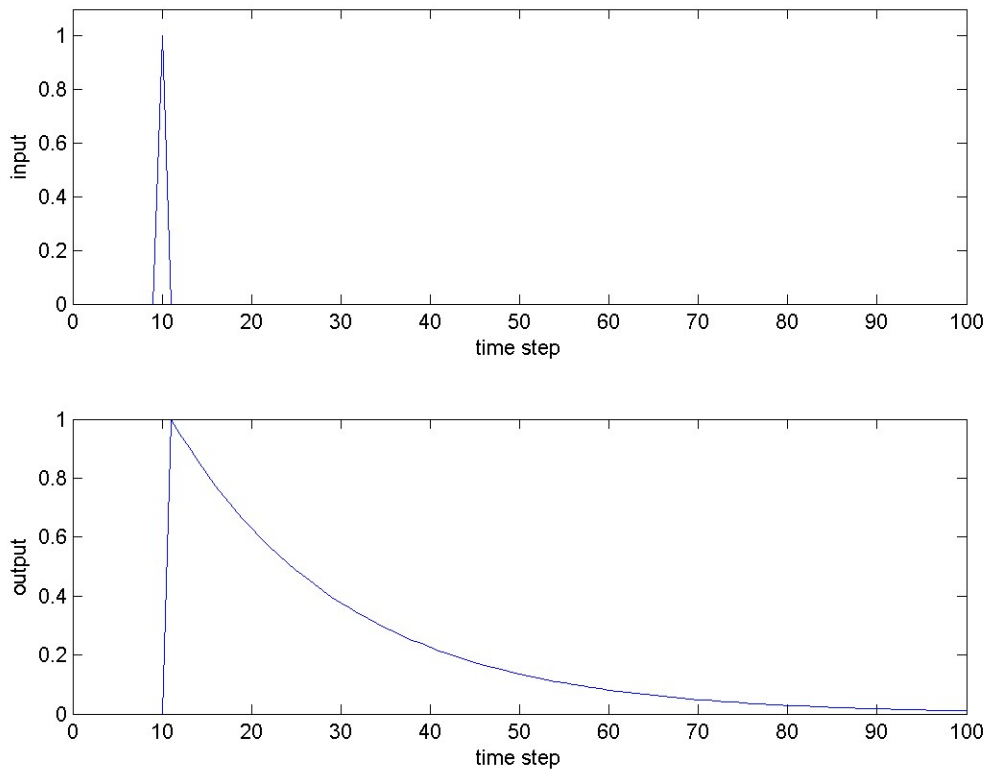


Figure 11 System output for a input pulse: a “leaky integrator”

```

# -*- coding: utf-8 -*-
import numpy as np
import matplotlib.pyplot as plt

def oneUnitWithPosFB():
    ,,,Simulates a single model neuron with positive feedback ,,,
    # set input flag (1 for impulse, 2 for step)
    inFlag = 1

    cut = -np.inf # set cut-off
    sat = np.inf # set saturation

    tEnd = 100 # set last time step
    nTs = tEnd+1 # find the number of time steps

    v = 1 # set the input weight
    w = 0.95 # set the feedback weight

    x = np.zeros(nTs) # open (define) an input hold vector
    start = 11 # set a start time for the input
    if inFlag == 1: # if the input should be a pulse
        x[start] = 1 # then set the input at only one time point
    elif inFlag == 2: # if the input instead should be a step, then
        x[start:nTs] = np.ones(nTs-start) #keep it up until the end

    y = np.zeros(nTs) # open (define) an output hold vector
    for t in range(2, nTs): # at every time step (skipping the first)

        y[t] = w*y[t-1] + v*x[t-1] # compute the output
    
```

```
y[t] = np.max([cut, y[t]]) # impose the cut-off constraint
y[t] = np.min([sat, y[t]]) # impose the saturation constraint

# plot results (no frills)
plt.subplot(211)
tBase = np.arange(tEnd+1)
plt.plot(tBase, x)
plt.axis([0, tEnd, 0, 1.1])
plt.xlabel('Time Step,')
plt.ylabel('Input,')
plt.subplot(212)
plt.plot(tBase, y)
plt.xlabel('Time Step,')
plt.ylabel('Output,')
plt.show()

if __name__ == '__main__':
    oneUnitWithPosFB()
```

2.3 Simulating a Simple Neural System

Even very simple neural systems can display a surprisingly versatile set of behaviors. An example is Wilson's model of the locust-flight central pattern generator. Here the system is described by

$$\vec{y}(t) = \mathbf{W} \cdot \vec{y}(t-1) + \vec{v}x(t-1)$$

\mathbf{W} is the connection matrix describing the recurrent connections of the neurons, and describes the input to the system.

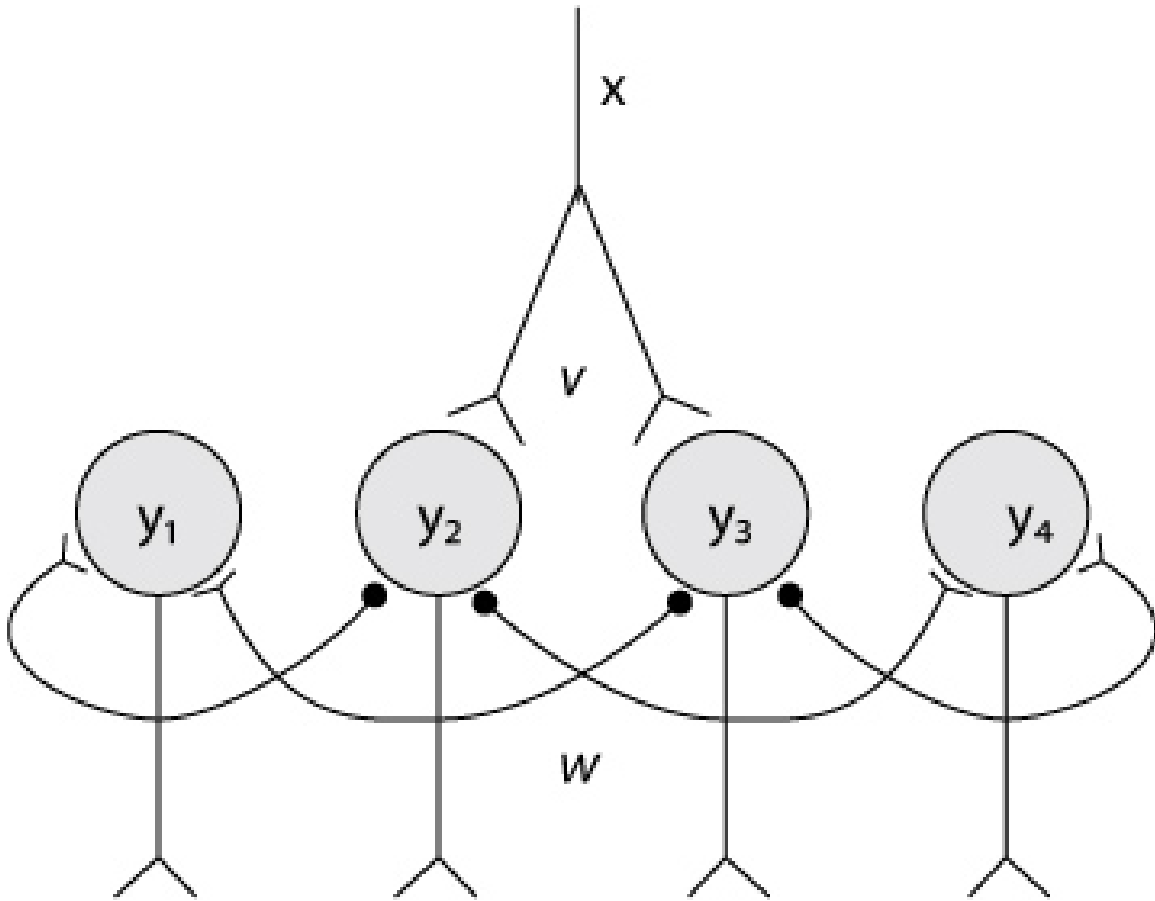


Figure 12 Input x connects to units y_i ($i=1,2,3,4$) with weights v_i , and units y_l ($l = 1,2,3,4$) connect to units y_k ($k = 1,2,3,4$) with weights w_{kl} . For clarity, the self-connections of y_2 and y_3 are not shown, and the individual forward and recurrent weights are not labeled. Based on Tom Anastasio's excellent book "Tutorial on Neural Systems Modeling".

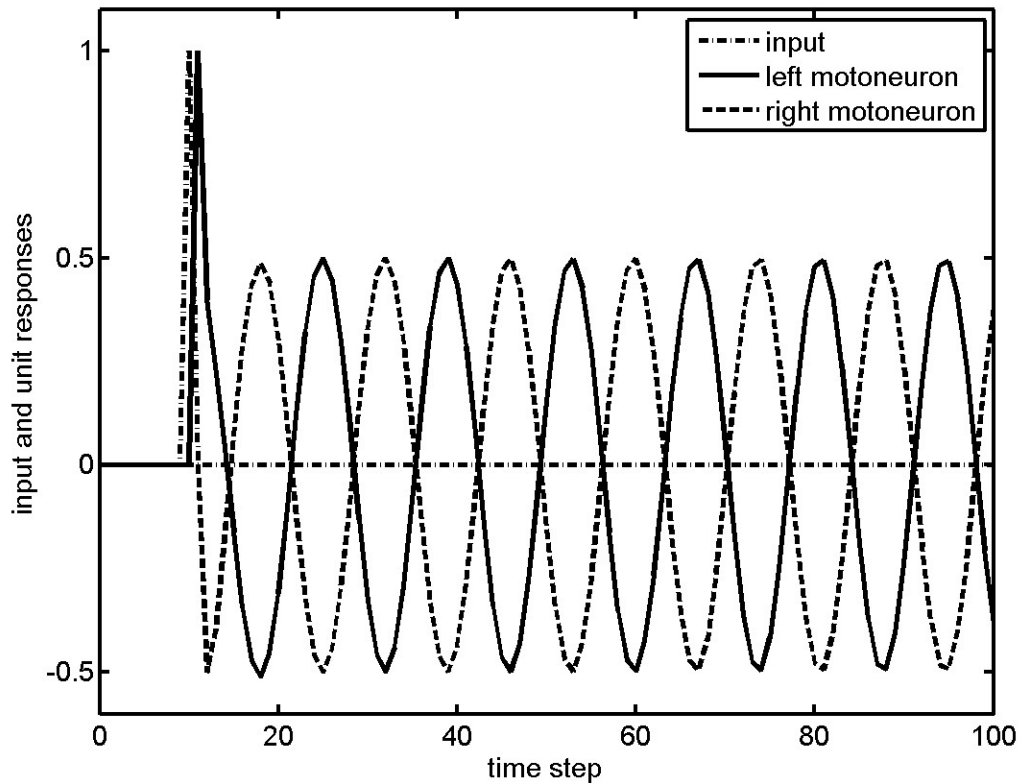


Figure 13 The response of units representing motoneurons in the linear version of Wilson's model of the locust-flight central pattern generator (CPG): A simple input pulse elicits a sustained antagonistic oscillation in neurons 2 and 3.

```
import numpy as np
import matplotlib.pyplot as plt

def printInfo(text, value):
    print(text)
    print(np.round(value, 2))

def WilsonCPG():
    ... implements a linear version of Wilson's
    locust flight central pattern generator (CPG) ...

    v1 = v3 = v4 = 0.          # set input weights
    v2 = 1.
    w11=0.9; w12=0.2; w13 = w14 = 0.    # feedback weights to unit
one
    w21=-0.95; w22=0.4; w23=-0.5; w24=0 # ... to unit two
    w31=0; w32=-0.5; w33=0.4; w34=-0.95 # ... to unit three
    w41 = w42 = 0.; w43=0.2; w44=0.9    # ... to unit four
    V=np.array([v1, v2, v3, v4])        # compose input weight matrix
(vector)
    W=np.array([[w11, w12, w13, w14],
                [w21, w22, w23, w24],
                [w31, w32, w33, w34],
                [w41, w42, w43, w44]])   # compose feedback weight
matrix
```

```

tEnd = 100          # set end time
tVec = np.arange(tEnd) # set time vector
nTs = tEnd         # find number of time steps
x = np.zeros(nTs)  # zero input vector
fly = 11          # set time to start flying
x[fly] = 1        # set input to one at fly time

y = np.zeros((4,nTs)) # zero output vector
for t in range(1,nTs): # for each time step
    y[:,t] = W.dot(y[:,t-1]) + V*x[t-1]; # compute output

# These calculations are interesting, but not absolutely
necessary
(eVal,eVec) = np.linalg.eig(W); # find eigenvalues and
eigenvectors
magEVal = np.abs(eVal)          # find magnitude of eigenvalues
angEVal = np.angle(eVal)*(180/np.pi) # find angles of eigenvalues

printInfo(,Eigenvectors: -----, eVec)
printInfo(,Eigenvalues: -----, eVal)
printInfo(,Angle of Eigenvalues: -----, angEVal)

# plot results (units y2 and y3 only)
plt.figure()
plt.rcParams[font.size,] = 14      # set the default fontsize
plt.rcParams[lines.linewidth,]=1

plt.plot(tVec, x, ,k-. , tVec, y[1:], ,k, , tVec,y[2:], ,k-- ,
linewidth=2.5)
plt.axis([0, tEnd, -0.6, 1.1])
plt.xlabel(,Time Step, ,fontsize=14)
plt.ylabel(,Input and Unit Responses, ,fontsize=14)
plt.legend((,Input, ,Left Motoneuron, ,Right Motoneuron,))
plt.show()

if __name__ == __main__:
    plt.close(,all,)
    WilsonCPG()

```

2.4 References

3 Visual System

3.1 Introduction

Generally speaking, visual systems rely on electromagnetic (EM) waves to give an organism more information about its surroundings. This information could be regarding potential mates, dangers and sources of sustenance. Different organisms have different constituents that make up what is referred to as a visual system.

The complexity of eyes range from something as simple as an eye spot, which is nothing more than a collection of photosensitive cells, to a fully fledged camera eye. If an organism has different types of photosensitive cells, or cells sensitive to different wavelength ranges, the organism would theoretically be able to perceive colour or at the very least colour differences. Polarisation, another property of EM radiation, can be detected by some organisms, with insects and cephalopods having the highest accuracy.

Please note, in this text, the focus has been on using EM waves to see. Granted, some organisms have evolved alternative ways of obtaining sight or at the very least supplementing what they see with extra-sensory information. For example, whales or bats, which use echo-location. This may be seeing in some sense of the definition of the word, but it is not entirely correct. Additionally, vision and visual are words most often associated with EM waves in the visual wavelength range, which is normally defined as the same wavelength limits of human vision. Since some organisms detect EM waves with frequencies below and above that of humans a better definition must be made. We therefore define the visual wavelength range as wavelengths of EM between 300nm and 800nm. This may seem arbitrary to some, but selecting the wrong limits would render parts of some bird's vision as non-vision. Also, with this range of wavelengths, we have defined for example the thermal-vision of certain organisms, like for example snakes as non-vision. Therefore snakes using their pit organs, which is sensitive to EM between 5000nm and 30,000nm (IR), do not "see", but somehow "feel" from afar. Even if blind specimens have been documented targeting and attacking particular body parts.

Firstly a brief description of different types of visual system sensory organs will be elaborated on, followed by a thorough explanation of the components in human vision, the signal processing of the visual pathway in humans and finished off with an example of the perceptual outcome due to these stages.

3.1.1 Sensory Organs

Vision, or the ability to see depends on visual system sensory organs or eyes. There are many different constructions of eyes, ranging in complexity depending on the requirements of the organism. The different constructions have different capabilities, are sensitive to different

wave-lengths and have differing degrees of acuity, also they require different processing to make sense of the input and different numbers to work optimally. The ability to detect and decipher EM has proved to be a valuable asset to most forms of life, leading to an increased chance of survival for organisms that utilise it. In environments without sufficient light, or complete lack of it, lifeforms have no added advantage of vision, which ultimately has resulted in atrophy of visual sensory organs with subsequent increased reliance on other senses (e.g. some cave dwelling animals, bats etc.). Interestingly enough, it appears that visual sensory organs are tuned to the optical window, which is defined as the EM wavelengths (between 300nm and 1100nm) that pass through the atmosphere reaching to the ground. This is shown in the figure below. You may notice that there exists other "windows", an IR window, which explains to some extent the thermal-"vision" of snakes, and a radiofrequency (RF) window, of which no known lifeforms are able to detect.

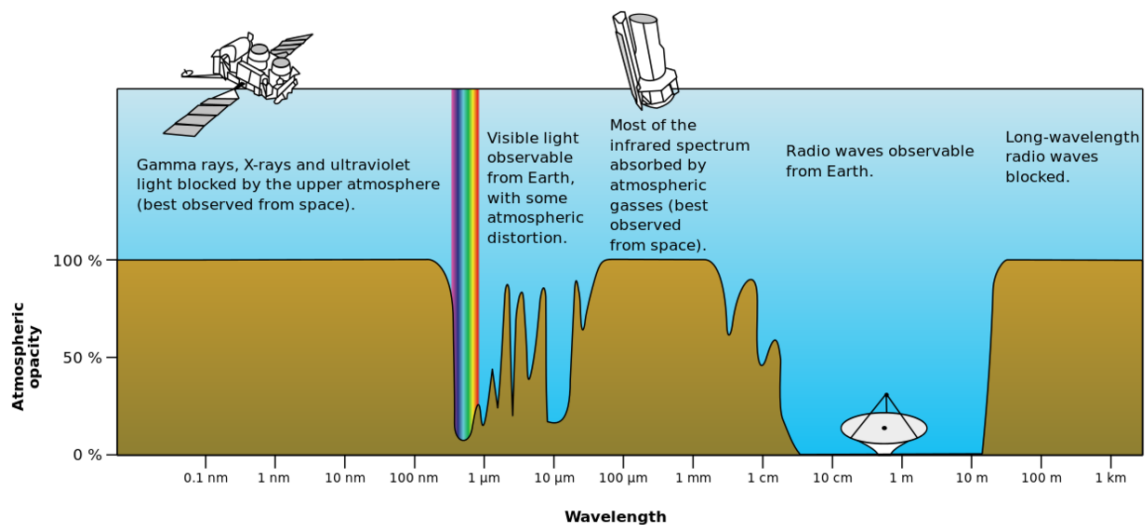


Figure 14

Through time evolution has yielded many eye constructions, and some of them have evolved multiple times, yielding similarities for organisms that have similar niches. There is one underlying aspect that is essentially identical, regardless of species, or complexity of sensory organ type, the universal usage of light-sensitive proteins called opsins. Without focusing too much on the molecular basis though, the various constructions can be categorised into distinct groups:

- Spot Eyes
- Pit Eyes
- Pinhole Eyes
- Lens Eyes
- Refractive Cornea Eyes
- Reflector Eyes
- Compound Eyes

The least complicated configuration of eyes enable organisms to simply sense the ambient light, enabling the organism to know whether there is light or not. It is normally simply a collection of photosensitive cells in a cluster in the same spot, thus sometimes referred to as spot eyes, eye spot or stemma. By either adding more angular structures or recessing the spot eyes, an organisms gains access to directional information as well, which is a vital requirement for image formation. These so called pit eyes are by far the most common types of visual sensory organs, and can be found in over 95% of all known species.



Figure 15 Pinhole eye

Taking this approach to the obvious extreme leads to the pit becoming a cavernous structure, which increases the sharpness of the image, alas at a loss in intensity. In other words, there is a trade-off between intensity or brightness and sharpness. An example of this can be found in the Nautilus, species belonging to the family Nautilidae, organisms considered to be living fossils. They are the only known species that has this type of eye, referred to as the pinhole eye, and it is completely analogous to the pinhole camera or the camera obscura. In addition, like more advanced cameras, Nautili are able to adjust the size of the aperture thereby increasing or decreasing the resolution of the eye at a respective decrease or increase in image brightness. Like the camera, the way to alleviate the intensity/resolution trade-off problem is to include a lens, a structure that focuses the light unto a central area, which most often has a higher density of photo-sensors. By adjusting the shape of the lens and moving it around, and controlling the size of the aperture or pupil, organisms can adapt to different conditions and focus on particular regions of interest in any visual scene. The last upgrade to the various eye constructions already mentioned is the inclusion of a refractive cornea. Eyes with this structure have delegated two thirds of the total optic power of the eye to the high refractive index liquid inside the cornea, enabling very high resolution vision. Most land animals, including humans have eyes of this particular construct. Additionally, many variations of lens structure, lens number, photosensor density, fovea shape, fovea number, pupil shape etc. exists, always, to increase the chances of survival for the organism in question. These variations lead to a varied outward appearance of eyes, even with a single eye construction category. Demonstrating this point, a collection of photographs of animals with the same eye category (refractive cornea eyes) is shown below.

Refractive Cornea Eyes

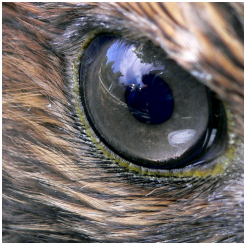


Figure 16
Hawk Eye



Figure 17
Sheep Eye



Figure 18 Cat
Eye



Figure 19 Hu-
man Eye

An alternative to the lens approach called reflector eyes can be found in for example mollusks. Instead of the conventional way of focusing light to a single point in the back of the eye using a lens or a system of lenses, these organisms have mirror like structures inside the chamber of the eye that reflects the light into a central portion, much like a parabola dish. Although there are no known examples of organisms with reflector eyes capable of image formation, at least one species of fish, the spookfish (*Dolichopteryx longipes*) uses them in combination with "normal" lensed eyes.



Figure 20 Compound eye

The last group of eyes, found in insects and crustaceans, is called compound eyes. These eyes consist of a number of functional sub-units called ommatidia, each consisting of a facet, or front surface, a transparent crystalline cone and photo-sensitive cells for detection. In addition each of the ommatidia are separated by pigment cells, ensuring the incoming light is as parallel as possible. The combination of the outputs of each of these ommatidia form a mosaic image, with a resolution proportional to the number of ommatidia units. For example, if humans had compound eyes, the eyes would have covered our entire faces to retain the same resolution. As a note, there are many types of compound eyes, but delving to deep into this topic is beyond the scope of this text.

Not only the type of eyes vary, but also the number of eyes. As you are well aware of, humans usually have two eyes, spiders on the other hand have a varying number of eyes, with most species having 8. Normally the spiders also have varying sizes of the different pairs of eyes and the differing sizes have different functions. For example, in jumping spiders 2 larger front facing eyes, give the spider excellent visual acuity, which is used mainly to target prey. 6 smaller eyes have much poorer resolution, but helps the spider to avoid potential dangers.

Two photographs of the eyes of a jumping spider and the eyes of a wolf spider are shown to demonstrate the variability in the eye topologies of arachnids.



Figure 21 Wolf Spider



Figure 22 Jumping Spider

3.2 Anatomy of the Visual System

We humans are visual creatures, therefore our eyes are complicated with many components. In this chapter, an attempt is made to describe these components, thus giving some insight into the properties and functionality of human vision.

Getting inside of the eyeball - Pupil, iris and the lens

Light rays enter the eye structure through the black aperture or pupil in the front of the eye. The black appearance is due to the light being fully absorbed by the tissue inside the eye. Only through this pupil can light enter into the eye which means the amount of incoming light is effectively determined by the size of the pupil. A pigmented sphincter surrounding the pupil functions as the eye's aperture stop. It is the amount of pigment in this iris, that give rise to the various eye colours found in humans.

In addition to this layer of pigment, the iris has 2 layers of ciliary muscles. A circular muscle called the pupillary sphincter in one layer, that contracts to make the pupil smaller. The other layer has a smooth muscle called the pupillary dilator, which contracts to dilate the

pupil. The combination of these muscles can thereby dilate/contract the pupil depending on the requirements or conditions of the person. The ciliary muscles are controlled by ciliary zonules, fibres that also change the shape of the lens and hold it in place.

The lens is situated immediately behind the pupil. Its shape and characteristics reveal a similar purpose to that of camera lenses, but they function in slightly different ways. The shape of the lens is adjusted by the pull of the ciliary zonules, which consequently changes the focal length. Together with the cornea, the lens can change the focus, which makes it a very important structure indeed, however only one third of the total optical power of the eye is due to the lens itself. It is also the eye's main filter. Lens fibres make up most of the material for the lense, which are long and thin cells void of most of the cell machinery to promote transparency. Together with water soluble proteins called crystallins, they increase the refractive index of the lens. The fibres also play part in the structure and shape of the lens itself.

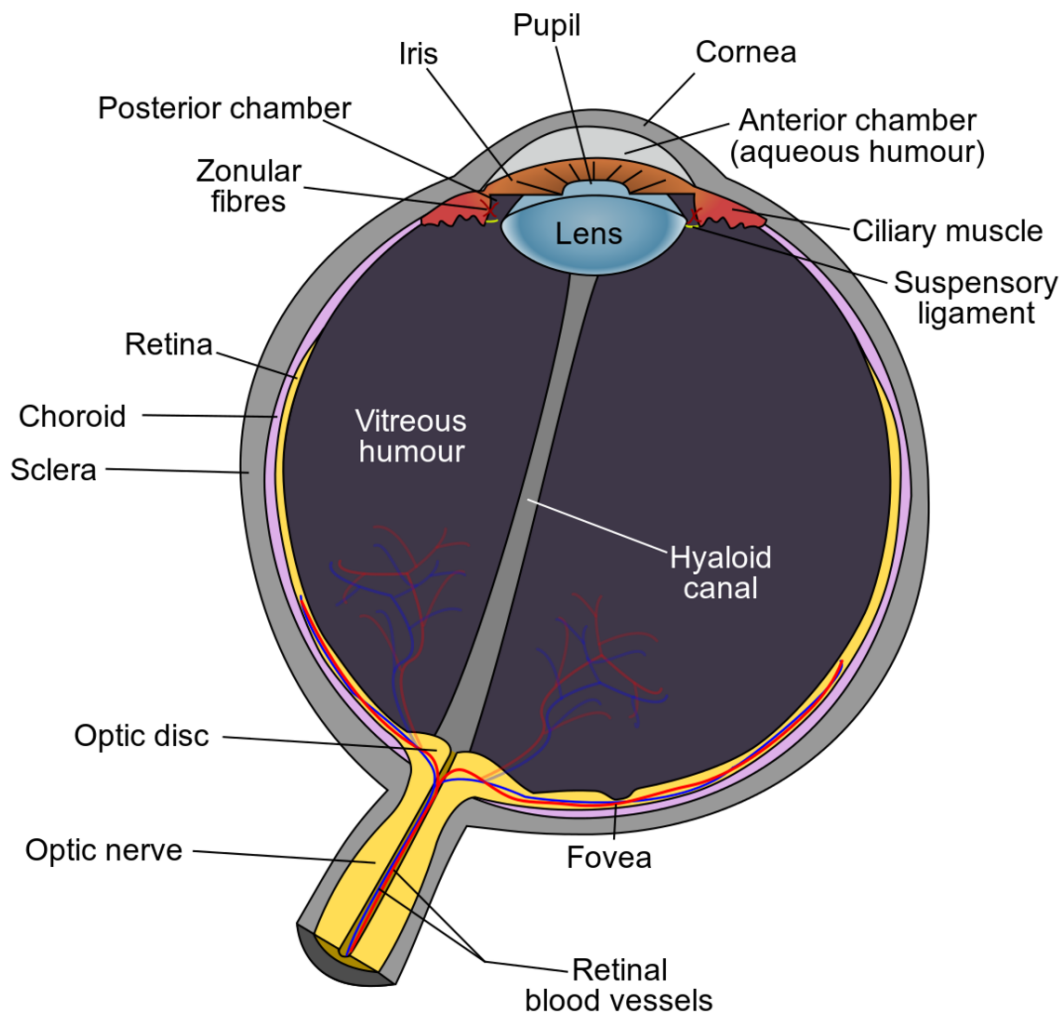


Figure 23 Schematic diagram of the human eye

Beamforming in the eye – Cornea and its protecting agent - Sclera

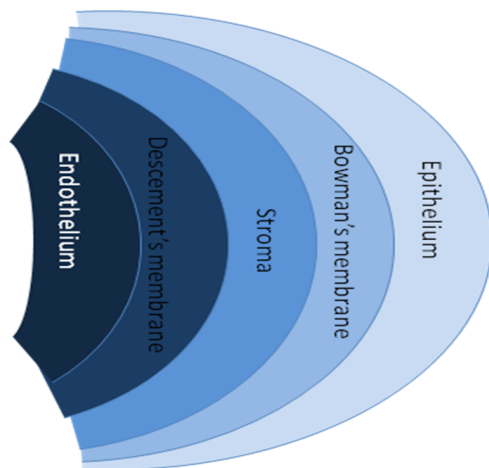


Figure 24 Structure of the Cornea

The cornea, responsible for the remaining 2/3 of the total optical power of the eye, covers the iris, pupil and lens. It focuses the rays that pass through the iris before they pass through the lens. The cornea is only 0.5mm thick and consists of 5 layers:

- Epithelium: A layer of epithelial tissue covering the surface of the cornea.
- Bowman's membrane: A thick protective layer composed of strong collagen fibres, that maintain the overall shape of the cornea.
- Stroma: A layer composed of parallel collagen fibrils. This layer makes up 90% of the cornea's thickness.
- Descemet's membrane and Endothelium: Are two layers adjusted to the anterior chamber of the eye filled with aqueous humor fluid produced by the ciliary body. This fluid moisturises the lens, cleans it and maintains the pressure in the eye ball. The chamber, positioned between cornea and iris, contains a trabecular meshwork body through which the fluid is drained out by Schlemm canal, through posterior chamber.

The surface of the cornea lies under two protective membranes, called the sclera and Tenon's capsule. Both of these protective layers completely envelop the eyeball. The sclera is built from collagen and elastic fibres, which protect the eye from external damages, this layer also gives rise to the white of the eye. It is pierced by nerves and vessels with the largest hole reserved for the optic nerve. Moreover, it is covered by conjunctiva, which is a clear mucous membrane on the surface of the eyeball. This membrane also lines the inside of the eyelid. It works as a lubricant and, together with the lacrimal gland, it produces tears, that lubricate and protect the eye. The remaining protective layer, the eyelid, also functions to spread this lubricant around.

Moving the eyes – extra-ocular muscles

The eyeball is moved by a complicated muscle structure of extra-ocular muscles consisting of four rectus muscles – inferior, medial, lateral and superior and two oblique – inferior and superior. Positioning of these muscles is presented below, along with functions:

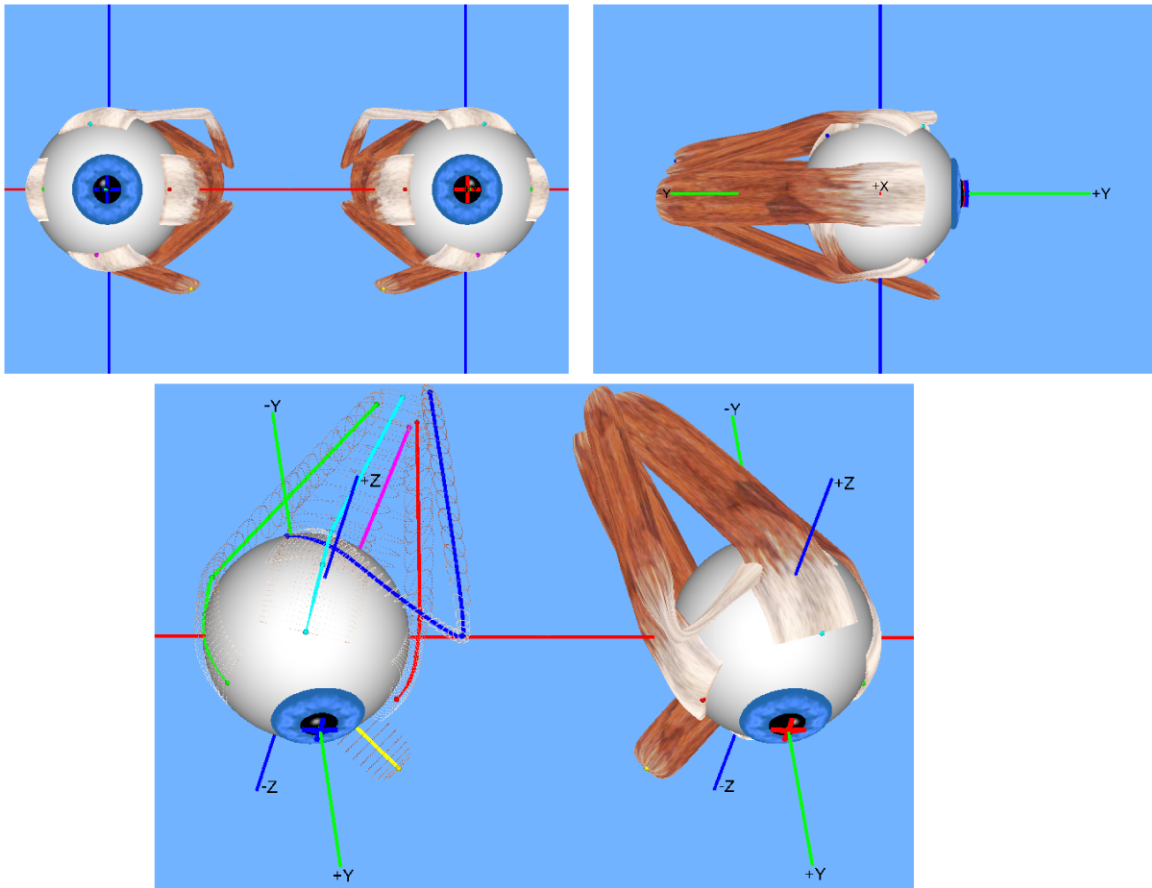


Figure 25 Extra-ocular muscles: Green - Lateral Rectus; Red - Medial Rectus; Cyan - Superior Rectus; Pink - Inferior Rectus; Dark Blue - Superior Oblique; Yellow - Inferior Oblique.

As you can see, the extra-ocular muscles (2,3,4,5,6,8) are attached to the sclera of the eyeball and originate in the annulus of Zinn, a fibrous tendon surrounding the optic nerve. A pulley system is created with the trochlea acting as a pulley and the superior oblique muscle as the rope, this is required to redirect the muscle force in the correct way. The remaining extra-ocular muscles have a direct path to the eye and therefore do not form these pulley systems. Using these extra-ocular muscles, the eye can rotate up, down, left, right and alternative movements are possible as a combination of these.

Other movements are also very important for us to be able to see. Vergence movements enable the proper function of binocular vision. Unconscious fast movements called saccades, are essential for people to keep an object in focus. The saccade is a sort of jittery movement performed when the eyes are scanning the visual field, in order to displace the point of fixation slightly. When you follow a moving object with your gaze, your eyes perform what is referred to as smooth pursuit. Additional involuntary movements called nystagmus are caused by signals from the vestibular system, together they make up the vestibulo-ocular reflexes.

The brain stem controls all of the movements of the eyes, with different areas responsible for different movements.

- Pons: Rapid horizontal movements, such as saccades or nystagmus
- Mesencephalon: Vertical and torsional movements
- Cerebellum: Fine tuning
- Edinger-Westphal nucleus: Vergence movements

Where the vision reception occurs – The retina

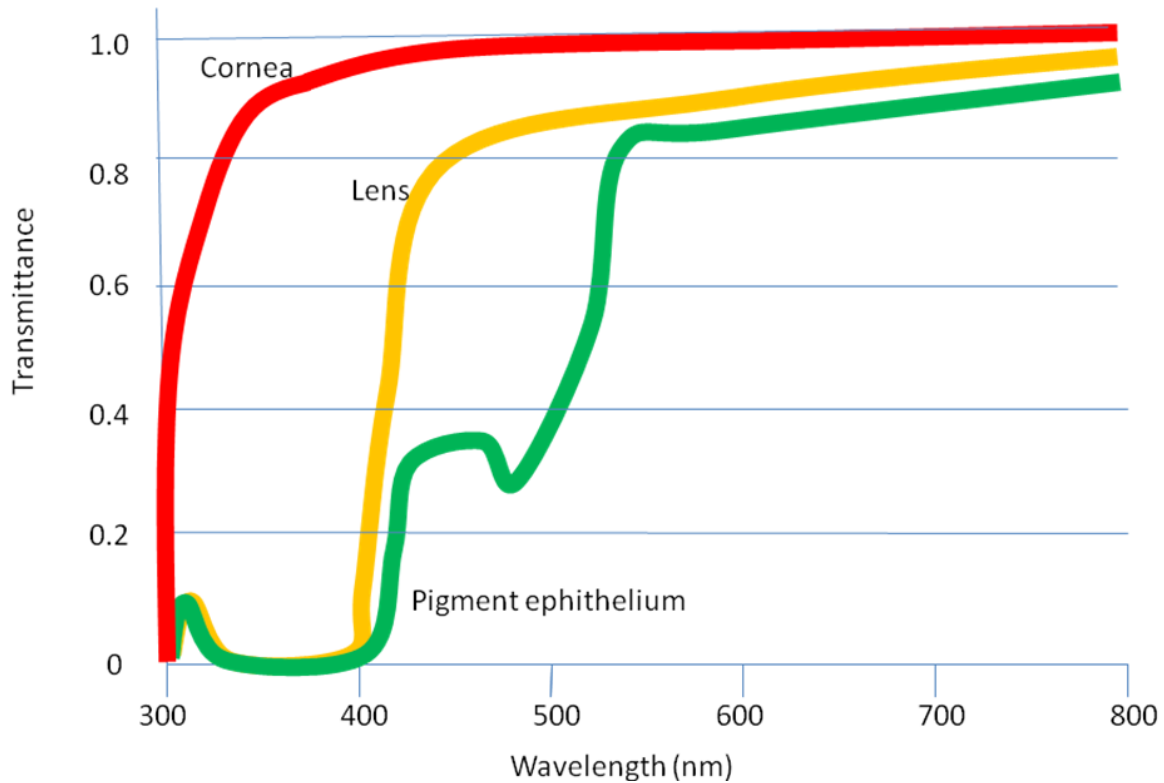


Figure 26 Filtering of the light performed by the cornea, lens and pigment epithelium

Before being transduced, incoming EM passes through the cornea, lens and the macula. These structures also act as filters to reduce unwanted EM, thereby protecting the eye from harmful radiation. The filtering response of each of these elements can be seen in the figure "Filtering of the light performed by cornea, lens and pigment epithelium". As one may observe, the cornea attenuates the lower wavelengths, leaving the higher wavelengths nearly untouched. The lens blocks around 25% of the EM below 400nm and more than 50% below 430nm. Finally, the pigment epithelium, the last stage of filtering before the photo-reception, affects around 30% of the EM between 430nm and 500nm.

A part of the eye, which marks the transition from non-photosensitive region to photosensitive region, is called the ora serrata. The photosensitive region is referred to as the retina, which is the sensory structure in the back of the eye. The retina consists of multiple layers presented below with millions of photoreceptors called rods and cones, which capture the light rays and convert them into electrical impulses. Transmission of these impulses is nervously initiated by the ganglion cells and conducted through the optic nerve, the single route by which information leaves the eye.

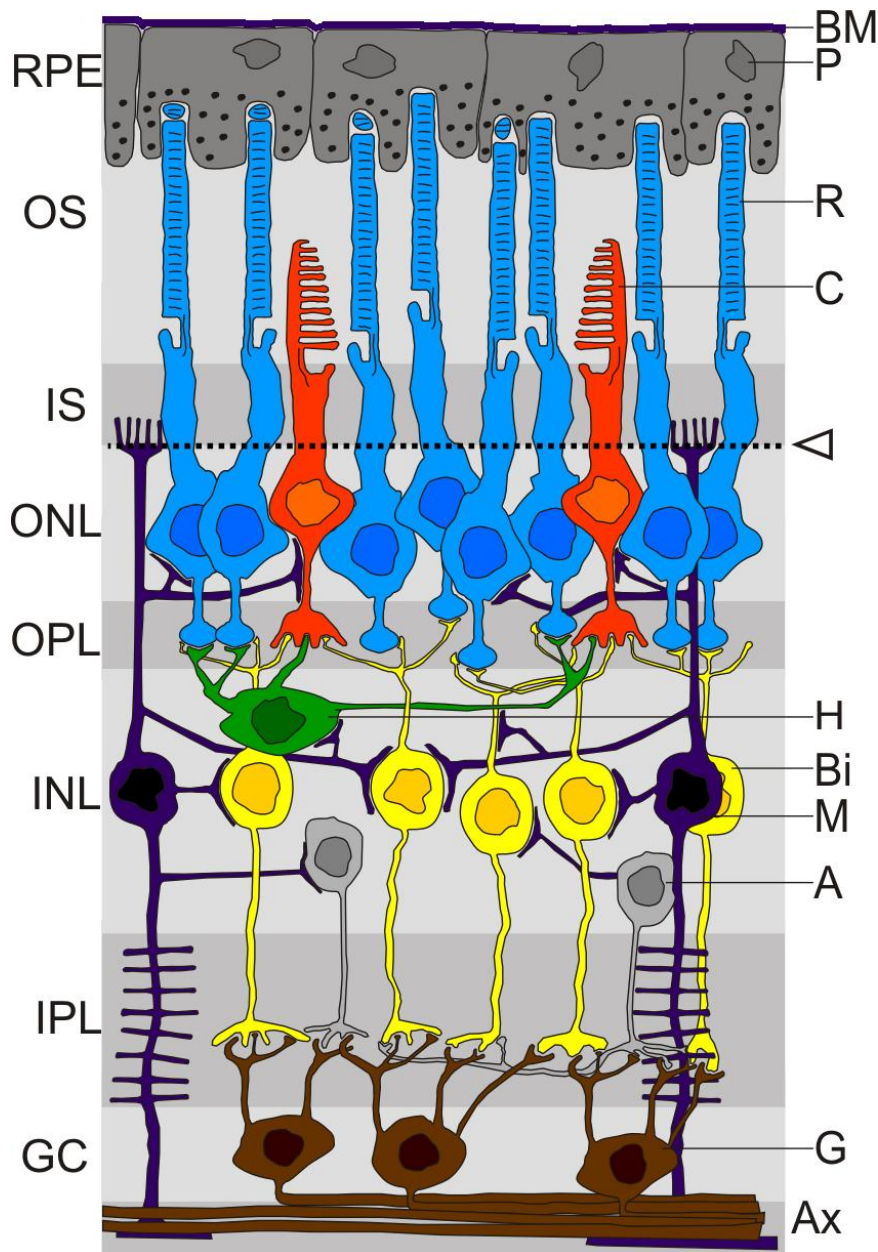


Figure 27 Structure of retina including the main cell components: RPE: retinal pigment epithelium; OS: outer segment of the photoreceptor cells; IS: inner segment of the photoreceptor cells; ONL: outer nuclear layer; OPL: outer plexiform layer; INL: inner nuclear layer IPL: inner plexiform layer; GC: ganglion cell layer; P: pigment epithelium cell; BM: Bruch-Membran; R: rods; C: cones; H: horizontal cell; B: bipolar cell; M: Müller cell; A: amacrine cell; G: ganglion cell; AX: Axon; arrow: Membrane limitans externa.

A conceptual illustration of the structure of the retina is shown on the right. As we can see, there are five main cell types:

- photoreceptor cells
- horizontal cells
- bipolar cells
- amacrine cells
- ganglion cells

Photoreceptor cells can be further subdivided into two main types called rods and cones. Cones are much less numerous than rods in most parts of the retina, but there is an enormous aggregation of them in the macula, especially in its central part called the fovea. In this central region, each photo-sensitive cone is connected to one ganglion-cell. In addition, the cones in this region are slightly smaller than the average cone size, meaning you get more cones per area. Because of this ratio, and the high density of cones, this is where we have the highest visual acuity.

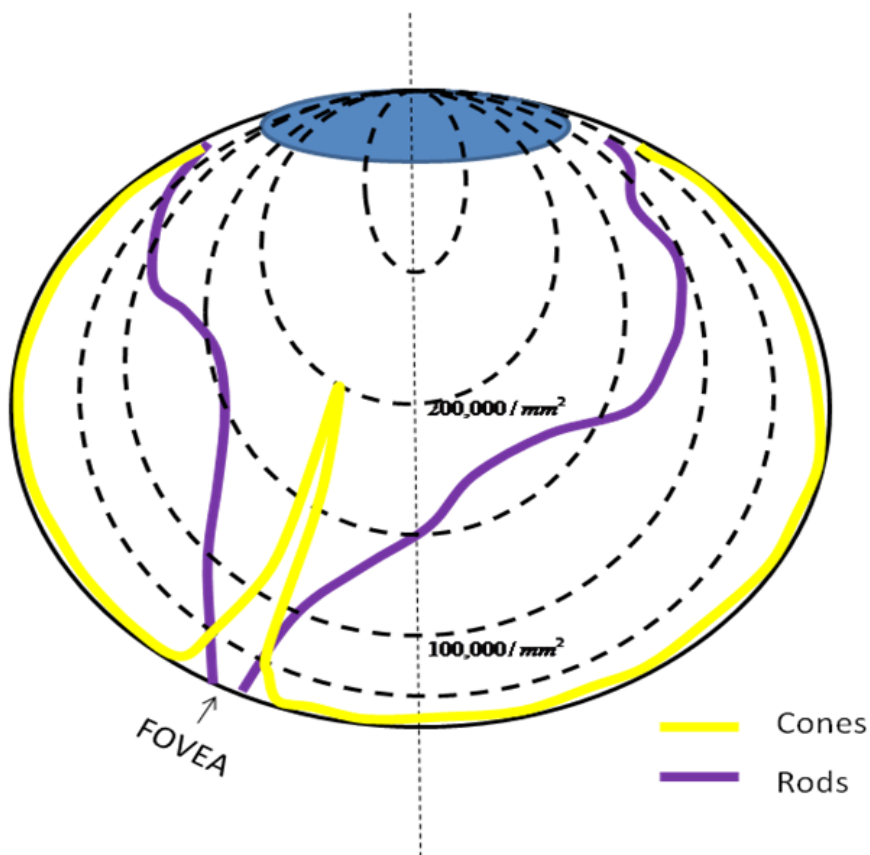
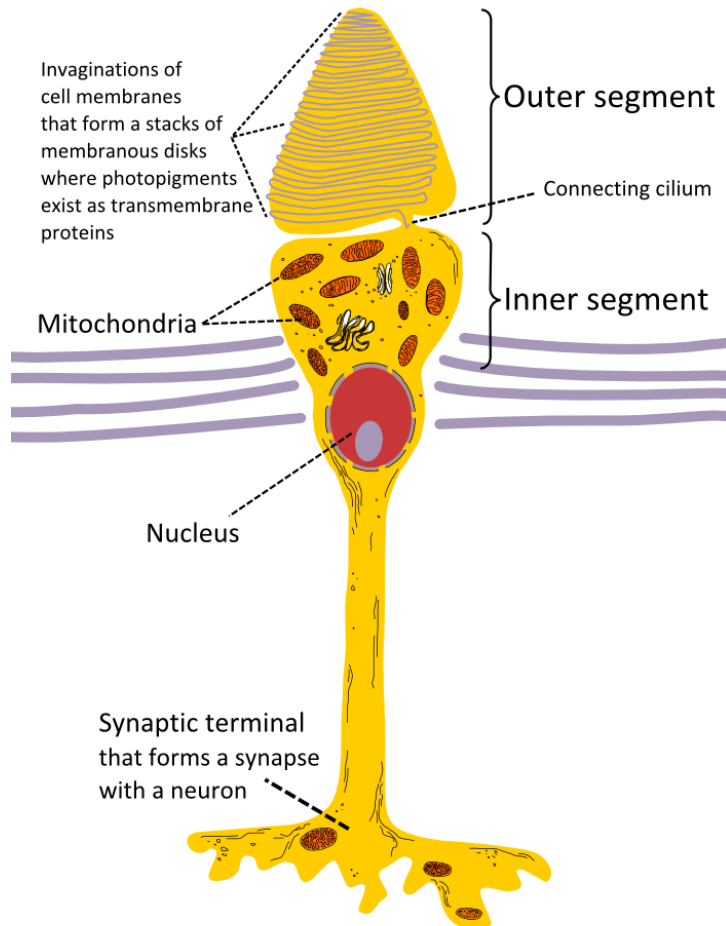


Figure 28 Density of rods and cones around the eye

There are 3 types of human cones, each of the cones responding to a specific range of wavelengths, because of three types of a pigment called photopsin. Each pigment is sensitive to red, blue or green wavelength of light, so we have blue, green and red cones, also called S-, M- and L-cones for their sensitivity to short-, medium- and long-wavelength respectively. It consists of protein called opsin and a bound chromophore called the retinal. The main building blocks of the cone cell are the synaptic terminal, the inner and outer segments, the interior nucleus and the mitochondria.

The spectral sensitivities of the 3 types of cones:

- 1. S-cones absorb short-wave light, i.e. blue-violet light. The maximum absorption wavelength for the S-cones is 420nm
- 2. M-cones absorb blue-green to yellow light. In this case The maximum absorption wavelength is 535nm
- 3. L-cones absorb yellow to red light. The maximum absorption wavelength is 565nm



Cone cell

Figure 29 Cone cell structure

The inner segment contains organelles and the cell's nucleus and organelles. The pigment is located in the outer segment, attached to the membrane as trans-membrane proteins within the invaginations of the cell-membrane that form the membranous disks, which are clearly visible in the figure displaying the basic structure of rod and cone cells. The disks maximize the reception area of the cells. The cone photoreceptors of many vertebrates contain spherical organelles called oil droplets, which are thought to constitute intra-ocular filters which may serve to increase contrast, reduce glare and lessen chromatic aberrations caused by the mitochondrial size gradient from the periphery to the centres.

Rods have a structure similar to cones, however they contain the pigment rhodopsin instead, which allows them to detect low-intensity light and makes them 100 times more sensitive than cones. Rhodopsin is the only pigment found in human rods, and it is found on the outer side of the pigment epithelium, which similarly to cones maximizes absorption area by employing a disk structure. Similarly to cones, the synaptic terminal of the cell joins it with a bipolar cell and the inner and outer segments are connected by cilium.

The pigment rhodopsin absorbs the light between 400-600nm, with a maximum absorption at around 500nm. This wavelength corresponds to greenish-blue light which means blue colours appear more intense in relation to red colours at night.

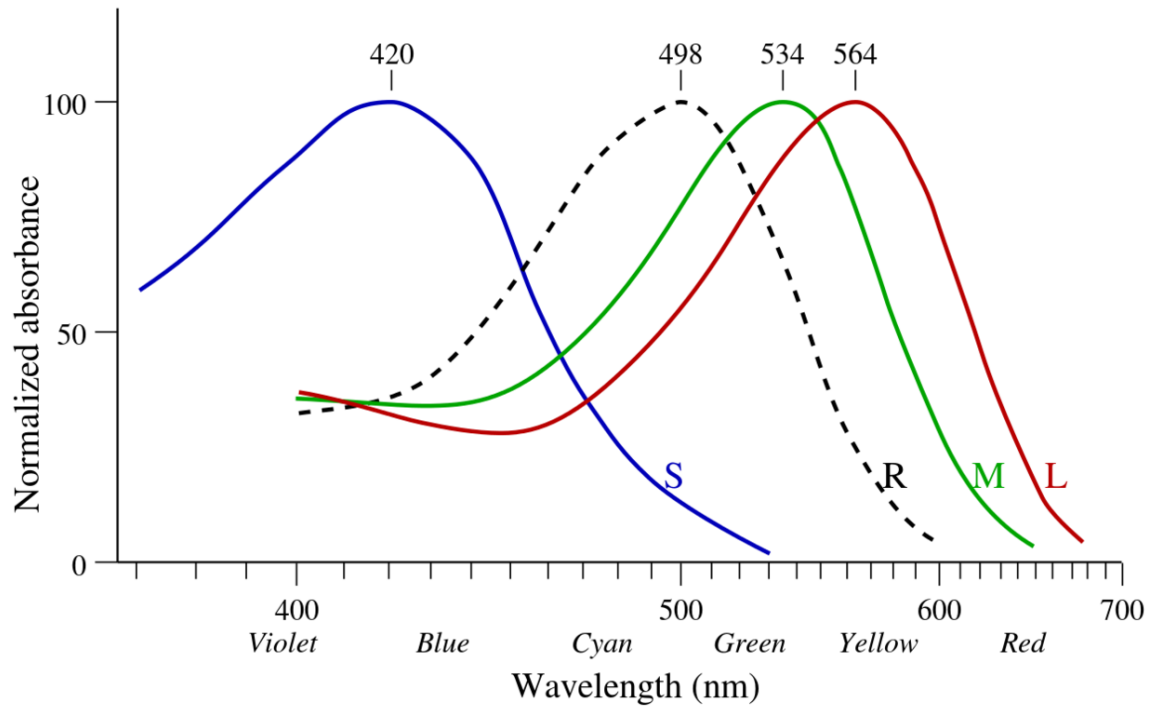


Figure 30 The sensitivity of cones and rods across visible EM

EM waves with wavelengths outside the range of 400 – 700 nm are not detected by either rods nor cones, which ultimately means they are not visible to human beings.

Horizontal cells occupy the inner nuclear layer of the retina. There are two types of horizontal cells and both types hyper-polarise in response to light i.e. they become more negative. Type A consists of a subtype called HII-H2 which interacts with predominantly S-cones. Type B cells have a subtype called HI-H1, which features a dendrite tree and an axon. The former contacts mostly M- and L-cone cells and the latter rod cells. Contacts with cones are made mainly by prohibitory synapses, while the cells themselves are joined into a network with gap junctions.

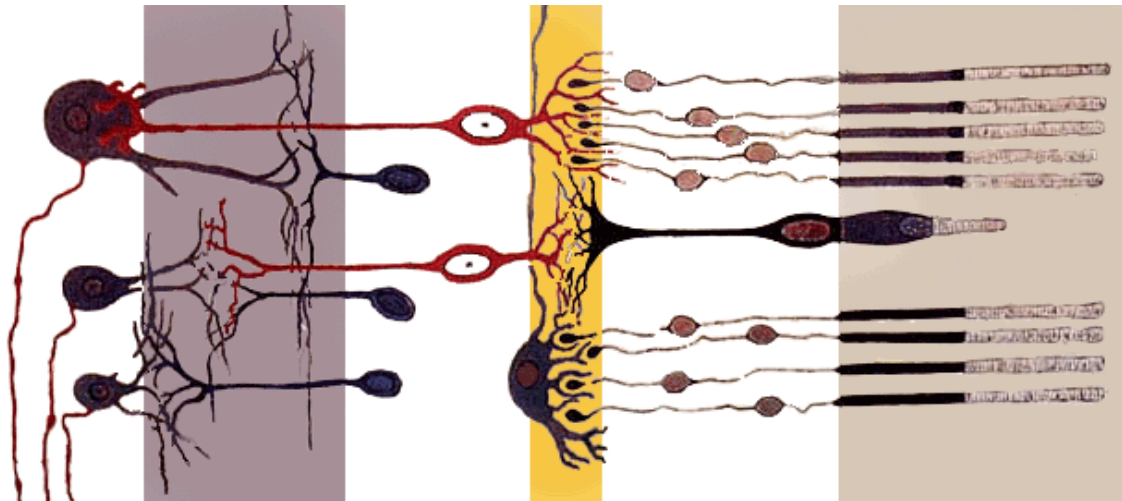


Figure 31 Cross-section of the human retina, with bipolar cells indicated in red.

Bipolar cells spread single dendrites in the outer plexiform layer and the perikaryon, their cell bodies, are found in the inner nuclear layer. Dendrites interconnect exclusively with cones and rods and we differentiate between one rod bipolar cell and nine or ten cone bipolar cells. These cells branch with amacrine or ganglion cells in the inner plexiform layer using an axon. Rod bipolar cells connect to triad synapses or 18-70 rod cells. Their axons spread around the inner plexiform layer synaptic terminals, which contain ribbon synapses and contact a pair of cell processes in dyad synapses. They are connected to ganglion cells with AII amacrine cell links.

Amacrine cells can be found in the inner nuclear layer and in the ganglion cell layer of the retina. Occasionally they are found in the inner plexiform layer, where they work as signal modulators. They have been classified as narrow-field, small-field, medium-field or wide-field depending on their size. However, many classifications exist leading to over 40 different types of amacrine cells.

Ganglion cells are the final transmitters of visual signal from the retina to the brain. The most common ganglion cells in the retina is the midget ganglion cell and the parasol ganglion cell. The signal after having passed through all the retinal layers is passed on to these cells which are the final stage of the retinal processing chain. All the information is collected here forwarded to the retinal nerve fibres and optic nerves. The spot where the ganglion axons fuse to create an optic nerve is called the optic disc. This nerve is built mainly from the retinal ganglion axons and Portort cells. The majority of the axons transmit data to the lateral geniculate nucleus, which is a termination nexus for most parts of the nerve and which forwards the information to the visual cortex. Some ganglion cells also react to light, but because this response is slower than that of rods and cones, it is believed to be related to sensing ambient light levels and adjusting the biological clock.

1

1 <http://en.wikibooks.org/wiki/Category%3A>

3.3 Signal Processing

As mentioned before the retina is the main component in the eye, because it contains all the light sensitive cells. Without it, the eye would be comparable to a digital camera without the CCD (Charge Coupled Device) sensor. This part elaborates on how the retina perceives the light, how the optical signal is transmitted to the brain and how the brain processes the signal to form enough information for decision making.

Creation of the initial signals - Photosensor Function

Vision invariably starts with light hitting the photo-sensitive cells found in the retina. Light-absorbing visual pigments, a variety of enzymes and transmitters in retinal rods and cones will initiate the conversion from visible EM stimuli into electrical impulses, in a process known as photoelectric transduction. Using rods as an example, the incoming visible EM hits rhodopsin molecules, transmembrane molecules found in the rods' outer disk structure. Each rhodopsin molecule consists of a cluster of helices called opsin that envelop and surround 11-cis retinal, which is the part of the molecule that will change due to the energy from the incoming photons. In biological molecules, moieties, or parts of molecules that will cause conformational changes due to this energy is sometimes referred to as chromophores. 11-cis retinal straightens in response to the incoming energy, turning into retinal (all-trans retinal), which forces the opsin helices further apart, causing particular reactive sites to be uncovered. This "activated" rhodopsin molecule is sometimes referred to as Metarhodopsin II. From this point on, even if the visible light stimulation stops, the reaction will continue. The Metarhodopsin II can then react with roughly 100 molecules of a G_s protein called transducing, which then results in α_s and $\beta\gamma$ after the GDP is converted into GTP. The activated α_s -GTP then binds to cGMP-phosphodiesterase(PDE), suppressing normal ion-exchange functions, which results in a low cytosol concentration of cation ions, and therefore a change in the polarisation of the cell.

The natural photoelectric transduction reaction has an amazing power of amplification. One single retinal rhodopsin molecule activated by a single quantum of light causes the hydrolysis of up to 10^6 cGMP molecules per second.

Photo Transduction

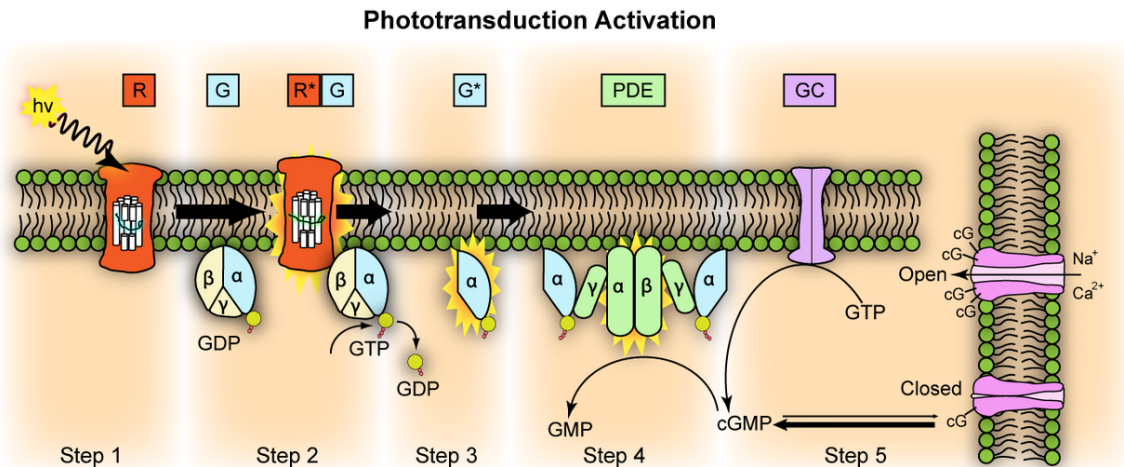


Figure 32 Representation of molecular steps in photoactivation (modified from Leskov et al., 2000). Depicted is an outer membrane disk in a rod. Step 1: Incident photon ($h\nu$) is absorbed and activates a rhodopsin by conformational change in the disk membrane to R^* . Step 2: Next, R^* makes repeated contacts with transducin molecules, catalyzing its activation to G^* by the release of bound GDP in exchange for cytoplasmic GTP (Step 3). The α and γ subunit G^* binds inhibitory γ subunits of the phosphodiesterase (PDE) activating its α and β subunits. Step 4: Activated PDE hydrolyzes cGMP. Step 5: Guanylyl cyclase (GC) synthesizes cGMP, the second messenger in the phototransduction cascade. Reduced levels of cytosolic cGMP cause cyclic nucleotide-gated channels to close preventing further influx of Na^+ and Ca^{2+} .

1. A light photon interacts with the retinal² in a photoreceptor³. The retinal undergoes isomerisation⁴, changing from the 11-*cis* to all-*trans* configuration.
2. Retinal⁵ no longer fits into the opsin binding site.
3. Opsin therefore undergoes a conformational change to metarhodopsin II.
4. Metarhodopsin II is unstable and splits, yielding opsin and all-*trans* retinal.
5. The opsin activates the regulatory protein transducin⁶. This causes transducin to dissociate from its bound GDP, and bind GTP, then the alpha subunit of transducin dissociates from the beta and gamma subunits, with the GTP still bound to the alpha subunit.
6. The alpha subunit-GTP complex activates phosphodiesterase⁷.
7. Phosphodiesterase breaks down cGMP to 5'-GMP. This lowers the concentration of cGMP and therefore the sodium channels close.
8. Closure of the sodium channels causes hyperpolarization of the cell due to the ongoing potassium current.
9. Hyperpolarization of the cell causes voltage-gated calcium channels to close.

2 <http://en.wikibooks.org/wiki/retinal>
 3 <http://en.wikibooks.org/wiki/photoreceptor>
 4 <http://en.wikibooks.org/wiki/isomerisation>
 5 <http://en.wikibooks.org/wiki/Retinal>
 6 <http://en.wikibooks.org/wiki/transducin>
 7 <http://en.wikibooks.org/wiki/phosphodiesterase>

10. As the calcium level in the photoreceptor cell drops, the amount of the neurotransmitter glutamate that is released by the cell also drops. This is because calcium is required for the glutamate-containing vesicles to fuse with cell membrane and release their contents.
11. A decrease in the amount of glutamate released by the photoreceptors causes depolarization of On center bipolar cells (rod and cone On bipolar cells) and hyperpolarization of cone Off bipolar cells.

Without visible EM stimulation, rod cells containing a cocktail of ions, proteins and other molecules, have membrane potential differences of around -40mV . Compared to other nerve cells, this is quite high (-65mV). In this state, the neurotransmitter glutamate is continuously released from the axon terminals and absorbed by the neighbouring bipolar cells. With incoming visible EM and the previously mentioned cascade reaction, the potential difference drops to -70mV . This hyper-polarisation of the cell causes a reduction in the amount of released glutamate, thereby affecting the activity of the bipolar cells, and subsequently the following steps in the visual pathway.

Similar processes exist in the cone-cells and in photosensitive ganglion cells, but make use of different opsins. Photopsin I through III (yellowish-green, green and blue-violet respectively) are found in the three different cone cells and melanopsin (blue) can be found in the photosensitive ganglion cells.

Processing Signals in the Retina

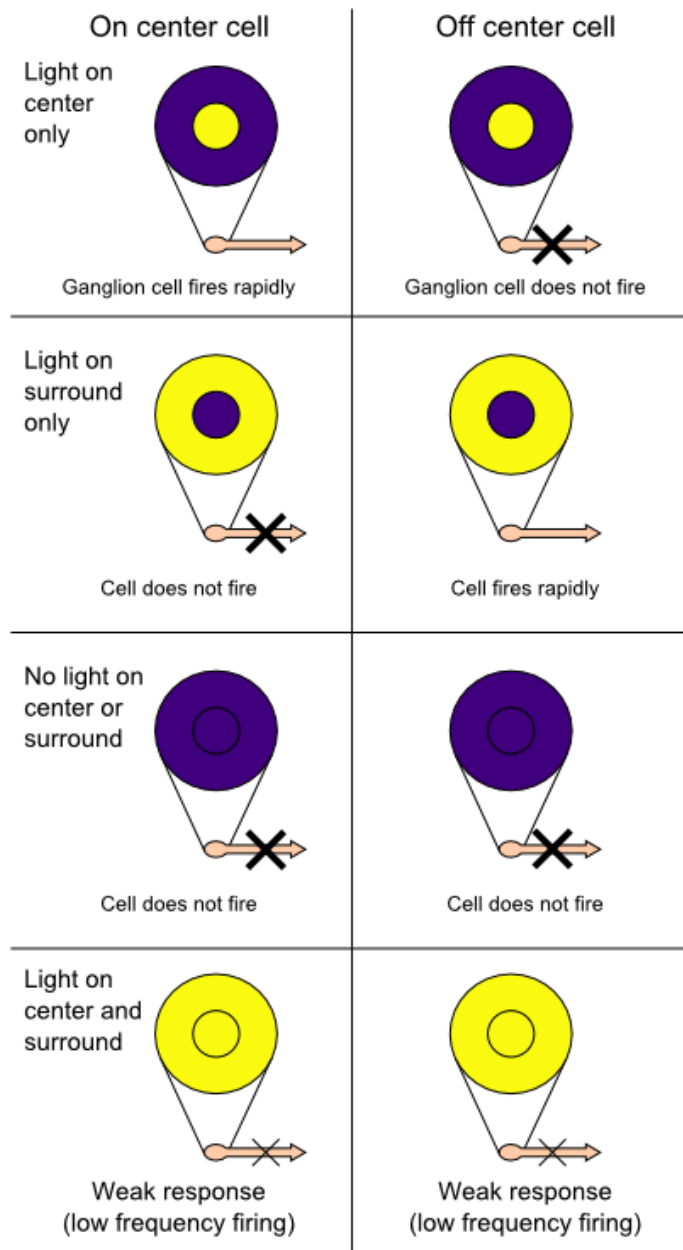


Figure 33

Different bipolar cells react differently to the changes in the released glutamate. The so called ON and OFF bipolar cells are used to form the direct signal flow from cones to bipolar cells. The ON bipolar cells will depolarise by visible EM stimulation and the corresponding ON ganglion cells will be activated. On the other hand the OFF bipolar cells are hyper polarised by the visible EM stimulation, and the OFF ganglion cells are inhibited. This is the basic pathway of the Direct signal flow. The Lateral signal flow will start from the rods, then go to the bipolar cells, the amacrine cells, and the OFF bipolar cells inhibited by the Rod-amacrine cells and the ON bipolar cells will stimulated via an electrical synapse, after

all of the previous steps, the signal will arrive at the ON or OFF ganglion cells and the whole pathway of the Lateral signal flow is established.

When the action potential (AP) in ON, ganglion cells will be triggered by the visible EM stimulus. The AP frequency will increase when the sensor potential increases. In other words, AP depends on the amplitude of the sensor's potential. The region of ganglion cells where the stimulatory and inhibitory effects influence the AP frequency is called receptive field (RF). Around the ganglion cells, the RF is usually composed of two regions: the central zone and the ring-like peripheral zone. They are distinguishable during visible EM adaptation. A visible EM stimulation on the centric zone could lead to AP frequency increase and the stimulation on the periphery zone will decrease the AP frequency. When the light source is turned off the excitation occurs. So the name of ON field (central field ON) refers to this kind of region. Of course the RF of the OFF ganglion cells act the opposite way and is therefore called "OFF field" (central field OFF). The RFs are organised by the horizontal cells. The impulse on the periphery region will be impulsed and transmitted to the central region, and there the so-called stimulus contrast is formed. This function will make the dark seem darker and the light brighter. If the whole RF is exposed to light, the impulse of the central region will predominate.

Signal Transmission to the Cortex

As mentioned previously, axons of the ganglion cells converge at the optic disk of the retina, forming the optic nerve. These fibres are positioned inside the bundle in a specific order. Fibres from the macular zone of the retina are in the central portion, and those from the temporal half of the retina take up the periphery part. A partial decussation or crossing occurs when these fibres are outside the eye cavity. The fibres from the nasal halves of each retina cross to the opposite halves and extend to the brain. Those from the temporal halves remain uncrossed. This partial crossover is called the optic chiasma, and the optic nerves past this point are called optic tracts, mainly to distinguish them from single-retinal nerves. The function of the partial crossover is to transmit the right-hand visual field produced by both eyes to the left-hand half of the brain only and vice versa. Therefore the information from the right half of the body, and the right visual field, is all transmitted to the left-hand part of the brain when reaches the posterior part of the fore-brain (diencephalon).

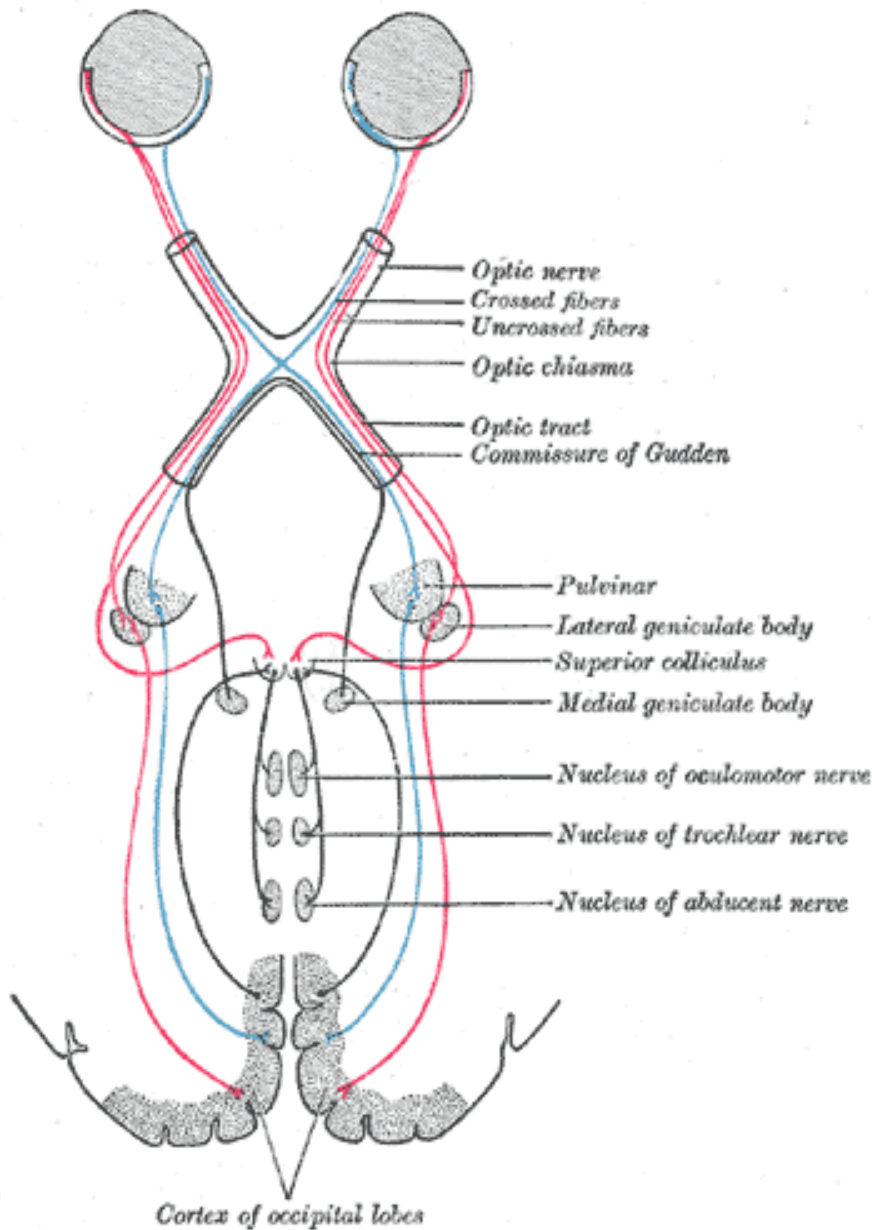


Figure 34 The pathway to the central cortex

The information relay between the fibers of optic tracts and the nerve cells occurs in the lateral geniculate bodies, the central part of the visual signal processing, located in the thalamus of the brain. From here the information is passed to the nerve cells in the occipital cortex of the corresponding side of the brain. Connections from the retina to the brain can be separated into a 'parvocellular pathway' and a "magnocellular pathway". The parvocellular pathways signals color and fine detail, whereas the magnocellular pathways detect fast moving stimuli.

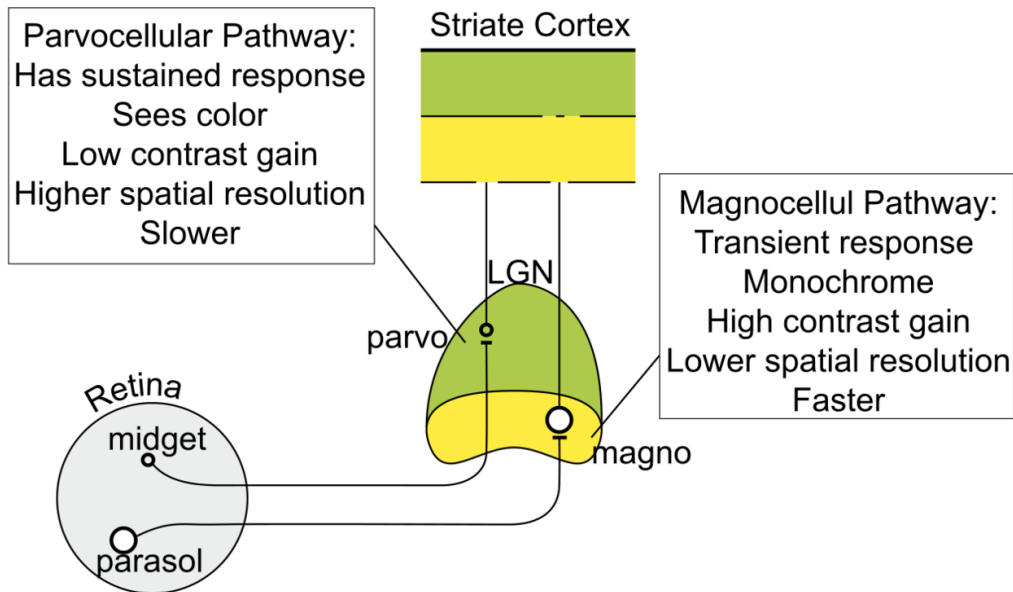


Figure 35 Connections from the retina to the brain can be separated into a "parvocellular pathway" and a "magnocellular pathway". The parvocellular pathway originates in midget cells in the retina, and signals color and fine detail; magnocellular pathway starts with parasol cells, and detects fast moving stimuli.

Signals from standard digital cameras correspond approximately to those of the parvocellular pathway. To simulate the responses of parvocellular pathways, researchers have been developing neuromorphic sensory systems, which try to mimic spike-based computation in neural systems. Thereby they use a scheme called "address-event representation" for the signal transmission in the neuromorphic electronic systems (Liu and Delbruck 2010 <http://www.ncbi.nlm.nih.gov/pubmed/20493680>).

Anatomically, the retinal Magno and Parvo ganglion cells respectively project to 2 ventral magnocellular layers and 4 dorsal parvocellular layers of the Lateral Geniculate Nucleus (LGN). Each of the six LGN layers receives inputs from either the ipsilateral or contralateral eye, i.e., the ganglion cells of the left eye cross over and project to layer 1, 4 and 6 of the right LGN, and the right eye ganglion cells project (uncrossed) to its layer 2, 3 and 5. From here the information from the right and left eye is separated.

Although human vision is combined by two halves of the retina and the signal is processed by the opposite cerebral hemispheres, the visual field is considered as a smooth and complete unit. Hence the two visual cortical areas are thought of as being intimately connected. This connection, called corpus callosum is made of neurons, axons and dendrites. Because the dendrites make synaptic connections to the related points of the hemispheres, electric stimulation of every point on one hemisphere indicates simulation of the interconnected point on the other hemisphere. The only exception to this rule is the primary visual cortex.

The synapses are made by the optic tract in the respective layers of the lateral geniculate body. Then these axons of these third-order nerve cells are passed up to the calcarine fissure in each occipital lobe of the cerebral cortex. Because bands of the white fibres and axons pair from the nerve cells in the retina go through it, it is called the striate cortex, which incidentally is our primary visual cortex, sometimes known as V1. At this point, impulses

from the separate eyes converge to common cortical neurons, which then enables complete input from both eyes in one region to be used for perception and comprehension. Pattern recognition is a very important function of this particular part of the brain, with lesions causing problems with visual recognition or blindsight.

Based on the ordered manner in which the optic tract fibres pass information to the lateral geniculate bodies and after that pass in to the striate area, if one single point stimulation on the retina was found, the response which produced electrically in both lateral geniculate body and the striate cortex will be found at a small region on the particular retinal spot. This is an obvious point-to-point way of signal processing. And if the whole retina is stimulated, the responses will occur on both lateral geniculate bodies and the striate cortex gray matter area. It is possible to map this brain region to the retinal fields, or more usually the visual fields.

Any further steps in this pathway is beyond the scope of this book. Rest assured that, many further levels and centres exist, focusing on particular specific tasks, like for example colour, orientations, spatial frequencies, emotions etc.

3.3.1 Cortical Processing - Visual Perception

Equipped with a firmer understanding of some of the more important concepts of the signal processing in the visual system, comprehension or perception of the processed sensory information is the last important piece in the puzzle. Visual perception is the process of translating information received by the eyes into an understanding of the external state of things. It makes us aware of the world around us and allows us to understand it better. Based on visual perception we learn patterns which we then apply later in life and we make decisions based on this and the obtained information. In other words, our survival depends on perception.

3.4 Retinal Implants

Since the late 20th century, restoring vision to blind people by means of artificial eye prostheses has been the goal of numerous research groups and some private companies around the world. Similar to cochlear implants, the key concept is to stimulate the visual nervous system with electric pulses, bypassing the damaged or degenerated photoreceptors on the human retina. In this chapter we will describe the basic functionality of a retinal implant, as well as the different approaches that are currently being investigated and developed. The two most common approaches to retinal implants are called “epiretinal” and “subretinal” implants, corresponding to eye prostheses located either on top or behind the retina respectively. We will not cover any non-retina related approaches to restoring vision, such as the BrainPort Vision System that aims at stimulating the tongue from visual input, cuff electrodes around the optic nerve, or stimulation implants in the primary visual cortex.

3.4.1 Retinal Structure and Functionality

Figure 1 depicts the schematic nervous structure of the human retina. We can differentiate between three layers of cells. The first, located furthest away from the eye lens, consists of the photoreceptors (rods and cones) whose purpose is to transduce incoming light into electrical signals that are then further propagated further to the intermediate layer, which is mainly composed of bipolar cells. These bipolar cells, which are connected to photoreceptors as well as cell types such as horizontal cells and amacrine cells, pass on the electrical signal to the retinal ganglion cells (RGC). For a detailed description on the functionality of bipolar cells, specifically with respect to their subdivision into ON- and OFF-bipolar cells, refer to chapter on Visual Systems. The uppermost layer, consisting of RGCs, collects the electric pulses from the horizontal cells and passes them on to the thalamus via the optic nerve. From there, signals are propagated to the primary visual cortex. There are some key aspects worthwhile mentioning about the signal processing within the human retina. First, while bipolar cells, as well as horizontal and amacrine, generate graded potentials, the RGCs generate action potentials instead. Further, the density of each cell type is not uniform across the retina. While there is an extremely high density of rods and cones in the area of the fovea, with in addition only very few photoreceptors connected to RGCs via the intermediate layer, a far lower density of photoreceptors is found in the peripheral areas of the retina with many photoreceptors connected to a single RGC. The latter also has direct implications on the receptive field of a RGC, as it tends to increase rapidly towards the outer regions of the retina, simply because of the lower photoreceptor density and the increased number of photoreceptors being connected to the same RGC.

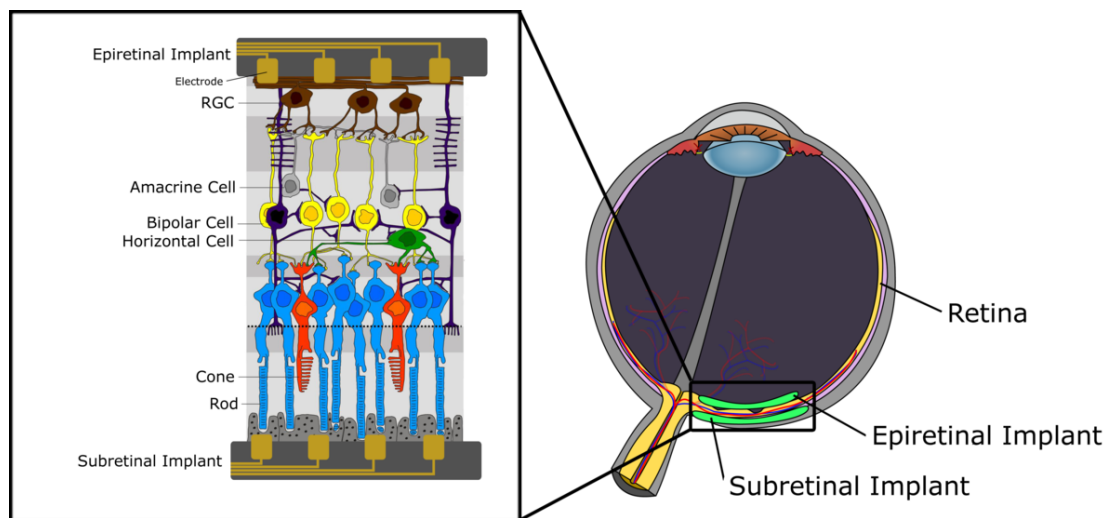


Figure 36 Schematic overview of the human eye and the location of retinal prostheses. Note the vertical layering of the retina tissue and the distances of the cell types to epiretinal and subretinal implants respectively.

3.4.2 Implant Use Case

Damage to the photoreceptor layer in the human can be caused by Retinitis pigmentosa, age-related macular degeneration and other diseases, eventually resulting in the affected person to become blind. However, the rest of the visual nervous system, both inside the retina as well as the visual nervous pathway in the brain, remains intact for several years after onset of blindness^{8 9}. This allows artificial stimulation of the remaining, still properly functioning retina cells, through electrodes, to restore visual information for the human patient. Thereby a retina prosthesis can be implanted either behind the retina, and is then referred to as subretinal implant. This brings the electrodes closest to the damaged photoreceptors and the still properly functioning bipolar cells, which are the real stimulation target here. (If the stimulation electrodes penetrate the choroid, which contains the blood supply of the retina, the implants are sometimes called "suprachoroidal" implants.) Or the implant may be put on top of the retina, closest to the Ganglion cell layer, aiming at stimulation of the RGCs instead. These implants are referred to as epiretinal implants. Both approaches are currently being investigated by several research groups. They both have significant advantages as well as drawbacks. Before we treat them in more detail separately, we describe some key challenges that need consideration in both cases.

3.4.3 Challenges

A big challenge for retinal implants comes from the extremely high spatial density of nervous cells in the human retina. There are roughly 125 million photoreceptors (rods and cones) and 1.5 million ganglion cells in the human retina, as opposed to approximately only 15000 hair cells in the human cochlea^{10 11}. In the fovea, where the highest visual acuity is achieved, as many as 150000 cones are located within one square millimeter. While there are much fewer RGCs in total compared to photoreceptors, their density in the foveal area is close to the density of cones, imposing a tremendous challenge in addressing the nervous cells in high enough spatial resolution with artificial electrodes. Virtually all current scientific experiments with retinal implants use micro-electrode arrays (MEAs) to stimulate the retina cells. High resolution MEAs achieve an inter-electrode spacing of roughly 50 micrometers, resulting in an electrode density of 400 electrodes per square millimeter. Therefore, a one to one association between electrodes and photoreceptors or RGCs respectively is impossible

-
- 8 Eberhart Zrenner, KarlUlrich Bartz-Schmidt, Heval Benav, Dorothea Besch, Anna Bruckmann, Veit-Peter Gabel, Florian Gekeler, Udo Greppmaier, Alex Harscher, Steffen Kibbel, Johannes Koch, Akos Kusnyerik, tobias Peters, Katarina Stingl, Helmut Sachs et al. . Subretinal electronic chips allow blind patients to read letters and combine them to words Subretinal electronic chips allow blind patients to read letters and combine them to words . , 2010
 - 9 Asaf Shoval, ChrisopherAdams, Moshe David-Pur, Mark Shein, Yael Hanein, Evelyne Sernagor . Carbon nanotube electrodes for effective interfacing with retinal tissue Carbon nanotube electrodes for effective interfacing with retinal tissue . , 2009
 - 10 Jost B. Jonas, UlrikeSchneider, Gottfried O.H. Naumann . Count and density of human retinal photoreceptors Count and density of human retinal photoreceptors . , (Springer) 1992
 - 11 Ashmore Jonathan . Cochlear Outer Hair Cell Motility Cochlear Outer Hair Cell Motility . , (American Physiological Society) 2008

in the foveal area with conventional electrode technology. However, spatial density of both photoreceptors as well as RGCs decrease quickly towards the outer regions of the retina, making one-to-one stimulation between electrodes and peripheral nerve cells more feasible¹². Another challenge is operating the electrodes within safe limits. Imposing charge densities above 0.1 mC/cm² may damage the nervous tissue¹³. Generally, the further a cell is away from the stimulating electrode, the larger is the current amplitude required for stimulation of the cell. Furthermore, the lower the stimulation threshold, the smaller the electrode may be designed and the compacter the electrodes may be placed on the MEAs, thereby enhancing the spatial stimulation resolution. Stimulation threshold is defined as the minimal stimulation strength necessary to trigger a nervous response in at least 50% of the stimulation pulses. For these reasons, a primary goal in designing retinal implants is to use as low a stimulation current as possible while still guaranteeing a reliable stimulation (i.e. generation of an action potential in the case of RGCs) of the target cell. This can either be achieved by placing the electrode as close as possible to the area of the target cell that reacts most sensitive to an applied electric field pulse or by making the cell projections, i.e. dendrites and/or axons, grow on top the electrode, allowing a stimulation of the cell with very low currents even if the cell body is located far away. Further, an implant fixed to the retina automatically follows the movements of the eyeball. While this entails some significant benefits, it also means that any connection to the implant - for adjusting parameters, reading out data, or providing external power for the stimulation - requires a cable that moves with the implant. As we move our eyes approximately three times a second, this exposes the cable and involved connections to severe mechanical stress. For a device that should remain functioning for an entire life time without external intervention, this imposes a severe challenge on the materials and technologies involved.

3.4.4 Subretinal Implants

As the name already suggest, subretinal implants are visual prosthesis located behind the retina. Therefore, the implant is located closest to the damaged photoreceptors, aiming at bypassing the rods and cones and stimulating the bipolar cells in the next nervous layer in the retina. The main advantage of this approach lies in relatively little visual signal processing that takes place between the photoreceptors and the bipolar cells that need to be imitated by the implant. That is, raw visual information, for example captured by a video camera, may be forwarded directly, or with only relatively rudimentary signal processing respectively, to the MEA stimulating the bipolar cells, rendering the procedure rather simple from a signal processing point of view. However, also this approach has some severe disadvantages. The high spatial resolution of photoreceptors in the human retina imposes a big challenge in

12 Chris Sekirnjak, PawelHottowy, Alexander Sher, Wladyslaw Dabrowski, Alan M. Litke, E.J. Chichilnisky . High-Resolution Electrical Stimulation of Primate Retina for Epiretinal Implant Design High-Resolution Electrical Stimulation of Primate Retina for Epiretinal Implant Design . , (Society of Neuroscience) 2008

13 Chris Sekirnjak, PawelHottowy, Alexander Sher, Wladyslaw Dabrowski, Alan M. Litke, E.J. Chichilnisky . High-Resolution Electrical Stimulation of Primate Retina for Epiretinal Implant Design High-Resolution Electrical Stimulation of Primate Retina for Epiretinal Implant Design . , (Society of Neuroscience) 2008

developing and designing a MEA with sufficiently high stimulation resolution and therefore low inter-electrode spacing. Furthermore, the stacking of the nervous layers in z-direction (with the x-y plane tangential to the retina curvature) adds another difficulty when it comes to placing the electrodes close to the bipolar cells. With the MAE located behind the retina, there is a significant spatial gap between the electrodes and the target cells that needs to be overcome. As mentioned above, an increased electrode to target cell distance forces the MAE to operate with higher currents, enlarging the electrode size, the number of cells within the stimulation range of a single electrode and the spatial separation between adjacent electrodes. All of this results in a decreased stimulation resolution as well as opposing the retina to the risk of tissue damage caused by too high charge densities. As shown below, one way to overcome large distances between electrodes and the target cells is to make the cells grow their projections over longer distances directly on top the electrode.

In late 2010, a German research group in collaboration with the private German company “Retina Implant AG”, published results from studies involving tests with subretinal implants in human subjects ¹⁴. A three by three millimeter microphotodiode array (MPDA) containing 1500 pixels, which each pixel consisting of an individual light-sensing photodiodes and an electrode, was implanted behind the retina of three patients suffering from blindness due to macular degeneration. The pixels were located approximately 70 micrometer apart each other, yielding a spatial resolution of roughly 160 electrodes per square millimeter – or, as indicated by the authors of the paper, a visual cone angle of 15 arcmin for each electrode. It should be noted, that, in contrast to implants using external video cameras to generate visual input, each pixel of the MPDA itself contains a light-sensitive photodiode, autonomously generating the electric current from the light received through the eyeball for its own associated electrode. So each MPDA pixel corresponds in its full functionality to a photoreceptor cell. This has a major advantage: Since the MPDA is fixed behind the human retina, it automatically drags along when the eyeball is being moved. And since the MPDA itself receives the visual input to generate the electric currents for the stimulation electrodes, movements of the head or the eyeball are handled naturally and need no artificial processing. In one of the patients, the MPDA was placed directly beneath the macula, leading to superior results in experimental tests as opposed to the other two patients, whose MPDA was implanted further away from the center of the retina. The results achieved by the patient with the implant behind the macula were quite extraordinary. He was able to recognize letters (5-8cm large) and read words as well as distinguish black-white patterns with different orientations ¹⁵.

The experimental results with the MPDA implants have also drawn attention to another visual phenomenon, revealing an additional advantage of the MPDA approach over implants

14 Eberhart Zrenner, KarlUlrich Bartz-Schmidt, Heval Benav, Dorothea Besch, Anna Bruckmann, Veit-Peter Gabel, Florian Gekeler, Udo Greppmaier, Alex Harscher, Steffen Kibbel, Johannes Koch, Akos Kusnyerik, tobias Peters, Katarina Stingl, Helmut Sachs et al. . Subretinal electronic chips allow blind patients to read letters and combine them to words Subretinal electronic chips allow blind patients to read letters and combine them to words . , 2010

15 Eberhart Zrenner, KarlUlrich Bartz-Schmidt, Heval Benav, Dorothea Besch, Anna Bruckmann, Veit-Peter Gabel, Florian Gekeler, Udo Greppmaier, Alex Harscher, Steffen Kibbel, Johannes Koch, Akos Kusnyerik, tobias Peters, Katarina Stingl, Helmut Sachs et al. . Subretinal electronic chips allow blind patients to read letters and combine them to words Subretinal electronic chips allow blind patients to read letters and combine them to words . , 2010

using external imaging devices: Subsequent stimulation of retinal cells quickly leads to decreased responses, suggesting that retinal neurons become inhibited after being stimulated repeatedly within a short period of time. This entails that a visual input projected onto a MEA fixed on or behind the retina will result in a sensed image that quickly fades away, even though the electric stimulation of the electrodes remains constant. This is due to the fixed electrodes on the retina stimulating the same cells on the retina all the time, rendering the cells less and less sensitive to a constant stimulus over time. However, the process is reversible, and the cells regain their initial sensitivity once the stimulus is absent again. So, how does an intact visionary system handle this effect? Why are healthy humans able to fix an object over time without it fading out? As mentioned in ¹⁶, the human eye actually continuously adjusts in small, unnoticeable eye movements, resulting in the same visual stimulus to be projected onto slightly different retinal spots over time, even as we tend to focus and fix the eye on some target object. This successfully circumvents the fading cell response phenomenon. With the implant serving both as photoreceptor and electrode stimulator, as it is the case with the MPDA, the natural small eye adjustments can be readily used to handle this effect in a straight forward way. Other implant approaches using external visual input (i.e. from video cameras) will suffer from their projected images fading away if stimulated continuously. Fast, artificial jittering of the camera images may not solve the problem as this external movement may not be in accordance with the eye movement and therefore, the visual cortex may interpret this simply as a wiggly or blurry scene instead of the desired steady long term projection of the fixed image. A further advantage of subretinal implants is the precise correlation between stimulated areas on the retina and perceived location of the stimulus in the visual field of the human subject. In contrast to RGCs, whose location on the retina may not directly correspond to the location of their individual receptive fields, the stimulation of a bipolar cell is perceived exactly at that point in the visual field that corresponds to the geometric location on the retina where that bipolar cell resides. A clear disadvantage of subretinal implants is the invasive surgical procedure involved.

3.4.5 Epiretinal Implants

Epiretinal implants are located on top of the retina and therefore closest to the retina ganglion cells (RGCs). For that reason, epiretinal implants aim at stimulating the RGCs directly, bypassing not only the damaged photoreceptors, but also any intermediate neural visual processing by the bipolar, horizontal and amacrine cells. This has some advantages: First of all, the surgical procedure for an epiretinal implant is far less critical than for a subretinal implant, since the prosthesis need not be implanted from behind the eye. Also, there are much fewer RGCs than photoreceptors or bipolar cells, allowing a more course grained stimulation with increased inter-electrode distance (at least in the peripheral regions of the retina), or an electrode density even superior to that of the actual RGC density, allowing for more flexibility and accuracy when stimulating the cells. A study on the epiretinal stimulation of peripheral parasol cells conducted on macaque retina provides quantitative details ¹⁷. Parasol cells are one type of RGCs forming the secondmost dense

¹⁶ Pritchard Roy . Stabilized Images on the Retina Stabilized Images on the Retina . ,

¹⁷ Chris Sekirnjak, PawelHottowy, Alexander Sher, Wladyslaw Dabrowski, Alan M. Litke, E.J. Chichilnisky . High-Resolution Electrical Stimulation of Primate Retina for Epiretinal Implant Design High-Resolution

visual pathway in the retina. Their main purpose is to encode the movement of objects in the visual field, thus sensing motion. The experiments were performed in vitro by placing the macaque retina tissue on a 61 electrode MEA (60 micrometer inter-electrode spacing). 25 individual parasol cells were indentified and stimulated electronically while properties such as stimulation threshold and best stimulation location were analyzed. The threshold current was defined as the lowest current that triggered a spike on the target cell in 50% of the stimulus pulses (pulse duration: 50 milliseconds) and was determined by incrementally increasing the stimulation strength until sufficient spiking response was registered. Please note two aspects: First, parasol cells as RGCs exhibit action potential behavior, as opposed to bipolar cells which work with graded potentials. Second, the electrodes on the MAE were both used for the stimulation pulses as well as for recording the spiking response from the target cells. 25 parasol cells were located on the 61 electrode MAE with a electrode density significantly higher than the parasol cell density, effectively yielding multiple electrodes within the receptive fields of a single parasol cell. In addition to measuring the stimulation thresholds necessary to trigger a reliable cell response, also the location of best stimulation was determined. The location of best stimulation refers to the location of the stimulating electrode with respect to the target cell where the lowest stimulation threshold was achieved. Surprisingly, this was found out to not be on the cell soma, as one would expect, but roughly 13 micrometers further down the axon path. From there on, the experiments showed the expected quadratic increase in stimulation threshold currents with respect to increasing electrode to soma distance. The study results also showed that all stimulation thresholds were well below the safety limits (around 0.05mC/cm², as opposed to 0.1mC/cm² being a (low) safety limit) and that the cell response to a stimulation pulse was fast (0.2 ms latency on average) and precise (small variance on latency). Further, the superior electrode density over parasol cell density allowed a reliable addressing of individual cells by the stimulation of the appropriate electrode, while preventing neighboring cells from also evoking a spike.

3.4.6 Overview of Alternative Technical Approaches

In this section, we give a short overview over some alternative approaches and technologies currently being under research.

Nanotube Electrode

Classic MAEs contain electrodes made out of titanium nitride or indium tin oxide exposing the implant to severe issues with long-term biocompatibility¹⁸. A promising alternative to metallic electrodes consists of carbon nanotubes (CNT) which combine a number of very advantageous properties. First, they are fully bio compatible since they are made from pure carbon. Second, their robustness makes them suited for long term implantation, a

Electrical Stimulation of Primate Retina for Epiretinal Implant Design . . , (Society of Neuroscience) 2008

18 Asaf Shoval, ChrisopherAdams, Moshe David-Pur, Mark Shein, Yael Hanein, Evelyne Sernagor . Carbon nanotube electrodes for effective interfacing with retinal tissue Carbon nanotube electrodes for effective interfacing with retinal tissue . . , 2009

key property for visual prosthesis. Further, the good electric conductivity allows them to operate as electrodes. And finally, their very porous nature leads to extremely large contact surfaces, encouraging the neurons to grow on top the CNTs, thus improving the neuron to electrode contact and lowering the stimulation currents necessary to elicit a cell response. However, CNT electrodes have only emerged recently and at this point only few scientific results are available.

Wireless Implant Approaches

One of the main technical challenges with retinal implant relates to the cabling that connects the MEA with the external stimuli, the power supply as well as the control signals. The mechanical stress on the cabling affects its long term stability and durability, imposing a big challenge on the materials used. Wireless technologies could be a way to circumvent any cabling between the actual retinal implant and external devices. The energy of the incoming light through the eye is not sufficient to trigger neural responses. Therefore, to make a wireless implant work, extra power must be provided to the implant. An approach presented by the Stanford School of Medecine uses an infrared LCD display to project the scene captured by a video camera onto goggles, reflecting infrared pulses onto the chip located on the retina. The chip also uses a photovoltaic rechargeable battery to provide the power required to transfer the IR light into sufficiently strong stimulation pulses. Similar to the subretinal approach, this also allows the eye to naturally fix and focus onto objects in the scene, as the eye is free to move, allowing different parts of the IR image on the goggles to be projected onto different areas on the chip located on the retina. Instead of using infrared light, inductive coils can also be used to transmit electrical power and data signals from external devices to the implant on the retina. This technology has been successfully implemented and tested in the EPIRET3 retinal implant ¹⁹. However, those tests were more a proof-of-concept, as only the patient's ability to sense a visual signal upon applying a stimulus on the electrodes was tested.

Directed Neural Growth

One way to allow a very precise neural stimulation with extremely low currents and even over longer distances is to make the neurons grow their projections onto the electrode. By applying the right chemical solution onto the retinal tissue, neural growth can be encouraged. This can be achieved by applying a layer of Laminin onto the MEA's surface. In order to control the neural paths, the Laminin is not applied uniformly across the MEA surface, but in narrow paths forming a pattern corresponding to the connections, the neurons should form. This process of applying the Laminin in a precise, pattered way, is called "microcontact printing". A picture of what these Lamini paths look like is shown in Figure 5. The successful directed neural growth achieved with this method allowed applying significantly lower stimulation currents compared to classic electrode stimulation while still able to reliably

19 Susanne Klauke, Michael Goertz, Stefan Rein, Dirk Hoehl, Uwe Thomas, Reinhard Eckhorn, Frank Bremmer, Thomas Wachtler . Stimulation with a Wireless Intraocular Epiretinal Implant Elicits Visual Percepts in Blind Humans Stimulation with a Wireless Intraocular Epiretinal Implant Elicits Visual Percepts in Blind Humans . , (The Association for Research in Vision and Ophthalmology) 2011

trigger neural response²⁰. Furthermore, the stimulation threshold no longer follows the quadratic increase with respect to electrode-soma distance, but remains constant at the same low level even for longer distances (>200 micrometer).

3.5 Other Visual Implants

In addition to the stimulation of the retina, also other elements of the visual system can be stimulated

3.5.1 Stimulation of the Optic Nerve

With cuff-electrodes, typically with only a few segments.

Advantages:

- Little trauma to the eye.

Challenges:

- Not very specific.

20 Neville Z. Mehenti, GrehS. Tsien, Theodore Leng, Harvey A. Fishman, Stacey F. Bent . A model retinal interface based on directed neuronal growth for single cell stimulation A model retinal interface based on directed neuronal growth for single cell stimulation . , (Springer) 2006

3.5.2 Cortical Implants

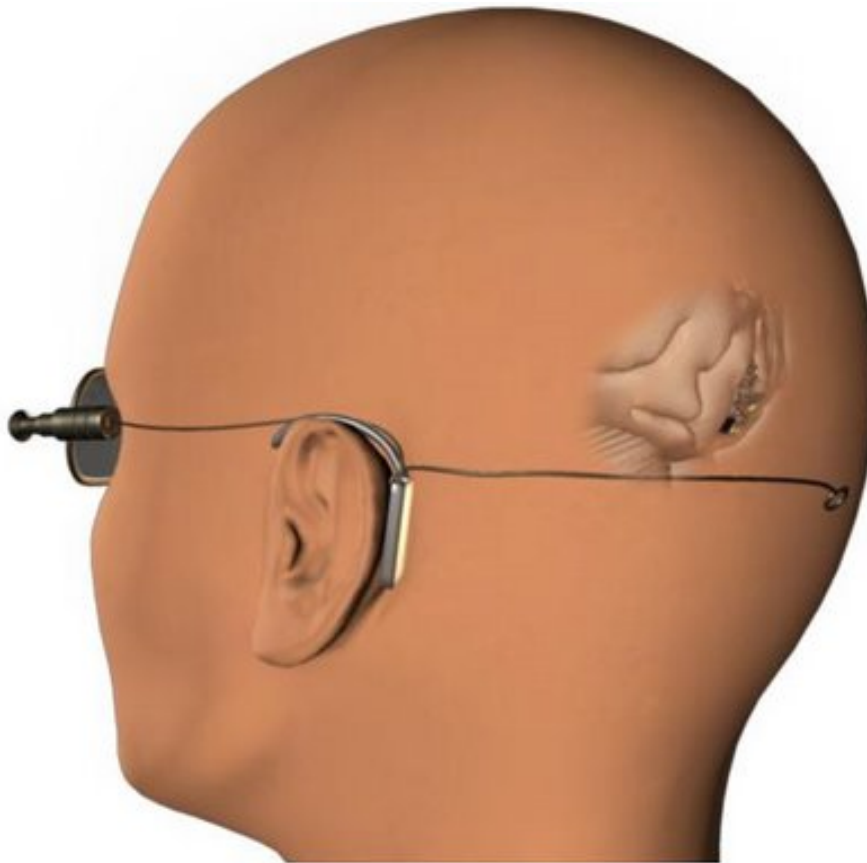


Figure 37 The Visual Cortical Implant

Dr. Mohamad Sawan²¹, Professor and Researcher at Polystim neurotechnologies Laboratory²² at the Ecole Polytechnique de Montreal, has been working on a visual prosthesis to be implanted into the human cortex. The basic principle of Dr. Sawan's technology consists in stimulating the visual cortex by implanting a silicon microchip on a network of electrodes made of biocompatible materials and in which each electrode injects a stimulating electrical current in order to provoke a series of luminous points to appear (an array of pixels) in the field of vision of the sightless person. This system is composed of two distinct parts: the implant and an external controller. The implant lodged in the visual cortex wirelessly receives dedicated data and energy from the external controller. This implantable part contains all the circuits necessary to generate the electrical stimuli and to oversee the changing microelectrode/biological tissue interface. On the other hand, the battery-operated outer control comprises a micro-camera which captures the image as well as a processor and a command generator which process the imaging data to select and translate the captured images and to generate and manage the electrical stimulation process and oversee the implant. The external controller and the implant exchange data in both directions by a

²¹ <http://www.polymtl.ca/recherche/rc/en/professeurs/details.php?NoProf=108/>

²² <http://www.polystim.ca/>

powerful transcutaneous radio frequency (RF) link. The implant is powered the same way. (Wikipedia http://en.wikipedia.org/wiki/Visual_prosthesis)

Advantages:

- Much larger area for stimulation: 2° radius of the central retinal visual field correspond to 1 mm^2 on the retina, but to 2100 mm^2 in the visual cortex.

Challenges:

- Implantation is more invasive.
- Parts of the visual field lie in a sulcus and are very hard to reach.
- Stimulation can trigger seizures.

23

3.6 Computer Simulation of the Visual System

In this section an overview in the simulation of processing done by the early levels of the visual system will be given. The implementation to reproduce the action of the visual system will thereby be done with MATLAB²⁴ and its toolboxes. The processing done by the early visual system was discussed in the section before and can be put together with some of the functions they perform in the following schematic overview. A good description of the image processing can be found in (Cormack 2000).

Schematic overview of the processing done by the early visual system Structure

Operations

2D Fourier Plane

World

$$I(x, y, t, \lambda)$$

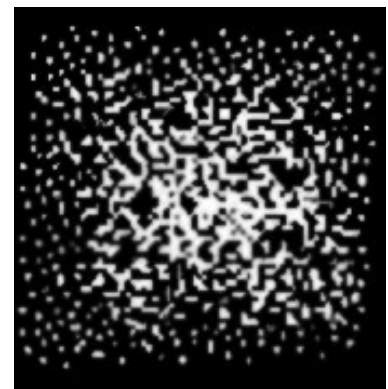


Figure 38

Optics
Photoreceptor Array

Low-pass spatial filtering
Sampling, more low-pass filtering, temporal lowhand-pass filtering, λ filtering, gain control, response compression



Figure 39

²³ <http://en.wikibooks.org/wiki/Category%3A>

²⁴ <http://en.wikibooks.org/wiki/MATLAB>

Schematic overview of the processing done by the early visual system Structure

Operations

2D Fourier Plane

LGN Cells

Spatiotemporal bandpass filtering, λ filtering, multiple parallel representations



Figure 40

Primary Visual Cortical Neurons: Simple & Complex

Simple cells: orientation, phase, motion, binocular disparity, & λ filtering
 Complex cells: no phase filtering (contrast energy detection)

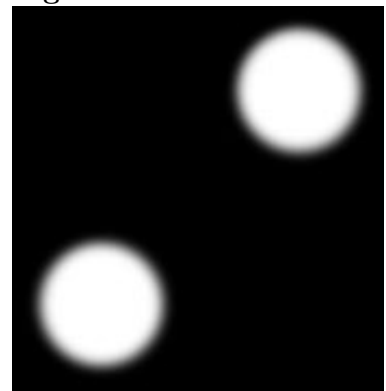


Figure 41

On the left, are some of the major structures to be discussed; in the middle, are some of the major operations done at the associated structure; in the right, are the 2-D Fourier representations of the world, retinal image, and sensitivities typical of a ganglion and cortical cell. (From Handbook of Image and Video Processing, A. Bovik)

As we can see in the above overview different stages of the image processing have to be considered to simulate the response of the visual system to a stimulus. The next section will therefore give a brief discussion in Image Processing. But first of all we will be concerned with the Simulation of Sensory Organ Components.

3.6.1 Simulating Sensory Organ Components

Anatomical Parameters of the Eye

The average eye has an anterior corneal radius of curvature of $r_C = 7.8$ mm, and an aqueous refractive index of 1.336. The length of the eye is $L_E = 24.2$ mm. The iris is approximately flat, and the edge of the iris (also called limbus) has a radius $r_L = 5.86$ mm.

Optics of the Eyeball

The optics of the eyeball are characterized by its 2-D spatial impulse response function, the Point Spread Function (PSF²⁵)

$$h(r) = 0.95 \cdot \exp(-2.6 \cdot |r|^{1.36}) + 0.05 \cdot \exp(-2.4 \cdot |r|^{1.74}),$$

in which r is the radial distance in minutes of arc from the center of the image.

Practical implementation

Obviously, the effect on a given digital image depends on the distance of that image from your eyes. As a simple place-holder, substitute this filter with a Gaussian filter with height 30, and with a standard deviation of 1.5.

In one dimension, a Gaussian is described by

$$g(x) = a \cdot \exp\left(-\frac{x^2}{2\sigma^2}\right).$$

Activity of Ganglion Cells

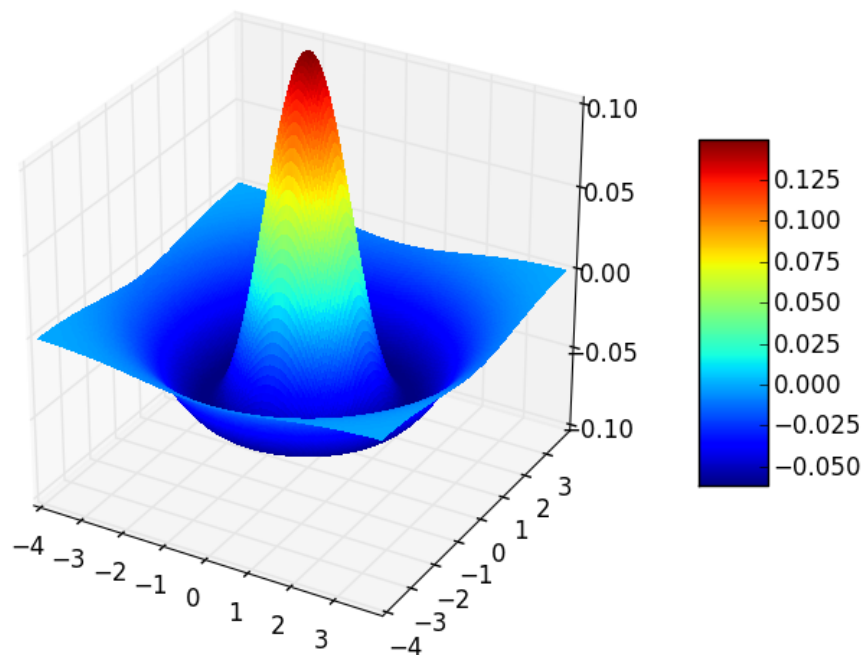


Figure 42 Mexican Hat function, with $\text{sigma1:sigma2} = 1:1.6$

²⁵ http://en.wikipedia.org/wiki/Point_spread_function

Ignoring the

- temporal response
- effect of wavelength (especially for the cones)
- opening of the iris
- sampling and distribution of photo receptors
- bleaching of the photo-pigment

we can approximate the response of ganglion cells with a **Difference of Gaussians** (DOG, Wikipedia http://en.wikipedia.org/wiki/Difference_of_gaussians)

$$f(x; \sigma) = \frac{1}{\sigma_1 \sqrt{2\pi}} \exp\left(-\frac{x^2}{2\sigma_1^2}\right) - \frac{1}{\sigma_2 \sqrt{2\pi}} \exp\left(-\frac{x^2}{2\sigma_2^2}\right).$$

The source code for a Python implementation is available under ²⁶.

The values of σ_1 and σ_2 have a ratio of approximately 1:1.6, but vary as a function of eccentricity. For midget cells (or P-cells), the Receptive Field Size (RFS) is approximately $RFS \approx 2 \cdot \text{Eccentricity}$,

where the RFS is given in arcmin, and the Eccentricity in mm distance from the center of the fovea (Cormack 2000).

Activity of simple cells in the primary visual cortex (V1)

Again ignoring temporal properties, the activity of simple cells in the primary visual cortex (V1) can be modeled with the use of Gabor filters (Wikipedia http://en.wikipedia.org/wiki/Gabor_filter). A Gabor filter is a linear filter whose impulse response is defined by a harmonic function (sinusoid) multiplied by a Gaussian function. The Gaussian function causes the amplitude of the harmonic function to diminish away from the origin, but near the origin, the properties of the harmonic function dominate

$$g(x, y; \lambda, \theta, \psi, \sigma, \gamma) = \exp\left(-\frac{x'^2 + \gamma^2 y'^2}{2\sigma^2}\right) \cos\left(2\pi \frac{x'}{\lambda} + \psi\right),$$

where

$$x' = x \cos \theta + y \sin \theta,$$

and

$$y' = -x \sin \theta + y \cos \theta.$$

In this equation, λ represents the wavelength of the cosine factor, θ represents the orientation of the normal to the parallel stripes of a Gabor function (Wikipedia http://en.wikipedia.org/wiki/Gabor_function), ψ is the phase offset, σ is the sigma of the Gaussian envelope

²⁶ Mexican Hat Function [Python] ²⁷. . Retrieved

and γ is the spatial aspect ratio, and specifies the ellipticity of the support of the Gabor function.

Gabor-like functions arise naturally, simply from the statistics of everyday scenes²⁸. An example how even the statistics of a simple image can lead to the emergence of Gabor-like receptive fields, written in Python, is presented in²⁹; and a (Python-)demonstration of the effects of filtering an image with Gabor-functions can be found at³¹.

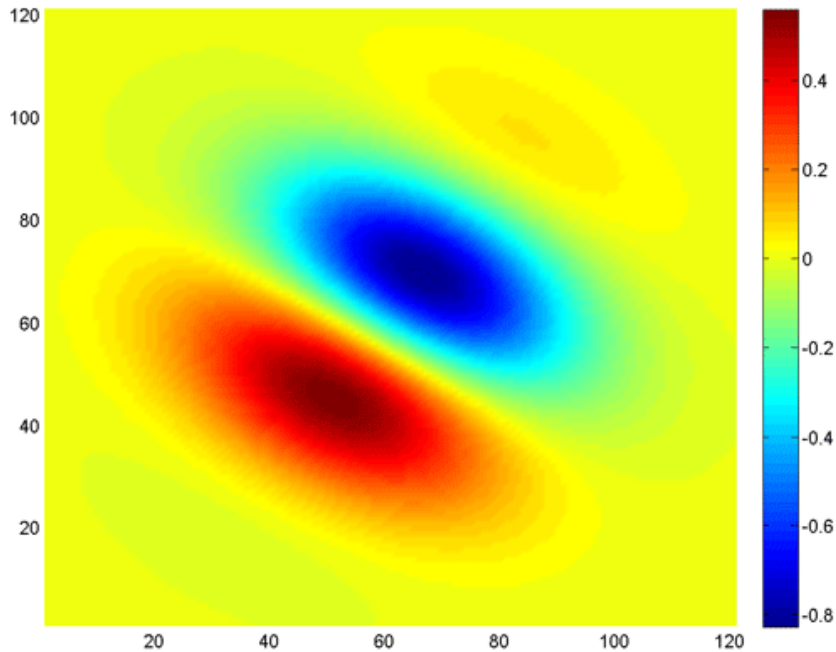


Figure 43 Gabor function, with $\sigma = 1$, $\theta = 1$, $\lambda = 4$, $\psi = 2$, $\gamma = 1$

This is an example implementation in MATLAB³³:

```
function gb = gabor_fn(sigma,theta,lambda,psi,gamma)

    sigma_x = sigma;
    sigma_y = sigma/gamma;

    % Bounding box
    nstds = 3;
    xmax =
    max(abs(nstds*sigma_x*cos(theta)),abs(nstds*sigma_y*sin(theta)));
```

28 Olshausen,B.A. and Field,D.J. . Emergence of simple-cell receptive field properties by learning a sparse code for natural images Emergence of simple-cell receptive field properties by learning a sparse code for natural images . *Nature* , **381** : 607-609 1996

29 Emergence of Gabor-like functions from a SimpleImage [Python]³⁰. . Retrieved

31 Demo-application of Gabor filters to an image [Python]³². . Retrieved

33 <http://en.wikibooks.org/wiki/MATLAB>

```

xmax = ceil(max(1,xmax));
ymax =
max(abs(nstds*sigma_x*sin(theta)),abs(nstds*sigma_y*cos(theta)));
ymax = ceil(max(1,ymax));
xmin = -xmax;
ymin = -ymax;
[x,y] = meshgrid(xmin:0.05:xmax,ymin:0.05:ymax);

% Rotation
x_theta = x*cos(theta) + y*sin(theta);
y_theta = -x*sin(theta) + y*cos(theta);

gb = exp(-.5*(x_theta.^2/sigma_x^2+y_theta.^2/sigma_y^2)).*
cos(2*pi/lambda*x_theta+psi);

end

```

And an equivalent Python implementation would be:

```

import numpy as np
import matplotlib.pyplot as mp

def gabor_fn(sigma = 1, theta = 1, g_lambda = 4, psi = 2, gamma = 1):
    # Calculates the Gabor function with the given parameters

    sigma_x = sigma
    sigma_y = sigma/gamma

    # Boundingbox:
    nstds = 3
    xmax = max( abs(nstds*sigma_x * np.cos(theta)), abs(nstds*sigma_y
* np.sin(theta)) )
    ymax = max( abs(nstds*sigma_x * np.sin(theta)), abs(nstds*sigma_y
* np.cos(theta)) )

    xmax = np.ceil(max(1,xmax))
    ymax = np.ceil(max(1,ymax))

    xmin = -xmax
    ymin = -ymax

    numPts = 201
    (x,y) = np.meshgrid(np.linspace(xmin, xmax, numPts),
np.linspace(ymin, ymax, numPts) )

    # Rotation
    x_theta = x * np.cos(theta) + y * np.sin(theta)
    y_theta = -x * np.sin(theta) + y * np.cos(theta)
    gb = np.exp( -0.5* (x_theta**2/sigma_x**2 +
y_theta**2/sigma_y**2) ) * \
        np.cos( 2*np.pi/g_lambda*x_theta + psi )

    return gb

if __name__ == '__main__':
    # Main function: calculate Gabor function for default parameters
    and show it
    gaborValues = gabor_fn()
    mp.imshow(gaborValues)
    mp.colorbar()
    mp.show()

```

3.6.2 Image Processing

One major technical tool to understand is the way a computer handles images. We have to know how we can edit images and what techniques we have to rearrange images.

Image Representation

Grayscale

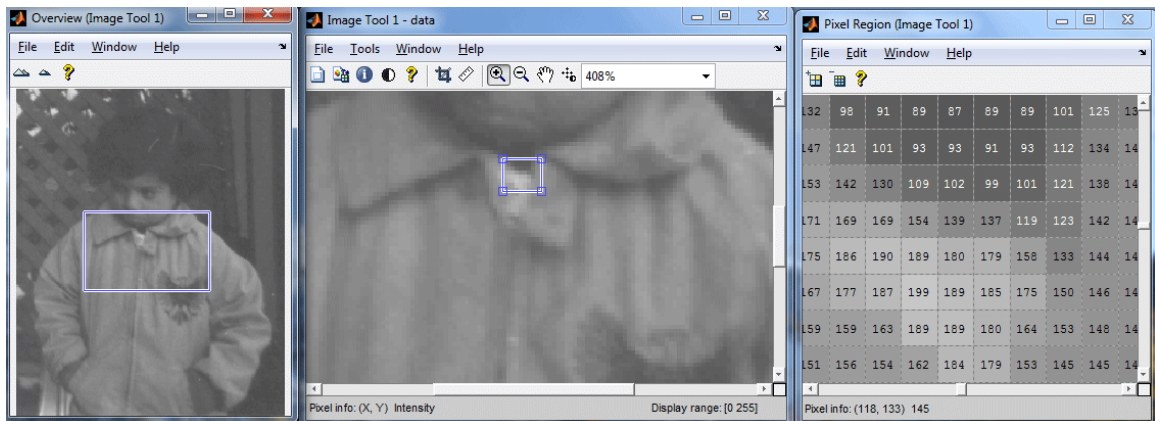


Figure 44 Representation of graylevel images.

For a computer an image is nothing more than a huge amount of little squares. These squares are called "pixel". In a grayscale image, each of this pixel carries a number n , often it holds $0 \leq n \leq 255$. This number n , represents the exactly color of this square in the image. This means, in a grayscale image we can use 256 different grayscales, where 255 means a white spot, and 0 means the square is black. To be honest, we could even use more than 256 different levels of gray. In the mentioned way, every pixels uses exactly 1 byte (or 8 bit) of memory to be saved. (Due to the binary system of a computer it holds: $2^8=256$) If you think it is necessary to have more different gray scales in your image, this is not a problem. You just can use more memory to save the picture. But just remember, this could be a hard task for huge images. Further quite often you have the problem that your sensing device (e.g. your monitor) can not show more than this 256 different gray colors.

Colour

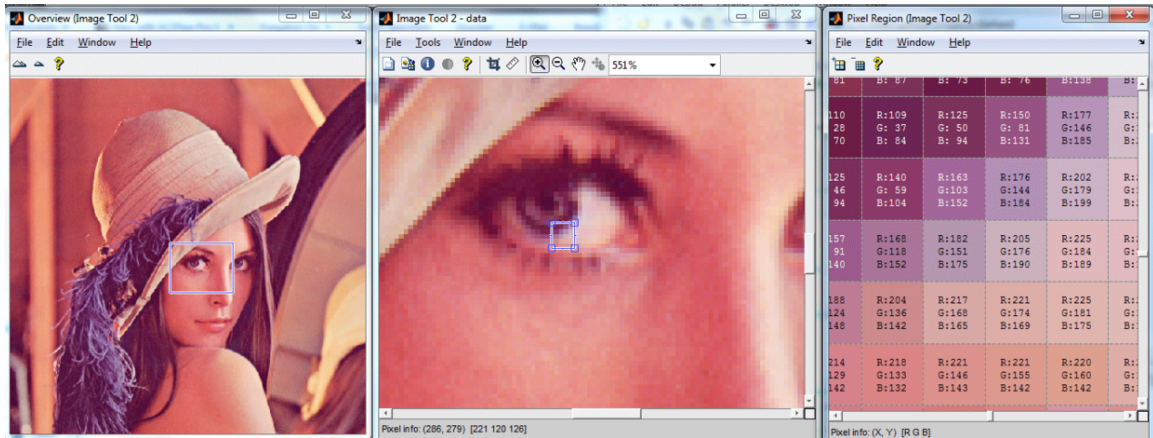


Figure 45 Image represented with RGB-notation

Representing a colourful image is only slightly more complicated than the grayscale picture. All you have to know is that the computer works with an additive colour mixture of the three main colors **Red**, **Green** and **Blue**. These are the so-called RGB colours.

Also these images are saved by pixels. But now every pixel has to know 3 values between 0 and 256, for every Color 1 value. So now we have $256^3 = 16,777,216$ different colours which can be represented. Similar to the grayscale images also here holds, that no color means black, and having all color means white. That means, the colour (0,0,0) is black, whereas (0,0,255) means blue and (255,255,255) is white.

Orientation

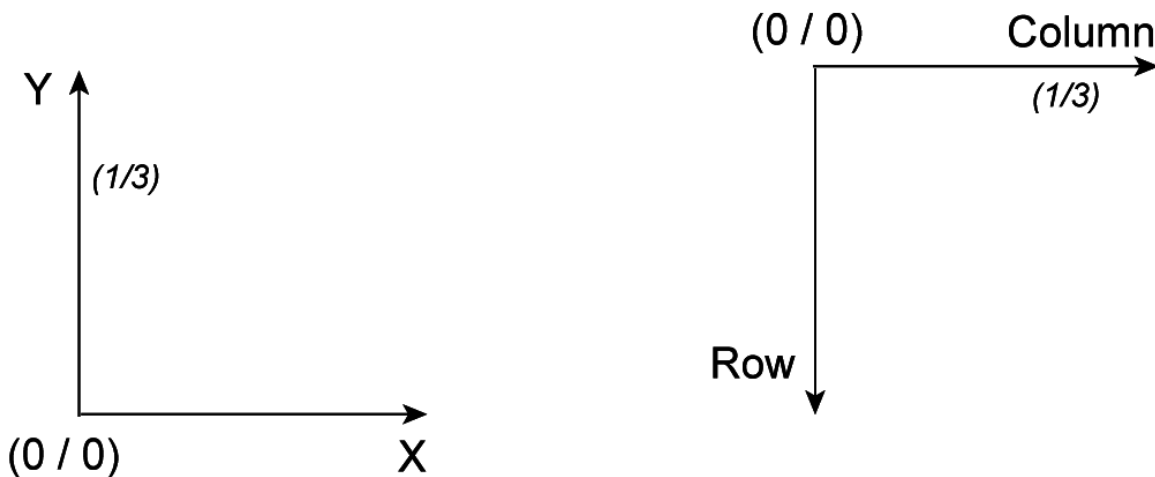


Figure 46

WARNING - There are two common, but different ways to describe the location of a point in 2 dimensions: 1) The x/y notation, with x typically pointing to the left 2) The row/column orientation Carefully watch out which coordinates you are using to describe your data, as the two descriptions are not consistent!

Image Filtering

1D Filter

In many technical applications, we find some primitive basis in which we easily can describe features. In 1 dimensional cases filters are not a big deal, therefore we can use this filters for changing images. The so called "Savitzky- Golay Filter" allows to smooth incoming signals. The filter was described in 1964 by Abraham Savitzky and Marcel J. E. Golay. It is a impulse-respond filter (IR).

For better understanding, lets look at a example. In 1d we usually deal with vectors. One such given vector, we call x and it holds: $x = (x_1, x_2, \dots, x_n)$ with $n \in \mathbb{N}$. Our purpose is to smooth that vector x . To do so all we need is another vector $(w) = (w_1, w_2, \dots, w_m)$ with $n > m \in \mathbb{N}$, this vector we call a weight vector.

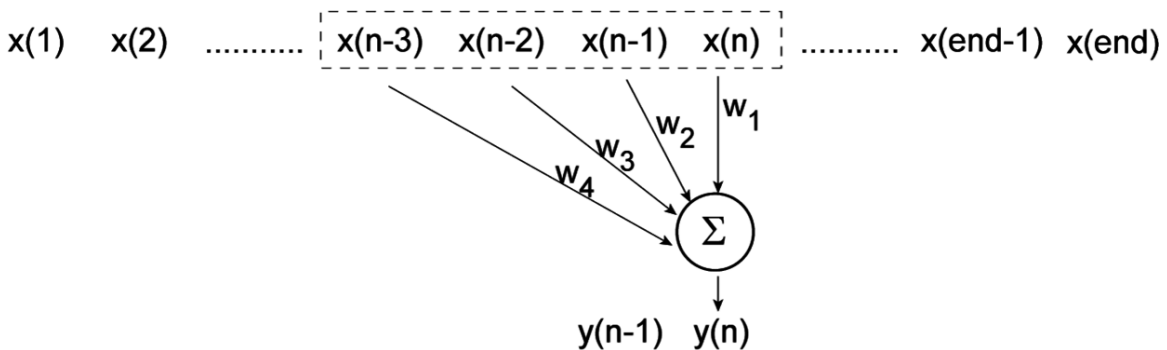


Figure 47

With $y(k) = \sum_{i=1}^m w(i)x(k - m + i)$ we now have a smoothed vector y . This vector is smoother than the vector before, because we only save the average over a few entries in the vector. These means the newly found vectorentries, depends on some entries right left and right of the entry to smooth. One major drawback of this approach is, the newly found vector y only has $n-m$ entries instead of n as the original vector x .

Drawing this new vector would lead to the same function as before, just with less amplitude. So no data is lost, but we have less fluctuation.

2D Filter

Going from the 1d case to the 2d case is done by simply make out of vectors matrices. As already mentioned, a gray-level image is for a computer or for a softwaretool as MATLAB nothing more, than a huge matrix filled with natural numbers, often between 0 and 255.

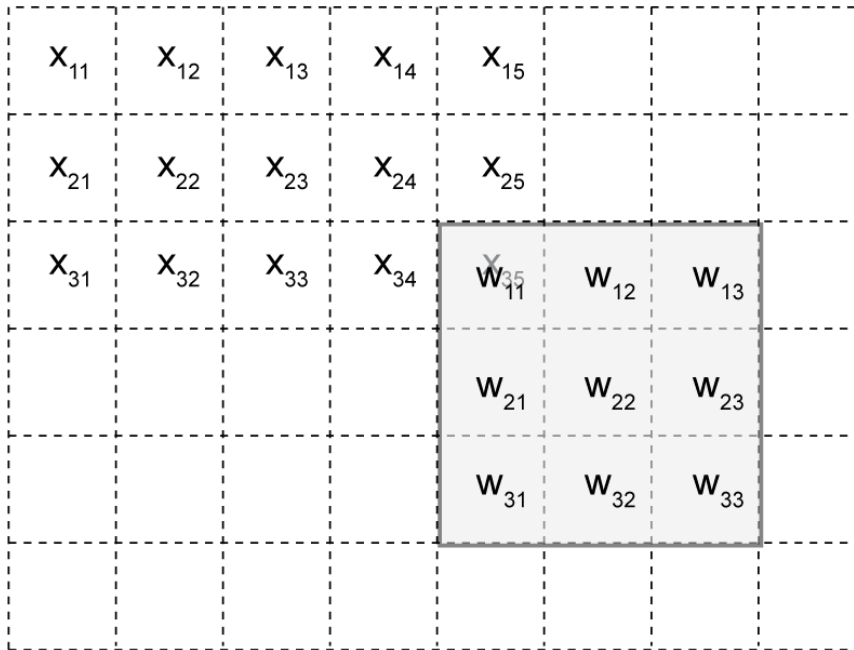


Figure 48

The weight vector is now a weight-matrix. But still we use the filter by adding up different matrix-element-multiplications. $y(n, m) = \sum_{i=1}^k \sum_{j=1}^l w_{ij} \times x(n-1+i, m-1+j)$

Dilation and Erosion

For linear filters as seen before, it holds that they are commutativ³⁴. Cite from wikipedia: "One says that x commutes with y under * if:

$$x * y = y * x "$$

In other words, it does not matter how many and in which sequence different linear filters you use. E.g. if a Savitzky-Golay filter is applied to some data, and then a second Savitzky-Golay filter for calculating the first derivative, the result is the same if the sequence of filters is reversed. It even holds, that there would have been **one** filter, which does the same as the **two** applied.

In contrast **morphological operations** on an image are non-linear operations and the final result depends on the sequence. If we think of any image, it is defined by pixels with values x_{ij} . Further this image is assumed to be a black-and-white image, so we have

$$x_{ij} = 0 \text{ or } 1, \forall i, j$$

To define a morphological operation we have to set a **structural element** SE. As example, a 3x3-Matrix as a part of the image.

³⁴ <http://en.wikipedia.org/wiki/Commutativity>

The definition of **erosion** E says:

$$E(M) = \begin{cases} 0, & \text{if } \sum_{i,j=0}^3 (se)_{ij} < 9 \\ 1, & \text{else} \end{cases}, \text{with } (se)_{ij}, M \in SE$$

So in words, if **any** of the pixels in the structural element M has value 0, the erosion sets the value of M, a specific pixel in M, to zero. Otherwise E(M)=1

And for the **dilation** D it holds, if **any** value in SE is 1, the dilation of M, D(M), is set to 1.

$$D(M) = \begin{cases} 1, & \text{if } \sum_{i,j=0}^3 (se)_{ij} \geq 1 \\ 0, & \text{else} \end{cases}, \text{with } (se)_{ij}, M \in SE$$

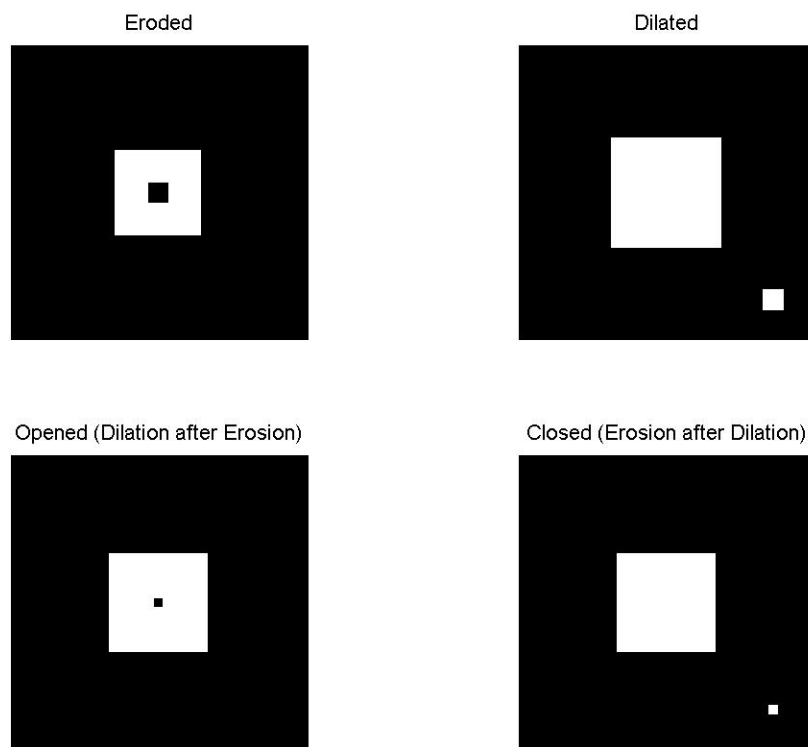


Figure 49

Compositions of Dilation and Erosion: Opening and Closing of Images

There are two compositions of dilation and erosion. One called **opening** the other called **closing**. It holds:

$$\textit{opening} = \textit{dilation} \circ \textit{erosion}$$

$$\textit{closing} = \textit{erosion} \circ \textit{dilation}$$

3.7 References

35

4 Auditory System

4.1 Introduction

The sensory system for the sense of hearing is the auditory system. This wikibook covers the physiology of the auditory system, and its application to the most successful neurosensory prosthesis - cochlear implants. The physics and engineering of acoustics are covered in a separate wikibook, *Acoustics*¹. An excellent source of images and animations is "Journey into the world of hearing"².

The ability to hear is not found as widely in the animal kingdom as other senses like touch, taste and smell. It is restricted mainly to vertebrates and insects. Within these, mammals and birds have the most highly developed sense of hearing. The table below shows frequency ranges of humans and some selected animals:

Humans	20-20'000 Hz
Whales	20-100'000 Hz
Bats	1'500-100'000 Hz
Fish	20-3'000 Hz

The organ that detects sound is the ear. It acts as receiver in the process of collecting acoustic information and passing it through the nervous system into the brain. The ear includes structures for both the sense of hearing and the sense of balance. It does not only play an important role as part of the auditory system in order to receive sound but also in the sense of balance and body position.



Figure 50
Mother and child



Figure 51
Humpback whales
in the singing
position



Figure 52 Big
eared townsend
bat



Figure 53 Hy-
phessobrycon
pulchripinnis fish

Humans have a pair of ears placed symmetrically on both sides of the head which makes it possible to localize sound sources. The brain extracts and processes different forms of data in order to localize sound, such as:

¹ <http://en.wikibooks.org/wiki/Acoustics>

² Journey into the world of hearing³. . Retrieved

- the shape of the sound spectrum at the tympanic membrane (eardrum)
- the difference in sound intensity between the left and the right ear
- the difference in time-of-arrival between the left and the right ear
- the difference in time-of-arrival between reflections of the ear itself (this means in other words: the shape of the pinna (pattern of folds and ridges) captures sound-waves in a way that helps localizing the sound source, especially on the vertical axis.

Healthy, young humans are able to hear sounds over a frequency range from 20 Hz to 20 kHz. We are most sensitive to frequencies between 2000 to 4000 Hz which is the frequency range of spoken words. The frequency resolution is 0.2% which means that one can distinguish between a tone of 1000 Hz and 1002 Hz. A sound at 1 kHz can be detected if it deflects the tympanic membrane (eardrum) by less than 1 Angstrom, which is less than the diameter of a hydrogen atom. This extreme sensitivity of the ear may explain why it contains the smallest bone that exists inside a human body: the stapes (stirrup). It is 0.25 to 0.33 cm long and weighs between 1.9 and 4.3 mg.

4.2 Anatomy of the Auditory System



Figure 54 Human (external) ear

The aim of this section is to explain the anatomy of the auditory system of humans. The chapter illustrates the composition of auditory organs in the sequence that acoustic information proceeds during sound perception.

Please note that the core information for “Sensory Organ Components” can also be found on the Wikipedia page “Auditory system”, excluding some changes like extensions and

specifications made in this article. (see also: Wikipedia Auditory system⁴)

The auditory system senses sound waves, that are changes in air pressure, and converts these changes into electrical signals. These signals can then be processed, analyzed and interpreted by the brain. For the moment, let's focus on the structure and components of the auditory system. The auditory system consists mainly of two parts:

- the ear and
- the auditory nervous system (central auditory system)

4.2.1 The ear

The ear is the organ where the first processing of sound occurs and where the sensory receptors are located. It consists of three parts:

- outer ear
- middle ear
- inner ear

⁴ http://en.wikipedia.org/wiki/Auditory_system

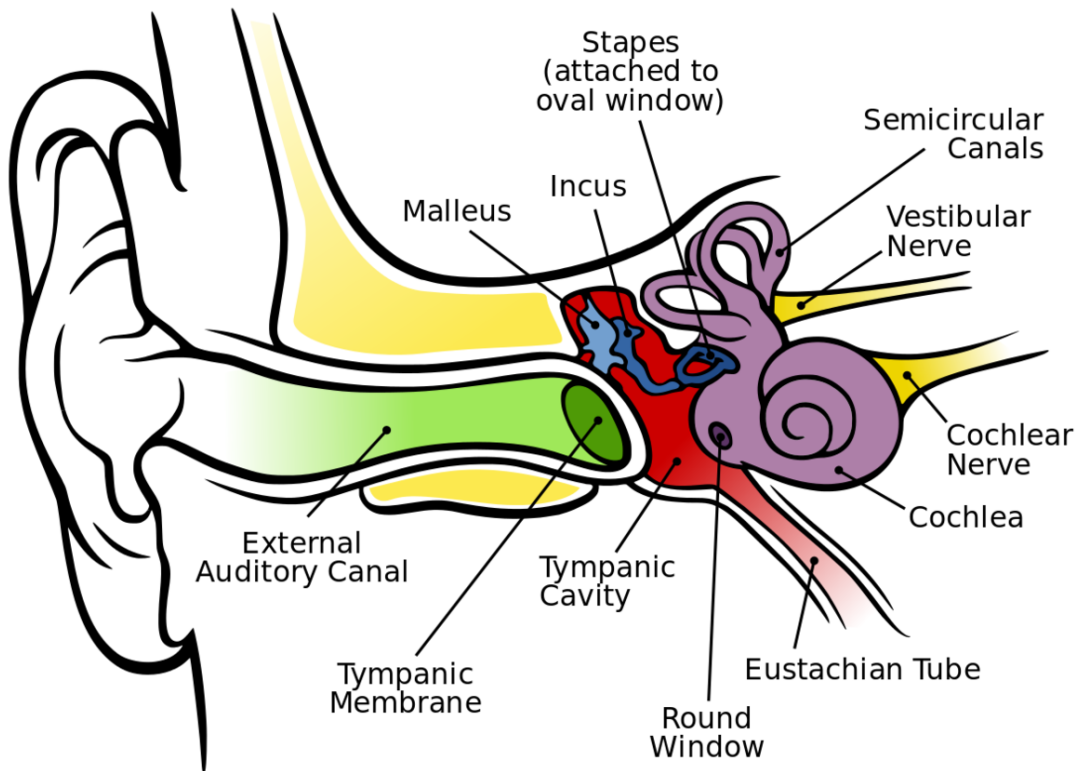


Figure 55 Anatomy of the human ear (green: outer ear / red: middle ear / purple: inner ear)

Outer ear

Function: Gathering sound energy and amplification of sound pressure.

The folds of cartilage surrounding the ear canal (external auditory meatus, external acoustic meatus) are called the pinna. It is the visible part of the ear. Sound waves are reflected and attenuated when they hit the pinna, and these changes provide additional information that will help the brain determine the direction from which the sounds came. The sound waves enter the auditory canal, a deceptively simple tube. The ear canal amplifies sounds that are between 3 and 12 kHz. At the far end of the ear canal is the tympanic membrane (eardrum), which marks the beginning of the middle ear.

Middle ear



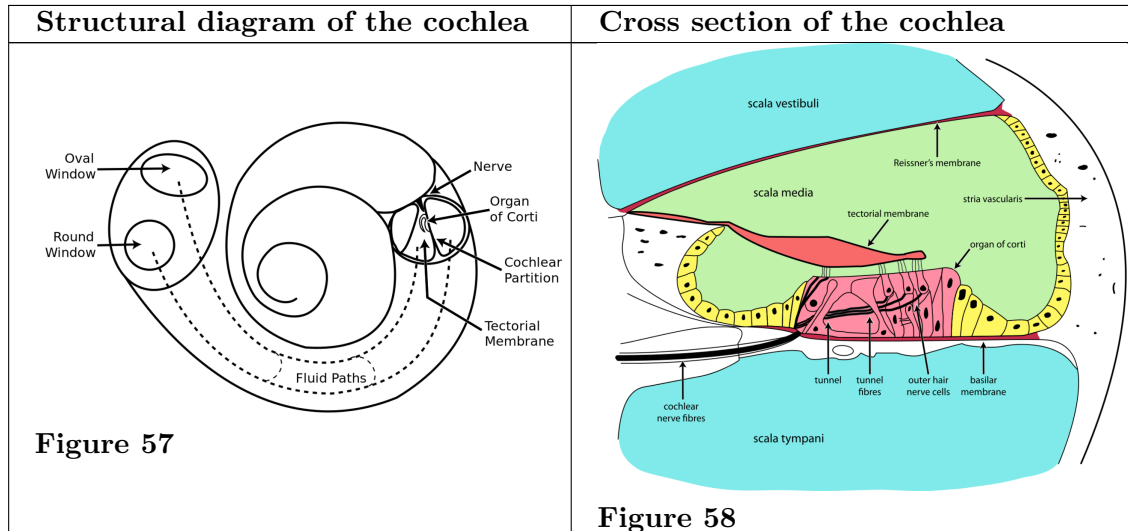
Figure 56 Micro-CT image of the ossicular chain showing the relative position of each ossicle.

Function: Transmission of acoustic energy from air to the cochlea.

Sound waves traveling through the ear canal will hit the tympanic membrane (tympanum, eardrum). This wave information travels across the air-filled tympanic cavity (middle ear cavity) via a series of bones: the malleus (hammer), incus (anvil) and stapes (stirrup). These ossicles act as a lever and a teletype, converting the lower-pressure eardrum sound vibrations into higher-pressure sound vibrations at another, smaller membrane called the oval (or elliptical) window, which is one of two openings into the cochlea of the inner ear. The second opening is called round window. It allows the fluid in the cochlea to move. The malleus articulates with the tympanic membrane via the manubrium, whereas the stapes articulates with the oval window via its footplate. Higher pressure is necessary because the inner ear beyond the oval window contains liquid rather than air. The sound is not amplified

uniformly across the ossicular chain. The stapedius reflex of the middle ear muscles helps protect the inner ear from damage. The middle ear still contains the sound information in wave form; it is converted to nerve impulses in the cochlea.

Inner ear



Function: Transformation of mechanical waves (sound) into electric signals (neural signals).

The inner ear consists of the cochlea and several non-auditory structures. The cochlea is a snail-shaped part of the inner ear. It has three fluid-filled sections: scala tympani (lower gallery), scala media (middle gallery, cochlear duct) and scala vestibuli (upper gallery). The cochlea supports a fluid wave driven by pressure across the basilar membrane separating two of the sections (scala tympani and scala media). The basilar membrane is about 3 cm long and between 0.5 to 0.04 mm wide. Reissner's membrane (vestibular membrane) separates scala media and scala vestibuli. Strikingly, one section, the scala media, contains an extracellular fluid similar in composition to endolymph, which is usually found inside of cells. The organ of Corti is located in this duct, and transforms mechanical waves to electric signals in neurons. The other two sections, scala tympani and scala vestibuli, are located within the bony labyrinth which is filled with fluid called perilymph. The chemical difference between the two fluids endolymph (in scala media) and perilymph (in scala tympani and scala vestibuli) is important for the function of the inner ear.

Organ of Corti

The organ of Corti forms a ribbon of sensory epithelium which runs lengthwise down the entire cochlea. The hair cells of the organ of Corti transform the fluid waves into nerve signals. The journey of a billion nerves begins with this first step; from here further processing leads to a series of auditory reactions and sensations.

4.2.2 Transition from ear to auditory nervous system

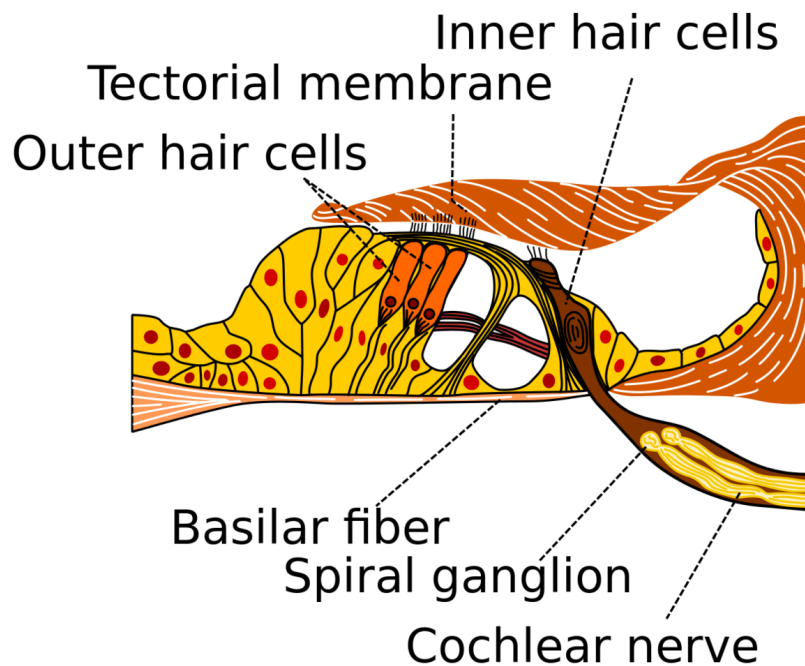


Figure 59 Section through the spiral organ of Corti

Hair cells

Hair cells are columnar cells, each with a bundle of 100-200 specialized cilia at the top, for which they are named. These cilia are the mechanosensors for hearing. The shorter ones are called stereocilia, and the longest one at the end of each haircell bundle is the kinocilium. The location of the kinocilium determines the on-direction, i.e. the direction of deflection inducing the maximum hair cell excitation. Lightly resting atop the longest cilia is the tectorial membrane, which moves back and forth with each cycle of sound, tilting the cilia and allowing electric current into the hair cell.

The function of hair cells is not fully established up to now. Currently, the knowledge of the function of hair cells allows to replace the cells by cochlear implants in case of hearing lost. However, more research into the function of the hair cells may someday even make it possible for the cells to be repaired. The current model is that cilia are attached to one another by “tip links”, structures which link the tips of one cilium to another. Stretching and compressing, the tip links then open an ion channel and produce the receptor potential in the hair cell. Note that a deflection of 100 nanometers already elicits 90% of the full receptor potential.

Neurons

The nervous system distinguishes between nerve fibres carrying information *towards* the central nervous system and nerve fibres carrying the information *away* from it:

- *Afferent neurons* (also sensory or receptor neurons) carry nerve impulses from receptors (sense organs) *towards* the central nervous system
- *Efferent neurons* (also motor or effector neurons) carry nerve impulses *away* from the central nervous system to effectors such as muscles or glands (and also the ciliated cells of the inner ear)

Afferent neurons innervate cochlear inner hair cells, at synapses where the neurotransmitter glutamate communicates signals from the hair cells to the dendrites of the primary auditory neurons. There are far fewer inner hair cells in the cochlea than afferent nerve fibers. The neural dendrites belong to neurons of the auditory nerve, which in turn joins the vestibular nerve to form the vestibulocochlear nerve, or cranial nerve number VIII.

Efferent projections from the brain to the cochlea also play a role in the perception of sound. Efferent synapses occur on outer hair cells and on afferent (towards the brain) dendrites under inner hair cells.

4.2.3 Auditory nervous system

The sound information, now re-encoded in form of electric signals, travels down the auditory nerve (acoustic nerve, vestibulocochlear nerve, VIIIth cranial nerve), through intermediate stations such as the cochlear nuclei and superior olivary complex of the brainstem and the inferior colliculus of the midbrain, being further processed at each waypoint. The information eventually reaches the thalamus, and from there it is relayed to the cortex. In the human brain, the primary auditory cortex is located in the temporal lobe.

Primary auditory cortex

The primary auditory cortex is the first region of cerebral cortex to receive auditory input. Perception of sound is associated with the right posterior superior temporal gyrus (STG). The superior temporal gyrus contains several important structures of the brain, including Brodmann areas 41 and 42, marking the location of the primary auditory cortex, the cortical region responsible for the sensation of basic characteristics of sound such as pitch and rhythm. The auditory association area is located within the temporal lobe of the brain, in an area called the Wernicke's area, or area 22. This area, near the lateral cerebral sulcus, is an important region for the processing of acoustic signals so that they can be distinguished as speech, music, or noise.

4.3 Auditory Signal Processing

Now that the anatomy of the auditory system has been sketched out, this topic goes deeper into the physiological processes which take place while perceiving acoustic information and converting this information into data that can be handled by the brain. Hearing starts with pressure waves hitting the auditory canal and is finally perceived by the brain. This section details the process transforming vibrations into perception.

4.3.1 Effect of the head

Sound waves with a wavelength shorter than the head produce a sound shadow on the ear further away from the sound source. When the wavelength is shorter than the head, diffraction of the sound leads to approximately equal sound intensities on both ears.

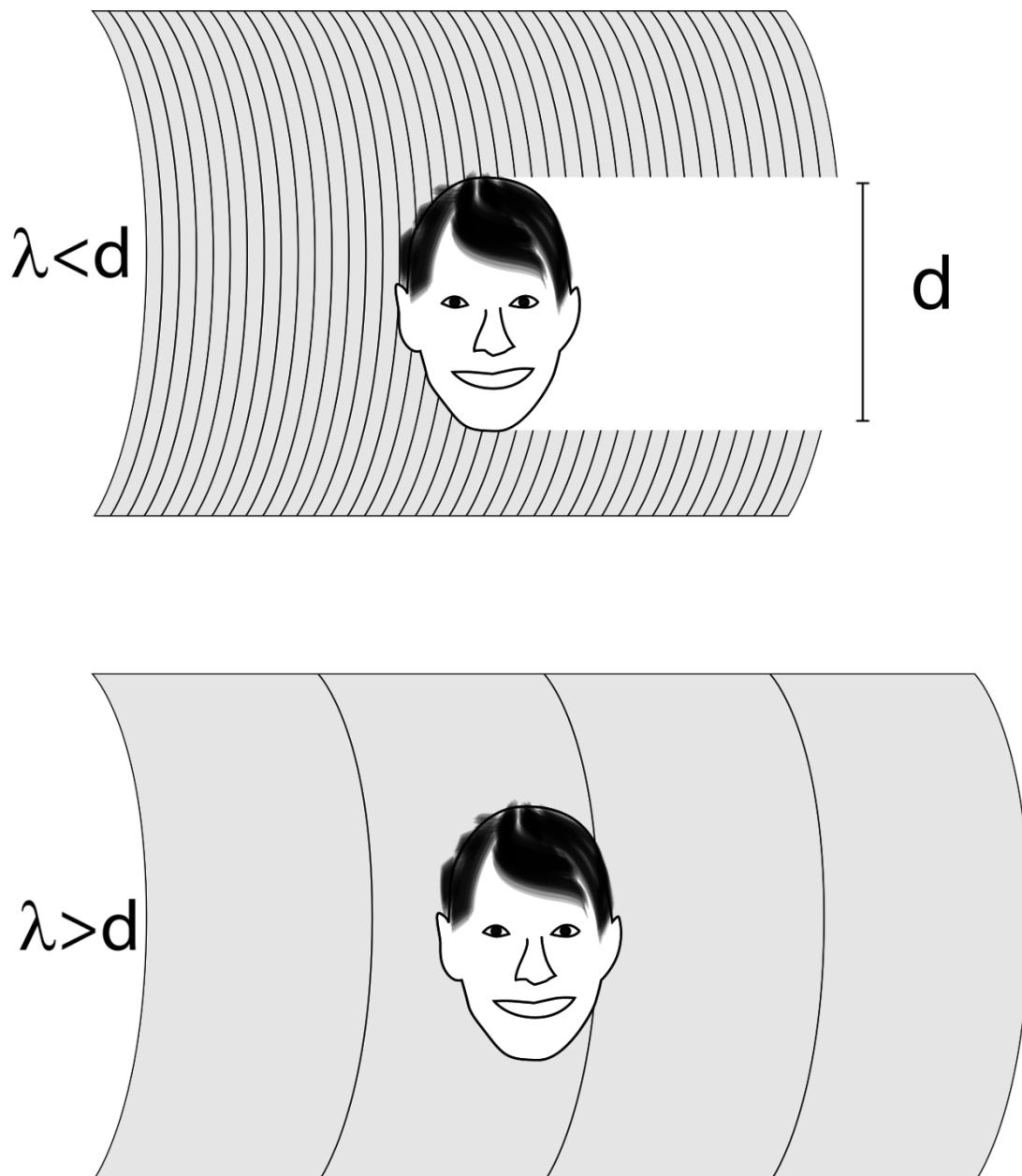


Figure 60 Difference in loudness and timing help us to localize the source of a sound signal.

4.3.2 Sound reception at the pinna

The pinna collects sound waves in air affecting sound coming from behind and the front differently with its corrugated shape. The sound waves are reflected and attenuated or amplified. These changes will later help sound localization.

In the external auditory canal, sounds between 3 and 12 kHz - a range crucial for human communication - are amplified. It acts as resonator amplifying the incoming frequencies.

4.3.3 Sound conduction to the cochlea

Sound that entered the pinna in form of waves travels along the auditory canal until it reaches the beginning of the middle ear marked by the tympanic membrane (eardrum). Since the inner ear is filled with fluid, the middle ear is kind of an impedance matching device in order to solve the problem of sound energy reflection on the transition from air to the fluid. As an example, on the transition from air to water 99.9% of the incoming sound energy is reflected. This can be calculated using:

$$\frac{I_r}{I_i} = \left(\frac{Z_2 - Z_1}{Z_2 + Z_1} \right)^2$$

with I_r the intensity of the reflected sound, I_i the intensity of the incoming sound and Z_k the wave resistance of the two media ($Z_{\text{air}} = 414 \text{ kg m}^{-2} \text{ s}^{-1}$ and $Z_{\text{water}} = 1.48 \cdot 10^6 \text{ kg m}^{-2} \text{ s}^{-1}$). Three factors that contribute the impedance matching are:

- the relative size difference between tympanum and oval window
- the lever effect of the middle ear ossicles and
- the shape of the tympanum.

Malleus

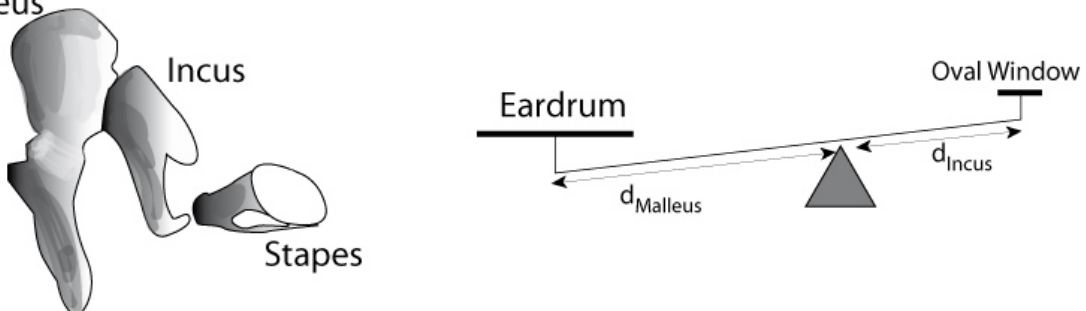


Figure 61 Mechanics of the amplification effect of the middle ear.

The longitudinal changes in air pressure of the sound-wave cause the tympanic membrane to vibrate which, in turn, makes the three chained ossicles malleus, incus and stirrup oscillate synchronously. These bones vibrate as a unit, elevating the energy from the tympanic membrane to the oval window. In addition, the energy of sound is further enhanced by the areal difference between the membrane and the stapes footplate. The middle ear acts as an impedance transformer by changing the sound energy collected by the tympanic membrane into greater force and less excursion. This mechanism facilitates transmission of sound-waves in air into vibrations of the fluid in the cochlea. The transformation results from the pistonlike in- and out-motion by the footplate of the stapes which is located in the oval window. This movement performed by the footplate sets the fluid in the cochlea into motion.

Through the *stapedius muscle*, the smallest muscle in the human body, the middle ear has a gating function: contracting this muscle changes the impedance of the middle ear, thus protecting the inner ear from damage through loud sounds.

4.3.4 Frequency analysis in the cochlea

The three fluid-filled compartments of the cochlea (scala vestibuli, scala media, scala tympani) are separated by the basilar membrane and the Reissner's membrane. The function of the cochlea is to separate sounds according to their spectrum and transform it into a neural code. When the footplate of the stapes pushes into the perilymph of the scala vestibuli, as a consequence the membrane of Reissner bends into the scala media. This elongation of Reissner's membrane causes the endolymph to move within the scala media and induces a displacement of the basilar membrane. The separation of the sound frequencies in the cochlea is due to the special properties of the basilar membrane. The fluid in the cochlea vibrates (due to in- and out-motion of the stapes footplate) setting the membrane in motion like a traveling wave. The wave starts at the base and progresses towards the apex of the cochlea. The transversal waves in the basilar membrane propagate with

$$c_{trans} = \sqrt{\frac{\mu}{\rho}}$$

with μ the shear modulus and ρ the density of the material. Since width and tension of the basilar membrane change, the speed of the waves propagating along the membrane changes from about 100 m/s near the oval window to 10 m/s near the apex.

There is a point along the basilar membrane where the amplitude of the wave decreases abruptly. At this point, the sound wave in the cochlear fluid produces the maximal displacement (peak amplitude) of the basilar membrane. The distance the wave travels before getting to that characteristic point depends on the frequency of the incoming sound. Therefore each point of the basilar membrane corresponds to a specific value of the stimulating frequency. A low-frequency sound travels a longer distance than a high-frequency sound before it reaches its characteristic point. Frequencies are scaled along the basilar membrane with high frequencies at the base and low frequencies at the apex of the cochlea.

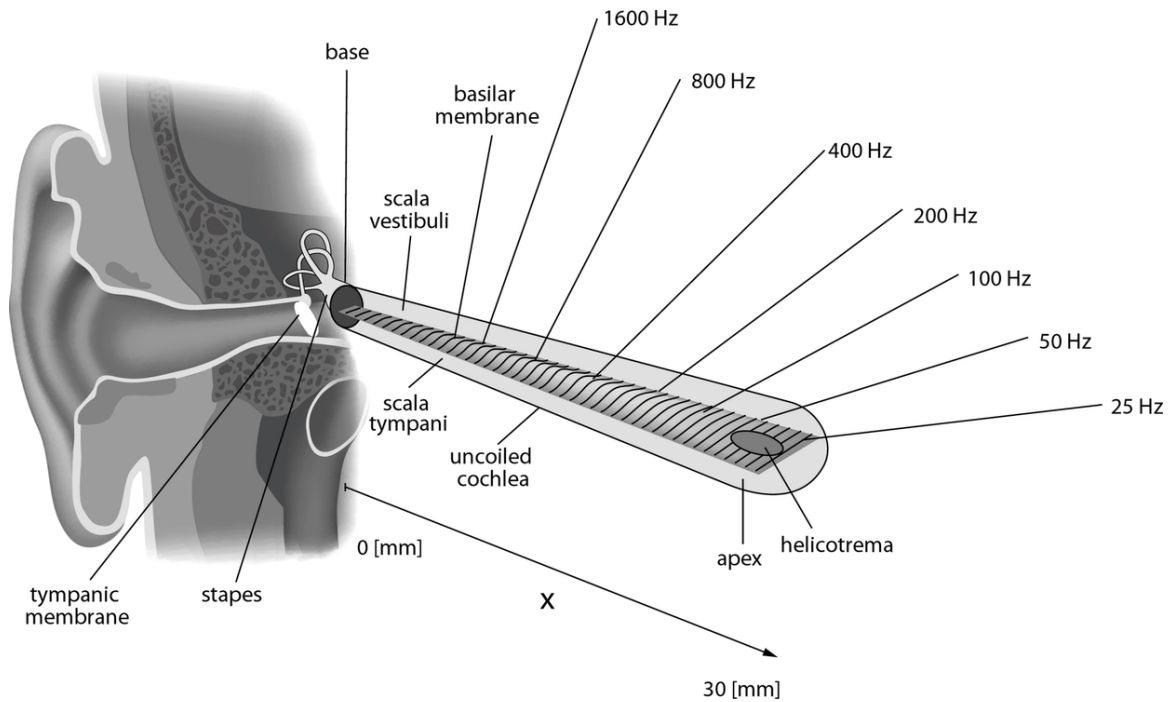


Figure 62 The position x of the maximal amplitude of the travelling wave corresponds in a 1-to-1 way to a stimulus frequency.

4.3.5 Sensory transduction in the cochlea

Most everyday sounds are composed of multiple frequencies. The brain processes the distinct frequencies, not the complete sounds. Due to its inhomogeneous properties, the basilar membrane is performing an approximation to a Fourier transform. The sound is thereby split into its different frequencies, and each hair cell on the membrane corresponds to a certain frequency. The loudness of the frequencies is encoded by the firing rate of the corresponding afferent fiber. This is due to the amplitude of the traveling wave on the basilar membrane, which depends on the loudness of the incoming sound.

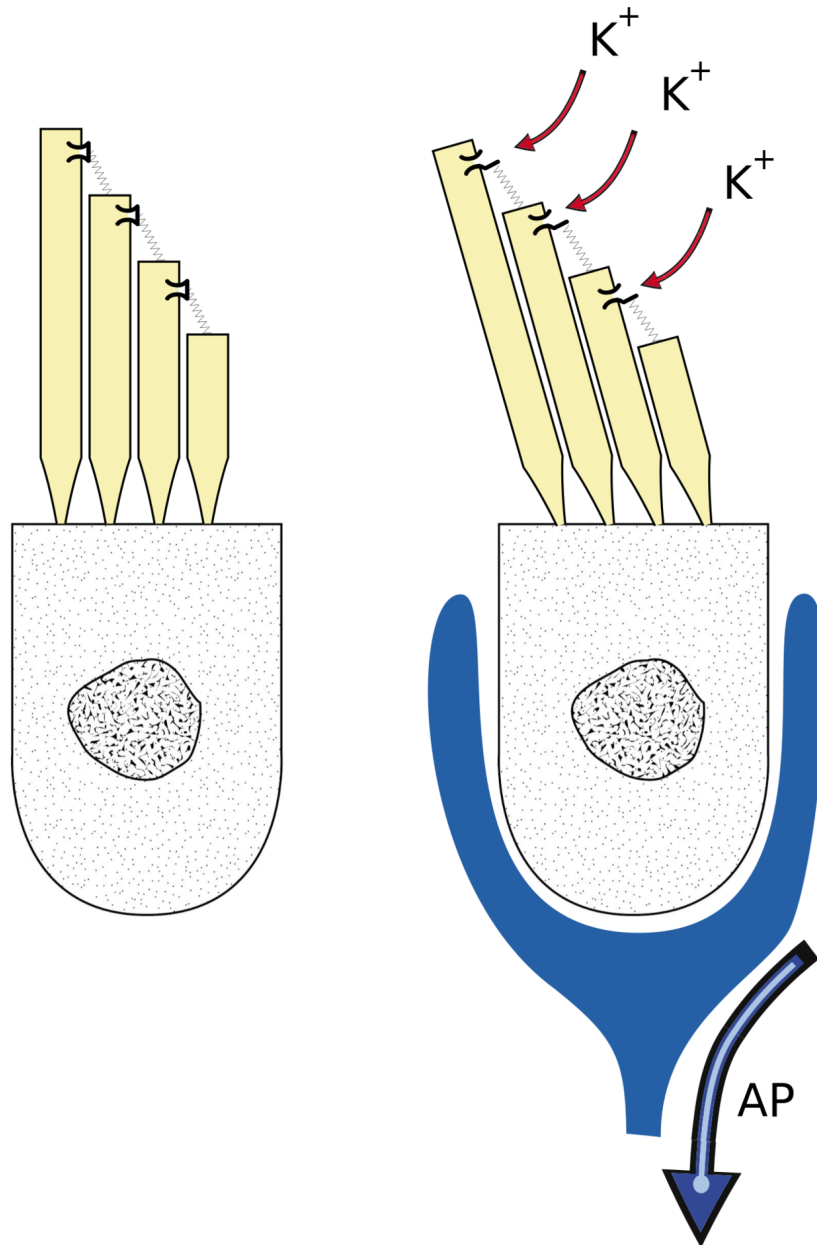


Figure 63 Transduction mechanism in auditory or vestibular hair cell. Tilting the hair cell towards the kinocilium opens the potassium ion channels. This changes the receptor potential in the hair cell. The resulting emission of neurotransmitters can elicit an action potential (AP) in the post-synaptic cell.

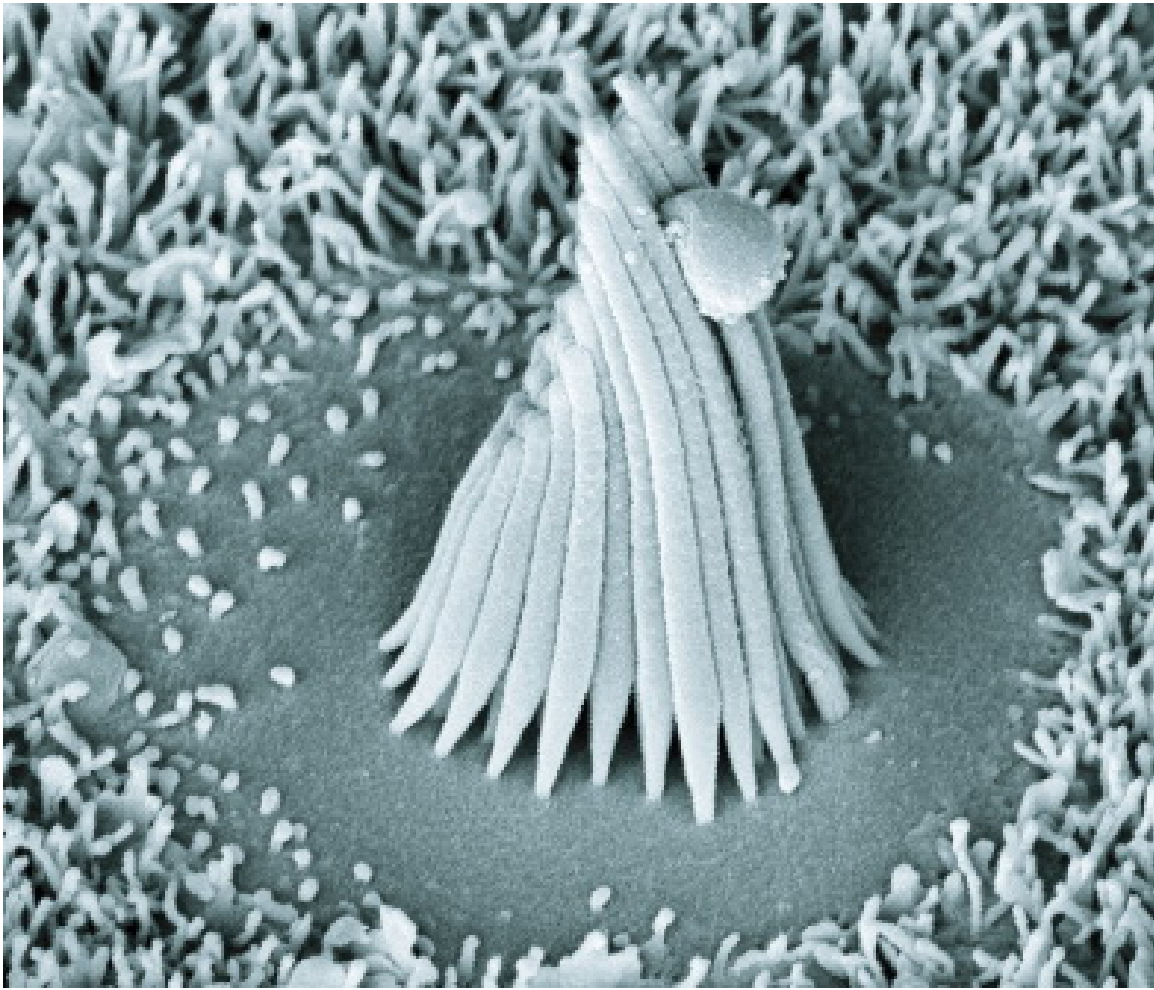


Figure 64 Auditory haircells are very similar to those of the vestibular system. Here an electron microscopy image of a frog's sacculus haircell.

The sensory cells of the auditory system, known as hair cells, are located along the basilar membrane within the organ of Corti. Each organ of Corti contains about 16'000 such cells, innervated by about 30'000 afferent nerve fibers. There are two anatomically and functionally distinct types of hair cells: the inner and the outer hair cells. Along the basilar membrane these two types are arranged in one row of inner cells and three to five rows of outer cells. Most of the afferent innervation comes from the inner hair cells while most of the efferent innervation goes to the outer hair cells. The inner hair cells influence the discharge rate of the individual auditory nerve fibers that connect to these hair cells. Therefore inner hair cells transfer sound information to higher auditory nervous centers. The outer hair cells, in contrast, amplify the movement of the basilar membrane by injecting energy into the motion of the membrane and reducing frictional losses but do not contribute in transmitting sound information. The motion of the basilar membrane deflects the stereocilias (hairs on the hair cells) and causes the intracellular potentials of the hair cells to decrease (depolarization) or increase (hyperpolarization), depending on the direction of the deflection. When the stereocilias are in a resting position, there is a steady state current flowing through the

channels of the cells. The movement of the stereocilia therefore modulates the current flow around that steady state current.

Lets look at the modes of action of the two different hair cell types separately:

- Inner hair cells:

The deflection of the hair-cell stereocilia opens mechanically gated ion channels that allow small, positively charged potassium ions (K^+) to enter the cell and causing it to depolarize. Unlike many other electrically active cells, the hair cell itself does not fire an action potential. Instead, the influx of positive ions from the endolymph in scala media depolarizes the cell, resulting in a receptor potential. This receptor potential opens voltage gated calcium channels; calcium ions (Ca^{2+}) then enter the cell and trigger the release of neurotransmitters at the basal end of the cell. The neurotransmitters diffuse across the narrow space between the hair cell and a nerve terminal, where they then bind to receptors and thus trigger action potentials in the nerve. In this way, neurotransmitter increases the firing rate in the VII-Ith cranial nerve and the mechanical sound signal is converted into an electrical nerve signal.

The repolarization in the hair cell is done in a special manner. The perilymph in Scala tympani has a very low concentration of positive ions. The electrochemical gradient makes the positive ions flow through channels to the perilymph. (see also: Wikipedia Hair cell⁵)

- Outer hair cells:

In humans outer hair cells, the receptor potential triggers active vibrations of the cell body. This mechanical response to electrical signals is termed somatic electromotility and drives oscillations in the cell's length, which occur at the frequency of the incoming sound and provide mechanical feedback amplification. Outer hair cells have evolved only in mammals. Without functioning outer hair cells the sensitivity decreases by approximately 50 dB (due to greater frictional losses in the basilar membrane which would damp the motion of the membrane). They have also improved frequency selectivity (frequency discrimination), which is of particular benefit for humans, because it enables sophisticated speech and music. (see also: Wikipedia Hair cell⁶)

With no external stimulation, auditory nerve fibres discharge action potentials in a random time sequence. This random time firing is called spontaneous activity. The spontaneous discharge rates of the fibers vary from very slow rates to rates of up to 100 per second. Fibers are placed into three groups depending on whether they fire spontaneously at high, medium or low rates. Fibers with high spontaneous rates (> 18 per second) tend to be more sensitive to sound stimulation than other fibers.

5 http://en.wikipedia.org/wiki/Hair_cell

6 http://en.wikipedia.org/wiki/Hair_cell

4.3.6 Auditory pathway of nerve impulses

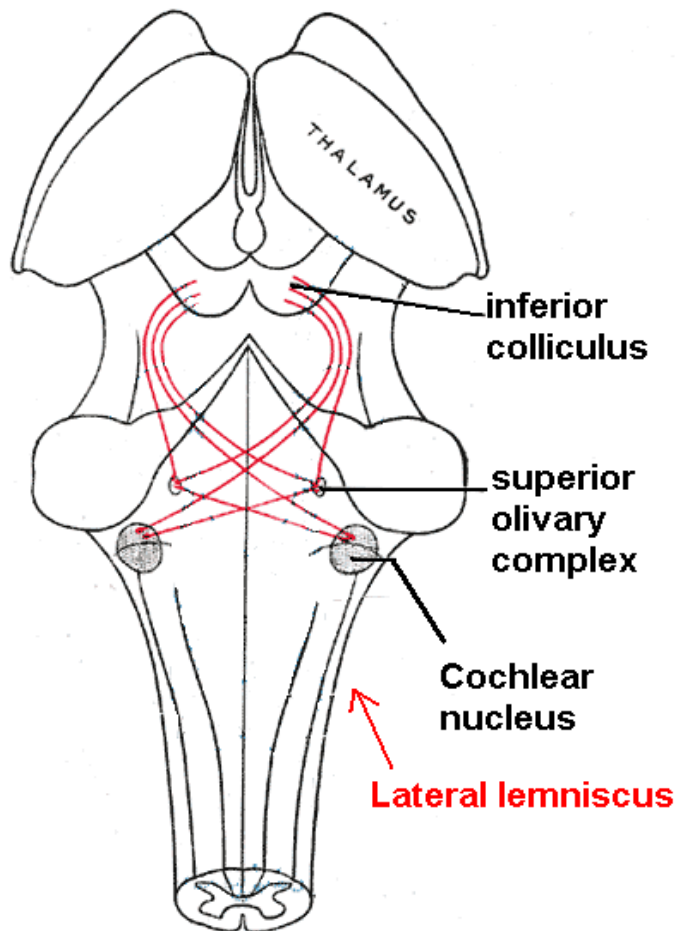


Figure 65 Lateral lemniscus in red, as it connects the cochlear nucleus, superior olivary nucleus and the inferior colliculus. Seen from behind.

So in the inner hair cells the mechanical sound signal is finally converted into electrical nerve signals. The inner hair cells are connected to auditory nerve fibres whose nuclei form the spiral ganglion. In the spiral ganglion the electrical signals (electrical spikes, action potentials) are generated and transmitted along the cochlear branch of the auditory nerve (VIIIth cranial nerve) to the cochlear nucleus in the brainstem.

From there, the auditory information is divided into at least two streams:

- Ventral Cochlear Nucleus:

One stream is the ventral cochlear nucleus which is split further into the posteroventral cochlear nucleus (PVCN) and the anteroventral cochlear nucleus (AVCN). The ventral cochlear nucleus cells project to a collection of nuclei called the superior olivary complex.

Superior olivary complex: Sound localization

The superior olivary complex - a small mass of gray substance - is believed to be involved in the localization of sounds in the azimuthal plane (i.e. their degree to the left or the right). There are two major cues to sound localization: Interaural level differences (ILD) and interaural time differences (ITD). The ILD measures differences in sound intensity between the ears. This works for high frequencies (over 1.6 kHz), where the wavelength is shorter than the distance between the ears, causing a head shadow - which means that high frequency sounds hit the averted ear with lower intensity. Lower frequency sounds don't cast a shadow, since they wrap around the head. However, due to the wavelength being larger than the distance between the ears, there is a phase difference between the sound waves entering the ears - the timing difference measured by the ITD. This works very precisely for frequencies below 800 Hz, where the ear distance is smaller than half of the wavelength. Sound localization in the median plane (front, above, back, below) is helped through the outer ear, which forms direction-selective filters.

There, the differences in time and loudness of the sound information in each ear are compared. Differences in sound intensity are processed in cells of the lateral superior olivary complex and timing differences (runtime delays) in the medial superior olivary complex. Humans can detect timing differences between the left and right ear down to 10 μ s, corresponding to a difference in sound location of about 1 deg. This comparison of sound information from both ears allows the determination of the direction where the sound came from. The superior olive is the first node where signals from both ears come together and can be compared. As a next step, the superior olivary complex sends information up to the inferior colliculus via a tract of axons called lateral lemniscus. The function of the inferior colliculus is to integrate information before sending it to the thalamus and the auditory cortex. It is interesting to know that the *superior* colliculus close by shows an interaction of auditory and visual stimuli.

- Dorsal Cochlear Nucleus:

The dorsal cochlear nucleus (DCN) analyzes the quality of sound and projects directly via the lateral lemniscus to the inferior colliculus.

From the inferior colliculus the auditory information from ventral as well as dorsal cochlear nucleus proceeds to the auditory nucleus of the thalamus which is the medial geniculate nucleus. The medial geniculate nucleus further transfers information to the primary auditory cortex, the region of the human brain that is responsible for processing of auditory information, located on the temporal lobe. The primary auditory cortex is the first relay involved in the conscious perception of sound.

4.3.7 Primary auditory cortex and higher order auditory areas

Sound information that reaches the primary auditory cortex (Brodmann areas 41 and 42). The primary auditory cortex is the first relay involved in the conscious perception of sound. It is known to be tonotopically organized and performs the basics of hearing: pitch and volume. Depending on the nature of the sound (speech, music, noise), is further passed

to higher order auditory areas. Sounds that are words are processed by Wernicke's area (Brodmann area 22). This area is involved in understanding written and spoken language (verbal understanding). The production of sound (verbal expression) is linked to Broca's area (Brodmann areas 44 and 45). The muscles to produce the required sound when speaking are contracted by the facial area of motor cortex which are regions of the cerebral cortex that are involved in planning, controlling and executing voluntary motor functions.

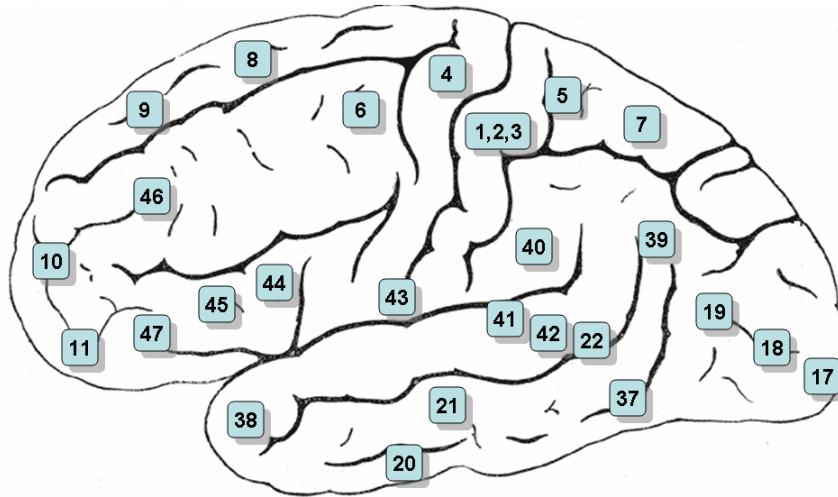


Figure 66 Lateral surface of the brain with Brodmann's areas numbered.

4.4 Human Speech

4.4.1 Terminology

Loudness

The intensity of sound is typically expressed in deciBel (dB), defined as

$$SPL = 20 * \log \frac{p}{p_0}$$

where SPL = "sound pressure level" (in dB), and the reference pressure is $p_0 = 2 * 10^{-5} \text{ N/m}^2$. Note that this is much smaller than the air pressure (ca. 10^5 N/m^2)! Also watch out, because sound is often expressed relative to "Hearing Level" instead of SPL.

- 0 - 20 dB SPL ... hearing level (0 dB for sinusoidal tones, from 1 kHz – 4 kHz)
- 60 dB SPL ... medium loud tone, conversational speech

Fundamental frequency, from the vibrations of the vocal cords in the larynx, is about 120 Hz for adult male, 250 Hz for adult female, and up to 400 Hz for children.

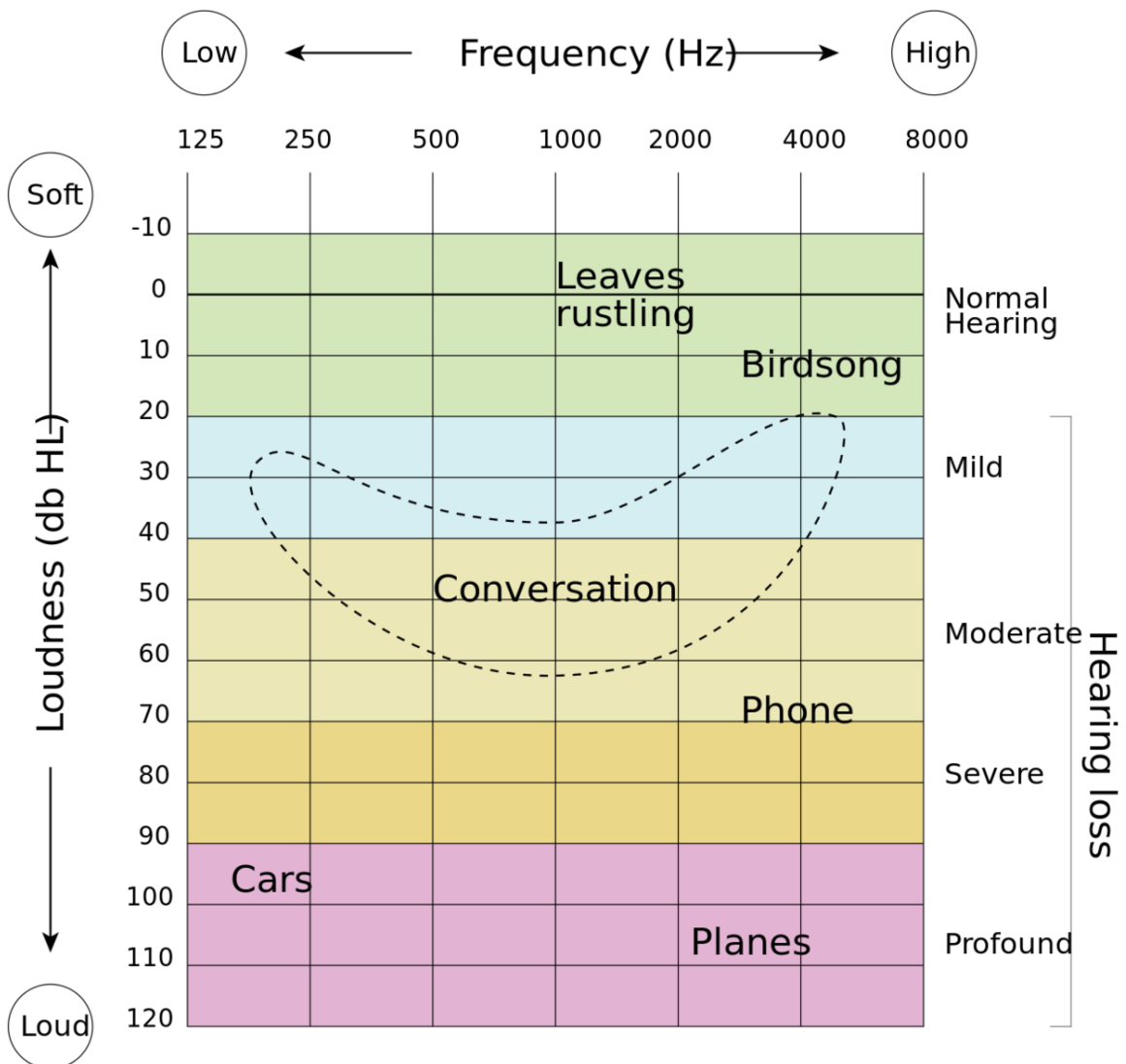


Figure 67 Frequency- and loudness-dependence of human hearing loss.

Formants

Formants are the dominant frequencies in human speech, and are caused by resonances of the signals from the vocal cord in our mouth etc. Formants show up as distinct peaks of energy in the sound's frequency spectrum. They are numbered in ascending order starting with the format at the lowest frequency.

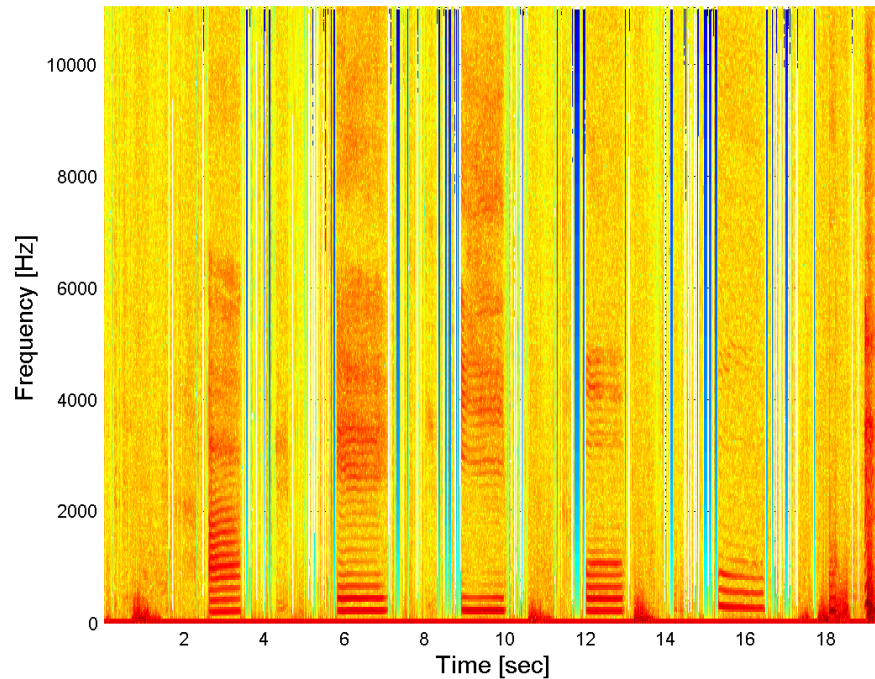


Figure 68 Spectrogram of the German vowels "a,e,i,o,u". These correspond approximately to the vowels in the English words "hut, hat, hit, hot, put". Calculated using the MATLAB command "spectrogram(data, 512,256, 512, fs)". The chapter Power Spectrum of Non-stationary Signals^a below describes the mathematics behind the spectrogram.

^a Chapter 4.4.1 on page 85

Phonemes

Speech is often considered to consist of a sequence of acoustic units called phons, which correspond to linguistic units called phonemes. Phonemes are the smallest units of sound that allows different words to be distinguished. The word "dog", for example, contains three phonemes. Changes to the first, second, and third phoneme respectively produce the words "log", "dig", and "dot". English is said to contain 40 different phonemes, specified as in /d/, /o/, /g/ for the word "dog".

4.4.2 Speech Perception

The ability of humans to decode speech signals still easily exceeds that of any algorithm developed so far. While automatic speech recognition has become fairly successful in recognizing clearly spoken speech in environments with high Signal-to-noise ratio, once the conditions become a bit less than ideal, recognition algorithms tend to perform vary poorly compared to humans. It seems from this that our computer speech recognition algorithms

have not yet come close to capturing the underlying algorithm that humans use to recognize speech.

Evidence has shown that the perception of speech takes quite a different route than the perception of other sounds in the brain. While studies on non-speech sound responses have generally found response to be graded with stimulus, speech studies have repeatedly found a discretization of response when a graded stimulus is presented. For instance, Lisker and Abramson,⁷ played a pre-voiced 'b/p' sound. Whether the sound is interpreted as a /b/ or a /p/ depends on the voice onset time (VOT). They found that when smoothly varying the VOT, there was a sharp change (at ~20ms after the consonant is played) where subjects switched their identification from /b/ to /p/. Furthermore, subjects had a great deal of difficulty differentiating between two sounds in the same category (e.g. pairs of sounds with a VOTs of -10ms to 10ms, which would both be /b/'s, than sounds with a 10ms to 30ms, which would be identified as a b and a p). This shows that some type of categorization scheme is going on. One of the main problems encountered when trying to build a model of speech perception is the so-called 'Lack of Invariance', which could more straightforwardly just be stated as the 'variance'. This term refers to the fact that a single phoneme (e.g. /p/ as in sPeech or Piety), has a great variety of waveforms that map to it, and that the mapping between an acoustic waveform and a phoneme is far from obvious and heavily context-dependent, yet human listeners reliably give the correct result. Even when the context is similar, a waveform will show a great deal of variance due to factors such as the pace of speech, the identity of the speaker and the tone in which he is speaking. So while there is no agreed-upon model of speech perception, the existing models can be split into two classes: Passive Perception and Active perception.

Passive Perception Models

Passive perception theories generally describe the problem of speech perception in the same way that most sensory signal-processing algorithms do: Some raw input signal goes in, and is processed through a hierarchy where each subsequent step extracts some increasingly abstract signal from the input. One of the early examples of a passive model was distinctive feature theory. The idea is to identify the presence of sets of binary values for certain features. For example, 'nasal/oral', 'vocalic/non-vocalic'. The theory is that a phoneme is interpreted as a binary vector of the presence or absence of these features. These features can be extracted from the spectrogram data. Other passive models, such as those described by Selfridge⁸ and Uttley,⁹ involve a kind of template-matching, where a hierarchy of processing layers extract features that are increasingly abstract and invariant to certain irrelevant features (such as identity of the speaker when classifying phonemes).

7 Lisker L., Abramson. "The voicing dimension: Some experiments in comparative phonetics".(1970)

8 Selfridge, O.C "Pandemonium: a paradigm for learning". 1959

9 Uttley, AM. 1966, "The transmission of information and effects of local feedback in theoretical and neural networks." (1966).

Active Perception Models

An entirely different take on speech perception are active-perception theories. These theories make the point that it would be redundant for the brain to have two parallel systems for speech perception and speech production, given that the ability produce a sound is so closely tied with the ability to identify it - proponents of these theories argue that it would be wasteful and complicated to maintain two separate databases-one containing the programs to identify phonemes, and another to produce them. They argue that speech perception is actually done by attempting to replicate the incoming signal, and thus using the same circuits for phoneme production as for identification. The Motor Theory of speech perception (Liberman et al., 1967), states that speech sounds are identified not by any sort of template matching, but by using the speech-generating mechanisms to try and regenerate a copy of the speech signal. It states that phonemes should not be seen as hidden signals within the speech, but as “cues” that the generating mechanism attempts to reproduce in a pre-speech signal. The theory states that speech-generating regions of the brain learn which speech-precursor signals will produce which sounds by the constant feedback loop of always hearing one's own speech. The babbling of babies, it is argued, is a way of learning this how to generate these “cue” sounds from pre-motor signals.¹⁰

A similar idea is proposed in the analysis-by-synthesis model, by Stevens and Halle.¹¹ This describes a generative model which attempts to regenerate a similar signal to the incoming sound. It essentially takes advantage of the fact that speech-generating mechanisms are similar between people, and that the characteristic features that one hears in speech can be reproduced by the speaker. As the speaker hears the sound, the speech centers attempt to generate the signal that's coming in. Comparators give constant feedback on the quality of the regeneration. The 'units of perception', are therefore not so much abstractions of the incoming sound, as pre-motor commands for generating the same speech.

Motor theories took a serious hit when a series of studies on what is now known as Broca's Aphasia were published. This condition impairs one's ability to produce speech sounds, without impairing the ability to comprehend them, whereas motor theory, taken in its original form, states that production and comprehension are done by the same circuits, so impaired speech production should imply impaired speech comprehension. The existence of Broca's aphasia appears to contradict this prediction.¹²

10 Liberman, A.M., Mattingly, IG, Turvey, MT. "Language codes and memory codes" (1967)

11 Stevens, KN, Halle, M. "Remarks on analysis by synthesis and distinctive features"

12 Hick, G. The role of mirror neurons in speech and language processing. (2010)

Current Models

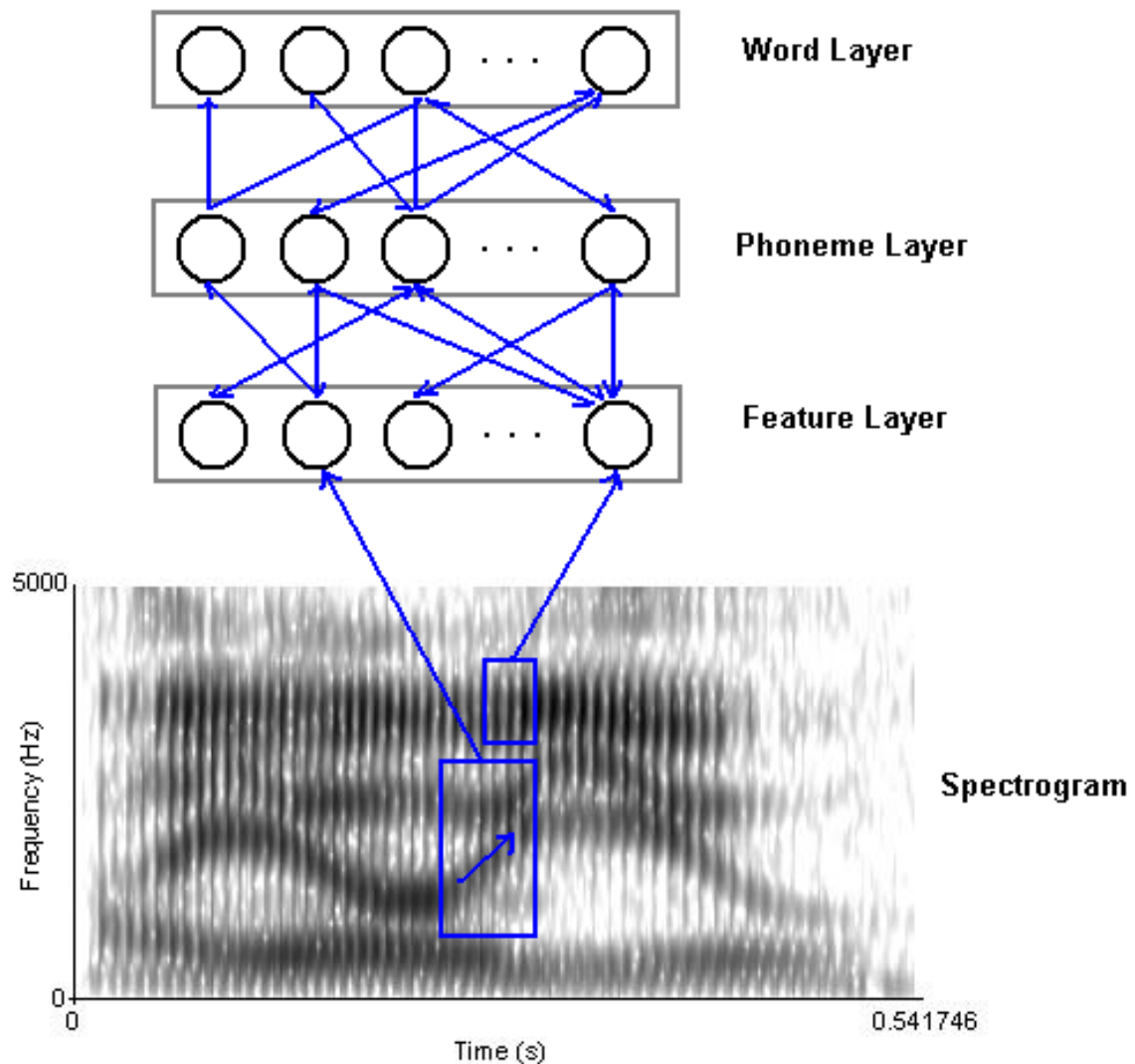


Figure 69 The TRACE model of speech perception. All connections beyond the input layer are bidirectional. Each unit represents some unit of speech such as a word or a phoneme.

One of the most influential computational models of speech perception is called TRACE.¹³ TRACE is a neural-network-like model, with three layers and a recurrent connection scheme. The first layer extracts features from an input spectrogram in temporal order, basically simulating the cochlea. The second layer extracts phonemes from the feature information, and the third layer extracts words from the phoneme information. The model contains feed-forward (bottom-up) excitatory connections, lateral inhibitory connections, and feedback (top-down) excitatory connections. In this model, each computational unit corresponds to some unit of perception (e.g. the phoneme /p/ or the word "preposterous"). The basic idea

¹³ McClelland, J.L. The TRACE Model of Speech Perception (1986)

is that, based on their input, units within a layer will compete to have the strongest output. The lateral inhibitory connections result in a sort of winner-takes-all circuit, in which the unit with the strongest input will inhibit its neighbors and become the clear winner. The feedback connections allow us to explain the effect of context-dependent comprehension - for example, suppose the phoneme layer, based on its bottom-up inputs, could not decide whether it had heard a /g/ or a /k/, but that the phoneme was preceded by 'an', and followed by 'ry'. Both the /g/ and /k/ units would initially be equally activated, sending inputs up to the word level, which would already contain excited units corresponding to words such as 'anaconda', 'angry', and 'ankle', which had been activated by the preceding 'an'. The excitement of the /g/ or /k/

4.5 Cochlear Implants

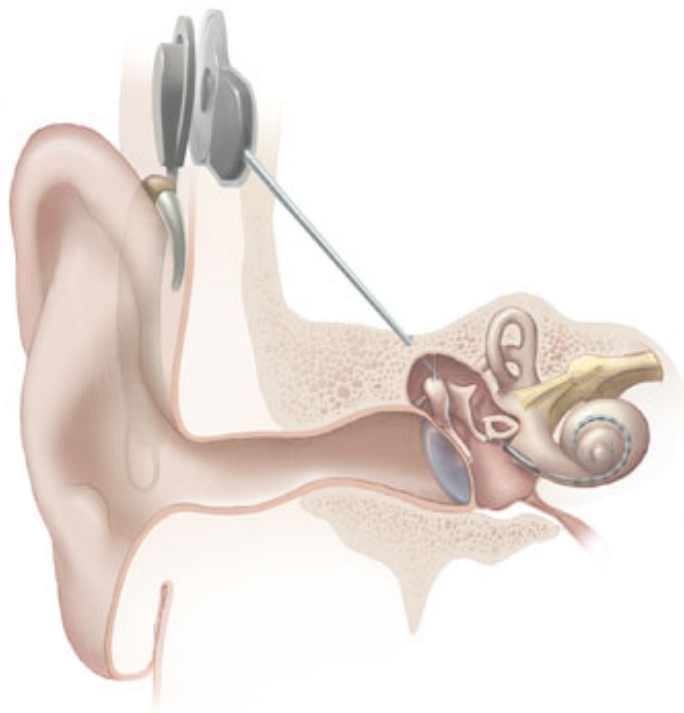


Figure 70 Cochlear implant

A cochlear implant (CI) is a surgically implanted electronic device that replaces the mechanical parts of the auditory system by directly stimulating the auditory nerve fibers through electrodes inside the cochlea. Candidates for cochlear implants are people with severe to profound sensorineural hearing loss in both ears and a functioning auditory nervous system. They are used by post-lingually deaf people to regain some comprehension of speech and other sounds as well as by pre-lingually deaf children to enable them to gain spoken language skills. (Diagnosis of hearing loss in newborns and infants is done using otoacoustic emissions, and/or the recording of auditory evoked potentials.) A quite recent evolution is the use of bilateral implants allowing recipients basic sound localization.

4.5.1 Parts of the cochlear implant

The implant is surgically placed under the skin behind the ear. The basic parts of the device include:

External:

- a microphone which picks up sound from the environment
- a speech processor which selectively filters sound to prioritize audible speech and sends the electrical sound signals through a thin cable to the transmitter,
- a transmitter, which is a coil held in position by a magnet placed behind the external ear, and transmits the processed sound signals to the internal device by electromagnetic induction,

Internal:

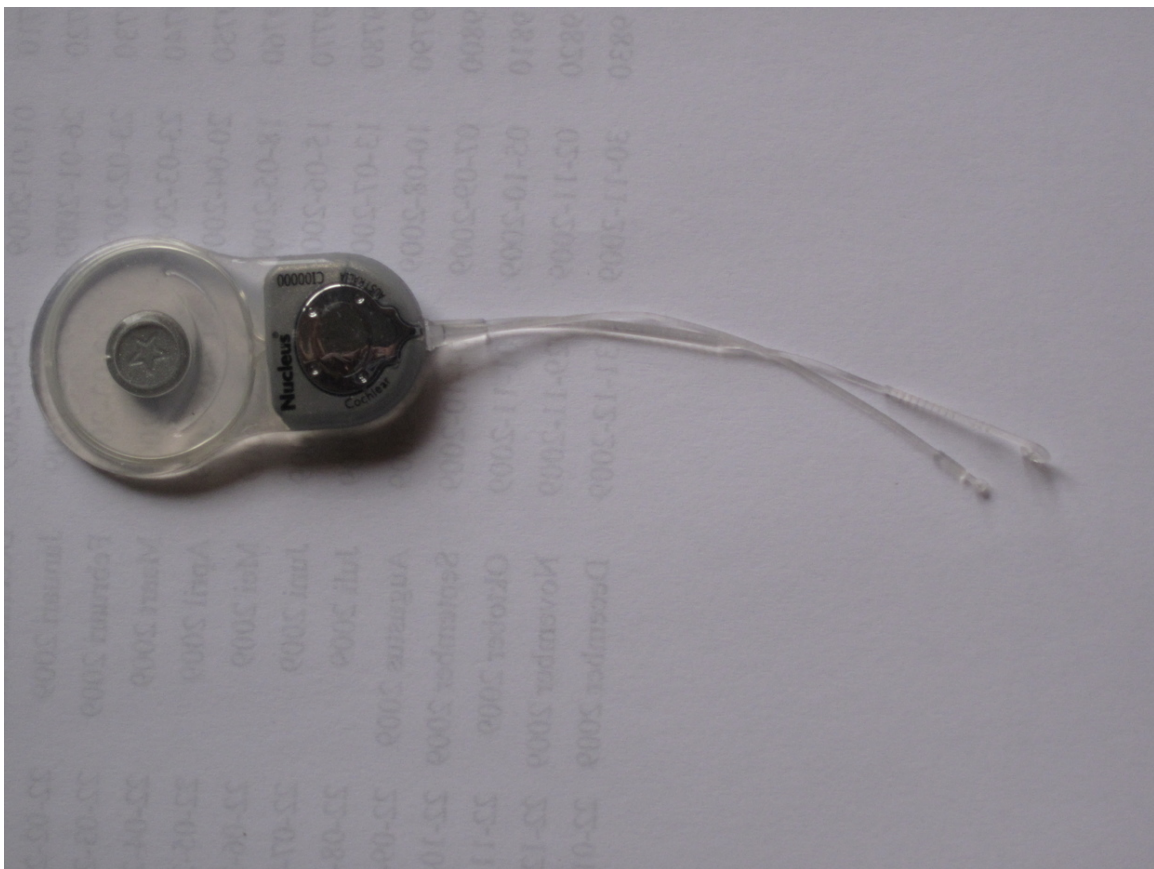


Figure 71 The internal part of a cochlear implant (model Cochlear Freedom 24 RE)

- a receiver and stimulator secured in bone beneath the skin, which converts the signals into electric impulses and sends them through an internal cable to electrodes,
- an array of up to 24 electrodes wound through the cochlea, which send the impulses to the nerves in the scala tympani and then directly to the brain through the auditory nerve system

4.5.2 Signal processing for cochlear implants

In normal hearing subjects, the primary information carrier for speech signals is the envelope, whereas for music, it is the fine structure. This is also relevant for tonal languages, like Mandarin, where the meaning of words depends on their intonation. It was also found that interaural time delays coded in the fine structure determine where a sound is heard from rather than interaural time delays coded in the envelope, although it is still the speech signal coded in the envelope that is perceived.

The speech processor in a cochlear implant transforms the microphone input signal into a parallel array of electrode signals destined for the cochlea. Algorithms for the optimal transfer function between these signals are still an active area of research. The first cochlear implants were single-channel devices. The raw sound was band-passed filtered to include only the frequency range of speech, then modulated onto a 16 kHz wave to allow the electrical signal to electrically couple to the nerves. This approach was able to provide very basic hearing, but was extremely limited in that it was completely unable to take advantage of the frequency-location map of the cochlea.

The advent of multi-channel implants opened the door to try a number of different speech-processing strategies to facilitate hearing. These can be roughly divided into Waveform and Feature-Extraction strategies.

Waveform Strategies

These generally involve applying a non-linear gain on the sound (as an input audio signal with a ~ 30 dB dynamic range must be compressed into an electrical signal with just a ~ 5 dB dynamic range), and passing it through parallel filter banks. The first waveform strategy to be tried was Compressed Analog approach. In this system, the raw audio is initially filtered with a gain-controlled amplifier (the gain-control reduces the dynamic range of the signal). The signal is then passed through parallel band-pass filters, and the output of these filters goes on to stimulate electrodes at their appropriate locations.

A problem with the Compressed Analog approach was that there was a strong interaction-effect between adjacent electrodes. If electrodes driven by two filters happened to be stimulating at the same time, the superimposed stimulation could cause unwanted distortion in the signals coming from hair cells that were within range of both of these electrodes. The solution to this was the Continuous Interleaved Sampling Approach - in which the electrodes driven by adjacent filters stimulate at slightly different times. This eliminates the interference effect between nearby electrodes, but introduces the problem that, due to the interleaving, temporal resolution suffers.

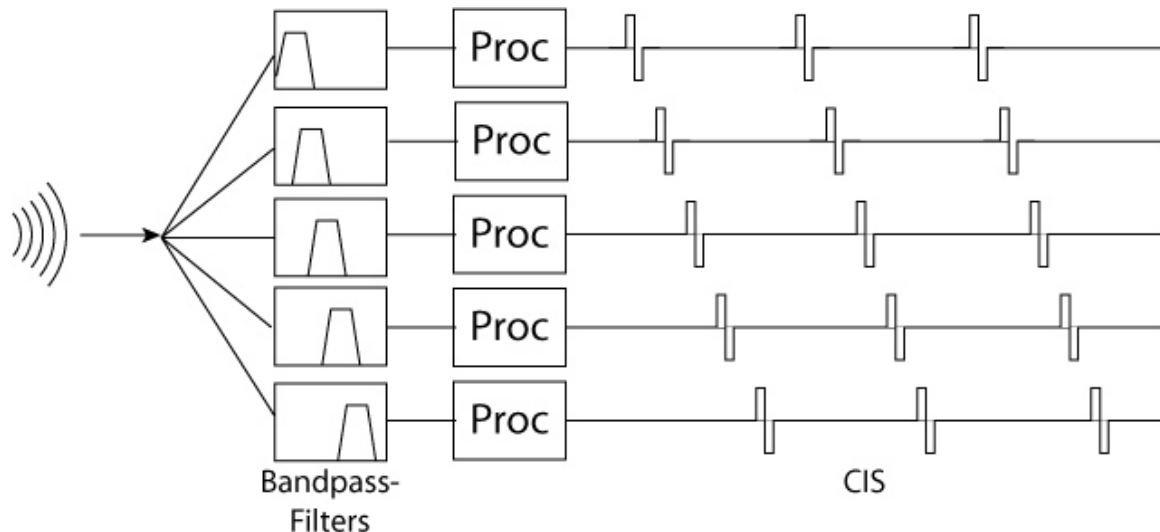


Figure 72 Schematic representation of Continuous Interleaved Sampling (CIS). The processing ("Proc") comprises the envelope detection, amplitude compression, digitization, and pulse modulation.

Feature-Extraction Strategies

These strategies focus less on transmitting filtered versions of the audio signal and more on extracting more abstract features of the signal and transmitting them to the electrodes. The first feature-extraction strategies looked for the formants (frequencies with maximum energy) in speech. In order to do this, they would apply wide band filters (e.g. 270 Hz low-pass for F0 - the base formant, 300 Hz-1 kHz for F1, and 1 kHz-4 kHz for F2), then calculate the formant frequency, using the zero-crossings of each of these filter outputs, and formant-amplitude by looking at the envelope of the signals from each filter. Only electrodes corresponding to these formant frequencies would be activated. The main limitation of this approach was that formants primarily identify vowels, and consonant information, which primarily resides in higher frequencies, was poorly transmitted. The MPEAK system later improved on this design by incorporating high-frequency filters which could better simulate unvoiced sounds (consonants) by stimulating high-frequency electrodes, and formant frequency electrodes at random intervals.¹⁴¹⁵¹⁶

14 <http://www.utdallas.edu/~loizou/cimplants/tutorial/tutorial.htm>

15 www.ohsu.edu/nod/documents/week3/Rubenstein.pdf

16 www.acoustics.bseeber.de/implant/ieee_talk.pdf

4.5.3 Current Developments

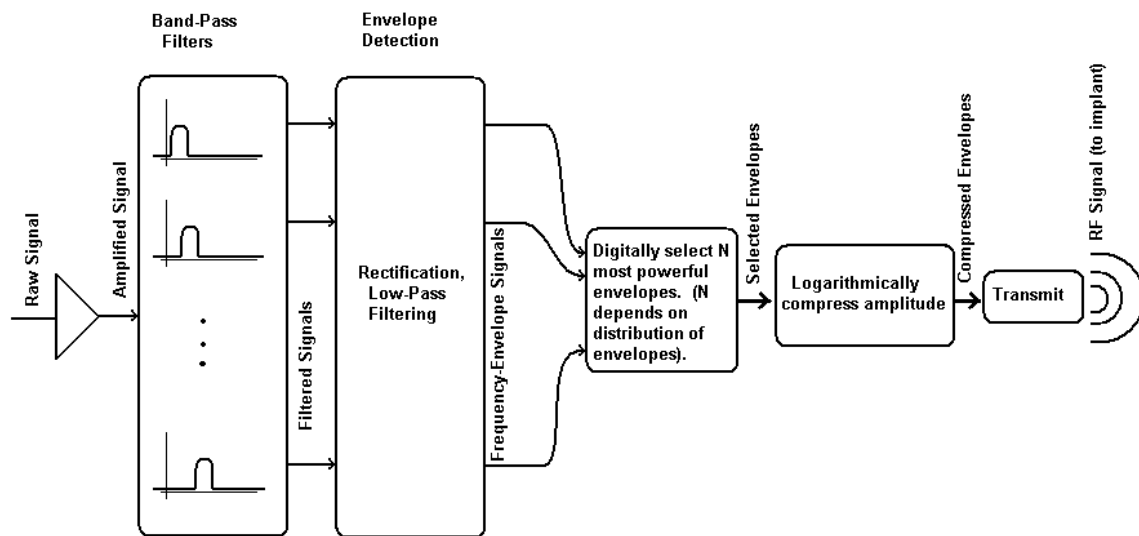


Figure 73 Block diagram of the SPEAK processing scheme

Currently, the leading strategy is the SPEAK system, which combines characteristics of Waveform and Feature-Detection strategies. In this system, the signal passes through a parallel array of 20 band-pass filters. The envelope is extracted from each of these and several of the most powerful frequencies are selected (how many depends on the shape of the spectrum), and the rest are discarded. This is known as a 'n-of-m' strategy. The amplitudes of these are then logarithmically compressed to adapt the mechanical signal range of sound to the much narrower electrical signal range of hair cells.

Multiple microphones

On its newest implants, the company Cochlea uses 3 microphones instead of one. The additional information is used for beam-forming, i.e. extracting more information from sound coming from straight ahead. This can improve the signal-to-noise ratio when talking to other people by up to 15dB, thereby significantly enhancing speech perception in noisy environments.

Integration CI – Hearing Aid

Preservation of low-frequency hearing after cochlear implantation is possible with careful surgical technique and with careful attention to electrode design. For patients with remaining low-frequency hearing, the company MedEl offers a combination of a cochlea implant for the higher frequencies, and classical hearing aid for the lower frequencies. This system, called EAS for electric-acoustic stimulation, uses with a lead of 18mm, compared to 31.5 mm for the full CI. (The length of the cochlea is about 36 mm.) This results in a significant improvement of music perception, and improved speech recognition for tonal languages.

Fine Structure

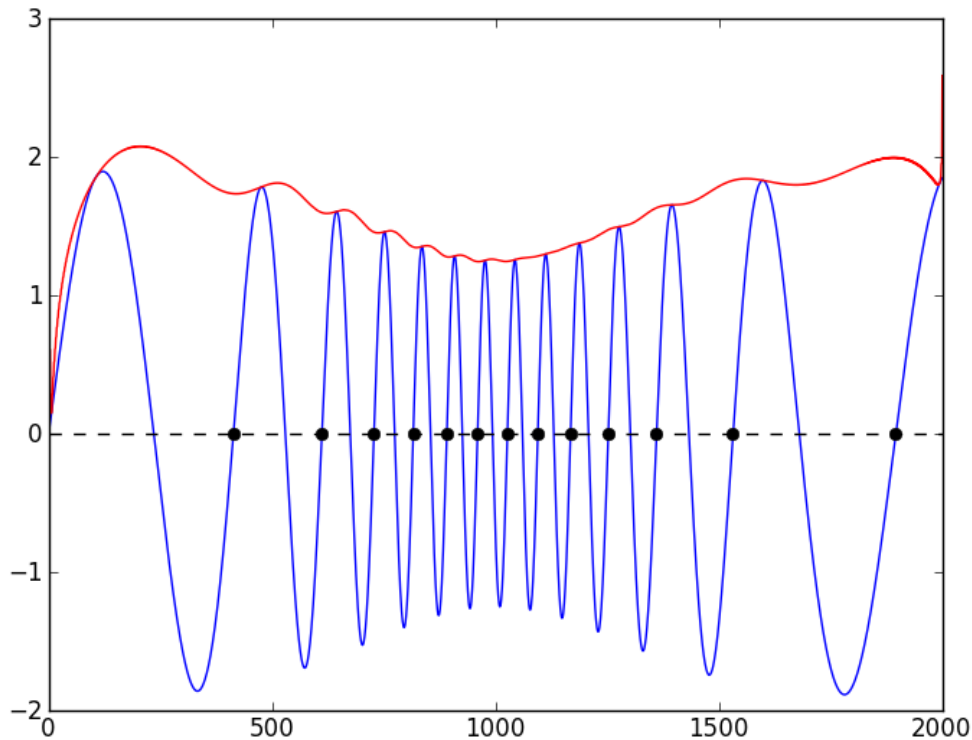


Figure 74 Graph showing how envelope (in red) and phase (black dots, for zero crossings) of a signal can be simply derived with the Hilbert Transform.

For high frequencies, the human auditory system uses only tonotopic coding for information. For low frequencies, however, also temporal information is used: the auditory nerve fires synchronously with the phase of the signal. In contrast, the original CIs only used the power spectrum of the incoming signal. In its new models, MedEl incorporates the timing information for low frequencies, which it calls fine structure, in determining the timing of the stimulation pulses. This improves music perception, and speech perception for tonal languages like Mandarin.

Mathematically, envelope and fine-structure of a signal can be elegantly obtained with the *Hilbert Transform* (see Figure). The corresponding Python code is available under.¹⁷

Virtual Electrodes

The numbers of electrodes available is limited by the size of the electrode (and the resulting charge and current densities), and by the current spread along the endolymph. To increase

¹⁷ Hilbert Transformation [Python] ¹⁸. . Retrieved

the frequency specificity, one can stimulate two adjacent electrodes. Subjects report to perceive this as a single tone at a frequency intermediate to the two electrodes.

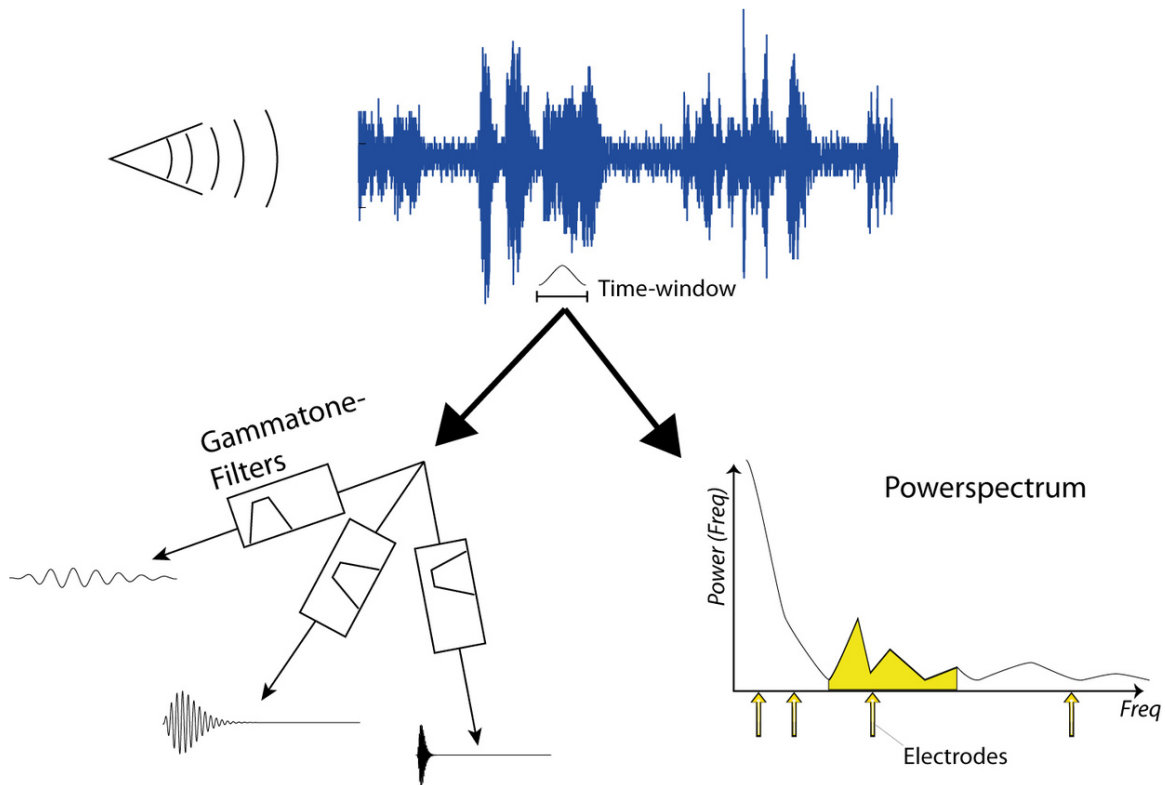


Figure 75 Simulation of the stimulation strength of a cochlear implant

4.5.4 Simulation of a cochlear implant

Sound processing in cochlear implant is still subject to a lot of research and one of the major product differentiations between the manufacturers. However, the basic sound processing is rather simple and can be implemented to gain an impression of the quality of sound perceived by patients using a cochlear implant. The first step in the process is to sample some sound and analyze its frequency. Then a time-window is selected, during which we want to find the stimulation strengths of the CI electrodes. There are two ways to achieve that: i) through the use of linear filters (see *Gammatone filters*¹⁹); or ii) through the calculation of the powerspectrum (see *Spectral Analysis*²⁰).

4.5.5 Cochlear implants and Magnetic Resonance Imaging

With more than 150 000 implantations worldwide, Cochlear Implants (CIs) have now become a standard method for treating severe to profound hearing loss. Since the benefits of CIs

¹⁹ Chapter 4.1 on page 67

²⁰ Chapter 4.1 on page 67

become more evident, payers become more willing to support CIs and due to the screening programs of newborns in most industrialized nations, many patients get CIs in infancy and will likely continue to have them throughout their lives. Some of them may require diagnostic scanning during their lives which may be assisted by imaging studies with Magnetic resonance imaging (MRI). For large segments of the population, including patients suffering from stroke, back pain or headache, MRI has become a standard method for diagnosis. MRI uses pulses of magnetic fields to generate images and current MRI machines are working with 1.5 Tesla magnet fields. 0.2 to 4.0 Tesla devices are common and the radiofrequency power can peak as high as 6 kW in a 1.5 Tesla machine.

Cochlear implants have been historically thought to incompatible with MRI with magnetic fields higher than 0.2 T. The external parts of the device always have to be removed. There are different regulations for the internal parts of the device. Current US Food and Drug Administration (FDA) guidelines allow limited use of MRI after CI implantation. The pulsar and Sonata (MED-EL Corp, Innsbruck, Austria) devices are approved for 0.2 T MRI with the magnet in place. The Hi-res 90K (Advanced Bionics Corp, Sylmar, CA, USA) and the Nucleus Freedom (Cochlear Americas, Englewood, CO, USA) are approved for up to 1.5 T MRI after surgical removal of the internal magnet. Each removal and replacement of the magnet can be done using a small incision under local anesthesia, but the procedure is likely to weaken the pocket of the magnet and to risk infection of the patient.

Cadaver studies have shown that there is a risk that the implant may be displaced from the internal device in a 1.5 T MRI scanner. However, the risk could be eliminated when a compression dressing was applied. Nevertheless, the CI produces an artifact that could potentially reduce the diagnostic value of the scan. The size of the artifact will be larger relative to the size of the patient's head and this might be particularly challenging for MRI scans with children. A recent study by Crane et al., 2010 found out that the artifact around the area of the CI had a mean anterior-posterior dimension of 6.6 ± 1.5 cm (mean \pm standard deviation) and a left-right dimension averaging 4.8 ± 1.0 cm (mean \pm standard deviation) (Crane et al., 2010). ⁽²¹⁾

4.6 Computer Simulations of the Auditory System

4.6.1 Working with Sound

Audio signals can be stored in a variety of formats. They can be uncompressed or compressed, and the encoding can be open or proprietary. On Windows systems, the most common format is the WAV-format. It contains a header with information about the number of channels, sample rate, bits per sample etc. This header is followed by the data themselves. The usual bitstream encoding is the linear pulse-code modulation (LPCM) format.

Many programming languages provide commands for reading and writing WAV-files. When working with data in other formats, you have two options:

21 Crane BT, Gottschalk B, Kraut M, Aygun N, Niparko JK (2010) Magnetic resonance imaging at 1.5 T after cochlear implantation. *Otol Neurotol* 31:1215-1220

- You can either you convert them into WAV-format, and go on from there. A very comprehensive free cross-platform solution to record, convert and stream audio and video is ffmpeg (<http://www.ffmpeg.org/>).
- Or you can obtain special programs moduls for reading/writing the desired format.

4.6.2 Reminder of Fourier Transformations

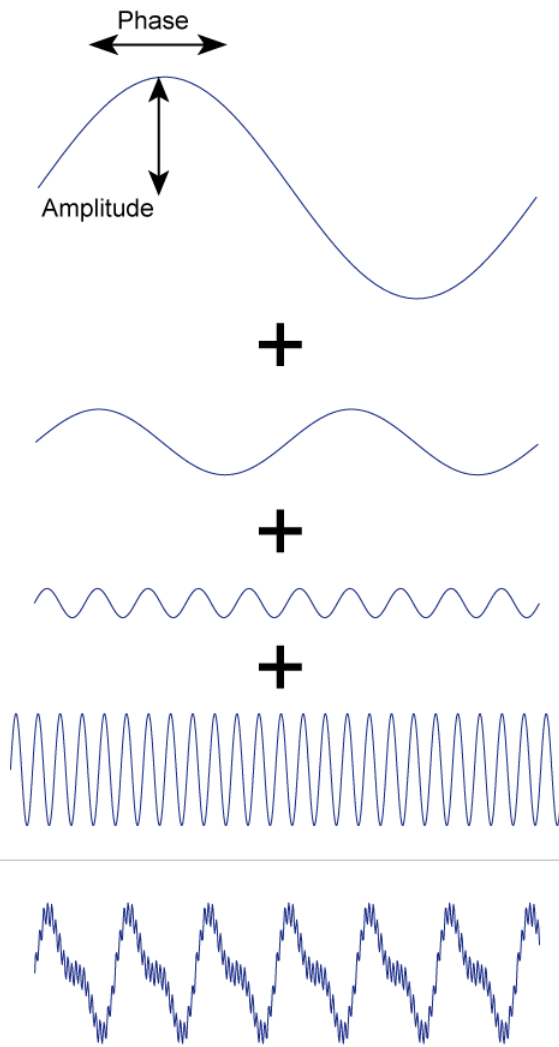
To transform a continuous function, one uses the *Fourier Integral*:

$$F(k) = \int_{-\infty}^{\infty} f(t) \cdot e^{-2\pi ikt} dt$$

where k represents frequency. Note that $F(k)$ is a complex value: its absolute value gives us the amplitude of the function, and its phase defines the phase-shift between cosine and sine components.

The inverse transform is given by

$$f(t) = \int_{-\infty}^{\infty} F(k) \cdot e^{2\pi ikt} dk$$



```
amp = [2 1 .1 .5];
freq = [1 2 10 20];
out = amp * sin(2*pi*freq*t);
```

Figure 76 Fourier Transformation: a sum of sine-waves can make up any repetitive waveform.

If the data are sampled with a constant sampling frequency and there are N data points,

$$f(\tau) = \sum_{n=0}^{N-1} F_n e^{2\pi i n \tau / N}$$

The coefficients F_n can be obtained by

$$F_n = \sum_{\tau=0}^{N-1} f(\tau) \cdot e^{-2\pi i n \tau / N}$$

Since there are a discrete, limited number of data points and with a discrete, limited number of waves, this transform is referred to as *Discrete Fourier Transform (DFT)*. The *Fast Fourier Transform (FFT)* is just a special case of the DFT, where the number of points is a power of 2: $N = 2^n$.

Note that each F_n is a complex number: its magnitude defines to the amplitude of the corresponding frequency component in the signal; and the phase of F_n defines the corresponding phase (see illustration). If the signal in the time domain "f(t)" is real valued, as is the case with most measured data, this puts a constraint on the corresponding frequency components: in that case we have

$$F_n = F_{N-n}^*$$

A frequent source of confusion is the question: "Which frequency corresponds to F_n ?" If there are N data points and the sampling period is " T_s ", the n^{th} frequency is given by

$$f_n = \frac{n}{N \cdot T_s}, 1 \leq n \leq N(\text{in Hz})$$

In other words, the lowest frequency is $\frac{1}{N \cdot T_s}$ [in Hz], while the highest independent frequency is $\frac{1}{2T_s}$ due to the Nyquist-Shannon theorem. Note that in MATLAB, the first return value corresponds to the offset of the function, and the second value to $n=1$!

4.6.3 Spectral Analysis of Biological Signals

Power Spectrum of Stationary Signals

Most FFT functions and algorithms return the complex Fourier coefficients F_n . If we are only interested in the magnitude of the contribution at the corresponding frequency, we can obtain this information by

$$P_n = F_n \cdot F_n^* = |F_n|^2$$

This is the *power spectrum* of our signal, and tells us how big the contribution of the different frequencies is.

Power Spectrum of Non-stationary Signals

Often one has to deal with signals that are changing their characteristics over time. In that case, one wants to know how the power spectrum changes with time. The simplest way is to take only a short segment of data at a time, and calculate the corresponding power spectrum. This approach is called *Short Time Fourier Transform (STFT)*. However in that case edge effects can significantly distort the signals, since we are assuming that our signal is periodic.

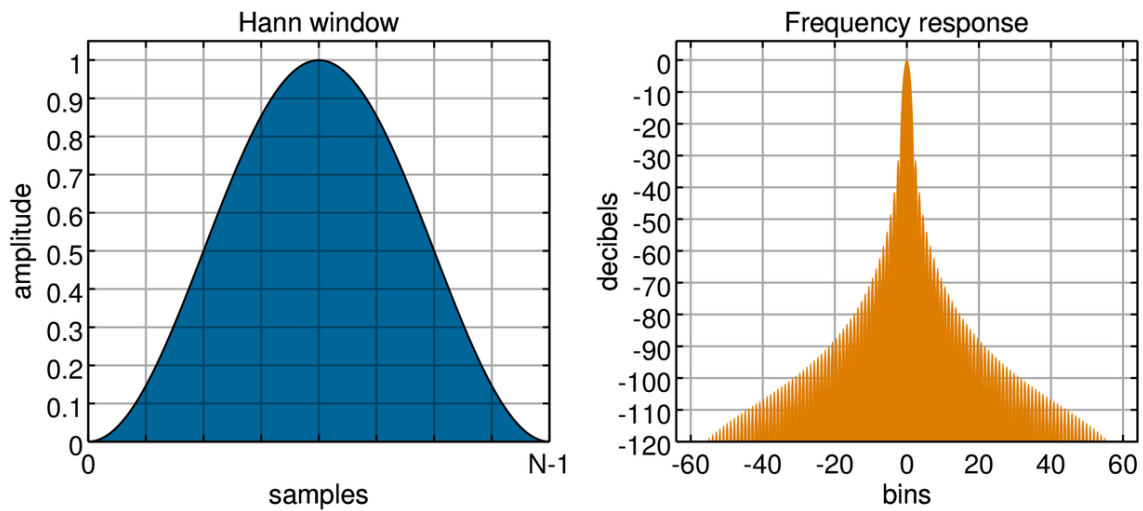


Figure 77 "Hanning window"

To eliminate edge artifacts, the signals can be filtered, or "windowed". An examples of such a window is shown in the figure above. While some windows provide better frequency resolution (e.g. the rectangular window), others exhibit fewer artifacts such as spectral leakage (e.g. Hanning window). For a selected section of the signal, the data resulting from windowing are obtained by multiplying the signal with the window (left Figure):

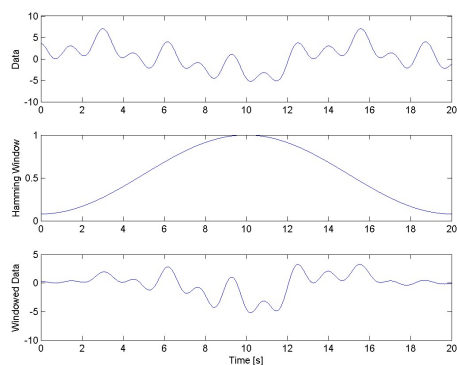


Figure 78 Effects of windowing a signal.

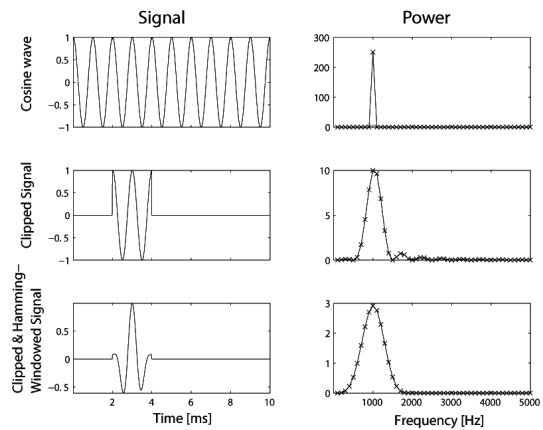


Figure 79

An example can show how cutting a signal, and applying a window to it, can affect the spectral power distribution, is shown in the right figure above. (The corresponding Python code can be found at ²²) Note that decreasing the width of the sample window increases the width of the corresponding powerspectrum!

Stimulation strength for one time window

To obtain the power spectrum for one selected time window, the first step is to calculate

²² Short Time Fourier Transform [Python] ²³. . Retrieved

the power spectrum through the Fast Fourier Transform (FFT) of the time signal. The result is the sound intensity in frequency domain, and the corresponding frequencies. The second step is to concentrate those intensities on a few distinct frequencies ("binning"). The result is a sound signal consisting of a few distinct frequencies - the location of the electrodes in the simulated cochlea. Back conversion into the time domain gives the simulated sound signal for that time window.

The following Python function does sound processing on a given signal.

```
import numpy as np

def pSpect(data, rate):
    ,,,Calculation of power spectrum and corresponding frequencies,
    using a Hamming window,,,
    nData = len(data)
    window = np.hamming(nData)
    fftData = np.fft.fft(data*window)
    PowerSpect = fftData * fftData.conj() / nData
    freq = np.arange(nData) * float(rate) / nData
    return (np.real(PowerSpect), freq)

def calc_stimstrength(sound, rate=1000, sample_freqs=[100, 200,
400]):
    ,,,Calculate the stimulation strength for a given sound,,,

    # Calculate the powerspectrum
    Pxx, freq = pSpect(sound, rate)

    # Generate matrix to sum over the requested bins
    num_electrodes = len(sample_freqs)
    sample_freqs = np.hstack((0, sample_freqs))
    average_freqs = np.zeros([len(freq), num_electrodes])
    for jj in range(num_electrodes):
        average_freqs[((freq>sample_freqs[jj]) *
(freq<sample_freqs[jj+1])),jj] = 1

    # Calculate the stimulation strength (the square root has to be
taken, to get the amplitude)
```

4.6.4 Sound Transduction by Pinna and Outer Ear

The outer ear is divided into two parts: the visible part on the side of the head (the pinna), and the external auditory meatus (outer ear canal) leading to the eardrum, as shown in the figure below. With such a structure, the outer ear contributes the 'spectral cues' for people's sound localization abilities, making people not only have the ability to detect and identify a sound, but also have the ability to localize a sound source. ²⁴

24 M.N. Semple . Auditory perception: Sounds in a virtual world Auditory perception: Sounds in a virtual world . *Nature* , **396** (Nature Publishing Group)(6713):721-724 1998

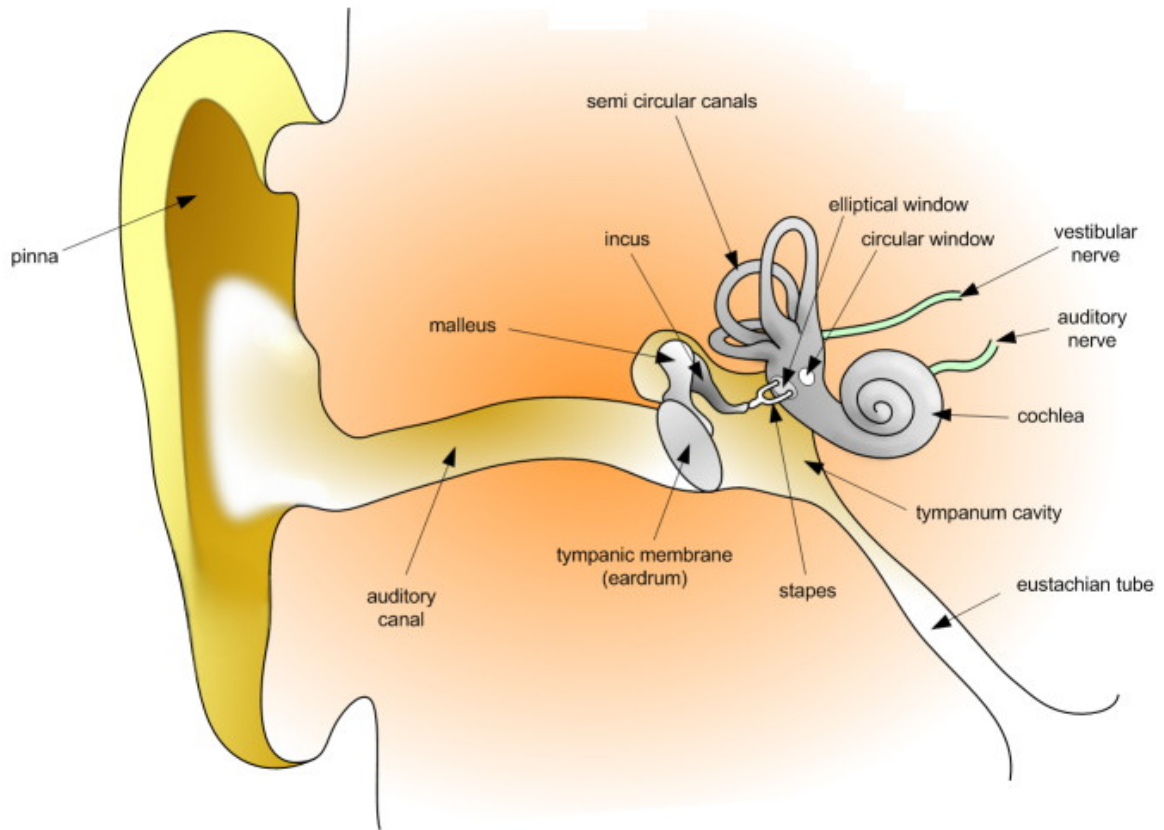


Figure 80 The Anatomy of Human Ear

Pinna Function

The Pinna's cone shape enables it to gather sound waves and funnel them into the out ear canal. On top of that, its various folds make the pinna a resonant cavity which amplifies certain frequencies. Furthermore, the interference effects resulting from the sound reflection caused by the pinna are directionally dependent and will attenuate other frequencies. Therefore, the pinna could be simulated as a filter function applied to the incoming sound, modulating its amplitude and phase spectra.

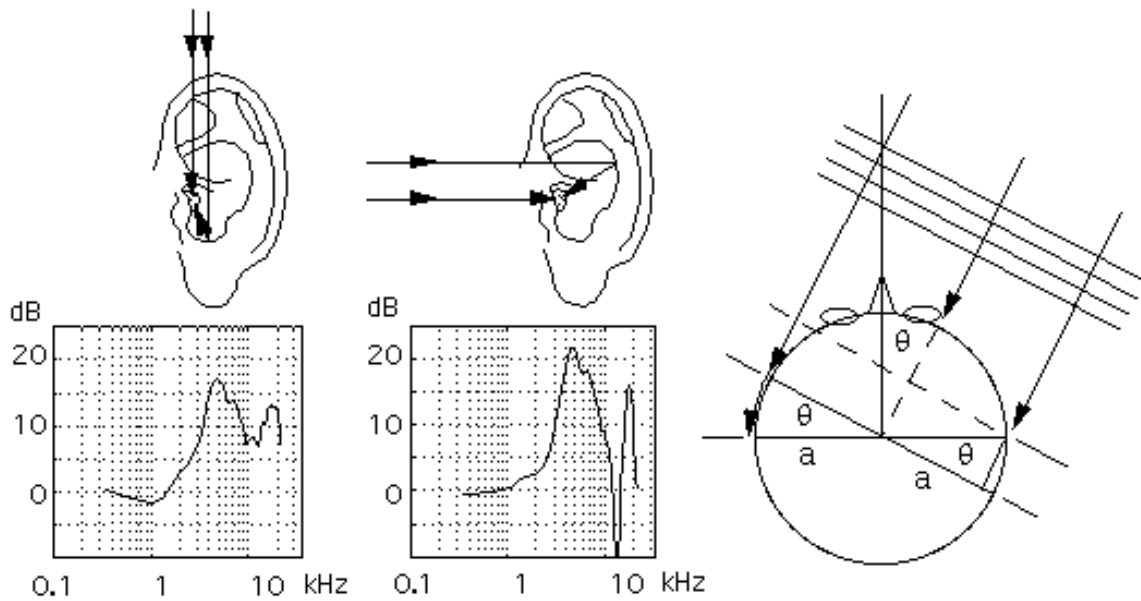


Figure 81 Frequency Responses for Sounds from Two Different Directions by the Pinna ^a

^a http://tav.net/audio/binaural_sound.htm

The resonance of the pinna cavity can be approximated well by 6 normal modes ²⁵. Among these normal modes, the first mode, which mainly depends on the concha depth (i.e. the depth of the bowl-shaped part of the pinna nearest the ear canal), is the dominant one.

The cancellation of certain frequencies caused by the pinna reflection is called “pinna notch”. ²⁶ As shown in the right figure ²⁷, sound transmitted by the pinna goes through two paths, a direct path and a longer reflected path. The different paths have different length, and thereby produce phase differences. When the frequency of incoming sound signal reaches certain criterion, which is that the path difference is half of the sound wavelength, the interference of sounds via direct and reflected paths will be destructive. This phenomenon is called “pinna notch”. Normally the notch frequency could happen in the range from 6k Hz to 16k Hz depending on the pinna shape. It is also seen that the frequency response of pinna is directionally dependent. This makes the pinna contribute to the spatial cues for sound localization.

²⁵ E.A.G. Shaw . Acoustical features of the human ear Acoustical features of the human ear . *Binaural and spatial hearing in real and virtual environments* , **25** (Mahwah, NJ: Lawrence Erlbaum):47 1997

²⁶ E.A.G. Shaw . Acoustical features of the human ear Acoustical features of the human ear . *Binaural and spatial hearing in real and virtual environments* , **25** (Mahwah, NJ: Lawrence Erlbaum):47 1997

Ear Canal Function

The outer ear canal is approximately 25 mm long and 8 mm in diameter, with a tortuous path from the entrance of the canal to the eardrum. The outer ear canal can be modeled as a cylinder closed at one end which leads to a resonant frequency around 3k Hz. This way the outer ear canal amplifies sounds in a frequency range important for human speech. ²⁸

Simulation of Outer Ear

Based on the main functions of the outer ear, it is easy to simulate the sound transduction by the pinna and outer ear canal with a filter, or a filter bank, if we know the characteristics of the filter.

Many researchers are working on the simulation of human auditory system, which includes the simulation of the outer ear. In the next chapter, a *Pinna-Related Transfer Function* model is first introduced, followed by two MATLAB toolboxes developed by Finnish and British research groups, respectively.

Model of Pinna-Related Transfer Function by Spagnol

This part is entirely from the paper published by S.Spagnol, M.Geronazzo, and F.Avanzini. In order to model the functions of the pinna, Spagnol developed a reconstruction model of the Pinna-Related Transfer Function (PRTF), which is a frequency response characterizing how sound is transduced by the pinna. This model is composed by two distinct filter blocks, accounting for resonance function and reflection function of the pinna respectively, as shown in the figure below.

28 Federico Avanzini . Algorithms for sound and music computing, Course Material of Informatica Musicale (http://www.dei.unipd.it/~musica/IM06/Dispense06/4_soundinspace.pdf) Algorithms for sound and music computing, Course Material of Informatica Musicale (http://www.dei.unipd.it/~musica/IM06/Dispense06/4_soundinspace.pdf) . , :4322007-2008

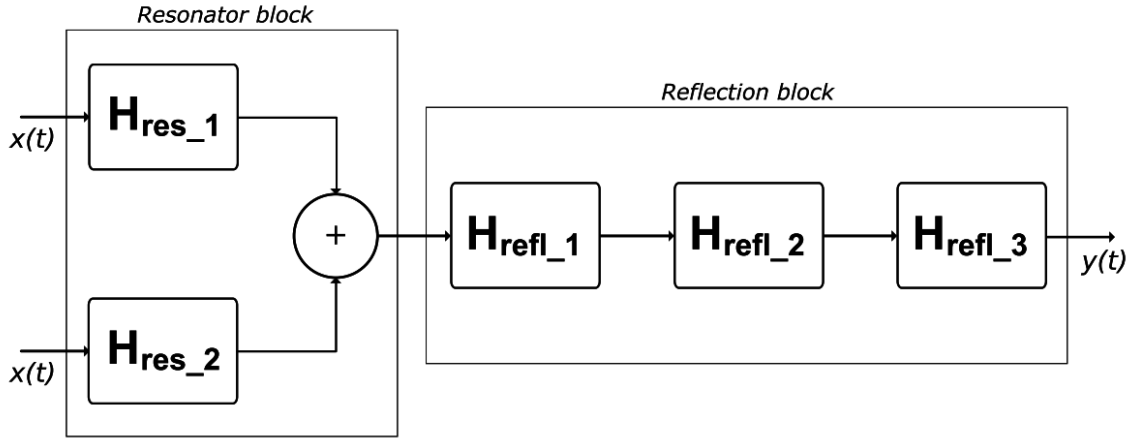


Figure 82 General Model for the Reconstruction of PRTFs^a

^a Spagnol, S. and Geronazzo, M. and Avanzini, F. . Structural modeling of pinna-related transfer functions Structural modeling of pinna-related transfer functions . , 2010

There are two main resonances in the interesting frequency range of the pinna²⁹, which can be represented by two second-order peak filters with fixed bandwidth $f_b = 5kH z^{30}$:

$$H_{res}(z) = \frac{V_0(1-h)(1-z^{-2})}{1+2dhz^{-1}+(2h-1)z^{-2}}$$

where

$$h = \frac{1}{1+\tan(\pi \frac{f_B}{f_s})}$$

$$d = -\cos(2\pi \frac{f_C}{f_s})$$

$$V_0 = 10^{\frac{G}{20}}$$

and f_s is the sampling frequency, f_C the central frequency, and G the notch depth.

For the reflection part, three second-order notch filters of the form³¹ are designed with the parameters including center frequency f_C , notch depth G , and bandwidth f_B .

$$H_{refl}(z) = \frac{1 + (1+k)\frac{H_0}{2} + d(1-k)z^{-1} + (-k - (1+k)\frac{H_0}{2})z^{-2}}{1 + d(1-k)z^{-1} - kz^{-2}}$$

where d is the same as previously defined for the resonance function, and

²⁹ Spagnol, S. and Geronazzo, M. and Avanzini, F. . Structural modeling of pinna-related transfer functions Structural modeling of pinna-related transfer functions . , 2010

³⁰ S. J. Orfanidis, ed., Introduction To Signal Processing. Prentice Hall, 1996.

³¹ U. Zölzer, ed., Digital Audio Effects. New York, NY, USA: J.Wiley & Sons, 2002.

$$V_0 = 10^{\frac{-G}{20}}$$

$$H_0 = V_0 - 1$$

$$k = \frac{\tan(\pi \frac{f_B}{f_s}) - V_0}{\tan(\pi \frac{f_B}{f_s}) + V_0}$$

each accounting for a different spectral notch.

By cascading the three in-series placed notch filters after the parallel two peak filters, an eighth-order filter is designed to model the PRTF.

By comparing the synthetic PRTF with the original one, as shown in the figures below, Spagnol concluded that the synthesis model for PRTF was overall effective. This model may have missing notches due to the limitation of cutoff frequency. Approximation errors may also be brought in due to the possible presence of non-modeled interfering resonances.

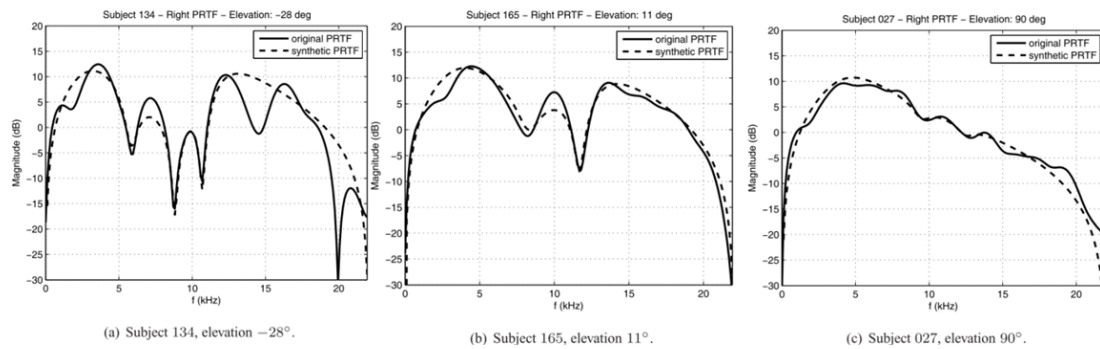


Figure 83 Original vs Synthetic PRTF Plots^a

^a Spagnol, S. and Geronazzo, M. and Avanzini, F. . Structural modeling of pinna-related transfer functions Structural modeling of pinna-related transfer functions . , 2010

HUTear MATLAB Toolbox

Pre-processing: Scale level to some SPL (dB) value
Outer and Middle Ear: ELC, MAF, or MAP correction.
Cochlea: Gammatone or gammachirp filterbank, etc.
Inner Hair Cell: Meddis's model or rectify-compress-filter model, etc.
Neural Adaption: Temporal window model, adaptive nonlinear networks, etc.
Post-processing: Decibels, scaling, detection devices.

Figure 84 Block Diagram of Generic Auditory Model of HUTear

HUTear is a MATLAB Toolbox for auditory modeling developed by Lab of Acoustics and Audio Signal Processing³² at Helsinki University of Technology³³. This open source toolbox could be downloaded from here³⁴. The structure of the toolbox is shown in the right figure.

In this model, there is a block for “Outer and Middle Ear” (OME) simulation. This OME model is developed on the basis of Glasberg and Moor³⁵. The OME filter is usually a linear filter. Auditory filter is generated with taking the "Equal Loudness Curves at 60 dB"(ELC)/"Minimum Audible Field"(MAF)/"Minimum Audible Pressure at ear canal"(MAP) correction into account. This model accounts for the outer ear simulation. By specifying different parameters with the "OEMtool", you may compare the MAP IIR approximation and MAP data, as shown in the figure below.

32 <http://www.acoustics.hut.fi/>

33 <http://www.aalto.fi/en/>

34 <http://www.acoustics.hut.fi/software/HUTear/HUTear2.tar.gz>

35 Glasberg, B.R. and Moore, B.C.J. . Derivation of auditory filter shapes from notched-noise data . *Hearing research* , **47** (Elsevier)(1-2):103-138 1990

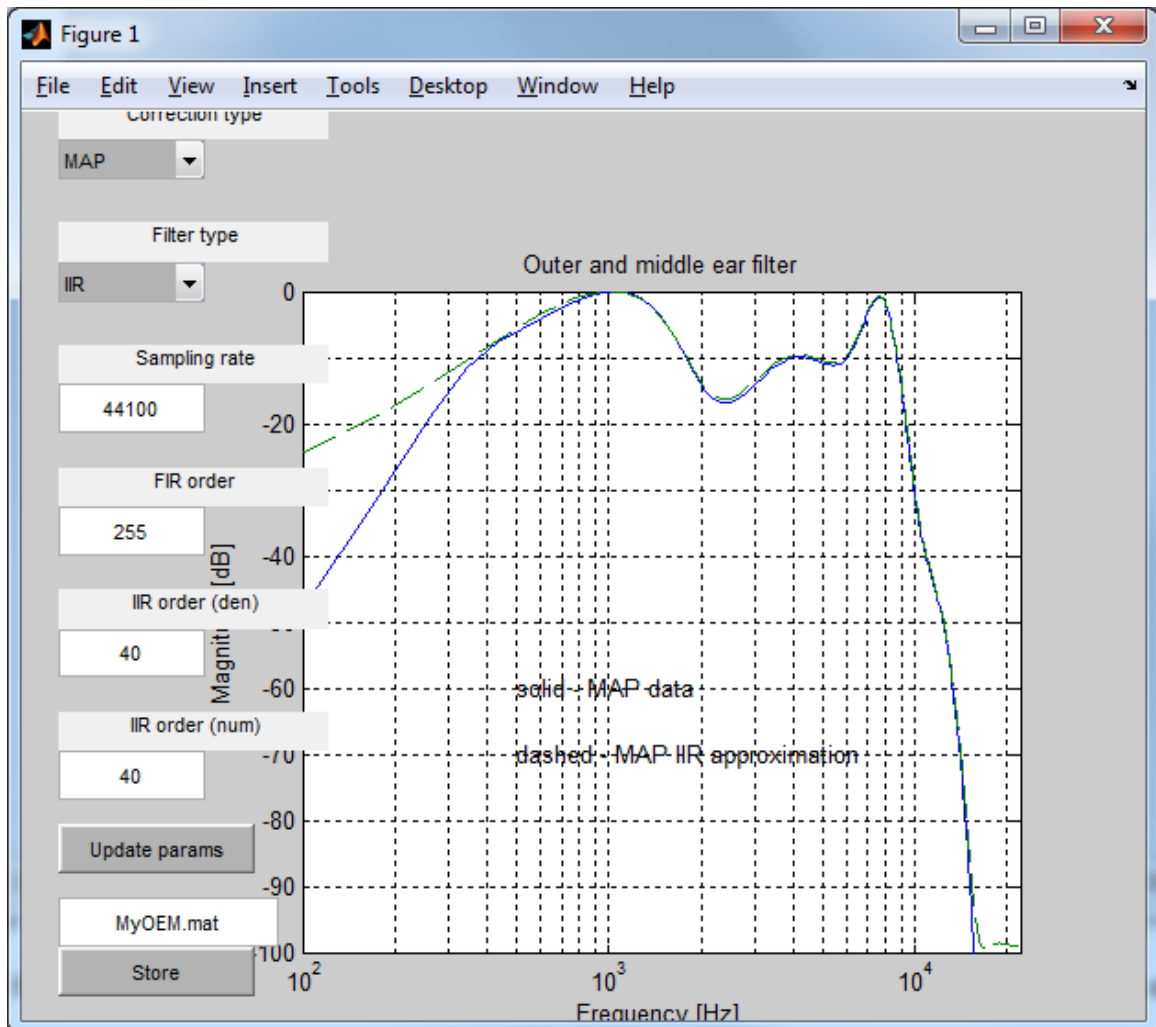


Figure 85 UI of OEMtool from HUTear Toolbox

MATLAB Model of the Auditory Periphery (MAP)

MAP is developed by researchers in the Hearing Research Lab³⁶ at University of Essex³⁷, England. Being a computer model of physiological basis of human hearing, MAP is an open-source code package for testing, developing the model, which could be downloaded from here³⁸. Its model structure is shown in the right figure.

36 <http://www.essex.ac.uk/psychology/department/HearingLab/Welcome.html>

37 <http://www.essex.ac.uk/>

38 http://www.essex.ac.uk/psychology/department/research/hearing_models.html

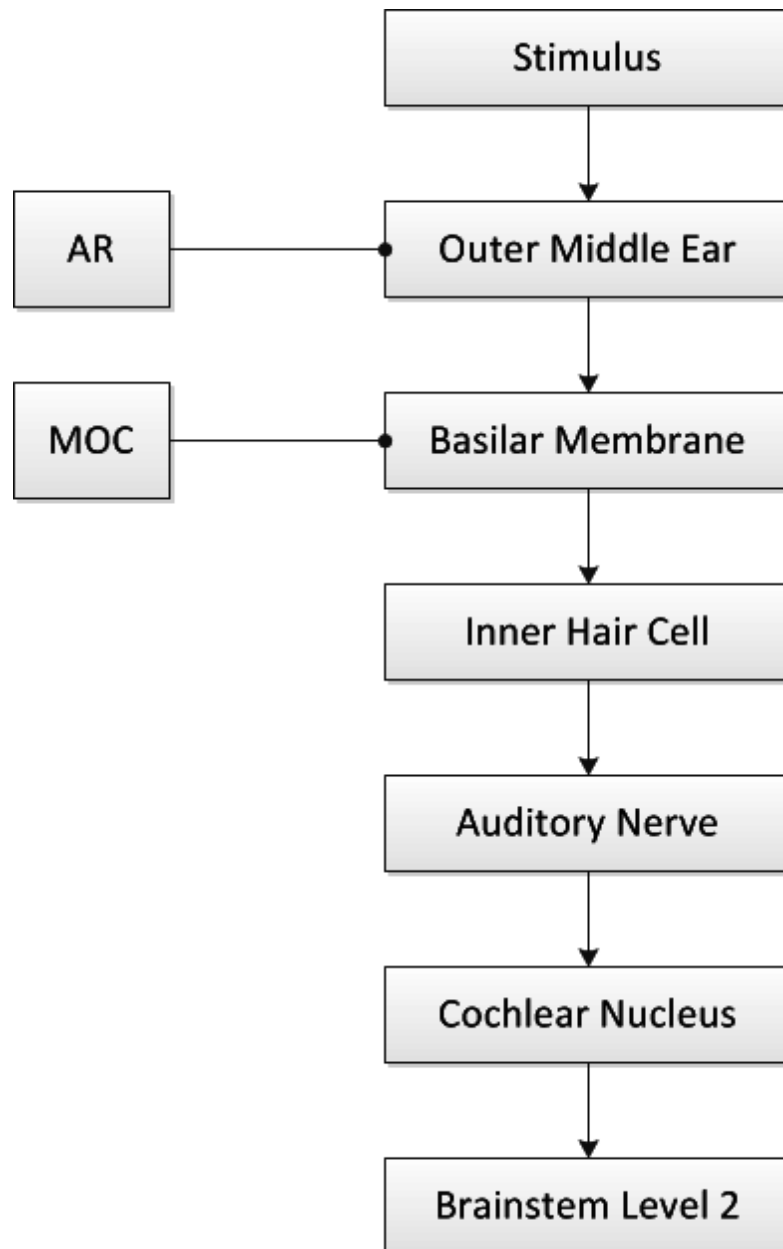


Figure 86 MAP Model Structure

Within the MAP model, there is the “Outer Middle Ear (OME)” sub-model, allowing the user to test and create an OME model. In this OME model, the function of the outer ear is modeled as a resonance function. The resonances are composed by two parallel bandpass filters, respectively, representing concha resonance and outer ear canal resonance. These two filters are specified by the pass frequency range, gain and order. By adding the output of resonance filters to the original sound pressure wave, the output of the outer ear model is obtained.

To test the OME model, run the function named “testOME.m”. A figure plotting the external ear resonances and stapes peak displacement will be displayed. (as shown in the figure below)

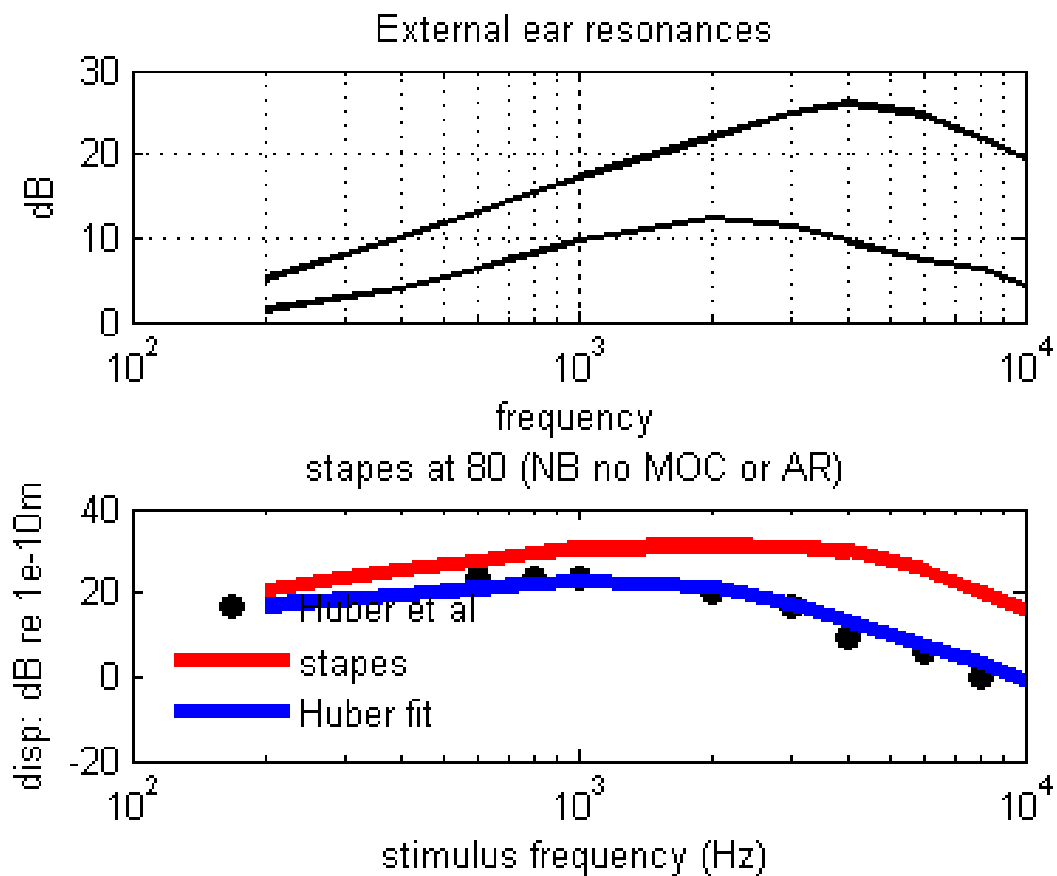


Figure 87 External Ear Resonances and Stapes Peak Displacement from OME Model of MAP

Summary

The outer ear, including pinna and outer ear canal, can be simulated as a linear filter, or a filter bank. This reflects its resonance and reflection effect to incoming sound. It is worth noting that since the pinna shape varies from person to person, the model parameters, like the resonant frequencies, depend on the subject.

One aspect not included in the models described above is the Head-Related Transfer Function(HRTF). The HRTF describes how an ear receives a sound from a point sound source in space. It is not introduced here because it goes beyond the effect of the outer ear (pinna and outer ear canal) as it is also influenced by the effects of head and torso. There

are plenty of literature and publications for HRTF for the interested reader. (wiki³⁹, tutorial 1⁴⁰, 2⁴¹, reading list for spatial audio research including HRTF⁴²)

4.6.5 Simulation of the Inner Ear

The shape and organisation of the basilar membrane means that different frequencies resonate particularly strongly at different points along the membrane. This leads to a tonotopic organisation of the sensitivity to frequency ranges along the membrane, which can be modeled as being an array of overlapping band-pass filters known as "auditory filters".⁴³ The auditory filters are associated with points along the basilar membrane and determine the frequency selectivity of the cochlea, and therefore the listener's discrimination between different sounds.⁴⁴ They are non-linear, level-dependent and the bandwidth decreases from the base to apex of the cochlea as the tuning on the basilar membrane changes from high to low frequency.⁴⁵⁴⁶ The bandwidth of the auditory filter is called the critical bandwidth, as first suggested by Fletcher (1940). If a signal and masker are presented simultaneously then only the masker frequencies falling within the critical bandwidth contribute to masking of the signal. The larger the critical bandwidth the lower the signal-to-noise ratio (SNR) and the more the signal is masked.

39 http://en.wikipedia.org/wiki/Head-related_transfer_function

40 <http://505606.pbworks.com/f/HRTF.pdf>

41 http://www.umiacs.umd.edu/~ramani/cmssc828d_audio/HRTF_INTRO.pdf

42 <https://ccrma.stanford.edu/~malcolm/SpatialAudioLiterature.html>

43 R. Munkong . . . , **25** :98--117 2008

44 Cochlear hearing loss . Whurr Publishers Ltd. , , 1998

45 Cochlear hearing loss . Whurr Publishers Ltd. , , 1998

46 B. C. J. Moore . Parallels between frequency selectivity measured psychophysically and in cochlear mechanics Parallels between frequency selectivity measured psychophysically and in cochlear mechanics . , :129-52 1986

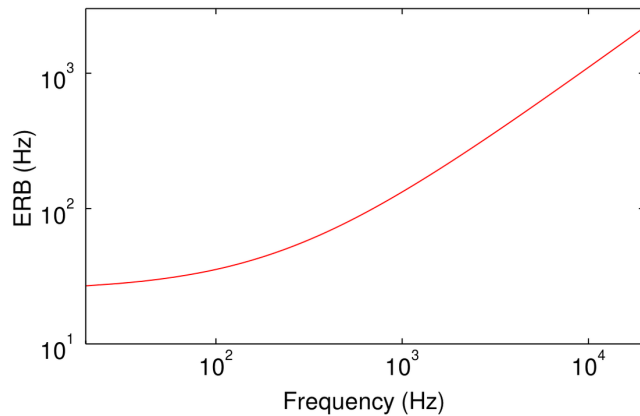


Figure 88 ERB related to centre frequency. The diagram shows the ERB versus centre frequency according to the formula of Glasberg and Moore.^a

^a Cochlear hearing loss . Whurr Publishers Ltd. , , 1998

Another concept associated with the auditory filter is the "equivalent rectangular bandwidth" (ERB). The ERB shows the relationship between the auditory filter, frequency, and the critical bandwidth. An ERB passes the same amount of energy as the auditory filter it corresponds to and shows how it changes with input frequency.⁴⁷ At low sound levels, the ERB is approximated by the following equation according to Glasberg and Moore:⁴⁸

$$ERB = 24.7 * (4.37F + 1)$$

where the ERB is in Hz and F is the centre frequency in kHz.

It is thought that each ERB is the equivalent of around 0.9mm on the basilar membrane.^{49,50}

47 Cochlear hearing loss . Whurr Publishers Ltd. , , 1998

48 Cochlear hearing loss . Whurr Publishers Ltd. , , 1998

49 Cochlear hearing loss . Whurr Publishers Ltd. , , 1998

50 B. C. J. Moore . Parallels between frequency selectivity measured psychophysically and in cochlear mechanics Parallels between frequency selectivity measured psychophysically and in cochlear mechanics . , :129-52 1986

Gammatone Filters

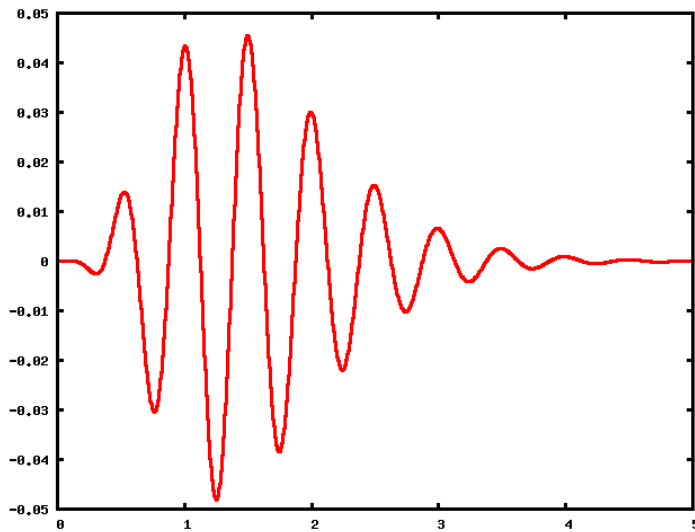


Figure 89 Sample gamma tone impulse response.

One filter type used to model the auditory filters is the "gammatone filter". It provides a simple linear filter for describing the movement of one location of the basilar membrane for a given sound input, which is therefore easy to implement. Linear filters are popular for modeling different aspects of the auditory system. In general, they are IIR-filters (*infinite impulse response*) incorporating feedforward and feedback, which are defined by

$$\sum_{j=0}^m a_{j+1}y(k-j) = \sum_{i=0}^n b_{i+1}x(k-i)$$

where $a_1=1$. In other words, the coefficients a_i and b_j uniquely determine this type of filter. The feedback-character of these filters can be made more obvious by re-shuffling the equation

$$y(k) = b_1x(k) + b_2x(k-1) + \dots + b_{n+1}x(k-n) - (a_2y(k-1) + \dots + a_{m+1}y(k-m))$$

(In contrast, FIR-filters, or *finite impulse response filters*, only involve feedforward: for them $a_i = 0$ for $i > 1$.)

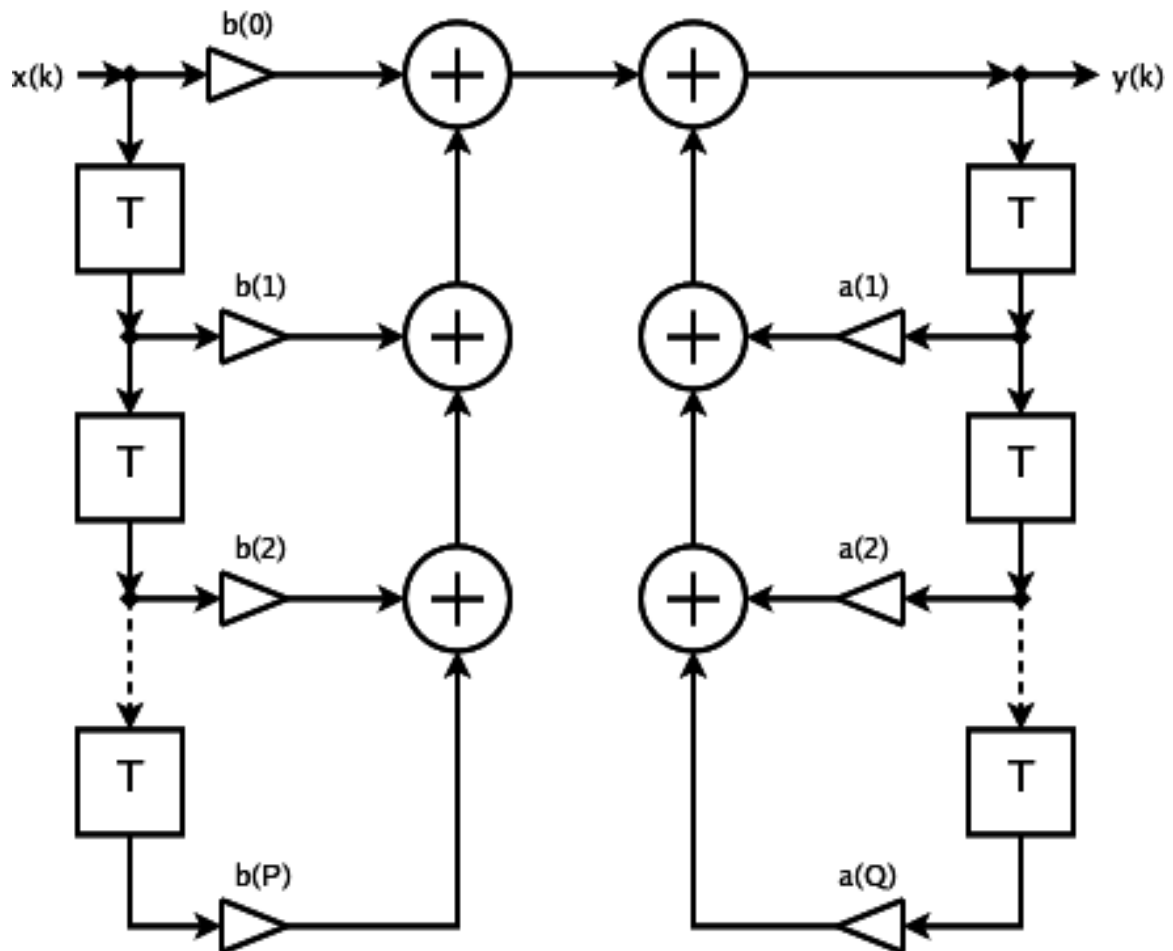


Figure 90 General description of an "Infinite Impulse Response" filter.

Linear filters cannot account for nonlinear aspects of the auditory system. They are nevertheless used in a variety of models of the auditory system. The gammatone impulse response is given by

$$g(t) = at^{n-1}e^{-2\pi bt} \cos(2\pi ft + \phi),$$

where f is the frequency, ϕ is the phase of the carrier, a is the amplitude, n is the filter's order, b is the filter's bandwidth, and t is time.

This is a sinusoid with an amplitude envelope which is a scaled gamma distribution function.

Variations and improvements of the gammatone model of auditory filtering include the gammachirp filter, the all-pole and one-zero gammatone filters, the two-sided gammatone filter, and filter cascade models, and various level-dependent and dynamically nonlinear versions of these.⁵¹

⁵¹ History and Future of Auditory Filter Models ⁵². IEEE . Retrieved

For computer simulations, efficient implementations of gammatone models are available for Matlab and for Python⁵³.

When working with gammatone filters, we can elegantly exploit *Parseval's Theorem* to determine the energy in a given frequency band:

$$\int_{-\infty}^{\infty} |f(t)|^2 dt = \int_{-\infty}^{\infty} |F(\omega)|^2 d\omega$$

4.7 References

⁵³ Gammatone Toolbox [Python]⁵⁴. . Retrieved

5 Vestibular System

5.1 Introduction

The main function of the balance system, or vestibular system, is to sense head movements, especially involuntary ones, and counter them with reflexive eye movements and postural adjustments that keep the visual world stable and keep us from falling. An excellent, more extensive article on the vestibular system is available on Scholarpedia ¹. An extensive review of our current knowledge about the vestibular system can be found in "The Vestibular System: a Sixth Sense" by J Goldberg et al ³.

5.2 Anatomy of the Vestibular System

5.2.1 Labyrinth

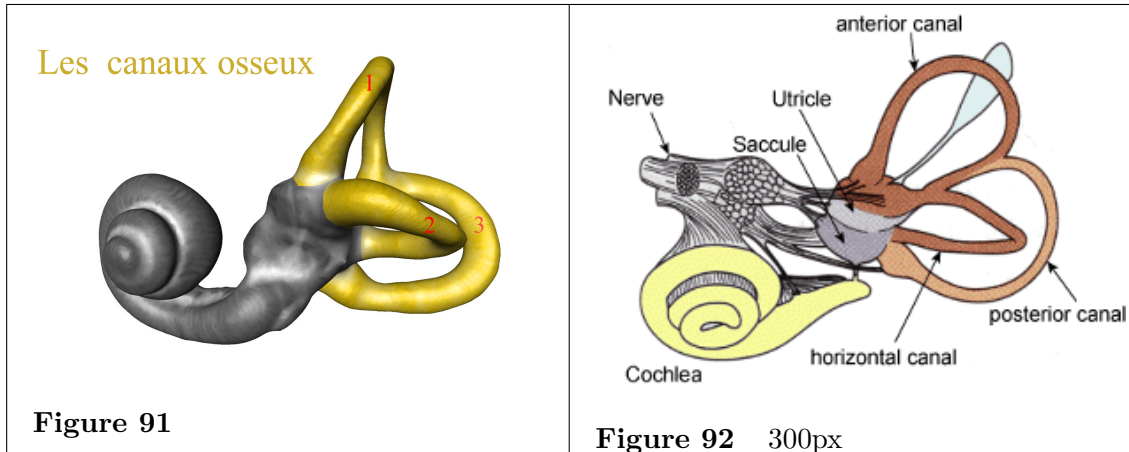
Together with the cochlea, the vestibular system is carried by a system of tubes called the *membranous labyrinth*. These tubes are lodged within the cavities of the bony labyrinth located in the inner ear. A fluid called *perilymph* fills the space between the bone and the membranous labyrinth, while another one called *endolymph* fills the inside of the tubes spanned by the membranous labyrinth. These fluids have a unique ionic composition suited to their function in regulating the electrochemical potential of hair cells, which are as we will later see the transducers of the vestibular system. The electric potential of endolymph is of about 80 mV more positive than perilymph.

Since our movements consist of a combination of linear translations and rotations, the vestibular system is composed of two main parts: The otolith organs, which sense linear accelerations and thereby also give us information about the head's position relative to gravity, and the semicircular canals, which sense angular accelerations.

Human bony labyrinth (Computed tomography 3D)	Internal structure of the human labyrinth
--	--

¹ Vestibular System ². Scholarpedia 3(1):3013 . Retrieved

³ The Vestibular System: a Sixth Sense" ⁴. Oxford University Press, USA . Retrieved



5.2.2 Otoliths

The otolith organs of both ears are located in two membranous sacs called the *utricle* and the *sacculle* which primary sense horizontal and vertical accelerations, respectively. They are located at the central part of the labyrinth, also called the *vestibule* of the ear. Both utricle and sacculle have a thickened portion of the membrane called the *macula*. A gelatinous membrane called the *otolithic membrane* sits atop the macula, and microscopic stones made of calcium carbonate crystal, the otoliths, are embedded on the surface of this membrane. On the opposite side, hair cells embedded in supporting cells project into this membrane.

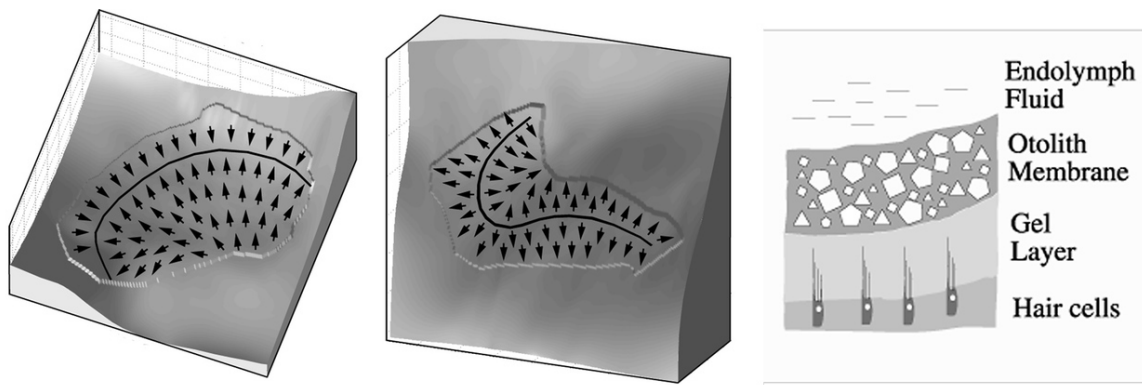


Figure 93 The otoliths are the human sensory organs for linear acceleration. The utricle (left) is approximately horizontally oriented; the sacculle (center) lies approximately vertical. The arrows indicate the local on-directions of the hair cells; and the thick black lines indicate the location of the striola. On the right you see a cross-section through the otolith membrane. The graphs have been generated by Rudi Jaeger, while we cooperated on investigations of the otolith dynamics.

5.2.3 Semicircular Canals

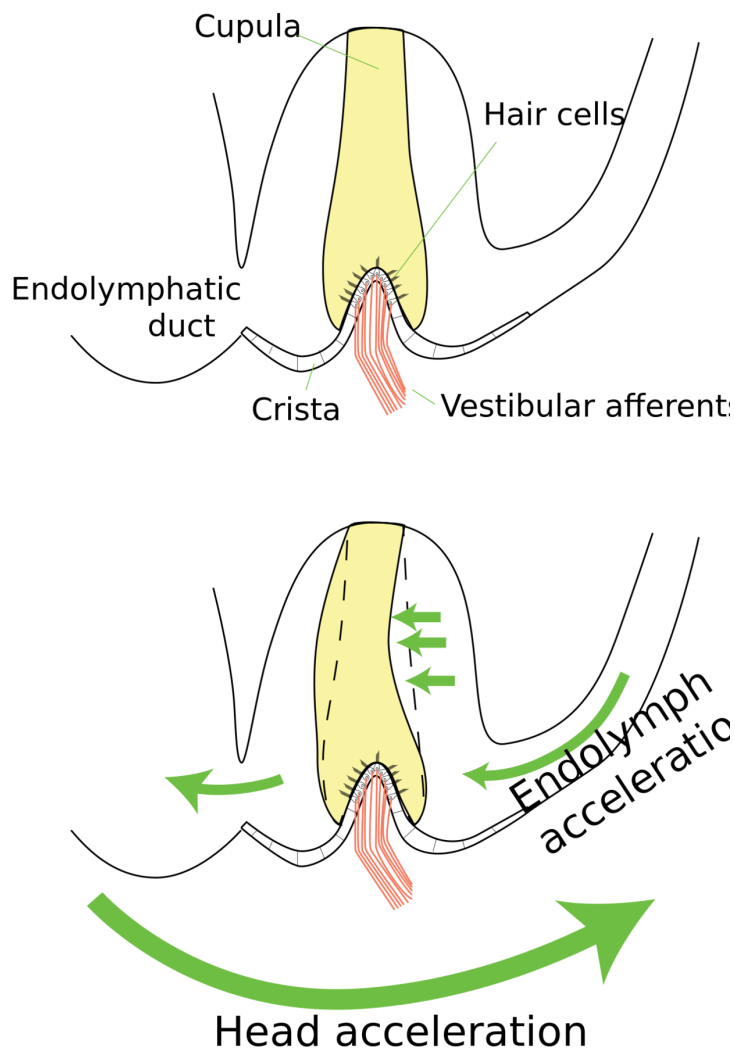


Figure 94 Cross-section through ampulla. Top: The cupula spans the lumen of the ampulla from the crista to the membranous labyrinth. Bottom: Since head acceleration exceeds endolymph acceleration, the relative flow of endolymph in the canal is opposite to the direction of head acceleration. This flow produces a pressure across the elastic cupula, which deflects in response.

Each ear has three semicircular canals. They are half circular, interconnected membranous tubes filled with endolymph and can sense angular accelerations in the three orthogonal planes. The radius of curvature of the human horizontal semicircular canal is 3.2 mm⁵.

5 Curthoys IS and Oman CM . Dimensions of the horizontal semicircular duct, ampulla and utricle in the human. Dimensions of the horizontal semicircular duct, ampulla and utricle in the human. . *Acta Otolaryngol* , **103** : 254–261 1987

The canals on each side are approximately orthogonal to each other. The orientation of the on-directions of the canals on the right side are ⁶:

Canal	X	Y	Z
Horizontal	0.32269	-0.03837	-0.94573
Anterior	0.58930	0.78839	0.17655
Posterior	0.69432	-0.66693	0.27042

(The axes are oriented such that the positive x-,y-,and z-axis point forward, left, and up, respectively. The horizontal plane is defined by Reid's line, the line connecting the lower rim of the orbita and the center of the external auditory canal. And the directions are such that a rotation about that vector, according to the right-hand-rule, excites the corresponding canal.) The *anterior and posterior semicircular canals* are approximately vertical, and the *horizontal semicircular canals* approximately horizontal. Each canal presents a dilatation at one end, called the *ampulla*. Each membranous ampulla contains a saddle-shaped ridge of tissue, the *crista*, which extends across it from side to side. It is covered by neuroepithelium, with hair cells and supporting cells. From this ridge rises a gelatinous structure, the *cupula*, which extends to the roof of the ampulla immediately above it, dividing the interior of the ampulla into two approximately equal parts.

5.2.4 Haircells

The sensors within both the otolith organs and the semicircular canals are the *hair cells*. They are responsible for the transduction of a mechanical force into an electrical signal and thereby build the interface between the world of accelerations and the brain.

6 Della Santina CC, Potyagaylo V, Migliaccio A, Minor LB, Carey JB . Orientation of Human Semicircular Canals Measured by Three-Dimensional Multi-planar CT Reconstruction. Orientation of Human Semicircular Canals Measured by Three-Dimensional Multi-planar CT Reconstruction. . *J Assoc Res Otolaryngol* , **6(3)** : 191-206 2005

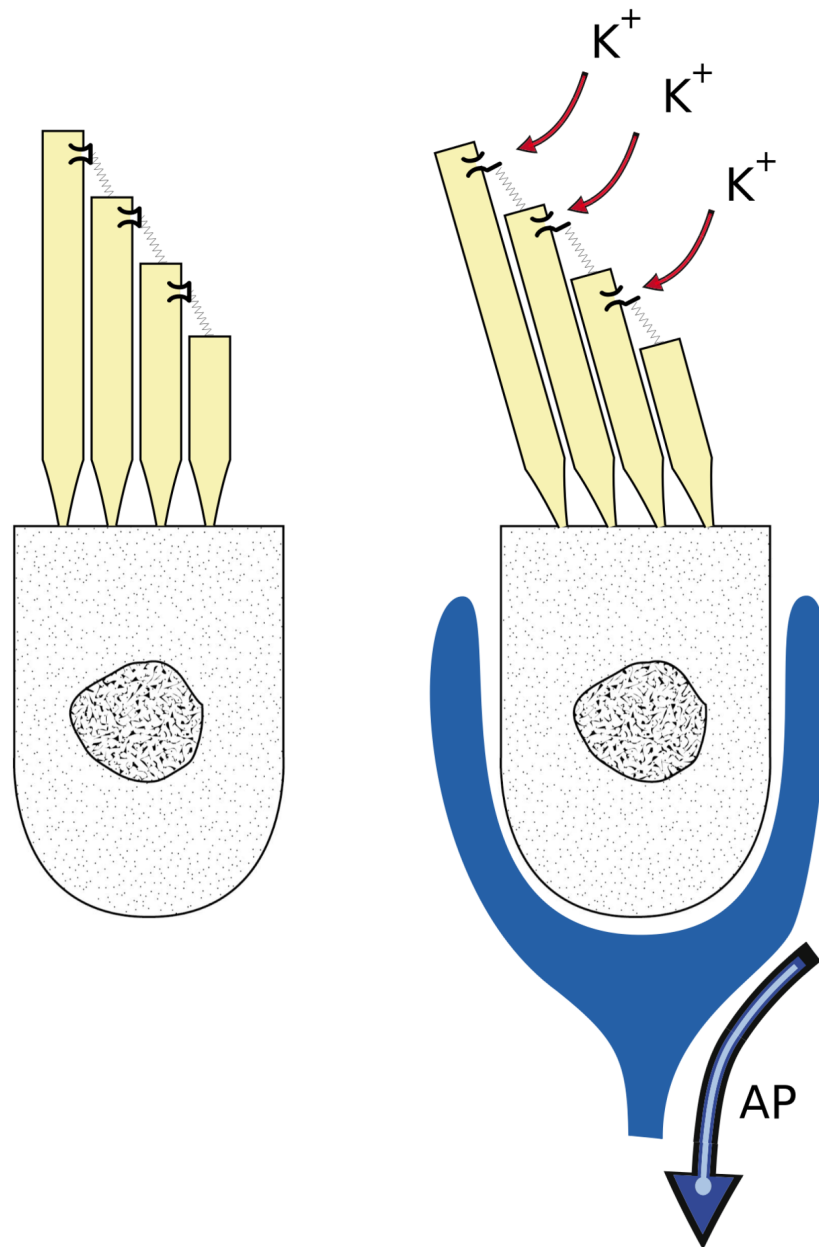


Figure 95 200px

Hair cells have a tuft of *stereocilia* that project from their apical surface. The thickest and longest stereocilia is the *kinocilium*. Stereocilia deflection is the mechanism by which all hair cells transduce mechanical forces. Stereocilia within a bundle are linked to one another by protein strands, called *tip links*, which span from the side of a taller stereocilium to the tip of its shorter neighbor in the array. Under deflection of the bundle, the tip links act as gating springs to open and close mechanically sensitive ion channels. *Afferent nerve excitation* works basically the following way: when all cilia are deflected toward the kinocilium, the gates open and cations, including potassium ions from the potassium rich endolymph, flow in and the membrane potential of the hair cell becomes more positive (depolarization). The hair cell itself does not fire action potentials. The depolarization activates voltage-sensitive

calcium channels at the basolateral aspect of the cell. Calcium ions then flow in and trigger the release of neurotransmitters, mainly glutamate, which in turn diffuse across the narrow space between the hair cell and a nerve terminal, where they then bind to receptors and thus trigger an increase of the action potentials firing rate in the nerve. On the other hand, *afferent nerve inhibition* is the process induced by the bending of the stereocilia away from the kinocilium (hyperpolarization) and by which the firing rate is decreased. Because the hair cells are chronically leaking calcium, the vestibular afferent nerve fires actively at rest and thereby allows the sensing of both directions (increase and decrease of firing rate). Hair cells are very sensitive and respond extremely quickly to stimuli. The quickness of hair cell response may in part be due to the fact that they must be able to release neurotransmitter reliably in response to a threshold receptor potential of only 100 μV or so.

Regular and Irregular Haircells

While afferent haircells in the auditory system are fairly homogeneous, those in the vestibular system can be broadly separated into two groups: "regular units" and "irregular units". Regular haircells have approximately constant interspike intervals, and fire constantly proportional to their displacement. In contrast, the inter-spike interval of irregular haircells is much more variable, and their discharge rate increases with increasing frequency; they can thus act as event detectors at high frequencies. Regular and irregular haircells also differ in their location, morphology and innervation.

5.3 Signal Processing

5.3.1 Peripheral Signal Transduction

Transduction of Linear Acceleration

The hair cells of the otolith organs are responsible for the transduction of a mechanical force induced by linear acceleration into an electrical signal. Since this force is the product of gravity plus linear movements of the head

$$\vec{F} = \vec{F}_g + \vec{F}_{inertial} = m(\vec{g} - \frac{d^2\vec{x}}{dt^2})$$

it is therefore sometimes referred to as *gravito-inertial force*. The mechanism of transduction works roughly as follows: The *otoconia*, calcium carbonate crystals in the top layer of the otoconia membrane, have a higher specific density than the surrounding materials. Thus a linear acceleration leads to a displacement of the otoconia layer relative to the connective tissue. The displacement is sensed by the hair cells. The bending of the hairs then polarizes the cell and induces afferent excitation or inhibition.

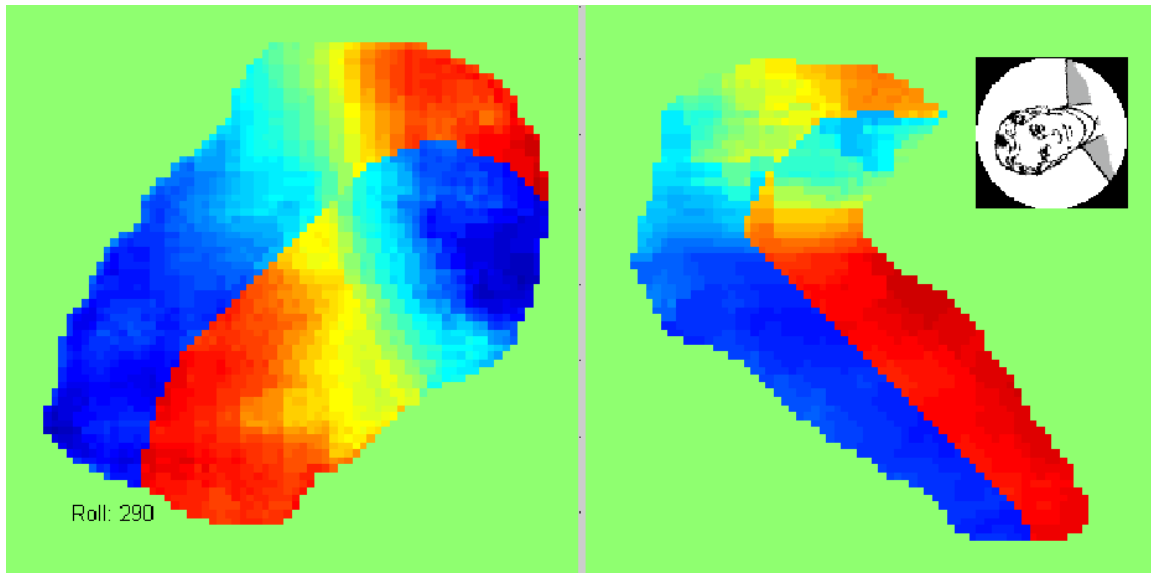


Figure 96 Excitation (red) and inhibition (blue) on utricle (left) and saccule (right), when the head is in a right-ear-down orientation. The displacement of the otoliths was calculated with the finite element technique, and the orientation of the haircells was taken from the literature.

While each of the three semicircular canals senses only one-dimensional component of rotational acceleration, linear acceleration may produce a complex pattern of inhibition and excitation across the maculae of both the utricle and saccule. The saccule is located on the medial wall of the vestibule of the labyrinth in the spherical recess and has its macula oriented vertically. The utricle is located above the saccule in the elliptical recess of the vestibule, and its macula is oriented roughly horizontally when the head is upright. Within each macula, the kinocilia of the hair cells are oriented in all possible directions.

Therefore, under linear acceleration with the head in the upright position, the saccular macula is sensing acceleration components in the vertical plane, while the utricular macula is encoding acceleration in all directions in the horizontal plane. The otolithic membrane is soft enough that each hair cell is deflected proportional to the local force direction. If \vec{n} denotes the direction of maximum sensitivity or *on-direction* of the hair cell, and the gravito-inertial force, the stimulation by static accelerations is given by

$$stim_{otolith} = \vec{F} \cdot \vec{n}$$

The direction and magnitude of the total acceleration is then determined from the excitation pattern on the otolith maculae.

Transduction of Angular Acceleration

The three semicircular canals are responsible for the sensing of angular accelerations. When the head accelerates in the plane of a semicircular canal, inertia causes the endolymph in the canal to lag behind the motion of the membranous canal. Relative to the canal walls, the

endolymph effectively moves in the opposite direction as the head, pushing and distorting the elastic cupula. Hair cells are arrayed beneath the cupula on the surface of the crista and have their stereocilia projecting into the cupula. They are therefore excited or inhibited depending on the direction of the acceleration.

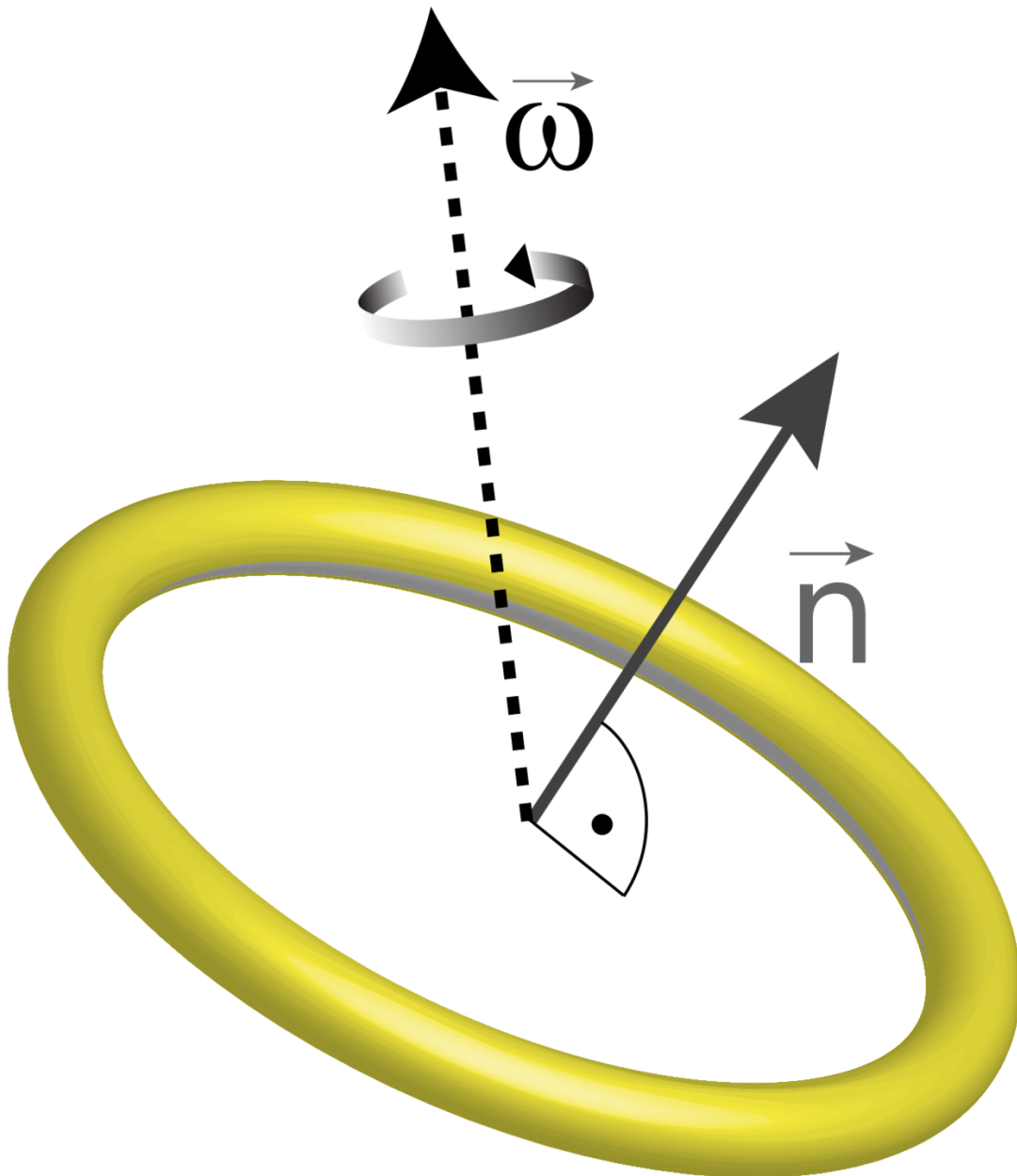


Figure 97 The stimulation of a human semicircular canal is proportional to the scalar product between a vector \vec{n} (which is perpendicular to the plane of the canal), and the vector $\vec{\omega}$ indicating the angular velocity.

This facilitates the interpretation of canal signals: if the orientation of a semicircular canal is described by the unit vector \vec{n} , the stimulation of the canal is proportional to the projection of the angular velocity $\vec{\omega}$ onto this canal

$$stim_{canal} = \vec{\omega} \cdot \vec{n}$$

The horizontal semicircular canal is responsible for sensing accelerations around a vertical axis, i.e. the neck. The anterior and posterior semicircular canals detect rotations of the head in the sagittal plane, as when nodding, and in the frontal plane, as when cartwheeling.

In a given cupula, all the hair cells are oriented in the same direction. The semicircular canals of both sides also work as a push-pull system. For example, because the right and the left horizontal canal cristae are “mirror opposites” of each other, they always have opposing (*push-pull principle*) responses to horizontal rotations of the head. Rapid rotation of the head toward the left causes depolarization of hair cells in the left horizontal canal's ampulla and increased firing of action potentials in the neurons that innervate the left horizontal canal. That same leftward rotation of the head simultaneously causes a hyperpolarization of the hair cells in the right horizontal canal's ampulla and decreases the rate of firing of action potentials in the neurons that innervate the horizontal canal of the right ear. Because of this mirror configuration, not only the right and left horizontal canals form a push-pull pair but also the right anterior canal with the left posterior canal (RALP), and the left anterior with the right posterior (LARP).

5.3.2 Central Vestibular Pathways

The information resulting from the vestibular system is carried to the brain, together with the auditory information from the cochlea, by the *vestibulocochlear nerve*, which is the eighth of twelve cranial nerves. The cell bodies of the bipolar afferent neurons that innervate the hair cells in the maculae and cristae in the vestibular labyrinth reside near the internal auditory meatus in the vestibular ganglion (also called Scarpa's ganglion, Figure Figure 10.1). The centrally projecting axons from the vestibular ganglion come together with axons projecting from the auditory neurons to form the eighth nerve, which runs through the internal auditory meatus together with the facial nerve. The primary afferent vestibular neurons project to the four vestibular nuclei that constitute the *vestibular nuclear complex* in the brainstem.

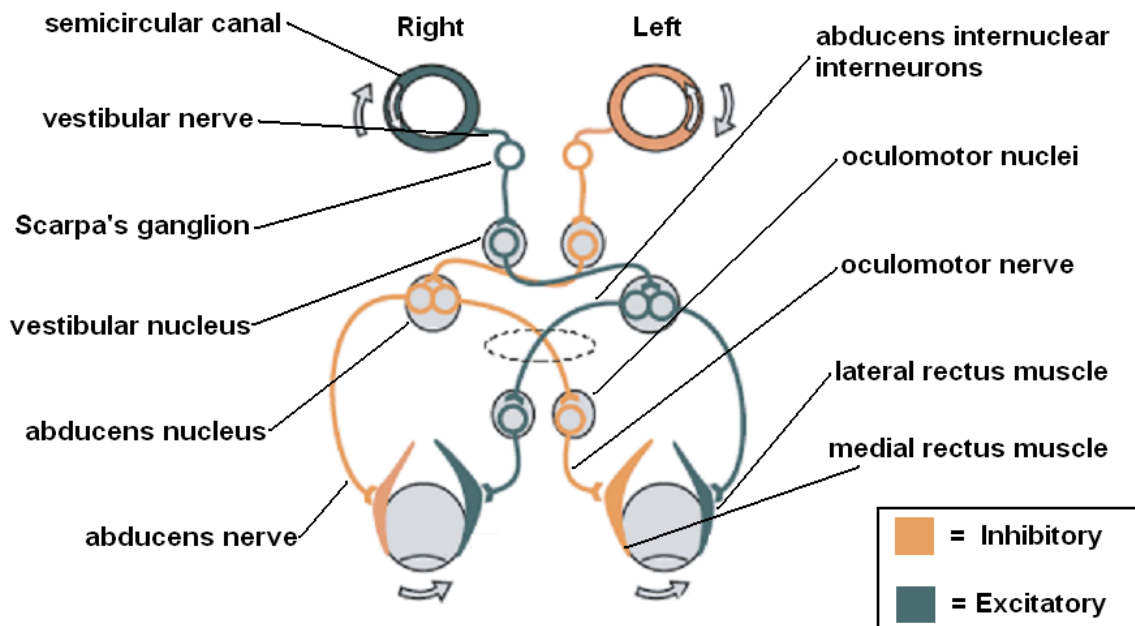


Figure 98 Vestibulo-ocular reflex.

5.3.3 Vestibulo-Ocular Reflex (VOR)

An extensively studied example of function of the vestibular system is the *vestibulo-ocular reflex* (VOR). The function of the VOR is to stabilize the image during rotation of the head. This requires the maintenance of stable eye position during horizontal, vertical and torsional head rotations. When the head rotates with a certain speed and direction, the eyes rotate with the same speed but in the opposite direction. Since head movements are present all the time, the VOR is very important for stabilizing vision.

How does the VOR work? The vestibular system signals how fast the head is rotating and the oculomotor system uses this information to stabilize the eyes in order to keep the visual image motionless on the retina. The vestibular nerves project from the vestibular ganglion to the vestibular nuclear complex, where the vestibular nuclei integrate signals from the vestibular organs with those from the spinal cord, cerebellum, and the visual system. From these nuclei, fibers cross to the contralateral abducens nucleus. There they synapse with two additional pathways. One pathway projects directly to the lateral rectus muscle of eye via the abducens nerve. Another nerve tract projects from the abducens nucleus by the abducens interneurons to the oculomotor nuclei, which contain motor neurons that drive eye muscle activity, specifically activating the medial rectus muscles of the eye through the oculomotor nerve. This short latency connection is sometimes referred to as *three-neuron-arc*, and allows an eye movement within less than 10 ms after the onset of the head movement.

For example, when the head rotates rightward, the following occurs. The right horizontal canal hair cells depolarize and the left hyperpolarize. The right vestibular afferent activity therefore increases while the left decreases. The vestibulocochlear nerve then carries this information to the brainstem and the right vestibular nuclei activity increases while the left

decreases. This makes in turn neurons of the left abducens nucleus and the right oculomotor nucleus fire at higher rate. Those in the left oculomotor nucleus and the right abducens nucleus fire at a lower rate. This results in the fact that the left lateral rectus extraocular muscle and the right medial rectus contract while the left medial rectus and the right lateral rectus relax. Thus, both eyes rotate leftward.

The *gain* of the VOR is defined as the change in the eye angle divided by the change in the head angle during the head turn

$$gain = \frac{\Delta_{Eye}}{\Delta_{Head}}$$

If the gain of the VOR is wrong, that is, different than one, then head movements result in image motion on the retina, resulting in blurred vision. Under such conditions, motor learning adjusts the gain of the VOR to produce more accurate eye motion. Thereby the cerebellum plays an important role in motor learning.

5.3.4 The Cerebellum and the Vestibular System

It is known that postural control can be adapted to suit specific behavior. Patient experiments suggest that the cerebellum plays a key role in this form of *motor learning*. In particular, the role of the cerebellum has been extensively studied in the case of adaptation of vestibulo-ocular control. Indeed, it has been shown that the gain of the vestibulo-ocular reflex adapts to reach the value of one even if damage occur in a part of the VOR pathway or if it is voluntarily modified through the use of magnifying lenses. Basically, there are two different hypotheses about how the cerebellum plays a necessary role in this adaptation. The first from (Ito 1972; Ito 1982) claims that the cerebellum itself is the site of learning, while the second from Miles and Lisberger (Miles and Lisberger 1981) claims that the vestibular nuclei are the site of adaptive learning while the cerebellum constructs the signal that drives this adaptation. Note that in addition to direct excitatory input to the vestibular nuclei, the sensory neurons of the vestibular labyrinth also provide input to the Purkinje cells in the flocculo-nodular lobes of the cerebellum via a pathway of mossy and parallel fibers. In turn, the Purkinje cells project an inhibitory influence back onto the vestibular nuclei. Ito argued that the gain of the VOR can be adaptively modulated by altering the relative strength of the direct excitatory and indirect inhibitory pathways. Ito also argued that a message of retinal image slip going through the inferior olivary nucleus carried by the climbing fiber plays the role of an error signal and thereby is the modulating influence of the Purkinje cells. On the other hand, Miles and Lisberger argued that the brainstem neurons targeted by the Purkinje cells are the site of adaptive learning and that the cerebellum constructs the error signal that drives this adaptation.

5.4 Computer Simulation of the Vestibular System

5.4.1 Semicircular Canals

Model without Cupula

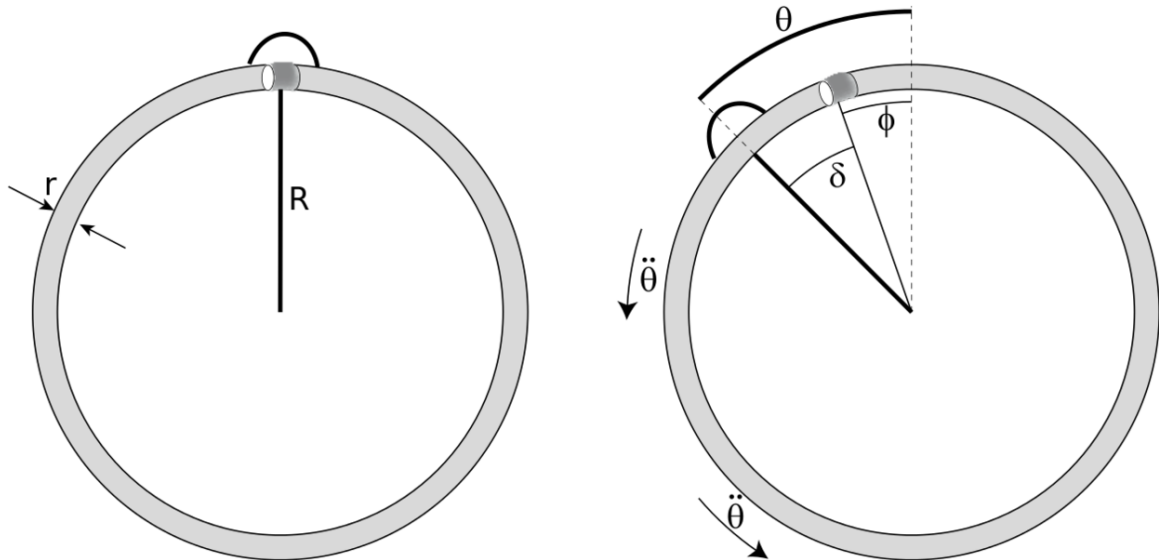


Figure 99 Simplified semicircular canal, without cupula.

Let us consider the mechanical description of the semi-circular canals (SCC). We will make very strong and reductive assumptions in the following description. The goal here is merely to understand the very basic mechanical principles underlying the semicircular canals.

The first strong simplification we make is that a semicircular canal can be modeled as a circular tube of “outer” radius R and “inner” radius r . (For proper hydro mechanical derivations see (Damiano and Rabbitt 1996) and Obrist (2005)). This tube is filled with endolymph.

The orientation of the semicircular canal can be described, in a given coordinate system, by a vector \vec{n} that is perpendicular to the plane of the canal. We will also use the following notations:

θ Rotation angle of tube [rad]

$\dot{\theta} \equiv \frac{d\theta}{dt}$ Angular velocity of the tube [rad/s]

$\ddot{\theta} \equiv \frac{d^2\theta}{dt^2}$ Angular acceleration of the tube [rad/s²]

ϕ Rotation angle of the endolymph inside the tube [rad], and similar notation for the time derivatives

$\delta = \theta - \phi$ movement between the tube and the endolymph [rad].

Note that all these variables are scalar quantities. We use the fact that the angular velocity of the tube can be viewed as the projection of the actual angular velocity vector of the head

$\vec{\omega}$ onto the plane of the semicircular canal described by \vec{n} to go from the 3D environment of the head to our scalar description. That is,

$$\dot{\theta} = \vec{\omega} \cdot \vec{n}$$

where the standard scalar product is meant with the dot.

To characterize the endolymph movement, consider a free floating piston, with the same density as the endolymph. Two forces are acting on the system:

1. The inertial moment $I\ddot{\phi}$, where I characterizes the inertia of the endolymph.
2. The viscous moment $B\dot{\delta}$, caused by the friction of the endolymph on the walls of the tube.

This gives the equation of motion

$$I\ddot{\phi} = B\dot{\delta}$$

Substituting $\phi = \theta - \delta$ and integrating gives

$$\dot{\theta} = \dot{\delta} + \frac{B}{I}\delta.$$

Let us now consider the example of a velocity step $\dot{\theta}(t)$ of constant amplitude ω . In this case, we obtain a displacement

$$\delta = \frac{I}{B}\omega \cdot (1 - e^{-\frac{B}{I}t})$$

and for $t \gg \frac{I}{B}$, we obtain the constant displacement

$$\delta \approx \frac{I}{B}\omega$$

Now, let us derive the time constant $T_1 \equiv \frac{I}{B}$. For a thin tube, $r \ll R$, the inertia is approximately given by

$$I = ml^2 \approx 2\rho\pi^2 r^2 R^3.$$

From the Poiseuille-Hagen Equation, the force F from a laminar flow with velocity v in a thin tube is

$$F = \frac{8\bar{V}\eta l}{r^2}$$

where $\bar{V} = r^2\pi v$ is the volume flow per second, η the viscosity and $l = 2\pi R$ the length of the tube.

With the torque $M = F \cdot R$ and the relative angular velocity $\Omega = \frac{v}{R}$, substitution provides

$$B = \frac{M}{\Omega} = 16\eta\pi^2 R^3$$

Finally, this gives the time constant T_1

$$T_1 = \frac{I}{B} = \frac{\delta r^2}{8\eta}$$

For the human balance system, replacing the variables with experimentally obtained parameters yields a time constant T_1 of about 0.01 s. This is brief enough that in equation (10.5) the \approx can be replaced by " $=$ ". This gives a system gain of

$$G \equiv \frac{\delta}{\omega} = \frac{I}{B} = T_1$$

Model with Cupula

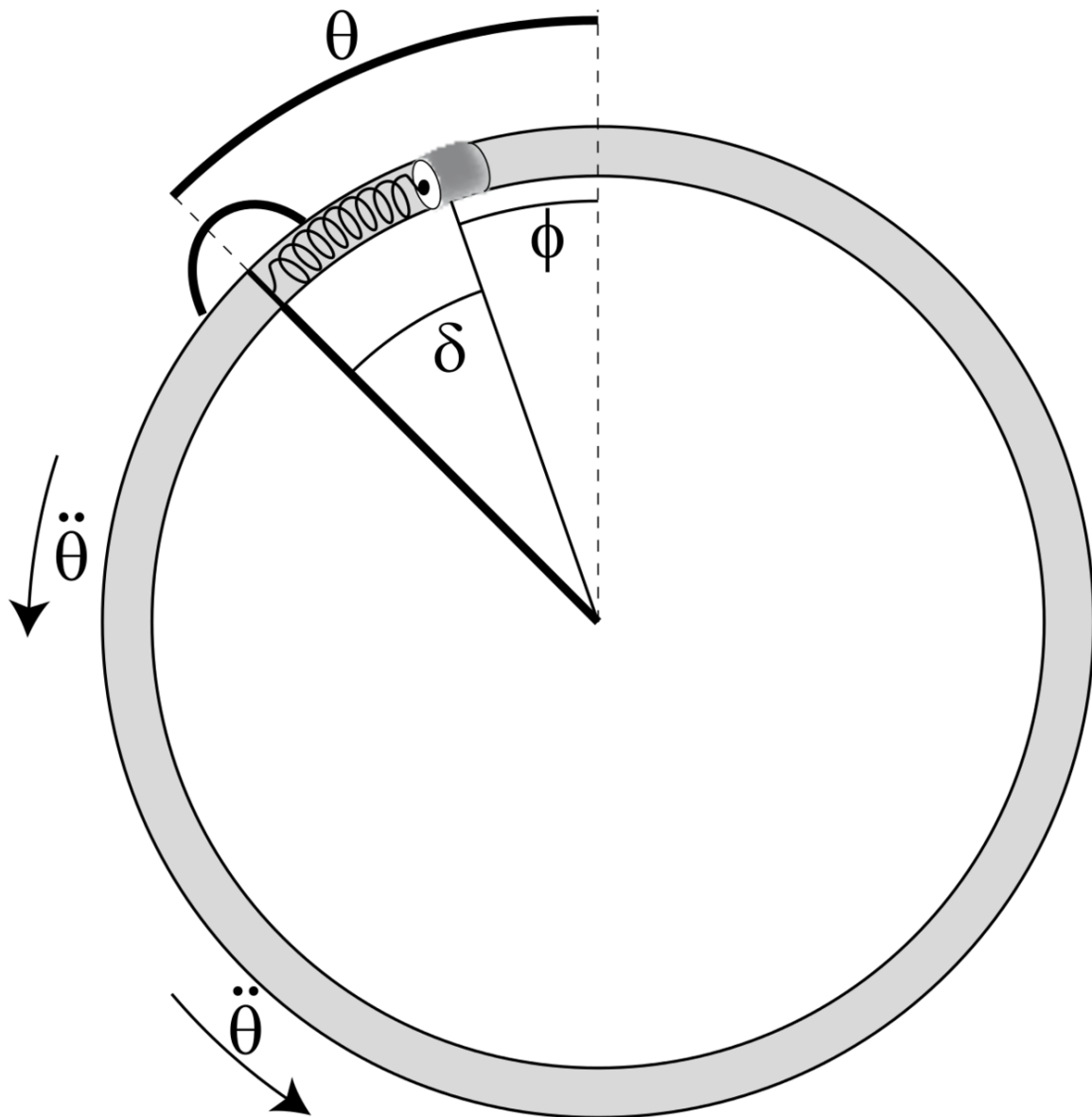


Figure 100 Effect of the cupula.

Our discussion until this point has not included the role of the cupula in the SCC: The cupula acts as an elastic membrane that gets displaced by angular accelerations. Through its elasticity the cupula returns the system to its resting position. The elasticity of the cupula adds an additional elastic term to the equation of movement. If it is taken into account, this equation becomes

$$\ddot{\theta} = \ddot{\delta} + \frac{B}{I} \dot{\delta} + \frac{K}{I} \delta$$

An elegant way to solve such differential equations is the *Laplace-Transformation*. The Laplace transform turns differential equations into algebraic equations: if the Laplace transform of a signal $x(t)$ is denoted by $X(s)$, the Laplace transform of the time derivative is

$$\frac{dx(t)}{dt} \xrightarrow{\text{Laplace Transform}} s \cdot X(s) - x(0)$$

The term $x(0)$ details the starting condition, and can often be set to zero by an appropriate choice of the reference position. Thus, the Laplace transform is

$$s^2 \tilde{\theta} = s^2 \tilde{\delta} + \frac{B}{I} s \tilde{\delta} + \frac{K}{I} \tilde{\delta}$$

where " $\tilde{\cdot}$ " indicates the Laplace transformed variable. With T_1 from above, and T_2 defined by

$$T_2 = \frac{B}{K}$$

we get the

$$\frac{\tilde{\delta}}{\tilde{\theta}} = \frac{T_1 s^2}{T_1 s^2 + s + \frac{1}{T_2}}$$

For humans, typical values for $T_2 = B/K$ are about 5 sec.

To find the poles of this transfer function, we have to determine for which values of s the denominator equals 0:

$$s_{1,2} = \frac{1}{T_1} \left(-1 \pm \sqrt{1 - 4 \frac{T_1}{T_2}} \right)$$

Since $T_2 \gg T_1$, and since

$$\sqrt{1-x} \approx 1 - \frac{x}{2} \text{ for } x \ll 1$$

we obtain

$$s_1 \approx -\frac{1}{T_1}, \text{ and } s_2 \approx -\frac{1}{T_2}$$

Typically we are interested in the cupula displacement δ as a function of head velocity $\dot{\theta} \equiv s\tilde{\theta}$:

$$\frac{\tilde{\delta}}{s\tilde{\theta}}(s) = \frac{T_1 T_2 s}{(T_1 s + 1)(T_2 s + 1)}$$

For typical head movements ($0.2 \text{ Hz} < f < 20\text{Hz}$), the system gain is approximately constant. In other words, for typical head movements the cupula displacement is proportional to the angular head velocity!

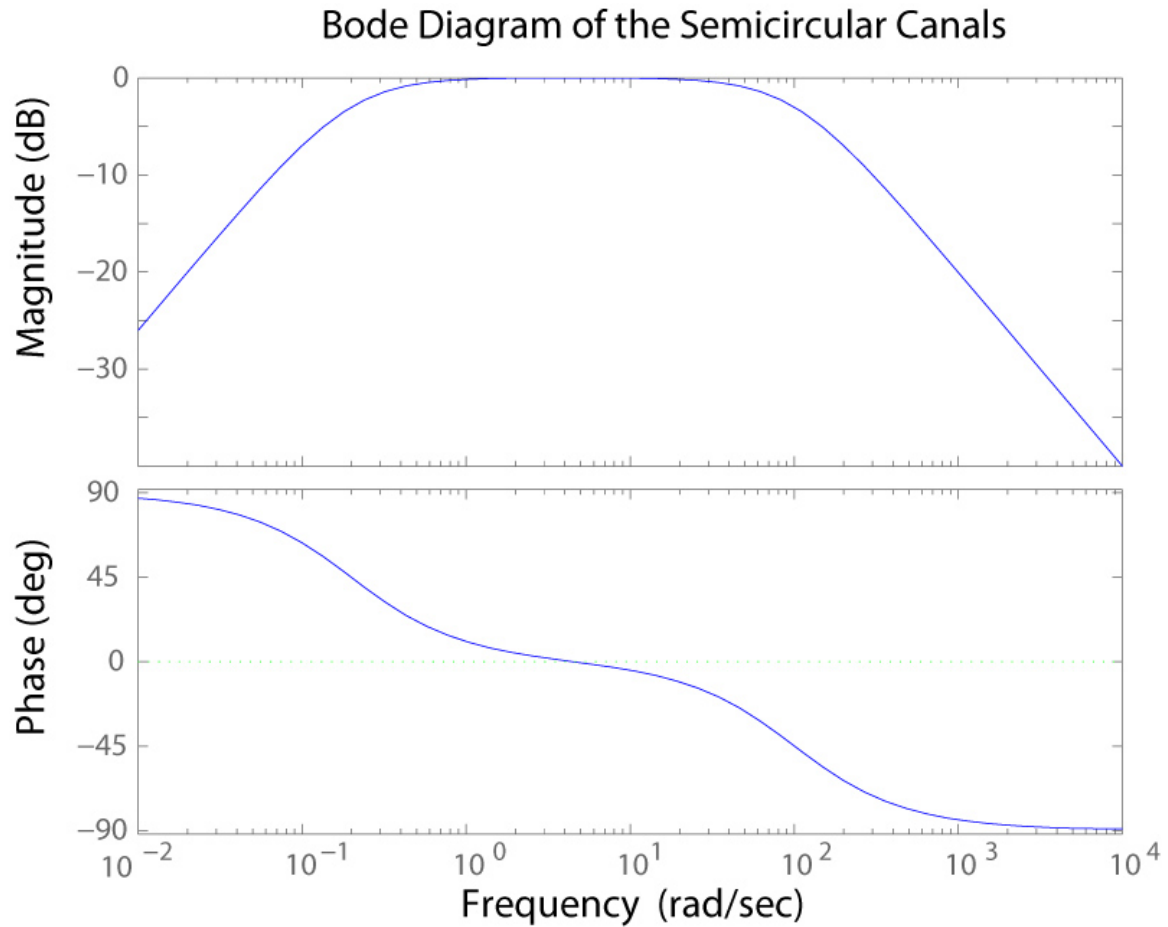


Figure 101 Bode plot of the cupula displacement of a function of head velocity, with $T_1 = 0.01$ sec, $T_2 = 5$ sec, and an amplification factor of $(T_1 + T_2) / (T_1 * T_2)$ to obtain a gain of approximately 0 for the central frequencies.

Control Systems

For Linear, Time-Invariant systems (LTI systems), the input and output have a simple relationship in the frequency domain :

$$Out(s) = G(s) * In(s)$$

where the *transfer function* $G(s)$ can be expressed by the algebraic function

$$G(s) = \frac{num(s)}{den(s)} = \frac{n(0) * s^0 + n(1) * s^1 + n(2) * s^2 + \dots}{d(0) * s^0 + d(1) * s^1 + d(2) * s^2 + \dots}$$

In other words, specifying the coefficients of the numerator (n) and denominator (d) uniquely characterizes the transfer function. This notation is used by some computational tools to simulate the response of such a system to a given input.

Different tools can be used to simulate such a system. For example, the response of a low-pass filter with a time-constant of 7 sec to an input step at 1 sec has the following transfer function

$$G(s) = \frac{1}{7s+1}$$

and can be simulated as follows:

With Simulink

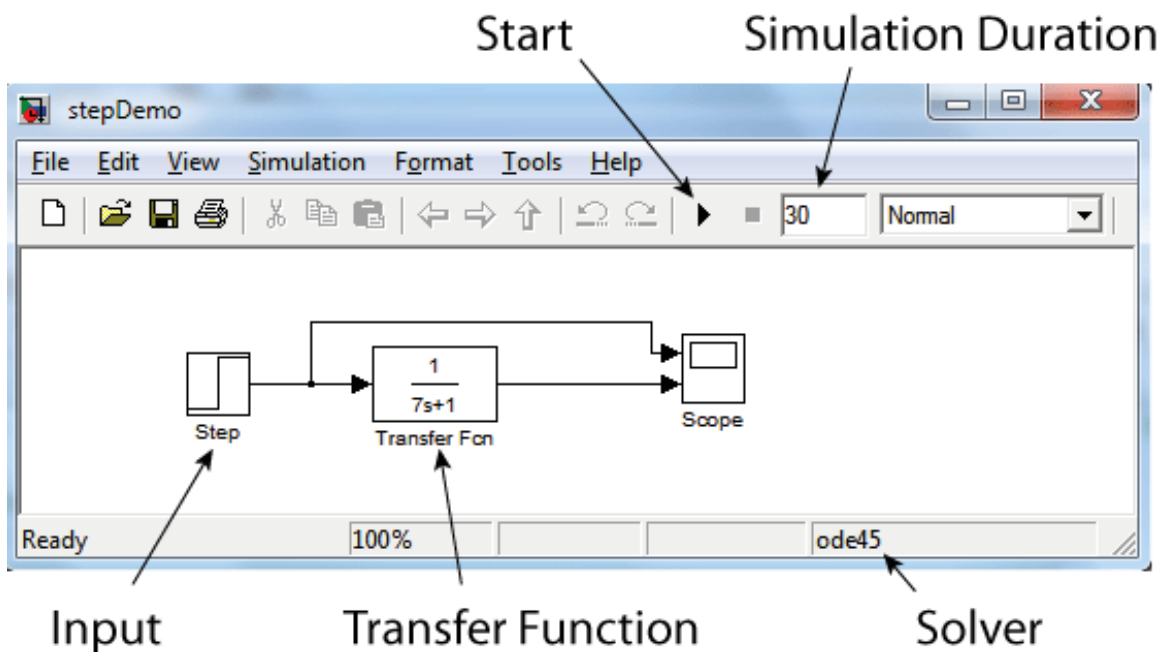


Figure 102 Step-response simulation of a lowpass filter with Simulink.

Commandline

If you work on the command line, you can use the *Control System Toolbox* of MATLAB or the module *signal* of the Python package *SciPy*:

MATLAB⁷ Control System Toolbox:

```
% Define the transfer function
```

⁷ <http://en.wikibooks.org/wiki/MATLAB>

```
num = [1];
tau = 7;
den = [tau, 1];
mySystem = tf(num,den)

% Generate an input step
t = 0:0.1:30;
inSignal = zeros(size(t));
inSignal(t>=1) = 1;

% Simulate and show the output
[outSignal, tSim] = lsim(mySystem, inSignal, t);
plot(t, inSignal, tSim, outSignal);
```

Python⁸ - SciPy:

```
# Import required packages
import numpy as np
import scipy.signal as ss
import matplotlib.pyplot as mp

# Define transfer function
num = [1]
tau = 7
den = [tau, 1]
mySystem = ss.lti(num, den)

# Generate inSignal
t = np.arange(0,30,0.1)
inSignal = np.zeros(t.size)
inSignal[t>=1] = 1

# Simulate and plot outSignal
tout, outSignal, xout = ss.lsim(mySystem, inSignal, t)
mp.plot(t, inSignal, tout, outSignal)
mp.show()
```

5.4.2 Otoliths

Consider now the mechanics of the otolith organs. Since they are made up by complex, visco-elastic materials with a curved shape, their mechanics cannot be described with analytical tools. However, their movement can be simulated numerically with the finite element technique. Thereby the volume under consideration is divided into many small volume elements, and for each element the physical equations are approximated by analytical functions.

⁸ <http://en.wikibooks.org/wiki/Python>

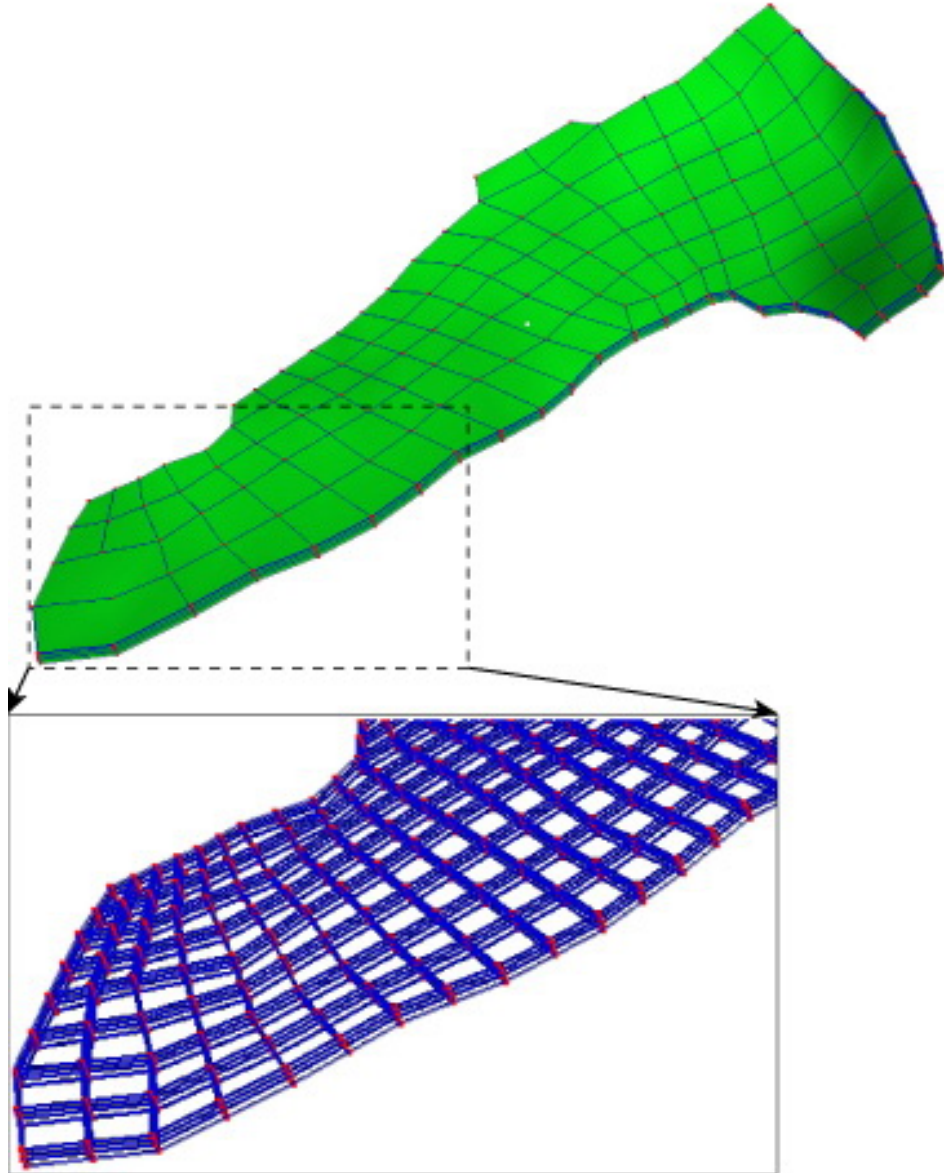


Figure 103 FE-Simulations: Small, finite elements are used to construct a mechanical model; here for example the saccule.

Here we will only show the physical equations for the visco-elastic otolith materials. The movement of each elastic material has to obey Cauchy's equations of motion:

$$\rho \frac{\partial^2 u_i}{\partial t^2} = \rho B_i + \sum_j \frac{\partial T_{ij}}{\partial x_j}$$

where ρ is the effective density of the material, u_i the displacements along the i -axis, B_i the i -component of the volume force, and T_{ij} the components of the Cauchy's strain tensor. x_j are the coordinates.

For linear elastic, isotropic material, *Cauchy's strain tensor* is given by

$$T_{ij} = \lambda e \delta_{ij} + 2\mu E_{ij}$$

where λ and μ are the *Lamé constants*; μ is identical with the shear modulus. $e = \text{div}(\vec{u})$, and E_{ij} is the stress tensor

$$E_{ij} = \frac{1}{2} \left(\frac{\partial u_i}{\partial x_j} + \frac{\partial u_j}{\partial x_i} \right).$$

This leads to Navier's Equations of motion

$$\rho \frac{\partial^2 u_i}{\partial t^2} = \rho B_i + (\lambda + \mu) \frac{\partial e}{\partial x_i} + \mu \sum_j \frac{\partial^2 u_i}{\partial x_j^2}$$

This equation holds for purely elastic, isotropic materials, and can be solved with the finite element technique. A typical procedure to find the mechanical parameters that appear in this equation is the following: when a cylindrical sample of the material is put under strain, the *Young coefficient* E characterizes the change in length, and the *Poisson's ratio* ν the simultaneous decrease in diameter. The Lamé constants λ and μ are related to E and ν by:

$$E = \frac{\mu(3\lambda + 2\mu)}{\lambda + \mu}$$

and

$$\nu = \frac{\lambda}{2(\lambda + \mu)}$$

5.5 References

9

6 Somatosensory System

6.1 Introduction

6.2 Sensory Organs

Our somatosensory system consists of sensors in the skin and sensors in our muscles, tendons, and joints. The receptors in the skin, the so called cutaneous receptors, tell us about temperature (*thermoreceptors*), pressure and surface texture (*mechano receptors*), and pain (*nociceptors*). The receptors in muscles and joints provide information about muscle length, muscle tension, and joint angles. (The following description is based on lecture notes from Laszlo Zaborszky, from Rutgers University.)

6.3 Sensory Organ Components

6.3.1 Cutaneous receptors

Mechanoreceptors

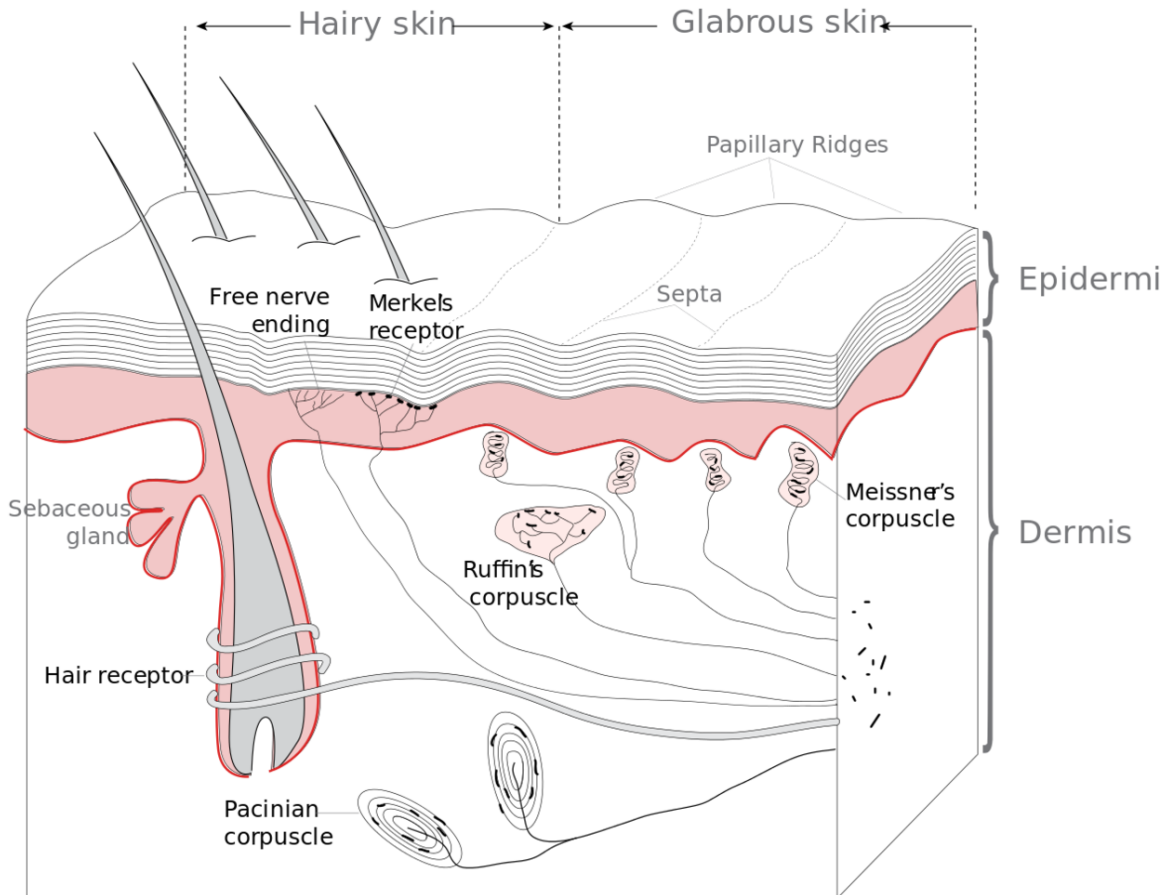


Figure 104 Receptors in the human skin: Mechanoreceptors can be free receptors or encapsulated. Examples for free receptors are the hair receptors at the roots of hairs. Encapsulated receptors are the Pacinian corpuscles and the receptors in the glabrous (hairless) skin: Meissner corpuscles, Ruffini corpuscles and Merkel's disks.

Sensory information from *Meissner corpuscles* and rapidly adapting afferents leads to adjustment of grip force when objects are lifted. These afferents respond with a brief burst of action potentials when objects move a small distance during the early stages of lifting. In response to rapidly adapting afferent activity, muscle force increases reflexively until the gripped object no longer moves. Such a rapid response to a tactile stimulus is a clear indication of the role played by somatosensory neurons in motor activity.

The slowly adapting *Merkel's receptors* are responsible for form and texture perception. As would be expected for receptors mediating form perception, Merkel's receptors are present at high density in the digits and around the mouth (50/mm² of skin surface), at lower density in other glabrous surfaces, and at very low density in hairy skin. This innervations density

shrinks progressively with the passage of time so that by the age of 50, the density in human digits is reduced to 10/mm². Unlike rapidly adapting axons, slowly adapting fibers respond not only to the initial indentation of skin, but also to sustained indentation up to several seconds in duration.

Activation of the rapidly adapting *Pacinian corpuscles* gives a feeling of vibration, while the slowly adapting *Ruffini corpuscles* respond to the lateral movement or stretching of skin.

	Rapidly adapting	Slowly adapting
Surface receptor / small receptive field	<i>Hair receptor, Meissner's corpuscle</i> : Detect an insect or a very fine vibration. Used for recognizing texture.	Merkel's receptor: Used for spatial details, e.g. a round surface edge or "an X" in brail.
Deep receptor / large receptive field	<i>Pacinian corpuscle</i> : "A diffuse vibration" e.g. tapping with a pencil.	<i>Ruffini's corpuscle</i> : "A skin stretch". Used for joint position in fingers.

Nociceptors

Nociceptors have free nerve endings. Functionally, skin nociceptors are either high-threshold mechanoreceptors or *polymodal receptors*. Polymodal receptors respond not only to intense mechanical stimuli, but also to heat and to noxious chemicals. These receptors respond to minute punctures of the epithelium, with a response magnitude that depends on the degree of tissue deformation. They also respond to temperatures in the range of 40-60°C, and change their response rates as a linear function of warming (in contrast with the saturating responses displayed by non-noxious thermoreceptors at high temperatures).

Pain signals can be separated into individual components, corresponding to different types of nerve fibers used for transmitting these signals. The rapidly transmitted signal, which often has high spatial resolution, is called *first pain* or *cutaneous pricking pain*. It is well localized and easily tolerated. The much slower, highly affective component is called *second pain* or *burning pain*; it is poorly localized and poorly tolerated. The third or *deep pain*, arising from viscera, musculature and joints, is also poorly localized, can be chronic and is often associated with referred pain.

Thermoreceptors

The thermoreceptors have free nerve endings. Interestingly, we have only two types of thermoreceptors that signal innocuous warmth and cooling respectively in our skin (however, some nociceptors are also sensitive to temperature, but capable of unambiguously signaling only noxious temperatures). The warm receptors show a maximum sensitivity at ~ 45°C, signal temperatures between 30 and 45°C, and cannot unambiguously signal temperatures higher than 45°C, and are unmyelinated. The cold receptors have their maximum sensitivity at ~ 27°C, signal temperatures above 17°C, and some consist of lightly myelinated fibers, while others are unmyelinated. Our sense of temperature comes from the comparison of the

signals from the warm and cold receptors. Thermoreceptors are poor indicators of absolute temperature but are very sensitive to changes in skin temperature.

Proprioceptors

The term *proprioceptive* or *kinesthetic sense* is used to refer to the perception of joint position, joint movements, and the direction and velocity of joint movement. There are numerous mechanoreceptors in the muscles, the muscle fascia, and in the dense connective tissue of joint capsules and ligaments. There are two specialized encapsulated, low-threshold mechanoreceptors: the *muscle spindle* and the *Golgi tendon organ*. Their adequate stimulus is stretching of the tissue in which they lie. Muscle spindles, joint and skin receptors all contribute to kinesthesia. Muscle spindles appear to provide their most important contribution to kinesthesia with regard to large joints, such as the hip and knee joints, whereas joint receptors and skin receptors may provide more significant contributions with regard to finger and toe joints.

Muscle Spindles

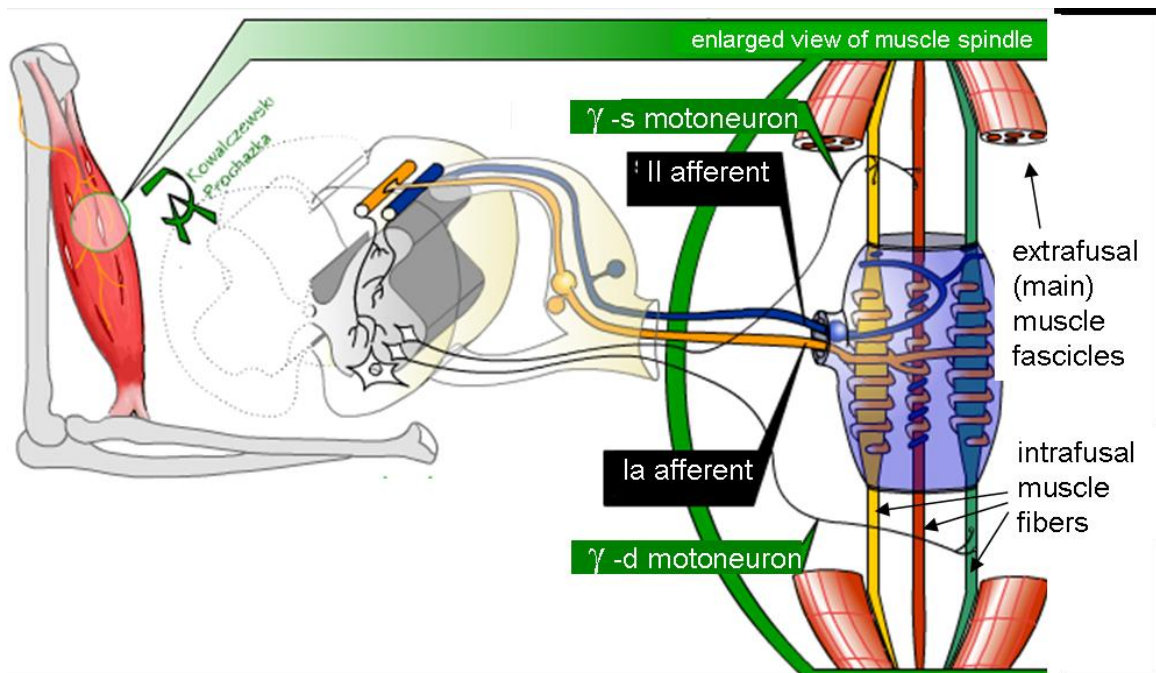


Figure 105 Mammalian muscle spindle showing typical position in a muscle (left), neuronal connections in spinal cord (middle) and expanded schematic (right). The spindle is a stretch receptor with its own motor supply consisting of several intrafusal muscle fibers. The sensory endings of a primary (group Ia) afferent and a secondary (group II) afferent coil around the non-contractile central portions of the intrafusal fibres. Gamma motoneurons activate the intrafusal muscle fibres, changing the resting firing rate and stretch-sensitivity of the afferents.

Scattered throughout virtually every striated muscle in the body are long, thin, stretch receptors called muscle spindles. They are quite simple in principle, consisting of a few small muscle fibers with a capsule surrounding the middle third of the fibers. These fibers are called *intrafusal fibers*, in contrast to the ordinary *extrafusal fibers*. The ends of the intrafusal fibers are attached to extrafusal fibers, so whenever the muscle is stretched, the intrafusal fibers are also stretched. The central region of each intrafusal fiber has few myofilaments and is non-contractile, but it does have one or more sensory endings applied to it. When the muscle is stretched, the central part of the intrafusal fiber is stretched and each sensory ending fires impulses.

Numerous specializations occur in this simple basic organization, so that in fact the muscle spindle is one of the most complex receptor organs in the body. Only three of these specializations are described here; their overall effect is to make the muscle spindle adjustable and give it a dual function, part of it being particularly sensitive to the length of the muscle in a static sense and part of it being particularly sensitive to the rate at which this length changes.

1. Intrafusal muscle fibers are of two types. All are multinucleated, and the central, non-contractile region contains the nuclei. In one type of intrafusal fiber, the nuclei are lined up single file; these are called *nuclear chain fiber*. In the other type, the nuclear region is broader, and the nuclei are arranged several abreast; these are called *nuclear bag fibers*. There are typically two or three nuclear bag fibers per spindle and about twice that many chain fibers.
2. There are also two types of sensory endings in the muscle spindle. The first type, called the primary ending, is formed by a single Ia (A-alpha) fiber, supplying every intrafusal fiber in a given spindle. Each branch wraps around the central region of the intrafusal fiber, frequently in a spiral fashion, so these are sometimes called *annulospiral endings*. The second type of ending is formed by a few smaller nerve fibers (II or A-Beta) on both sides of the primary endings. These are the secondary endings, which are sometimes referred to as *flower-spray endings* because of their appearance. Primary endings are selectively sensitive to the onset of muscle stretch but discharge at a slower rate while the stretch is maintained. Secondary endings are less sensitive to the onset of stretch, but their discharge rate does not decline very much while the stretch is maintained. In other words, both primary and secondary endings signal the static length of the muscle (static sensitivity) whereas only the primary ending signals the length changes (movement) and their velocity (dynamic sensitivity). The change of firing frequency of group Ia and group II fibers can then be related to static muscle length (static phase) and to stretch and shortening of the muscle (dynamic phases).
3. Muscle spindles also receive a motor innervation. The large motor neurons that supply extrafusal muscle fibers are called *alpha motor neurons*, while the smaller ones supplying the contractile portions of intrafusal fibers are called *gamma neurons*. Gamma motor neurons can regulate the sensitivity of the muscle spindle so that this sensitivity can be maintained at any given muscle length.

Golgi tendon organ

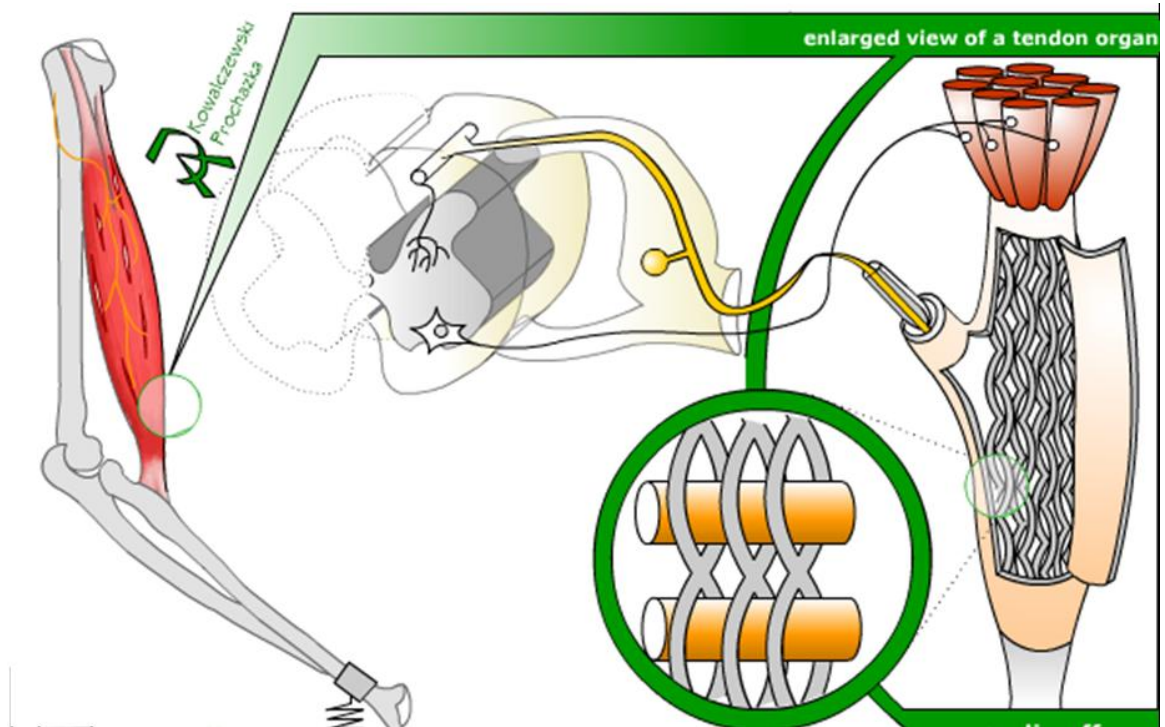


Figure 106 Mammalian tendon organ showing typical position in a muscle (left), neuronal connections in spinal cord (middle) and expanded schematic (right). The tendon organ is a stretch receptor that signals the force developed by the muscle. The sensory endings of the Ib afferent are entwined amongst the musculotendinous strands of 10 to 20 motor units.

The Golgi tendon organ is located at the musculotendinous junction. There is no efferent innervation of the tendon organ, therefore its sensitivity cannot be controlled from the CNS. The tendon organ, in contrast to the muscle spindle, is coupled in series with the extrafusal muscle fibers. Both passive stretch and active contraction of the muscle increase the tension of the tendon and thus activate the tendon organ receptor, but active contraction produces the greatest increase. The tendon organ, consequently, can inform the CNS about the “muscle tension”. In contrast, the activity of the muscle spindle depends on the “muscle length” and not on the tension. The muscle fibers attached to one tendon organ appear to belong to several motor units. Thus the CNS is informed not only of the overall tension produced by the muscle but also of how the workload is distributed among the different motor units.

Joint receptors

The joint receptors are low-threshold mechanoreceptors and have been divided into four groups. They signal different characteristics of joint function (position, movements, direction and speed of movements). The free receptors or type 4 joint receptors are nociceptors.

6.4 Proprioceptive Signal Processing

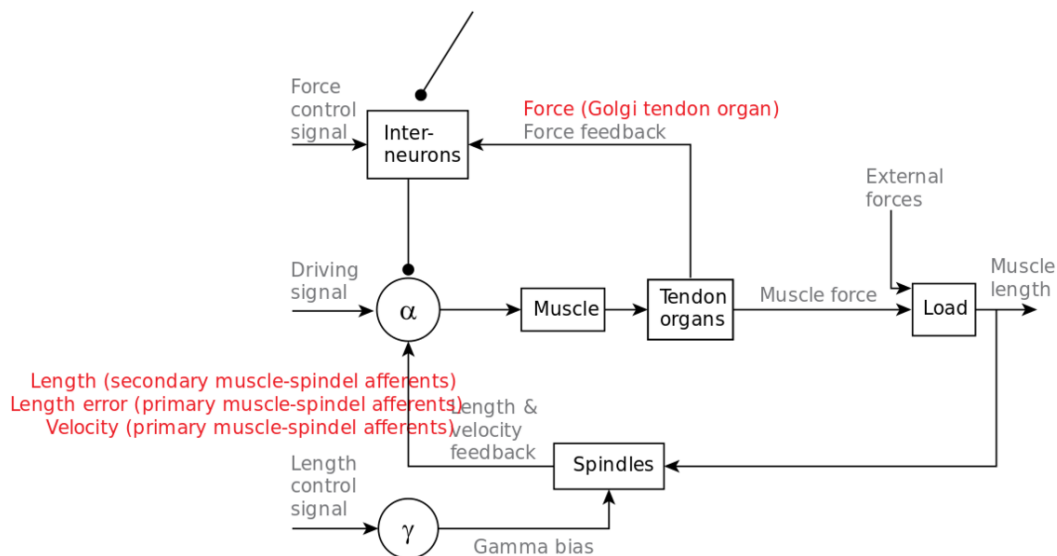


Figure 107 Feedback loops for proprioceptive signals for the perception and control of limb movements. Arrows indicate excitatory connections; filled circles inhibitory connections.

6.5 Modelling muscle spindles and afferent response

The response of the muscle spindles in mammals to muscle stretch has been thoroughly studied, and various models have been proposed. However, due to the difficulty in obtaining accurate data of the afferent and fusimotor responses during muscular movement, these models have usually been quite limited. For example, several of the earliest models account only for the afferent response, ignoring the fusimotor activity.

6.5.1 Mileusnic et al. (2006) model

One recent model, developed by Mileusnic et al. (2006), portrays the muscle spindle as consisting of several (typically 4 to 11) nuclear chain fibres, and two different nuclear bag fibres, connected in parallel as shown here in the figure below. The muscle fibres respond to three inputs: fascicle length, dynamic fusimotor input and static fusimotor input. The *bag₁* fibre is mainly responsible for detecting dynamic fusimotor input, while the *bag₂* and chain fibres are mainly responsible for detecting static fusimotor input. All fibres respond to changes in the fascicle length, and are modelled in largely the same way but with different coefficients to account for their different physiological properties. The responses of the three types of fibres are summed to generate the primary and secondary afferent activities. The primary afferent activity is affected by the response of all three types of muscle fibres, while the secondary afferent activity only depends on the *bag₂* and chain fibre responses.

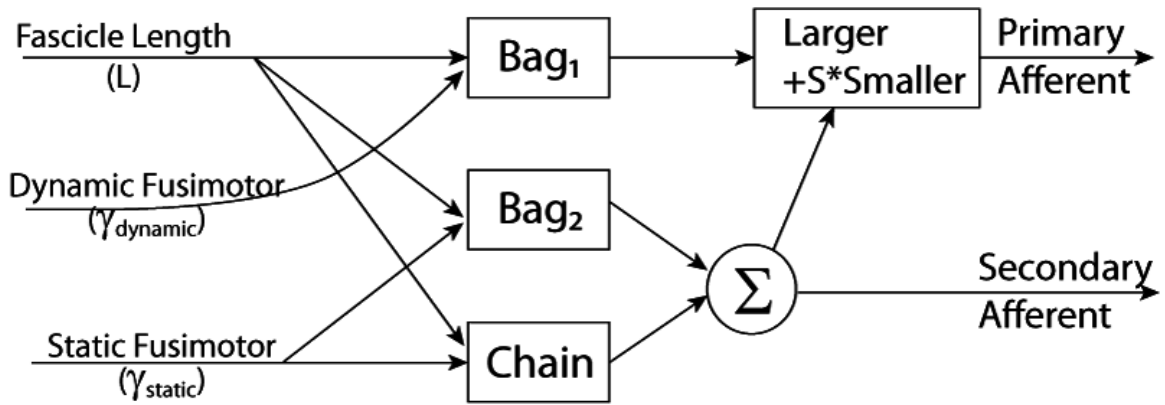


Figure 108

6.5.2 Hasan (1983) model

Another comprehensive model of muscle spindles was proposed by Hasan in 1983¹. This representation of muscle fibres and spindles is based closely on their physical properties. The muscle spindle is represented as two separate regions connected in series: sensory and non-sensory. The firing rate of the spindle afferent depends on the state of the two regions². The lengths of the two regions can be labelled $z(t)$ for the sensory and $y(t)$ for the non-sensory region. The tension $f(t)$ in the two regions is equal, since they are placed in series. The sensory zone can be assumed to act like a spring (equation (3)), while in the non-sensory region, tension is a non-linear function of $y(t)$ (equation (2) derived by Hasan).

$$f(t) = k_1(y(t) - c)(1 + [\frac{y'(t)}{a}]^{\frac{1}{3}}) \quad (2)$$

$$f(t) = k_2 z(t) \quad (3)$$

The total length of the muscle spindle, $x(t)$ is the sum of the length of the two regions (equation (4)).

$$x(t) = z(t) + y(t) \quad (4)$$

Using this substitution and rearranging, we can derive the following expression for the length of the sensory zone (equation (5)):

$$z'(t) = x'(t) - a(\frac{bz(t) - x(t) + c}{x(t) - z(t) - c})^3 \quad (5)$$

Here, parameter a represents the sensitivity of the tension to velocity in the non-sensory zone, parameter $b = (k_1 + k_2)/k_1$ and parameter c determines the zero-length tension which influences the background firing rate of the afferent. The length of the sensory zone depends not only on the current length and velocity of the spindle, but on the history of the length changes.

The firing rate, $g(t)$ in Hasan's model depends on a combination of the sensory zone length and its first derivative (equation (6)), with an experimentally derived weighting.

1 Hasan 1983 [^]{<http://www.example.org>} , Hasan 1983

2 Hasan 1983 [^]{<http://www.example.org>} , Hasan 1983

$$g(t) = z(t) + 0.1z'(t) \quad (6)$$

Model parameters

Approximate values for the model parameters a, b and c were suggested by Hasan (1983), and differ for voluntary and passive movements. A summary of these values is presented in the table below. Type of ending Condition A (mm/s) B C (mm)

Type of ending	Condition	A (mm/s)	B	C (mm)
Primary	Passive	0.3	250	-15
Primary	Gamma - dynamic	0.1	125	-15
Primary	Gamma - static	100	100	-25
Secondary	Passive	50	50	-20

In the model, these values are assumed to be static for the duration of a movement, however this is not believed to be the case.

6.6 Internal models of limb dynamics

In addition to modelling the response of muscle spindle afferents to muscle stretch, several groups have worked on modelling the signals which are sent from the brain to the spindle efferents in order for muscles to complete specific movements. The complexity here lies in the fact that the brain must be able to adapt to unexpected changes in the dynamics of planned movements, using feedback from the spindle afferents.

Studies in this area suggest that humans achieve this using internal models, which are built through an “error-feedback-learning” process, and transform planned muscle states into the motor commands required to achieve them. To generate the motor commands for a particular reaching movement, the brain performs calculations based on the expected dynamics of the planned movement. However, any unexpected changes in these dynamics while the movement is being executed (e.g. external strain placed on the muscle) will lead to errors in expected muscle length (Gottlieb 1994, Shadmehr and Muss-Ivaldi 1994). These errors are communicated to the brain through the muscle spindle afferents, which experience a different sensory state to what is expected. The brain then reacts to these error signals with short and long latency responses, which work to minimise the error, but cannot eliminate it completely due to the delay in the system.

Studies suggest that the error can be eliminated in a subsequent attempt at the movement under the same dynamics, and this is where the “error-feedback-learning” idea comes from (Thoroughman and Shadmehr 1999). The corrections which are generated by the brain form an internal model, which maps a desired action (in kinematic coordinates) to the necessary motor commands (as torques). This internal model can be represented as a weighted combination of basis elements:

$$torque = \sum w_i g_i(\theta, \theta', \theta'' \dots)$$

Here each basis g_i represents some characteristic of the muscle's sensory state, and the motor command is a “population code”. Population coding is a method of representing stimuli as

the combined activity of many neurons (in contrast to rate coding). In order to use such a model, we need to know how the bases represent particular limb or muscle positions, and the neuronal firing rates associated with them. The bases can, in principle, represent every aspect of the state: position, velocity, acceleration and even higher derivatives. However, this high dimensionality makes it very difficult to derive relationships experimentally between each dimension of the bases and the firing rates. ³

³ <http://en.wikibooks.org/wiki/Category%3A>

7 Olfactory System

7.1 Introduction

Probably the oldest sensory system in the nature, the **olfactory system** concerns the sense of smell. The olfactory system is physiologically strongly related to the gustatory system, so that the two are often examined together. Complex flavors require both taste and smell sensation to be recognized. Consequently, food may taste “different” if the sense of smell does not work properly (e.g. head cold).

Generally the two systems are classified as visceral sense because of their close association with gastrointestinal function. They are also of central importance while speaking of emotional and sexual functions.

Both taste and smell receptors are chemoreceptors that are stimulated by molecules soluted respectively in mucus or saliva. However these two senses are anatomically quite different. While smell receptors are distance receptors that do not have any connection to the thalamus, receptors pass up the brainstem to the thalamus and project to the postcentral gyrus along with those for touch and pressure sensibility for the mouth.

In this article we will first focus on the organs composing the **olfactory system**, then we will characterize them in order to understand their functionality and we will end explaining the transduction of the signal and the commercial application such as the eNose.

7.2 Sensory Organs

In vertebrates the main **olfactory system** detects odorants that are inhaled through the nose where they come to contact with the olfactory epithelium, which contains the olfactory receptors.

Olfactory sensitivity is directly proportional to the area in the nasal cavity near the septum reserved to the olfactory mucous membrane, which is the region where the olfactory receptor cells are located. The extent of this area is a specific between animals species. In dogs, for example, the sense of smell is highly developed and the area covered by this membrane is about $75 - 150 \text{ cm}^2$; these animals are called macrosmatic animals. Differently in humans the olfactory mucous membrane cover an area about $3 - 5 \text{ cm}^2$, thus they are known as microsomatic animals.

In humans there are about 10 million olfactory cells, each of which have 350 different receptor types composing the olfactory mucous membrane. The 350 different receptors are characteristic for only one odorant type. The bond with one odorant molecule starts a molecular chain reaction, which transforms the chemical perception into an electrical signal.

The electrical signal proceeds through the olfactory nerve's axons to the olfactory bulbs. In this region there are between 1000 and 2000 glomerular cells which combine and interpret the potentials coming from different receptors. This way it is possible to unequivocally characterise e.g. the coffee aroma, which is composed by about 650 different odorants. Humans can distinguish between about 10.000 odors.

The signal then goes forth to the olfactory cortex where it will be recognized and compared with known odorants (i.e. olfactory memory) involving also an emotional response to the olfactory stimuli.

It is also interesting to note that the human genome has about 600 – 700 genes (~2% of the complete genome) specialized in characterizing the olfactory receptors, but only 350 are still used to build the **olfactory system**. This is a proof of the evolution change in the necessity of humans in using the olfaction.

7.3 Sensory Organ Components

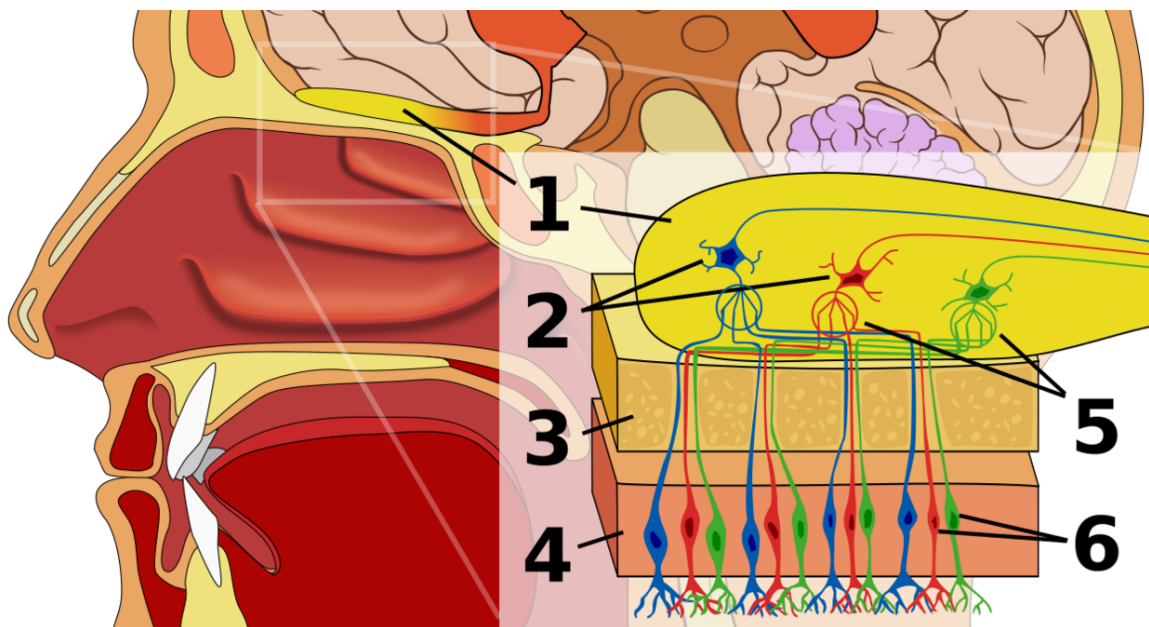


Figure 109 1: Olfactory bulb 2: Mitral cells 3: Bone 4: Nasal Epithelium 5: Glomerulus 6: Olfactory receptor cells

Similar to other sensory modalities, olfactory information must be transmitted from peripheral olfactory structures, like the olfactory epithelium, to more central structures, meaning the olfactory bulb and cortex. The specific stimuli has to be integrated, detected and transmitted to the brain in order to reach sensory consciousness. However the **olfactory system** is different from other sensory systems in three fundamental ways as depicted in the book of Paxianos G. and Mai J.K., "The human Nervous System".

1. Olfactory receptor neurons are continuously replaced by mitotic division of the basal cells of the olfactory epithelium. The motivation of this is the high vulnerability of the neurons, which are directly exposed to the environment.
2. Because of phylogenetic relationship, olfactory sensory activity is transferred directly from the olfactory bulb to the olfactory cortex, without a thalamic relay.
3. Neural integration and analysis of olfactory stimuli may not involve topographic organization beyond the olfactory bulb, meaning that spatial or frequency axis are not needed to project the signal.

7.3.1 Olfactory Mucous Membrane

The olfactory mucous membrane contains the olfactory receptor cells and in humans it covers an area about $3 - 5 \text{ cm}^2$ in the roof of the nasal cavity near the septum. Because the receptors are continuously regenerated it contains both the supporting cells and progenitor cells of the olfactory receptors. Interspersed between these cells are 10 – 20 million receptor cells.

Olfactory receptors are olfactory neurons with a short and thick dendrite. Their extended end is called an olfactory rod, from which cilia project to the surface of the mucus. These neurons have a length of 2 micrometers and have between 10 and 20 cilia of diameter about 0.1 micrometers.

The axons of the olfactory receptor neurons go through the cribriform plate of the ethmoid bone and enter the olfactory bulb. This passage is in absolute the most sensitive of the **olfactory system**; the damage of the cribriform plate (e.g. breaking the nasal septum) can imply the destruction of the axons compromising the sense of smell.

A further particularity of the mucous membrane is that with a period of a few weeks it is completely renewed.

7.3.2 Olfactory Bulbs

In humans the olfactory bulb is located anteriorly with respect to the cerebral hemisphere and remains connected to it only by a long olfactory stalk. Furthermore in mammals it is separated into layers and consists of a concentric lamina structure with well-defined neuronal somata and synaptic neuropil.

After passing the cribriform plate the olfactory nerve fibers ramify in the most superficial layer (olfactory nerve layer). When these axons reach the olfactory bulb the layer gets thicker and they terminate in the primary dendrites of the mitral cells and tufted cells forming in this way the complex globular synapses called olfactory glomeruli. Both these cells send other axons to the olfactory cortex and appear to have the same functionality but in fact tufted cells are smaller and consequently have also smaller axons.

The axons from several thousand receptor neurons cover one or two glomeruli in a corresponding zone of the olfactory bulb; this suggests that the glomeruli are the unit structures for the olfactory discrimination.

In order to avoid threshold problems in addition to mitral and tufted cells, the olfactory bulb contains also two type of cells with inhibitory properties: periglomerular cells and granule cells. The first will connect two different glomeruli, the second, without using any axons, build a reciprocal synapses with the lateral dendrites of the mitral and tufted cells. By releasing GABA the granule cell on the one side of these synapse are able to inhibits the mitral (or tufted) cells, while on the other side of the synapses the mitral (or tufted) cells are able to excite the granule cells by releasing glutamate. Nowadays about 8.000 glomeruli and 40.000 mitral cells have been counted in young adults. Unfortunately this huge number of cells decrease progressively with the age compromising the structural integrity of the different layers.

7.3.3 Olfactory Cortex

The axons of the mitral and tufted cells pass through the granule layer, the intermediate olfactory stria and the lateral olfactory stria to the olfactory cortex. This tract forms in humans the bulk of the olfactory peduncle. As depicted in the book of Paxianos G. and Mai J.K., "The human Nervous System", the primary olfactory cortical areas can be easily described by a simple structure composed of three layers: a broad plexiform layer (first layer); a compact pyramidal cell somata layer (second layer) and a deeper layer composed by both pyramidal and nonpyramidal cells (third layer). Furthermore, in contrast to the olfactory bulb, only a little spatial encoding can be observed; "that is, small areas of the olfactory bulb virtually project the entire olfactory cortex, and small areas of the cortex receive fibers from virtually the entire olfactory bulb" [3].

In general the olfactory tract can be divided in five major regions of the cerebrum: Anterior olfactory nucleus, the olfactory tubercle, the piriform cortex, Anterior cortical nucleus of the amygdala and the entorhinal cortex. Olfactory information is transmitted from primary olfactory cortex to several other parts of the forebrain, including orbital cortex, amigdala, hippocampus, central striatum, hypothalamus and mediodorsal thalamus.

Interesting is also to note that in humans, the piriform cortex can be activated by sniffing, whereas the to activate the lateral and the anterior orbitofrontal gyri of the frontal lobe only the smell is required. This is possible because in general the orbitofrontal activation is grater on the right side than the left side, this directly imply an asymmetry in the corticals reception of the olfaction. A further implication of the emotional response to olfactory stimuli as olfactory memories can be assigned to the fibers projection to the amigdala of the entorhinal cortex.

A good and complete description of the substructure of the olfactory cortex can be found in the book of Paxianos G. and Mai J.K., "The human Nervous System".

7.4 Signal Processing

Examples of olfactory thresholds from William, "Review of Medial Physiology".	
Substance	mg/L of Ari

Examples of olfactory thresholds from William, "Review of Medial Physiology".	
Substance	mg/L of Ari
Ethyl ether	5.83
Chloroform	3.30
Pyridine	0.03
Oil of peppermint	0.02
Iodoform	0.02
Butyric acid	0.009
Propyl mercaptan	0.006
Artificial musk	0.00004
Methyl mercaptan	0.0000004

Only substances which comes in contact with the olfactory epithelium can be excite the olfactory receptors. The right table shows some threshold for some representative substances. These values give an impression of the huge sensitivity of the olfactory receptors.

It is remarkable that humans can recognize more than 10'000 different odors but they should at least differ about the 30% before they can be distinguished. Compared to the visual system, such precision would mean a 1% change in light intensity, where as compared to hearing the direction perception may be indicated by the slight difference in the time of arrival of odoriferous molecules in the two nostrils [4]. It is amazing how the same number of carbon atoms (normally between 3 and 20) in odors molecules can leads to different odors just by slightly change in the structural configuration.

7.4.1 Signal Transduction

An interesting feature of the olfactory system is how a simple sense organ that apparently lacks a high degree of complexity can mediate discrimination of more than 10'000 different odors. On the one hand this is made possible by the huge number of different odorant receptor. The gene family for the olfactory receptor is infect the largest family studied so far in mammals. On the other hand the neural net of the olfactory system's provide with their 1800 glomeruli a large two dimensional map in the olfactory bulb that is unique to each odorant. In addition, the extracellular field potential in each glomerulus oscillates, and the granule cells appear to regulate the frequency of the oscillation. The exact function of the oscillation is unknown, but it probably also helps to focus the olfactory signal reaching the cortex [3].

7.4.2 Smell measurement

Olfaction, as described in the research of R. Haddad et al., consists of a set of transforms from physical space of odorant molecules (olfactory physicochemical space), through a neural space of information processing (olfactory neural space), into a perceptual space of smell (olfactory perceptual space). The rules of these transforms depend on obtaining valid metrics for each of those spaces.

Olfactory perceptual space

As the perceptual space represent the “input” of the smell measurement, it’s aim is to describe the odors in the most simple possible way. Odor are infect ordered so that their reciprocal distance in space confers them similarity. This mean that odors the more two odors are near each other in this space the more are they expected to be similar. This space is thus defined by so called perceptual axes characterized by some arbitrarily chosen “unit” odors.

Olfactory neural space

As suggested by its name the neural spaces are generated from neural responses. This gives rise to an extensive database of odorant-induced activity, which can be used to formulate an olfactory space where the concept of similarity serves as a guiding principal. Using this procedure different odorant are than expected to be similar if they generate a similar neuronal response. This database can be navigated at the Glomerular Activity Response Archive <http://gara.bio.uci.edu/>.

Olfactory physicochemical space

The need of identify the molecular encryption of the biological interaction, make the physicochemical space the most complex one of the olfactory space described so far. R. Haddad suggest that one possibility is to span this space would to represent each odorant by a very large number of molecular descriptors by use either a variance metric or a distance metric. In his first description single odorants may have many physicochemical features and one expect these feature to present themselves at various probabilities within the world of molecules that have a smell. In such metric the orthogonal basis generated from the description of the odorant leads to represent each odorant by a single value. While in the second, the metric represents each odorant with a vector of 1664 values, on the basis of Euclidean distances between odorants in the 1664 physicochemical space. Whereas the first metric enabled the prediction of perceptual attributes, the second enabled the prediction of odorant-induced neuronal response patterns.

7.4.3 Electronic measurement of odors

Nowadays odors can be measured electronically in a huge amount of different way, some examples are: mass spectrography, gas chromatography, raman spectra and most recently electronic nose. In general they assume that different olfactory receptors have different affinities to specific molecular physicochemical properties, and that the different activation of these receptors gives rise to a spatio-temporal pattern of activity that reflects odors.

Electronic Nose

eNose are analytic devices for mimicking the principle of biological olfaction that have as main component an array of non specific chemical sensors. Combining electronics, path

recognition and modern technology, the eNoses uses gas sensors to translate the chemical signal into an electrical signal when an odorant volatiles from samples reach the gas sensor array. Usually the pattern recognition is used to perform either the quantitative or the qualitative identification. In order to reproduce the olfactory epithelium a gas sensor array is sealed in a chamber of the eNose. A cross-sensitive chemical sensors will then act as olfactory neuron transferring the odor information from a chemical into an electric form similar to the one process which occur in the olfactory bulb where the signal is integrated and enhanced. The information is then elaborated by an artificial neuronal network, which provide coding, processing and storage. The gas sensor array transforms odor information from the sample space into a measurement space. This is a key procedure for information processing within an eNose. Gas sensors with different transduction principles and different fabrication techniques provide various ways to obtain odor information. Commercially a lot of different sensor types are available the most frequently used sensor types include metal oxide semiconductors (MOS), quartz crystal microbalances (QCM), conducting polymers (CP) and surface acoustic wave (SAW) sensors. A big influence in the choice of the sensor is made by the fast response, reversibility, repeatability and high sensitivity of the sensor. While constructing the sensor array for a eNose the sensors are selected to be cross-selective to different odors, such that their sensitivity is overlapped with the same odor, to make the most of type-limited sensors for obtaining adequate odor information. In general the amount of raw data generated from the array of sensor's is huge, so that the information has to be transferred from a high dimensional space into a lower one. Pattern recognition are then needed to encode the signal into a so called classification space. Both are important and necessary for designing a powerful information processing algorithm and constructing an array with high quality gas sensors. Many pattern recognition methods have been introduced into eNose, including parameterized and non-parameterized multivariate statistical methods. Artificial neural network have various significant advantages: (i) Self-adaptive, (ii) capability of error tolerance and generalization suitable for treating the problems (iii) parallel processing and distributed storage.

7.5 References

1. Schmidt, Lang (2007). "Ohysiologie des Menschen", *Soringer*, 30. Auflage.
2. Faller A., Schünke M. (2008). "Der Körper des Menschen", *Thieme*, 15. Auflage.
3. Paxianos G., Mai J.K. (2004). "The human Nervous System", *Elsevier academic press*, 2nd Edition.
4. William. "Review of Medial Physiology", *Lange*, 22th Edition.
5. Haddad R. ed al (2008). "Measuring smells", *Elsevier Ltd*, 18:438-444
6. Mamlouk A.M., Martinez T. (2004). "One dimensions of the olfactory perception space", *Elsevier B.V.*
7. >Guang L ed al (2009), "Progress in bionic information processing techniques for an electronic nose based on olfactory models", *Chinese Science Bulletin*, 54(4)521-53Z

1

1 <http://en.wikibooks.org/wiki/Category%3A>

8 Gustatory_System

8.1 Introduction

The Gustatory System or sense of taste allows us to perceive different flavors from substances like food, drinks, medicine etc. Molecules that we taste or tastants are sensed by cells in our mouth, which send information to the brain. These specialized cells are called taste cells and can sense 5 main tastes: bitter, salty, sweet, sour and umami (savory). All the variety of flavors that we know are combinations of molecules which fall into these categories.

Measuring the degree by which a substance presents one of the basic tastes is done subjectively by comparing its taste to a taste of a reference substance according to relative indexes of different substances. For the bitter taste quinine (found in tonic water) is used to rate how bitter a substance is. Saltiness can be rated by comparing to a dilute salt solution. The sourness is compared to diluted hydrochloric acid (H^+Cl^-). Sweetness is measured relative to sucrose. The values of these reference substances are defined as 1.

8.1.1 Bitter

(Coffee, mate, beer, tonic water etc.)

It is considered by many as unpleasant. In general bitterness is very interesting because a large number of bitter compounds are known to be toxic so the bitter taste is considered to provide an important protective function. Plant leaves often contain toxic compounds. Herbivores have a tendency to prefer immature leaves, which have higher protein content and lower poison levels than mature leaves. It seems that even if the bitter taste is not very pleasant at first, there is a tendency to overcome this aversion because coffee and drinks containing rich amount of caffeine and are widely consumed. Sometimes bitter agents are added to substances to prevent accidental ingestion.

8.1.2 Salty

(Table salt)

The salty taste is primarily produced by the presence of cations such as Li^+ (lithium ions), K^+ (potassium ions) and more commonly Na^+ (sodium). The saltiness of substances is compared to sodium chloride, which is typically used as table salt (Na^+Cl^-). Potassium chloride K^+Cl^- is the principal ingredient used in salt substitutes and has an index of 0.6 (see below part 5) compared to 1 of Na^+Cl^- .

8.1.3 Sour

(Lemon, orange, wine, spoiled milk and candies containing citric acid)

Sour taste can be mildly pleasant and it is linked to salty flavor but more exacerbated. Typically sour are fruits, which are over-ripened, spoiled milk, rotten meat, and other spoiled foods, which can be dangerous. It also tastes acids (H^+ ions) which taken in large quantities can cause irreversible tissue damage. Sourness is rated compared to hydrochloric acid ($H+Cl^-$), which has a sourness index of 1.

8.1.4 Sweet

(Sucrose (table sugar), cake, ice cream etc.)

Sweetness is regarded as a pleasant sensation and is produced by the presence of mostly sugars. Sweet substances are rated relative to sucrose, which has an index of 1. Nowadays there are many artificial sweeteners in the market, these include saccharin, aspartame and sucralose but it is still not clear how these substitutes activate the receptors.

8.1.5 Umami (savory or tasty)

(Cheese, soy sauce etc.)

Recently, monosodium glutamate (umami) has been added as the fifth taste. This taste signals the presence of L-glutamate and it is a very important for the Eastern cuisines.

8.2 Sensory Organs

8.2.1 Tongue and Taste Buds



Figure 110 Human tongue

Taste cells are epithelial and are clustered in taste buds located in the tongue, soft palate, epiglottis, pharynx and the esophagus the tongue being the primary organ of the Gustatory System.

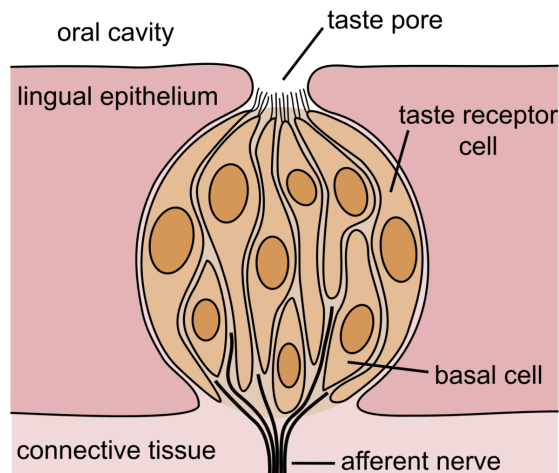


Figure 111 Schematic drawing of a taste bud

Taste buds are located in papillae along the surface of the tongue. There are three types of papillae in human: fungiform located in the anterior part containing approximately five taste buds, circumvallate papillae which are bigger and more posterior than the previous ones and the foliate papillae that are in the posterior edge of the tongue. Circumvallate and foliate papillae contain hundreds of taste buds. In each taste bud there are different types of cells: basal, dark, intermediate and light cells. Basal cells are believed to be the stem cells that give rise to the other types. It is thought that the rest of the cells correspond to different stages of differentiation where the light cells are the most mature type of cells. An alternative idea is that dark, intermediate and light cells correspond to different cellular lineages. Taste cells are short lived and are continuously regenerated. They contain a taste pore at the surface of the epithelium where they extend microvilli, the site where sensory transduction takes place. Taste cells are innervated by fibers of primary gustatory neurons. They contact sensory fibers and these connections resemble chemical synapses, they are excitable with voltage-gated channels: K^+ , Na^+ and Ca^{2+} channels capable of generating action potentials. Although the reaction from different tastants varies, in general tastants interact with receptors or ion channels in the membrane of a taste cells. These interactions depolarize the cell directly or via second messengers and in this way the receptor potential generates action potentials within the taste cells, which lead to Ca^{2+} influx through Ca^{2+} voltage-gated channels followed by the release of neurotransmitters at the synapses with the sensory fibers.

8.2.2 Tongue map

The idea that the tongue is most sensitive to certain tastes in different regions was a long time misconception, which has now been proved to be wrong. All sensations come from all regions of the tongue.

8.2.3 Supertasters

An average person has about 5'000 taste buds. A "supertaster" is a person whose sense of taste is significantly more sensitive than average. The increase in the response is thought to be because they have more than 20'000 taste buds, or due to an increased number of fungiform papillae.

8.3 Transduction of Taste

As mentioned before we distinguish between 5 types of basic tastes: bitter, salty, sour, sweet and umami. There is one type of taste receptor for each flavor known and each type of taste stimulus is transduced by a different mechanisms. In general bitter, sweet and umami are detected by G protein-coupled receptors and salty and sour are detected via ion channels.

8.3.1 Bitter

Bitter compounds act through G protein coupled receptors (GPCR's) also known as a seven-transmembrane domains, which are located in the walls of the taste cells. Taste receptors of type 2 (T2Rs) which is a group of GPCR's is thought respond to bitter stimuli. When the bitter-tasting ligand binds to the GPCR it releases the G protein gustducin, its 3 subunits break apart and activate phosphodiesterase, which in turn converts a precursor within the cell into a secondary messenger, closing the K⁺ channels. This secondary messenger stimulates the release of Ca²⁺, contributing to depolarization followed by neurotransmitter release. It is possible that bitter substances that are permeable to the membrane are sensed by mechanisms not involving G proteins.

8.3.2 Salt

The amiloride-sensitive epithelial sodium channel (ENaC), a type of ion channel in the taste cell wall, allows Na⁺ ions to enter the cell down an electrochemical gradient, altering the membrane potential of the taste cells by depolarizing the cell. This leads to an opening of voltage-gated Ca²⁺ channels, followed by neurotransmitter release.

8.3.3 Sour

The sour taste signals the presence of acidic compounds (H⁺ ions) and there are three receptors: 1) The ENaC, (the same protein involved in salty taste). 2) There are also H⁺ gated channels; one is the K⁺ channel, which allows K⁺ outflux of the cell. H⁺ ions block these so the K⁺ stays inside the cell. 3) A third channel undergoes a configuration change when a H⁺ attaches to it leading to an opening of the channel and allowing an influx of Na⁺ down the concentration gradient into the cell, leading to the opening of a voltage gated Ca²⁺ channels. These three receptors work in parallel and lead to depolarization of the cell followed by neurotransmitter release.

8.3.4 Sweet

Sweet transduction is mediated by the binding of a sweet tastant to GPCR's located in the apical membrane of the taste cell. Saccharide activates the GPCR, which releases gustducin and this in turn activates cAMP (cyclic adenylylate monophosphate). cAMP will activate the cAMP kinase that will phosphorylate the K⁺ channels and eventually inactivate them, leading to depolarization of the cell and followed by neurotransmitter release.

8.3.5 Umami (Savory)

Umami receptors involve also GPCR's, the same way as bitter and sweet receptors. Glutamate binds a type of the metabotropic glutamate receptor mGluR4 causing a G-protein complex to activate a secondary receptor, which ultimately leads to neurotransmitter release. In particular how the intermediate steps work, is currently unknown.

8.4 Signal Processing

In humans, the sense of taste is transmitted to the brain via three cranial nerves. The VII facial nerve carries information from the anterior 2/3 part of the tongue and soft palate. The IX nerve or glossopharyngeal nerve carries taste sensations from the posterior 1/3 part of the tongue and the X nerve or vagus nerve carries information from the back of the oral cavity and the epiglottis.

The gustatory cortex is the brain structure responsible for the perception of taste. It consists of the anterior insula on the insular lobe and the frontal operculum on the inferior frontal gyrus of the frontal lobe. Neurons in the gustatory cortex respond to the five main tastes.

Taste cells synapse with primary sensory axons of the mentioned cranial nerves. The central axons of these neurons in the respective cranial nerve ganglia project to rostral and lateral regions of the nucleus of the solitary tract in the medulla. Axons from the rostral (gustatory) part of the solitary nucleus project to the ventral posterior complex of the thalamus, where they terminate in the medial half of the ventral posterior medial nucleus. This nucleus projects to several regions of the neocortex, which include the gustatory cortex.

Gustatory cortex neurons exhibit complex responses to changes in concentration of tastant. For one tastant, the same neuron might increase its firing and for an other tastant, it may only respond to an intermediate concentration.

8.5 Taste and Other Senses

In general the Gustatory Systems does not work alone. While eating, consistency and texture are sensed by the mechanoreceptors from the somatosensory system. The sense of taste is also correlated with the olfactory system because if we lack the sense of smell it makes it difficult to distinguish the flavor.

8.5.1 Spicy food

(black peppers, chili peppers, etc.)

It is not a basic taste because this sensation does not arise from taste buds. Capsaicin is the active ingredient in spicy food and causes “hotness” or “spiciness” when eaten. It stimulates temperature fibers and also nociceptors (pain) in the tongue. In the nociceptors it stimulates the release of substance P, which causes vasodilatation and release of histamine causing hyperalgesia (increased sensitivity to pain).

In general basic tastes can be appetitive or aversive depending on the effect that the food has on us but also essential to the taste experience are the presentation of food, color, texture, smell, previous experiences, expectations, temperature and satiety.

8.6 Taste disorders

8.6.1 Ageusia (complete loss of taste)

Ageusia is a partial or complete loss in the sense of taste and sometimes it can be accompanied by the loss of smell.

8.6.2 Dysgeusia (abnormal taste)

Is an alteration in the perception associated with the sense of taste. Tastes of food and drinks vary radically and sometimes the taste is perceived as repulsive. The causes of dysgeusia can be associated with neurologic disorders.

1

1 <http://en.wikibooks.org/wiki/Category%3A>

9 Sensory Systems in Non-Primates

Primates are animals belonging to the highest order of mammals. Primates include humans and the nonhuman primates, the apes, monkeys, lemurs, tree-shrews, lorises, bush babies and tarsiers. They are characterized by a voluminous and complicated brain. They have excellent sight and are highly adapted to an arboreal existence, including the possession by some of a prehensile tail. Non primates on the other hand do have a much less developed brain. But as we learn more about the rest of the animal world, it's becoming pretty clear that non-primates are pretty intelligent too. Some examples include pigs, octopus, and crows.¹

In many branches of mythology, the crow plays a shrewd trickster, and in the real world, crows are proving to be quite a clever species. Crows have been found to engage in feats such as tool use, the ability to hide and store food from season to season, episodic-like memory, and the ability to use personal experience to predict future conditions.

As it turns out, being piggy is actually a pretty smart tactic. Pigs are probably the most intelligent domesticated animal on the planet. Although their raw intelligence is most likely commensurate with a dog or cat, their problem-solving abilities top those of felines and canine pals.

If pigs are the most intelligent of the domesticated species, octopuses take the cake for invertebrates. Experiments in maze and problem-solving have shown that they have both short-term and long-term memory. Octopuses can open jars, squeeze through tiny openings, and hop from cage to cage for a snack. They can also be trained to distinguish between different shapes and patterns. In a kind of play-like activity (one of the hallmarks of higher intelligence species) octopuses have been observed repeatedly releasing bottles or toys into a circular current in their aquariums and then catching them.

9.1 Octopus

9.1.1 Introduction

One of the most interesting non-primate is the octopus. The most interesting feature about this non-primate is its arm movement. In these invertebrates, the control of the arm is especially complex because the arm can be moved in any direction, with a virtually infinite number of degrees of freedom. In the octopus, the brain only has to send a command to the arm to do the action—the entire recipe of how to do it is embedded in the arm itself. Observations indicate that octopuses reduce the complexity of controlling their arms by

¹ K. Gammon, Life's Little Mysteries (<http://www.lifeslittlemysteries.com/1647-smartest-non-primates.html>) . TechMediaNetwork.

keeping their arm movements to set, stereotypical patterns. To find out if octopus arms have minds of their own, the researchers cut off the nerves in an octopus arm from the other nerves in its body, including the brain. They then tickled and stimulated the skin on the arm. The arm behaved in an identical fashion to what it would in a healthy octopus. The implication is that the brain only has to send a single move command to the arm, and the arm will do the rest.

In this chapter we discuss in detail the sensory system of an octopus and focus on the sensory motor system in this non-primate.

Octopus - The intelligent non-primate

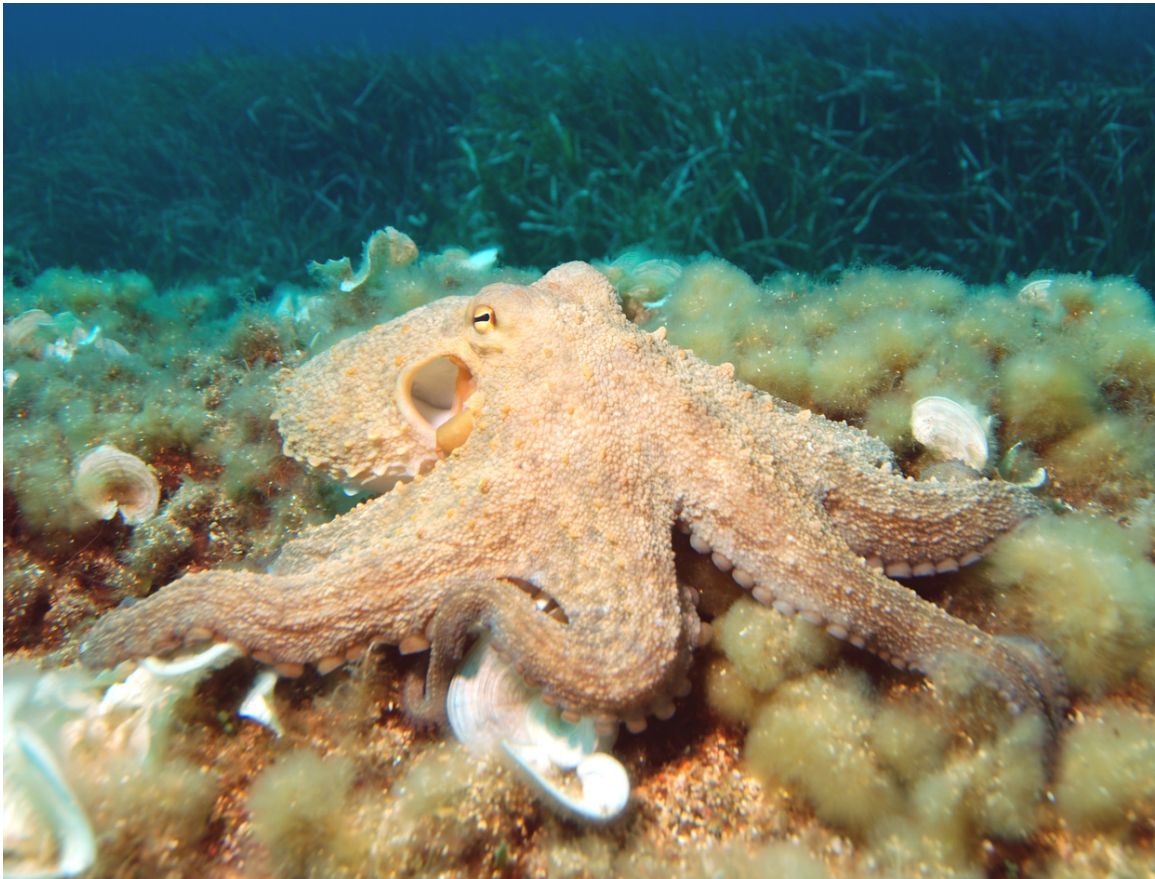


Figure 112 The Common Octopus, *Octopus vulgaris*.

Octopuses have two eyes and four pairs of arms, and they are bilaterally symmetric. An octopus has a hard beak, with its mouth at the center point of the arms. Octopuses have no internal or external skeleton (although some species have a vestigial remnant of a shell inside their mantle), allowing them to squeeze through tight places. Octopuses are among the most intelligent and behaviorally flexible of all invertebrates.

The most interesting feature of the octopuses is their arm movements. For goal directed arm movements, the nervous system in octopus generates a sequence of motor commands that

brings the arm towards the target. Control of the arm is especially complex because the arm can be moved in any direction, with a virtually infinite number of degrees of freedom. The basic motor program for voluntary movement is embedded within the neural circuitry of the arm itself.²

9.1.2 Arm Movements in Octopus

In the hierarchical organization in octopus, the brain only has to send a command to the arm to do the action. The entire recipe of how to do it is embedded in the arm itself. By the use of the arms octopus walks, seizes its prey, or rejects unwanted objects and also obtains a wide range of mechanical and chemical information about its immediate environment.

Octopus arms, unlike human arms, are not limited in their range of motion by elbow, wrist, and shoulder joints. To accomplish goals such as reaching for a meal or swimming, however, an octopus must be able to control its eight appendages. The octopus arm can move in any direction using virtually infinite degrees of freedom. This ability results from the densely packed flexible muscle fibers along the arm of the octopus.

Observations indicate that octopuses reduce the complexity of controlling their arms by keeping their arm movements to set, stereotypical patterns.³ For example, the reaching movement always consists of a bend that propagates along the arm toward the tip. Since octopuses always use the same kind of movement to extend their arms, the commands that generate the pattern are stored in the arm itself, not in the central brain. Such a mechanism further reduces the complexity of controlling a flexible arm. These flexible arms are controlled by an elaborate peripheral nervous system containing 5×10^7 neurons distributed along each arm. 4×10^5 of these are motor neurons, which innervate the intrinsic muscles of the arm and locally control muscle action.

Whenever it is required, the nervous system in octopus generates a sequence of motor commands which in turn produces forces and corresponding velocities making the limb reach the target. The movements are simplified by the use of optimal trajectories made through vectorial summation and superposition of basic movements. This requires that the muscles are quite flexible.

9.1.3 The Nervous System of the Arms

The eight arms of the octopus are elongated, tapering, muscular organs, projecting from the head and regularly arranged around the mouth. The inner surface of each arm bears a double row of suckers, each sucker alternating with that of the opposite row. There are about 300 suckers on each arm.⁴

2 G. S. et al., Control of Octopus Arm Extension by a Peripheral Motor Program . Science 293, 1845, 2001.

3 Y. Gutfreund, Organization of octopus arm movements: a model system for studying the control of flexible arms. Journal of Neuroscience 16, 7297, 1996.

4 P. Graziadei, The anatomy of the nervous system of Octopus vulgaris, J. Z. Young. Clarendon, Oxford, 1971.

The arms perform both motor and sensory functions. The nervous system in the arms of the octopus is represented by the nerve ganglia, subserving motor and inter-connecting functions. The peripheral nerve cells represent the sensory systems. There exists a close functional relationship between the nerve ganglia and the peripheral nerve cells.

General anatomy of the arm

The muscles of the arm can be divided into three separate groups, each having a certain degree of anatomical and functional independence:

1. Intrinsic muscles of the arm,
2. Intrinsic muscles of the suckers, and
3. Acetabulo-brachial muscles (connects the suckers to the arm muscles).

Each of these three groups of muscles comprises three muscle bundles at right angles to one another. Each bundle is innervated separately from the surrounding units and shows a remarkable autonomy. In spite of the absence of a bony or cartilaginous skeleton, octopus can produce arm movements using the contraction and relaxation of different muscles. Behaviorally, the longitudinal muscles shorten the arm and play major role in seizing objects carrying them to mouth, and the oblique and transverse muscles lengthen the arms and are used by octopus for rejecting unwanted objects.

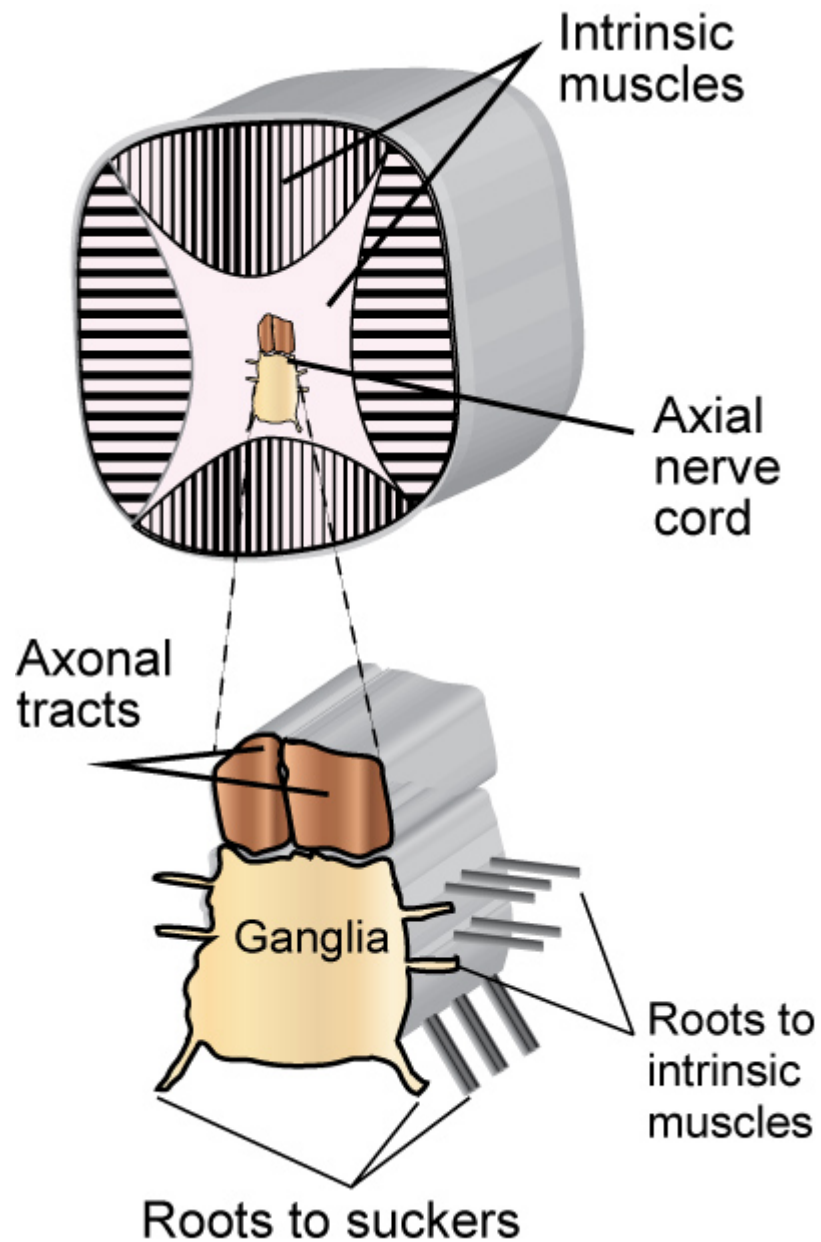


Figure 113 Cross section of an octopus arm: The lateral roots innervate the intrinsic muscles, the ventral roots the suckers.

Six main nerve centers lie in the arm and are responsible for the performance of these sets of muscles. The axial nerve cord is by far the most important motor and integrative center of the arm. The eight cords one in each arm contains altogether 3.5×10^8 neurons. Each axial cord is linked by means of connective nerve bundles with five sets of more peripheral nerve centers, the four intramuscular nerve cords, lying among the intrinsic muscles of the arm, and the ganglia of the suckers, situated in the peduncle just beneath the acetabular cup of each sucker.

All these small peripheral nerves contain motor neurons and receive sensory fibers from deep muscle receptors which play the role of local reflex centers. The motor innervation of the muscles of the arm is thus provided not only by the motor neurons of the axial nerve cord, which receives pre-ganglionic fibers from the brain, but also by these more peripheral motor centers.

Sensory Nervous system

The arms contain a complex and extensive sensory system. Deep receptors in the three main muscle systems of the arms, provide the animal with a widespread sensory apparatus for collecting information from muscles. Many primary receptors lie in the epithelium covering the surface of the arm. The sucker, and particularly its rim, has the greatest number of these sensory cells, while the skin of the arm is rather less sensitive. Several tens of thousands of receptors lie in each sucker.

Three main morphological types of receptors are found in arms of an octopus. These are round cells, irregular multipolar cells, and tapered ciliated cells. All these elements send their processes centripetally towards the ganglia. The functional significance of these three types of receptors is still not very well known and can only be conjectured. It has been suggested that the round and multipolar receptors may record mechanical stimuli, while ciliated receptors are likely to be chemo-receptors.

The ciliated receptors do not send their axons directly to the ganglia but the axons meet encapsulated neurons lying underneath the epithelium and make synaptic contacts with the dendritic processes of these. This linkage helps in reduction of input between primary nerve cells. Round and multipolar receptors on the other hand send their axons directly to the ganglia where the motor neurons lie.

9.1.4 Functioning of peripheral nervous system in arm movements

Behavioral experiments suggest that information regarding the movement of the muscles does not reach the learning centers of the brain, and morphological observations prove that the deep receptors send their axons to peripheral centers such as the ganglion of the sucker or the intramuscular nerve cords.⁵ The information regarding the stretch or movement of the muscles is used in local reflexes only.

When the dorsal part of the axial nerve cord that contains the axonal tracts from the brain is stimulated by electrical signals, movements in entire arm are still noticed. The movements are triggered by the stimulation which is provided and is not directly driven by the stimuli coming from the brain. Thus, arm extensions are evoked by stimulation of the dorsal part of the axial nerve cord. In contrast, the stimulation of the muscles within the same area or the ganglionic part of the cord evokes only local muscular contractions. The implication is that the brain only has to send a single move command to the arm, and the arm will do the rest.

A dorsally oriented bend propagates along the arm causing the suckers to point in the direction of the movement. As the bend propagates, the part of the arm proximal to the bend

⁵ M. J. Wells, The orientation of octopus. *Ergeb. Biol.* 26, 40-54, 1963.

remains extended. For further conformations that an octopus arm has a mind of its own, the nerves in an octopus arm have been cut off from the other nerves in its body, including the brain. Movements resembling normal arm extensions were initiated in amputated arms by electrical stimulation of the nerve cord or by tactile stimulation of the skin or suckers.

It has been noted that the bend propagations are more readily initiated when a bend is created manually before stimulation. If the fully relaxed arm is stimulated, the initial movement is triggered by the stimuli, which follows the same bend propagation. The nervous system of the arm thus, not only drives local reflexes but controls complex movements involving the entire arm.

These evoked movements are almost kinematically identical to the movements of freely behaving octopus. When stimulated, a severed arm shows an active propagation of the muscle activity as in natural arm extensions. Movements evoked from similar initial arm postures result in similar paths, while different starting postures result in different final paths.

As the extensions evoked in denervated octopus arms are qualitatively and kinematically similar to natural arm extensions, an underlying motor program seems to be controlling the movements which are embedded in the neuromuscular system of the arm, which does not require central control.

9.2 Fish

Fish are aquatic animals with great diversity. There are over 32'000 species of fish, making it the largest group of vertebrates.

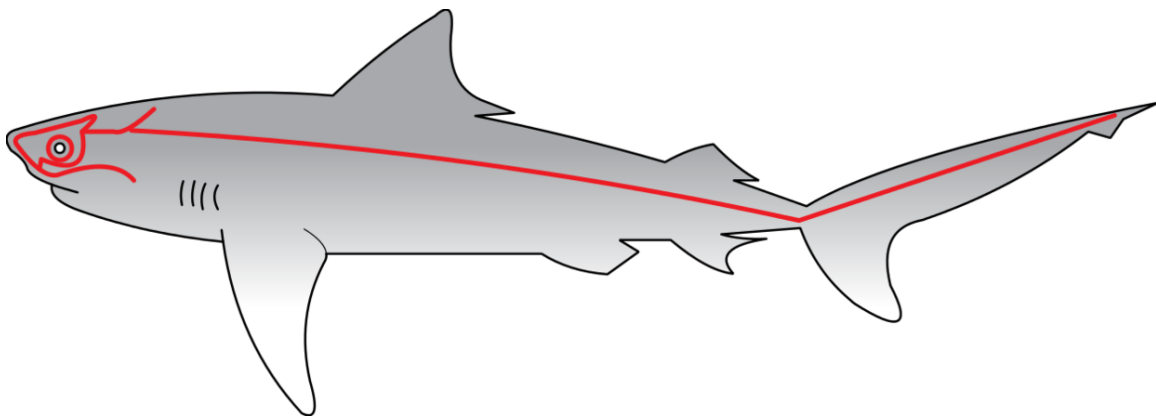


Figure 114 The lateral line sensory organ shown on a shark.

Most fish possess highly developed sense organs. The eyes of most daylight dwelling fish are capable of color vision. Some can even see ultra violet light. Fish also have a very good sense of smell. Trout for example have special holes called “nares” in their head that they use to register tiny amounts of chemicals in the water. Migrating salmon coming from the ocean use this sense to find their way back to their home streams, because they remember what they smell like. Especially ground dwelling fish have a very strong tactile sense in their

lips and barbels. Their taste buds are also located there. They use these senses to search for food on the ground and in murky waters.

Fish also have a lateral line system, also known as the lateral system. It is a system of tactile sense organs located in the head and along both sides of the body. It is used to detect movement and vibration in the surrounding water.

9.2.1 Function

Fish use the lateral line sense organ to sense prey and predators, changes in the current and its orientation and they use it to avoid collision in schooling.

Coombs et al. have shown [1] that the lateral line sensory organ is necessary for fish to detect their prey and orient towards it. The fish detect and orient themselves towards movements created by prey or a vibrating metal sphere even when they are blinded. When signal transduction in the lateral lines is inhibited by cobalt chloride application, the ability to target the prey is greatly diminished.

The dependency of fish on the lateral line organ to avoid collisions in schooling fish was demonstrated by Pitcher et al. in 1976, where they show that optically blinded fish can swim in a school of fish, while those with a disabled lateral line organ cannot [2].

9.2.2 Anatomy

The lateral lines are visible as two faint lines that run along either side of the fish body, from its head to its tail. They are made up of a series of mechanoreceptor cells called neuromasts. These are either located on the surface of the skin or are, more frequently, embedded within the lateral line canal. The lateral line canal is a mucus filled structure that lies just beneath the skin and transduces the external water displacement through openings from the outside to the neuromasts on the inside. The neuromasts themselves are made up of sensory cells with fine hair cells that are encapsulated by a cylindrical gelatinous cupula. These reach either directly into the open water (common in deep sea fish) or into the lymph fluid of the lateral line canal. The changing water pressures bend the cupula, and in turn the hair cells inside. Similar to the hair cells in all vertebrate ears, a deflection towards the shorter cilia leads to a hyperpolarization (decrease of firing rate) and a deflection in the opposite direction leads to depolarization (increase of firing rate) of the sensory cells. Therefore the pressure information is transduced to digital information using rate coding that is then passed along the lateral line nerve to the brain. By integrating many neuromasts through their afferent and efferent connections, complex circuits can be formed. This can make them respond to different stimulation frequencies and consequently coding for different parameters, like acceleration or velocity [3].

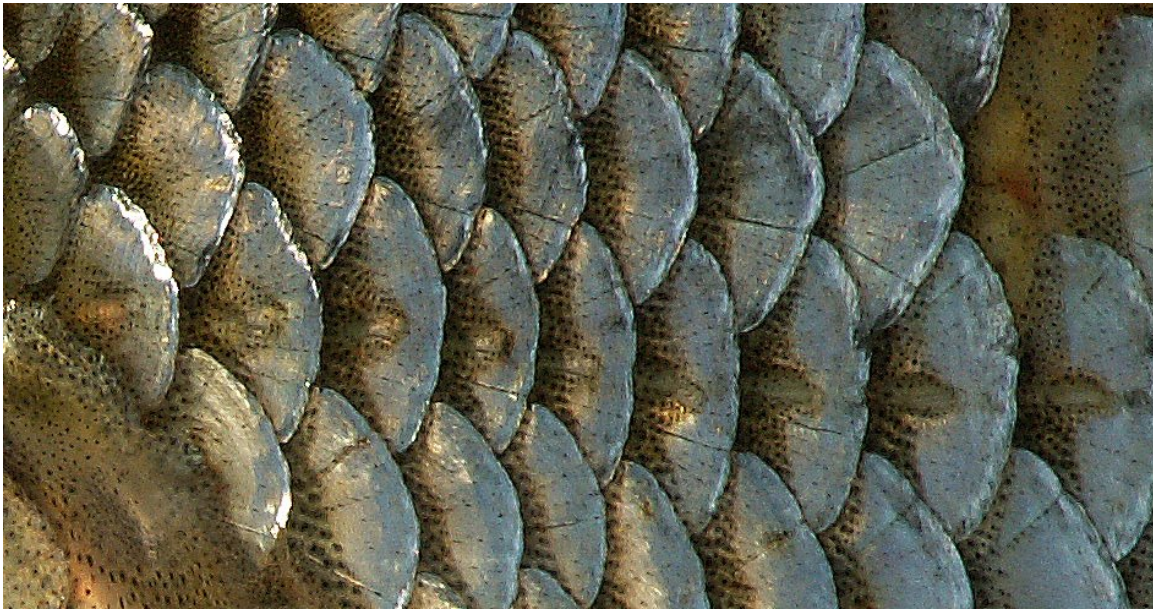


Figure 115 Some scales of the lateral line (center) of a *Rutilus rutilus*

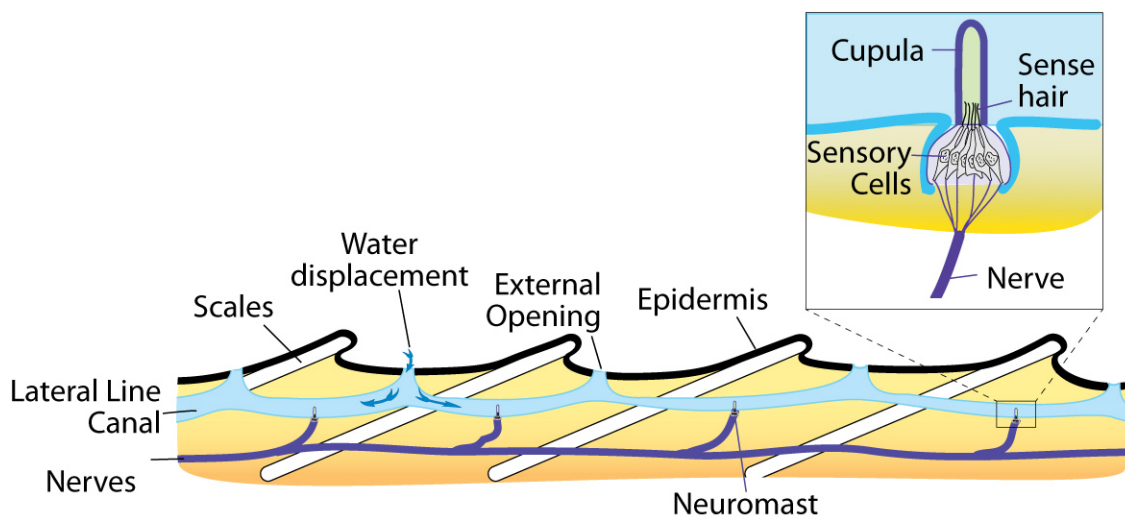


Figure 116 Sketch of the anatomy of the lateral line sensory system.

In sharks and rays, some neuromasts have undergone an interesting evolution. They have evolved into electroreceptors called ampullae of Lorenzini. They are mostly concentrated around the head of the fish and can detect a change of electrical stimuli as small as 0.01 microvolt [4]. With this sensitive instrument these fish are able to detect tiny electrical potentials generated by muscle contractions and can thus find their prey over large distances, in murky waters or even hidden under the sand. It has been suggested that sharks also use this sense for migration and orientation, since the ampullae of Lorenzini are sensitive enough to detect the earth's electromagnetic field.

9.2.3 Convergent Evolution

Cephalopods:

Cephalopods such as squids, octopuses and cuttlefish have lines of ciliated epidermal cells on head and arms that resemble the lateral lines of fish. Electrophysiological recordings from these lines in the common cuttlefish (*Sepia officinalis*) and the brief squid (*Lolliguncula brevis*) have identified them as an invertebrate analogue to the mechanoreceptive lateral lines of fish and aquatic amphibians [5].

Crustaceans:

Another convergence to the fish lateral line is found in some crustaceans. Contrary to fish, they don't have the mechanosensory cells on their body, but have them spaced at regular intervals on long trailing antennae. These are held parallel to the body. This forms two 'lateral lines' parallel to the body that have similar properties to those of fish lateral lines and are mechanically independent of the body [6].

Mammals:

In aquatic manatees the postcranial body bears tactile hairs. They resemble the mechanosensory hairs of naked mole rats. This arrangement of hair has been compared to the fish lateral line and complement the poor visual capacities of the manatees. Similarly, the whiskers of harbor seals are known to detect minute water movements and serve as a hydrodynamic receptor system. This system is far less sensitive than the fish equivalent. [7]

9.3 Flies

9.3.1 Introduction



Figure 117 Halteres of the Crane fly

Halteres are sensory organs present in many flying insects. Widely thought to be an evolutionary modification of the rear pair of wings on such insects, halteres provide gyroscopic sensory data, vitally important for flight. Although the fly has other relevant systems to aid in flight, the visual system of the fly is too slow to allow for rapid maneuvers. Additionally, to be able to fly adeptly in low light conditions, a requirement to avoid predation, such a sensory system is necessary. Indeed, without halteres, flies are incapable of sustained, controlled flight. Since the 18th century, scientists have been aware of the role halteres play in flight, but it was only recently that the mechanisms by which they operate have been better explored. ^{6 7}

6 J. L. Fox and T. L. Daniel . A neural basis for gyroscopic force measurement in the halteres of *Holorusia*. A neural basis for gyroscopic force measurement in the halteres of *Holorusia*. . *J Comp Physiol* , **194** :887-8972008

7 Rhoe A. Thompson . Haltere Mediated Flight Stabilization in Diptera: Rate Decoupling, Sensory Encoding, and Control Realization. Haltere Mediated Flight Stabilization in Diptera: Rate Decoupling, Sensory Encoding, and Control Realization. . *PhD thesis* , (University of Florida)2009

9.3.2 Anatomy

The haltere evolved from the rearmost of two pairs of wings. While the first has maintained its usage for flight, the posterior pair has lost its flight functions and has adopted a slightly different shape. The haltere is visually comprised of three structural components: a knob-shaped end, a thin shaft, and a slightly wider base. The knob contains approximately 13 innervated hairs, while the base contains two chordotonal organs, each innervated by about 20-30 nerves. Chordotonal organs are sense organs thought to be solely responsive to extension, though they remain relatively unknown. The base is also covered by around 340 campaniform sensilla, which are small fibers which respond preferentially to compression in the direction in which they are elongated. Each of these fibers is also innervated. Relative to the stalk of the haltere, both the chordotonal organs and the campaniform sensilla have an orientation of approximately 45 degrees, which is optimal for measuring bending forces on the haltere. The halteres move contrary (anti-phase) to the wings during flight. The sensory components can be categorized into three groups⁸): those sensitive to vertical oscillations of the haltere, including the dorsal and ventral scapal plates, dorsal and ventral Hicks papillae (both the plates and papillae are subcategories of the aforementioned campaniform sensilla), and the small chordotonal organ. The basal plate (another manifestation of the sensilla) and the large chordotonal organ are sensitive to gyroscopic torque acting on the haltere, and there is also a population of undifferentiated papillae which are responsive to all strains acting on the base of the haltere. This provides an additional method for flies to distinguish between the direction of force being applied to the haltere.

Genetics

As Homeobox genes were being discovered and explored for the first time, it was found that the deletion or inactivation of the Hox gene Ultrabithorax (Ubx) causes the halteres to develop into a normal pair of wings. This was a very compelling early result as to the nature of Hox genes. Manipulations to the Antennapedia gene can similarly cause legs to become severely deformed, or can cause a set of legs to develop instead of antennae on the head.

9.3.3 Function

The halteres function by detecting Coriolis forces, sensing the movement of air across the potentially rotating fly body. Studies have indicated that the angular velocity of the body is encoded by the Coriolis forces measured by the halteres⁹. Active halteres can recruit any neighboring units, influencing nearby muscles and causing dramatic changes in the flight dynamics. Halteres have been shown to have extremely fast response times, allowing these flight changes to be performed much more quickly than if the fly were to rely on its visual system. In order to distinguish between different rotational components, such as pitch

8 J. W. S. Pringle . The gyroscopic mechanism of the halteres of diptera. The gyroscopic mechanism of the halteres of diptera. . *Phil Trans R Soc Lond B* , **233** (602):347-3841948

9 J. W. S. Pringle . The gyroscopic mechanism of the halteres of diptera. The gyroscopic mechanism of the halteres of diptera. . *Phil Trans R Soc Lond B* , **233** (602):347-3841948

and roll, the fly must be able to combine signals from the two halteres, which must not be coincident (coincident signals would diminish the ability of the fly to differentiate the rotational axes). The halteres are capable of contributing to image stabilization, as well as in-flight attitude control, which was established by numerous authors noting a reaction from the head and wings to inputs from the components of the rotation rate vector. Contributions from halteres to head and neck movements have been noted, explaining their role in gaze stabilization. The fly therefore uses input from the halteres to establish where to fixate its gaze, an interesting integration of the two senses.

9.3.4 Mathematics

Recordings have indicated that halteres are capable of responding to stimuli at the same (double-wingbeat) frequency as Coriolis forces, the proof of concept that allows further mathematical analysis of how these measurements can occur. The vector cross-product of the halteres' angular velocity and the rotation of the body provide the Coriolis force vector to the fly. This force is at the same frequency as the wingbeat in both the pitch and roll planes, and is doubly fast in the yaw plane. Halteres are capable of providing a rate damping signal to affect rotations. This is because the Coriolis force is proportional to the fly's own rotation rate. By measuring the Coriolis force, the halteres can send an appropriate signal to their affiliated muscles, allowing the fly to properly control its flight. The large amplitude of haltere motion allows for the calculation of the vertical and horizontal rates of rotation. Because of the large disparity in haltere movement between vertical and horizontal movement, Ω_1 , the vertical component of the rotation rate, generates a force of double the frequency of the horizontal component. It is widely thought that this twofold frequency difference is what allows the fly to distinguish between the vertical and horizontal components. If we assume that the haltere moves sinusoidally, a reasonably accurate approximation of its real-world behavior, the angular position γ can be modeled as: $\gamma = \frac{\pi}{2} \sin(\omega t)$ where ω is the haltere beat frequency, and the amplitude is 180, a close approximation to the real life range of motion. The body rotational velocities can be computed, given the known rates (the roll, pitch, and yaw components are labeled below with 1, 2, and 3, respectively) from the two halteres' (Ω_b being the left and Ω_c being the right haltere) reference frames, respective to the body of the fly with the following calculations¹⁰:

$$W_1 = -\frac{\Omega_{b3} + \Omega_{c3}}{2 \sin(\alpha)}$$

$$W_2 = \frac{\Omega_{b3} - \Omega_{c3}}{2 \cos(\alpha)}$$

$$W_3 = -\frac{\Omega_{b1} + \Omega_{c1}}{2}$$

α represents the haltere angle of rotation from the body plane, and the Ω terms are, as mentioned, the angular velocity of the haltere with respect to the body. Knowing this, one could roughly simulate input to the halteres using the equation for forces on the end knob

¹⁰ Rhoe A. Thompson . Haltere Mediated Flight Stabilization in Diptera: Rate Decoupling, Sensory Encoding, and Control Realization. Haltere Mediated Flight Stabilization in Diptera: Rate Decoupling, Sensory Encoding, and Control Realization. . *PhD thesis* , (University of Florida)2009

of a haltere:

$$F = mg - ma_i - ma_F - m\dot{\Omega}_i \times r_i - m\Omega_i \times (\Omega_i \times r_i) - 2m\Omega_i \times v_i$$

m is the mass of the knob of the haltere, g is the acceleration due to gravity, $\{r_i, v_i\}$ and a_i are the position, velocity, and acceleration of the knob relative to the body of the fly in the i direction, a_F is the fly's linear acceleration, and Ω_i and $\dot{\Omega}_i$ are the angular velocity and acceleration components for the direction i , respectively, of the fly in space. The Coriolis force is simulated by the $2m\Omega \times v_i$ term. Because the sensory signal generated is proportional to the forces exerted on the halteres, this would allow the haltere signal to be simulated. If attempting to reconcile the force equation with the rotational component equations, it is worthwhile to remember that the force equation must be calculated separately for both halteres.

9.4 Butterflies



Figure 118 The sense of balance of butterflies sits at the base of the antennae.

Butterflies and moths keep their balance with *Johnston's organ*: this is an organ at the base of a butterfly's antennae, and is responsible for maintaining the butterfly's sense of balance and orientation, especially during flight.

9.5 References

10 Appendix

10.1 Spectrum

If light passes through a prism, a colour spectrum will be formed at the other end of the prism ranging from red to violet. The wavelength of the red light is from 650nm to 700nm, and the violet light is at around 400nm to 420nm. This is the EM range detectable for the human eye.

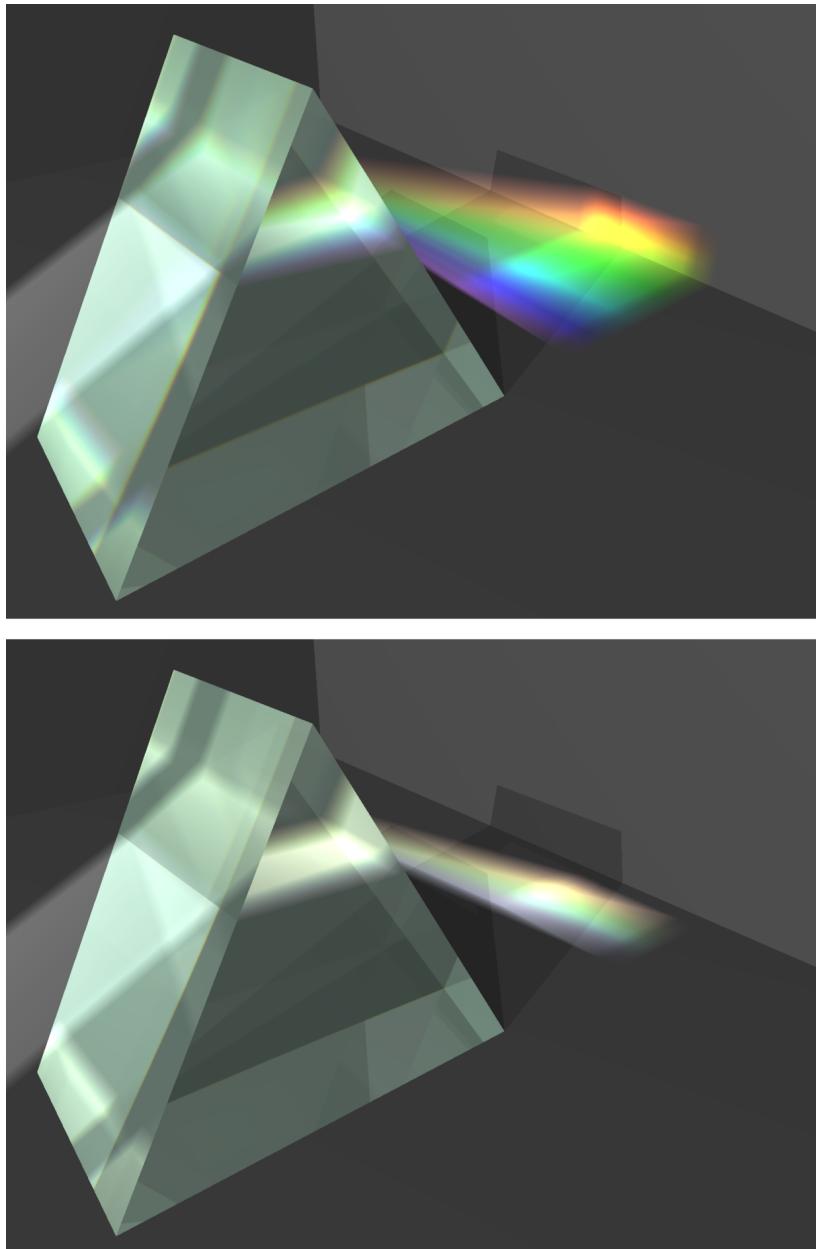


Figure 119 Colour spectrum produced by a prism

10.2 Colour Models

The colour triangle is often used to illustrate the colour-mixing effect. The triangle entangles the visible spectrum, and a white dot is located in the middle of the triangle. Because of additive colour mixing property of red (700nm), green(546nm) and blue(435nm), every colour can be produced by mixing those three colours.

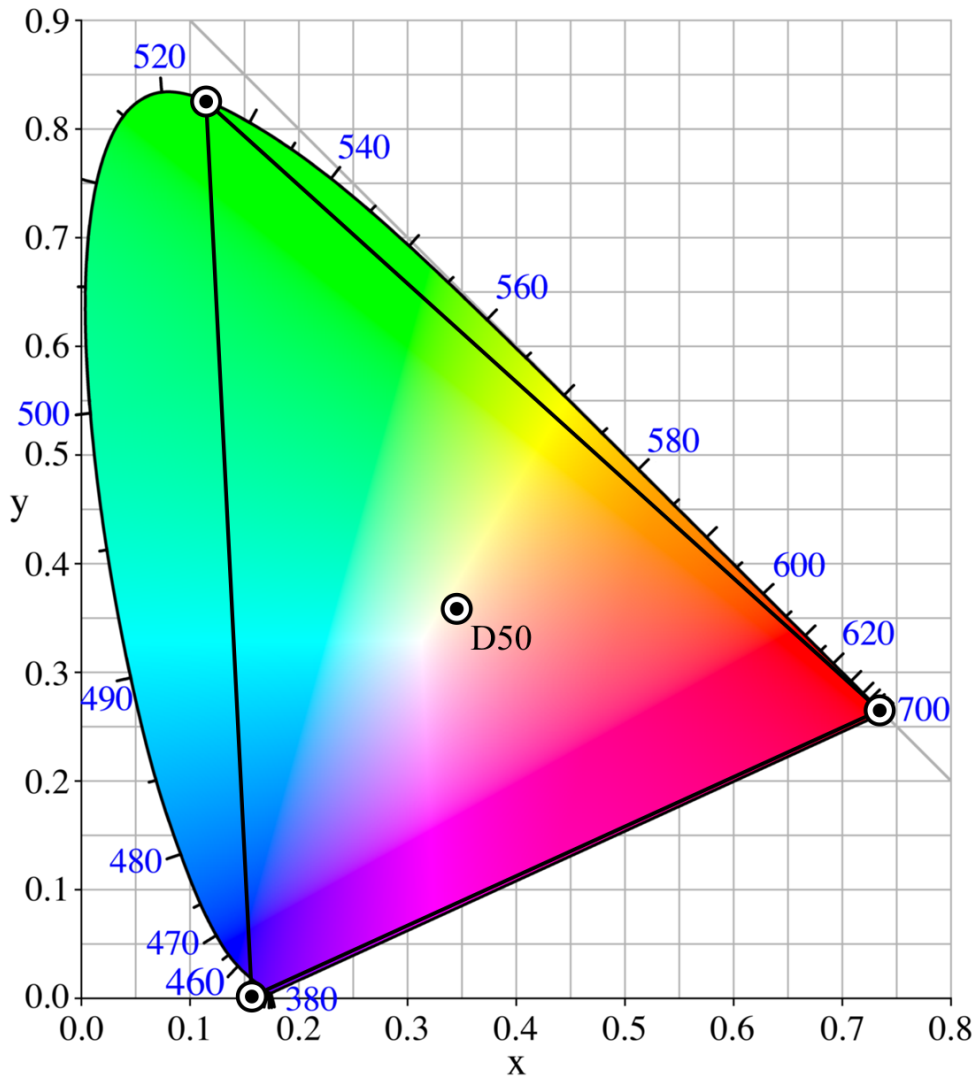


Figure 120 The RGB color-triangle

1

10.3 History of *Sensory Systems*

This Wikibook was started by engineers studying at ETH Zurich as part of the course Computational Simulations of Sensory Systems. The course combines physiology with an emphasis on the sensory systems, programming and signal processing. There is a plethora of information regarding these topics on the internet and in the literature, but there's a distinct lack of concise texts and books on the fusion of these 3 topics. The world needs a structured and thorough overview of biology and biological systems from an engineering

¹ <http://en.wikibooks.org/wiki/Category%3A>

point of view, which is what this book is trying to correct. We will start off with the Visual System, focusing on the biological and physiological aspects, mainly because this will be used in part to grade our performance in the course. The other part being the programming aspects have already been evaluated and graded. It is the authors' wishes that eventually information on physiology/biology, signal processing AND programming shall be added to each of the sensory systems. Also we hope that more sections will be added to extend the book in ways previously not thought of.

The original title of the Wikibook, *Biological Machines*, stressed the technical aspects of sensory system. However, as the wikibook evolved it became a comprehensive overview of human sensory systems, with additional emphasis on technical aspects of these systems. This focus is better represented with *Sensory Systems*, the new wikibook title since December 2011.

2

11 Sources

Visual System

- <http://www.yorku.ca/eye/>
- <http://www.eyedesignbook.com/> <-- Watch out, religious fanatic here.
- <http://users.rcn.com/jkimball.ma.ultranet/BiologyPages/>
- <http://www.physpharm.fmd.uwo.ca/undergrad/sensesweb/>
- http://www.optometry.co.uk/articles/docs/0b3e55d71662f4e8381aea8637c48f4f_stafford20010112.pdf
- Biology of Spiders by Rainer F. Foelix - Vision page 82-93
- Photoreceptors and light signalling by Alfred Batschauer, Royal Society of Chemistry (Great Britain), Published by Royal Society of Chemistry, 2003, ISBN 085404311X, 9780854043118
- <http://emedicine.medscape.com/article/835021-overview>
- <http://www.stlukeseye.com/Anatomy/>
- http://www.absoluteastronomy.com/topics/Rod_cell#encyclopedia
- <http://hubel.med.harvard.edu/>
- <http://www.absoluteastronomy.com/topics/Photopsin>
- Structural differences of cone 'oil-droplets' in the light and dark adapted retina of *Poecilia reticulata* P., Yvette W. Kunz and Christina Wise
- Advances in organ biology, Volume 10, Pages 1-395 (2005)
- <<http://www.search.eb.com/eb/art-53283>>"optic chiasm: visual pathways." Online Art. Encyclopædia Britannica Online.
- Color atlas of physiology, Despopoulos, A. and Silbernagl, S., 2003, Thieme
- Neurotransmitter systems in the retina, Ehinger, B., Retina, 2-4, 305, 1982

1

Auditory System

- *Intraoperative Neurophysiological Monitoring*, 2nd Edition, Aage R. Møller, Humana Press 2006, Totowa, New Jersey, pages 55-70
- *The Science and Applications of Acoustics*, 2nd Edition, Daniel R. Raichel, Springer Science&Business Media 2006, New York, pages 213-220
- *Physiology of the Auditory System*, P. J. Abbas, 1993, in: *Cummings Otolaryngology: Head and Neck Surgery*, 2nd edition, Mosby Year Book, St. Louis
- <http://thalamus.wustl.edu/course/audvest.html>
- <http://faculty.washington.edu/chudler/hearing.html>

1 <http://en.wikibooks.org/wiki/Category%3A>

- *Computer Simulations of Sensory Systems*, Lecture Script Ver 1.3 March 2010, T. Haslwanter, Upper Austria University of Applied Sciences, Linz, Austria,

Gustatory System

- A. Carleton, R. Accolla, S. A. Simon, *Trends Neurosci* 33, 326 (Jul).
- P. Dalton, N. Doolittle, H. Nagata, P. A. Breslin, *Nat Neurosci* 3, 431 (May, 2000).
- J. A. Gottfried, R. J. Dolan, *Neuron* 39, 375 (Jul 17, 2003).
- K. L. Mueller et al., *Nature* 434, 225 (Mar 10, 2005).
- J. B. Nitschke et al., *Nat Neurosci* 9, 435 (Mar, 2006).
- T. Okubo, C. Clark, B. L. Hogan, *Stem Cells* 27, 442 (Feb, 2009).
- D. V. Smith, S. J. St John, *Curr Opin Neurobiol* 9, 427 (Aug, 1999).
- D. A. Yarmolinsky, C. S. Zuker, N. J. Ryba, *Cell* 139, 234 (Oct 16, 2009).
- G. Q. Zhao et al., *Cell* 115, 255 (Oct 31, 2003).
- Kandel, E., Schwartz, J., and Jessell, T. (2000) *Principles of Neural Science*. 4th edition. McGraw Hill, New York.

12 Authors

This list contains the names of all the authors that have contributed to this text. If you have added, modified or contributed in any way, please add your name to this list.

Name	Institution
Thomas Haslwanter ¹	Upper Austria University of Applied Sciences / ETH Zurich
Aleksander George Slater	Imperial College London / ETH Zurich
Piotr Jozef Sliwa	Imperial College London / ETH Zurich
Qian Cheng	ETH Zurich
Salomon Wettstein	ETH Zurich
Philipp Simmler	ETH Zurich
Renate Gander	ETH Zurich
Gerick Lee	University of Zurich & ETH Zurich
Gabriela Michel	ETH Zurich
Peter O'Connor	ETH Zurich
Nikhil Biyani	ETH Zurich
Mathias Buerki	ETH Zurich
Jianwen Sun	ETH Zurich
Maurice Göldi	University of Zurich

2

¹ <http://en.wikibooks.org/wiki/User%3AThomas.haslwanter>

² <http://en.wikibooks.org/wiki/Category%3A>

13 Contributors

Edits	User
3	A mu ¹
12	Adrignola ²
4	Avicennasis ³
9	CommonsDelinker ⁴
7	Dirk Hünninger ⁵
5	GerickINI ⁶
2	Goeldi ma ⁷
64	J sun ⁸
4	J36miles ⁹
1	Jomegat ¹⁰
24	Mbuerki ¹¹
6	Nikhilbiyani ¹²
1	Pole from sweden ¹³
9	Psimmler ¹⁴
5	QUBot ¹⁵
8	QuiteUnusual ¹⁶
59	Rega ¹⁷
2	S2709pr ¹⁸
23	Salomonw ¹⁹
36	Skela ²⁰
306	Thomas.haslwanter ²¹

1	http://en.wikibooks.org/w/index.php?title=User:A_mu
2	http://en.wikibooks.org/w/index.php?title=User:Adrignola
3	http://en.wikibooks.org/w/index.php?title=User:Avicennasis
4	http://en.wikibooks.org/w/index.php?title=User:CommonsDelinker
5	http://en.wikibooks.org/w/index.php?title=User:Dirk_H%C3%BCnniger
6	http://en.wikibooks.org/w/index.php?title=User:GerickINI
7	http://en.wikibooks.org/w/index.php?title=User:Goeldi_ma
8	http://en.wikibooks.org/w/index.php?title=User:J_sun
9	http://en.wikibooks.org/w/index.php?title=User:J36miles
10	http://en.wikibooks.org/w/index.php?title=User:Jomegat
11	http://en.wikibooks.org/w/index.php?title=User:Mbuerki
12	http://en.wikibooks.org/w/index.php?title=User:Nikhilbiyani
13	http://en.wikibooks.org/w/index.php?title=User:Pole_from_sweden
14	http://en.wikibooks.org/w/index.php?title=User:Psimmler
15	http://en.wikibooks.org/w/index.php?title=User:QUBot
16	http://en.wikibooks.org/w/index.php?title=User:QuiteUnusual
17	http://en.wikibooks.org/w/index.php?title=User:Rega
18	http://en.wikibooks.org/w/index.php?title=User:S2709pr
19	http://en.wikibooks.org/w/index.php?title=User:Salomonw
20	http://en.wikibooks.org/w/index.php?title=User:Skela
21	http://en.wikibooks.org/w/index.php?title=User:Thomas.haslwanter

- 3 Tklauser²²
- 3 Tolva²³
- 12 Zurlos²⁴

22 <http://en.wikibooks.org/w/index.php?title=User:Tklauser>

23 <http://en.wikibooks.org/w/index.php?title=User:Tolva>

24 <http://en.wikibooks.org/w/index.php?title=User:Zurlos>

List of Figures

- GFDL: Gnu Free Documentation License. <http://www.gnu.org/licenses/fdl.html>
- cc-by-sa-3.0: Creative Commons Attribution ShareAlike 3.0 License. <http://creativecommons.org/licenses/by-sa/3.0/>
- cc-by-sa-2.5: Creative Commons Attribution ShareAlike 2.5 License. <http://creativecommons.org/licenses/by-sa/2.5/>
- cc-by-sa-2.0: Creative Commons Attribution ShareAlike 2.0 License. <http://creativecommons.org/licenses/by-sa/2.0/>
- cc-by-sa-1.0: Creative Commons Attribution ShareAlike 1.0 License. <http://creativecommons.org/licenses/by-sa/1.0/>
- cc-by-2.0: Creative Commons Attribution 2.0 License. <http://creativecommons.org/licenses/by/2.0/>
- cc-by-2.0: Creative Commons Attribution 2.0 License. <http://creativecommons.org/licenses/by/2.0/deed.en>
- cc-by-2.5: Creative Commons Attribution 2.5 License. <http://creativecommons.org/licenses/by/2.5/deed.en>
- cc-by-3.0: Creative Commons Attribution 3.0 License. <http://creativecommons.org/licenses/by/3.0/deed.en>
- GPL: GNU General Public License. <http://www.gnu.org/licenses/gpl-2.0.txt>
- LGPL: GNU Lesser General Public License. <http://www.gnu.org/licenses/lgpl.html>
- PD: This image is in the public domain.
- ATTR: The copyright holder of this file allows anyone to use it for any purpose, provided that the copyright holder is properly attributed. Redistribution, derivative work, commercial use, and all other use is permitted.
- EURO: This is the common (reverse) face of a euro coin. The copyright on the design of the common face of the euro coins belongs to the European Commission. Authorised is reproduction in a format without relief (drawings, paintings, films) provided they are not detrimental to the image of the euro.
- LFK: Lizenz Freie Kunst. <http://artlibre.org/licence/lal/de>
- CFR: Copyright free use.

- EPL: Eclipse Public License. <http://www.eclipse.org/org/documents/epl-v10.php>

Copies of the GPL, the LGPL as well as a GFDL are included in chapter Licenses²⁵. Please note that images in the public domain do not require attribution. You may click on the image numbers in the following table to open the webpage of the images in your webbrowser.

²⁵ Chapter 14 on page 201

1	NOAA	PD
2	Barfooz ²⁶ at the English Wikipedia ²⁷ .	GFDL
3	Original uploader was Kbradnam ²⁸ at en.wikipedia ²⁹ (Original text : <i>Zeynep F. Altun, Editor of www.wormatlas.org</i>)	cc-by-sa-2.5
4	Thomas.haslwanter ³⁰	cc-by-sa-3.0
5	Lokal_Profil ³¹ Original: Dhp1080 ³²	
6	Original by en:User:Chris 73 ³³ , updated by en:User:Diberri ³⁴ , converted to SVG by tiZom ³⁵	GFDL
7	Nrets ³⁶ Original uploader was Nrets ³⁷ at en.wikipedia ³⁸	GFDL
8	Thomas.haslwanter ³⁹	cc-by-sa-3.0
9	Thomas.haslwanter ⁴⁰	cc-by-sa-3.0
10	Thomas.haslwanter ⁴¹	cc-by-sa-3.0
11	Thomas.haslwanter ⁴²	cc-by-sa-3.0
12	Thomas.haslwanter ⁴³	cc-by-sa-3.0
13	Thomas.haslwanter ⁴⁴	cc-by-sa-3.0
14	NASA (original); SVG by Mysid ⁴⁵ .	PD
15	Hans Hillewaert ⁴⁶	cc-by-sa-3.0
16	Steve Jurvetson ⁴⁷	cc-by-2.0
17	George Gastin ⁴⁸	GFDL
18	Zema zZz ⁴⁹	cc-by-sa-3.0
19	che ⁵⁰ {{user:che/credit	cc-by-sa-2.5
20	Richard Bartz ⁵¹ , Munich aka Makro Freak ⁵²	cc-by-sa-2.5

- 26 <http://en.wikipedia.org/wiki/User%3ABarfooz>
27 <http://en.wikipedia.org/wiki/Main%20Page>
28 <http://en.wikibooks.org/wiki/%3Aen%3AUser%3AKbradnam>
29 <http://en.wikipedia.org>
30 <http://en.wikibooks.org/wiki/User%3AThomas.haslwanter>
31 http://en.wikibooks.org/wiki/%3AUser%3ALokal_Profil
32 <http://en.wikibooks.org/wiki/user%3ADhp1080>
33 <http://en.wikibooks.org/wiki/%3Aen%3AUser%3AChris%2073>
34 <http://en.wikibooks.org/wiki/%3Aen%3AUser%3ADiberri>
35 <http://en.wikibooks.org/wiki/User%3ATomtheman5>
36 <http://en.wikibooks.org/wiki/%3Aen%3AUser%3ANrets>
37 <http://en.wikibooks.org/wiki/%3Aen%3AUser%3ANrets>
38 <http://en.wikipedia.org>
39 <http://en.wikibooks.org/wiki/User%3AThomas.haslwanter>
40 <http://en.wikibooks.org/wiki/User%3AThomas.haslwanter>
41 <http://en.wikibooks.org/wiki/User%3AThomas.haslwanter>
42 <http://en.wikibooks.org/wiki/User%3AThomas.haslwanter>
43 <http://en.wikibooks.org/wiki/User%3AThomas.haslwanter>
44 <http://en.wikibooks.org/wiki/User%3AThomas.haslwanter>
45 <http://en.wikipedia.org/wiki/User%3AMysid>
46 <http://en.wikibooks.org/wiki/User%3ABiopics>
47 <http://www.flickr.com/people/jurvetson/>
48 <http://en.wikibooks.org/wiki/User%3AGeorge%20Gastin>
49 <http://en.wikibooks.org/wiki/User%3AZema%20zZz>
50 <http://en.wikibooks.org/wiki/User%3AChe>
51 <http://en.wikibooks.org/wiki/User%3ARichard%20Bartz>
52 <http://en.wikibooks.org/wiki/User%3AMakro%20Freak>

21	Opoterser ⁵³	cc-by-sa-3.0
22	Opoterser ⁵⁴	GFDL
23	Rhcastilhos	PD
24	Piotr Sliwa. Original uploader was A mu ⁵⁵ at en.wikibooks ⁵⁶	
25	Thomas.haslwanter ⁵⁷	cc-by-sa-3.0
26	Piotr Sliwa	PD
27	Peter Hartmann ⁵⁸ at de.wikipedia ⁵⁹ , edited by Marc Gabriel Schmid ⁶⁰	GFDL
28	Piotr Sliwa. Original uploader was Skela ⁶¹ at en.wikibooks ⁶²	PD
29	Ivo Kruusamägi ⁶³	cc-by-sa-3.0
30		GFDL
31	Santiago Ramón y Cajal (1852 - 1934); uploaded to en.wikipedia by en:User:Meduz ⁶⁴ . source = Santiago Ramón y Cajal, <i>Histologie Du Système Nerveux de l'Homme et Des Vertébrés</i> , Maloine, Paris, 1911 date = 1911	PD
32	Jason J. Corneveaux, wiki user: Caddymob ⁶⁵ (talk ⁶⁶)	GFDL
33	original uploaded to en by user:delldot ⁶⁷ , modified by Xoneca ⁶⁸	PD
34		PD
35	Thomas.haslwanter ⁶⁹	GFDL
36	Mbuerki ⁷⁰	cc-by-sa-3.0
37	Mohamad Sawan ⁷¹	GFDL
38		GFDL
39		GFDL
40		GFDL
41		GFDL
42	Thomas.haslwanter ⁷²	cc-by-sa-3.0
43	Thomas.haslwanter ⁷³	cc-by-sa-3.0
44	Thomas.haslwanter ⁷⁴	cc-by-sa-3.0

-
- 53 <http://en.wikibooks.org/wiki/User%3AOpoterser>
 - 54 <http://en.wikibooks.org/wiki/User%3AOpoterser>
 - 55 <http://en.wikibooks.org/wiki/%3Awikibooks%3Aen%3AUser%3AA%20mu>
 - 56 <http://en.wikibooks.org>
 - 57 <http://en.wikibooks.org/wiki/User%3AThomas.haslwanter>
 - 58 <http://en.wikibooks.org/wiki/%3Ade%3AUser%3AHartpete>
 - 59 <http://de.wikipedia.org>
 - 60 <http://en.wikibooks.org/wiki/%3Ade%3AUser%3AMarc%20Gabriel%20Schmid>
 - 61 <http://en.wikibooks.org/wiki/%3Awikibooks%3Aen%3AUser%3ASkela>
 - 62 <http://en.wikibooks.org>
 - 63 <http://en.wikibooks.org/wiki/User%3AKruusam%2E4gi>
 - 64 <http://en.wikibooks.org/wiki/%3Aen%3AUser%3AMeduz>
 - 65 <http://en.wikibooks.org/wiki/User%3ACaddymob>
 - 66 <http://en.wikibooks.org/wiki/User%20talk%3ACaddymob>
 - 67 <http://en.wikibooks.org/wiki/user%3Ade1ldot>
 - 68 <http://en.wikibooks.org/wiki/User%3AXoneca>
 - 69 <http://en.wikibooks.org/wiki/User%3AThomas.haslwanter>
 - 70 <http://en.wikibooks.org/wiki/User%3AMbuerki>
 - 71 <http://en.wikibooks.org/wiki/Mohamad%20Sawan>
 - 72 <http://en.wikibooks.org/wiki/User%3AThomas.haslwanter>
 - 73 <http://en.wikibooks.org/wiki/User%3AThomas.haslwanter>
 - 74 <http://en.wikibooks.org/wiki/User%3AThomas.haslwanter>

45	Thomas.haslwanter ⁷⁵	cc-by-sa-3.0
46	Thomas.haslwanter ⁷⁶	cc-by-sa-3.0
47	Thomas.haslwanter ⁷⁷	cc-by-sa-3.0
48	Thomas.haslwanter ⁷⁸	cc-by-sa-3.0
49	Thomas.haslwanter ⁷⁹	cc-by-sa-3.0
50		cc-by-2.0
51		PD
52	PD-USGov, exact author unknown	PD
53	Waugenberg ⁸⁰	cc-by-sa-3.0
54	David Benbennick ⁸¹	GFDL
55	Chittka L, Brockmann	cc-by-2.5
56	Mattia Ferrazzini	cc-by-sa-3.0
57	<ul style="list-style-type: none"> • Cochlea.png⁸²: Original uploader was Dicklyon⁸³ at en.wikipedia⁸⁴ • derivative work: Fred the Oyster⁸⁵ 	
58	<ul style="list-style-type: none"> • Cochlea-crosssection.png⁸⁶: Original uploader was Oarih⁸⁷ at en.wikipedia⁸⁸ • derivative work: Fred the Oyster⁸⁹ 	
59	Madhero88 ⁹⁰	cc-by-sa-3.0
60	Thomas.haslwanter ⁹¹	GFDL
61	Thomas.haslwanter ⁹²	GFDL
62	Kern A, Heid C, Steeb W-H, Stoop N, Stoop R	cc-by-2.5
63	Thomas.haslwanter ⁹³	GFDL
64	A. James Hudspeth, M.D., Ph.D.	cc-by-sa-3.0
65	User:Mikael Häggström ⁹⁴	PD
66		PD
67	Thomas.haslwanter ⁹⁵	GFDL

- 75 <http://en.wikibooks.org/wiki/User%3AThomas.haslwanter>
76 <http://en.wikibooks.org/wiki/User%3AThomas.haslwanter>
77 <http://en.wikibooks.org/wiki/User%3AThomas.haslwanter>
78 <http://en.wikibooks.org/wiki/User%3AThomas.haslwanter>
79 <http://en.wikibooks.org/wiki/User%3AThomas.haslwanter>
80 <http://en.wikibooks.org/wiki/User%3AWaugenberg>
81 <http://en.wikibooks.org/wiki/User%3ADbenbenn>
82 <http://en.wikibooks.org/wiki/%3AFile%3ACochlea.png>
83 <http://en.wikibooks.org/wiki/%3Aen%3AUser%3ADicklyon>
84 <http://en.wikipedia.org>
85 <http://en.wikibooks.org/wiki/User%3AFred%20the%20Oyster>
86 <http://en.wikibooks.org/wiki/%3AFile%3ACochlea-crosssection.png>
87 <http://en.wikibooks.org/wiki/%3Aen%3AUser%3AOarih>
88 <http://en.wikipedia.org>
89 <http://en.wikibooks.org/wiki/User%3AFred%20the%20Oyster>
90 <http://en.wikibooks.org/wiki/User%3AMadhero88>
91 <http://en.wikibooks.org/wiki/User%3AThomas.haslwanter>
92 <http://en.wikibooks.org/wiki/User%3AThomas.haslwanter>
93 <http://en.wikibooks.org/wiki/User%3AThomas.haslwanter>
94 <http://en.wikibooks.org/wiki/User%3AMikael%20H%E4ggstr%F6m>
95 <http://en.wikibooks.org/wiki/User%3AThomas.haslwanter>

68	Thomas.haslwanter ⁹⁶	cc-by-sa-3.0
69	Petrocan ⁹⁷	cc-by-sa-3.0
70		PD
71	Edwtie ⁹⁸	GFDL
72	Thomas.haslwanter ⁹⁹	cc-by-sa-3.0
73	Petrocan ¹⁰⁰	cc-by-sa-3.0
74	Thomas.haslwanter ¹⁰¹	cc-by-sa-3.0
75	Thomas.haslwanter ¹⁰²	cc-by-sa-3.0
76	Thomas.haslwanter ¹⁰³	cc-by-sa-3.0
77	Bob K ¹⁰⁴ (original version), Olli Niemitalo ¹⁰⁵	PD
78	Thomas.haslwanter ¹⁰⁶	cc-by-sa-3.0
79	Thomas.haslwanter ¹⁰⁷	cc-by-sa-3.0
80	User:Dan Pickard ¹⁰⁸	PD
81	T.A.V. Multimedia. Andreu & Vila.	cc-by-2.5
82	Spagnol, S. and Geronazzo, M. and Avanzini, F.	
83	Spagnol, S. and Geronazzo, M. and Avanzini, F.	
84	J sun ¹⁰⁹	cc-by-sa-3.0
85	J sun ¹¹⁰	cc-by-sa-3.0
86	J sun ¹¹¹	cc-by-sa-3.0
87	J sun ¹¹²	cc-by-sa-3.0
88	User:Dicklyon ¹¹³ Richard F. Lyon	PD
89	Roger wilco ¹¹⁴	PD
90		GFDL
91	José Braga	GFDL
92	user:Thomas.haslwanter ¹¹⁵	GFDL
93	Thomas.haslwanter ¹¹⁶	GFDL
94	Thomas.haslwanter ¹¹⁷	GFDL
95	Thomas.haslwanter ¹¹⁸	GFDL

- 96 <http://en.wikibooks.org/wiki/User%3AThomas.haslwanter>
- 97 <http://en.wikibooks.org/wiki/User%3APetrocan>
- 98 <http://en.wikibooks.org/wiki/User%3AEdwtie>
- 99 <http://en.wikibooks.org/wiki/User%3AThomas.haslwanter>
- 100 <http://en.wikibooks.org/wiki/User%3APetrocan>
- 101 <http://en.wikibooks.org/wiki/User%3AThomas.haslwanter>
- 102 <http://en.wikibooks.org/wiki/User%3AThomas.haslwanter>
- 103 <http://en.wikibooks.org/wiki/User%3AThomas.haslwanter>
- 104 <http://en.wikibooks.org/wiki/User%3ABob%20K>
- 105 <http://en.wikibooks.org/wiki/User%3A01li%20Niemitalo>
- 106 <http://en.wikibooks.org/wiki/User%3AThomas.haslwanter>
- 107 <http://en.wikibooks.org/wiki/User%3AThomas.haslwanter>
- 108 <http://en.wikibooks.org/wiki/User%3ADan%20Pickard>
- 109 <http://en.wikibooks.org/wiki/User%3AJ%20sun>
- 110 <http://en.wikibooks.org/wiki/User%3AJ%20sun>
- 111 <http://en.wikibooks.org/wiki/User%3AJ%20sun>
- 112 <http://en.wikibooks.org/wiki/User%3AJ%20sun>
- 113 <http://en.wikibooks.org/wiki/User%3ADicklyon>
- 114 <http://en.wikibooks.org/wiki/User%3ARoger%20wilco>
- 115 <http://en.wikibooks.org/wiki/%3Auser%3AThomas.haslwanter>
- 116 <http://en.wikibooks.org/wiki/User%3AThomas.haslwanter>
- 117 <http://en.wikibooks.org/wiki/User%3AThomas.haslwanter>
- 118 <http://en.wikibooks.org/wiki/User%3AThomas.haslwanter>

96	Thomas.haslwanter ¹¹⁹	GFDL
97	Thomas.haslwanter ¹²⁰	GFDL
98	User:Mikael Häggström ¹²¹	GFDL
99	Thomas.haslwanter ¹²²	GFDL
100	Thomas.haslwanter ¹²³	GFDL
101	Thomas.haslwanter ¹²⁴	GFDL
102	Thomas.haslwanter ¹²⁵	cc-by-sa-3.0
103	Thomas.haslwanter ¹²⁶	GFDL
104	Thomas.haslwanter ¹²⁷	GFDL
105	Neuromechanics ¹²⁸	PD
106	Neuromechanics ¹²⁹	PD
107	Thomas.haslwanter ¹³⁰	GFDL
108	Thomas.haslwanter ¹³¹	cc-by-sa-3.0
109	Chabacano	cc-by-sa-2.5
110	gabymichel	GFDL
111	NEUROtiker ¹³²	GFDL
112	albert kok	GFDL
113	Thomas.haslwanter ¹³³	cc-by-sa-3.0
114	Chris huh ¹³⁴	PD
115	Piet Spaans Viridiflavus ¹³⁵	cc-by-sa-2.5
116	Thomas.haslwanter ¹³⁶	cc-by-sa-3.0
117	Original uploader was Pinzo ¹³⁷ at en.wikipedia ¹³⁸	CFR
118	{{User:Muhammad Mahdi Karim/	
119		GFDL
120	Original uploader was Entirety ¹³⁹ at en.wikipedia ¹⁴⁰	PD

- 119 <http://en.wikibooks.org/wiki/User%3AThomas.haslwanter>
120 <http://en.wikibooks.org/wiki/User%3AThomas.haslwanter>
121 <http://en.wikibooks.org/wiki/User%3AMikael%20H%E4ggstr%F6m>
122 <http://en.wikibooks.org/wiki/User%3AThomas.haslwanter>
123 <http://en.wikibooks.org/wiki/User%3AThomas.haslwanter>
124 <http://en.wikibooks.org/wiki/User%3AThomas.haslwanter>
125 <http://en.wikibooks.org/wiki/User%3AThomas.haslwanter>
126 <http://en.wikibooks.org/wiki/User%3AThomas.haslwanter>
127 <http://en.wikibooks.org/wiki/User%3AThomas.haslwanter>
128 <http://en.wikibooks.org/wiki/User%3ANeuromechanics>
129 <http://en.wikibooks.org/wiki/User%3ANeuromechanics>
130 <http://en.wikibooks.org/wiki/User%3AThomas.haslwanter>
131 <http://en.wikibooks.org/wiki/User%3AThomas.haslwanter>
132 <http://en.wikibooks.org/wiki/User%3ANEUROtiker>
133 <http://en.wikibooks.org/wiki/User%3AThomas.haslwanter>
134 <http://en.wikibooks.org/wiki/User%3AChris%20huh>
135 <http://en.wikibooks.org/wiki/User%3AViridiflavus>
136 <http://en.wikibooks.org/wiki/User%3AThomas.haslwanter>
137 <http://en.wikibooks.org/wiki/%3Aen%3AUser%3APinzo>
138 <http://en.wikipedia.org>
139 <http://en.wikibooks.org/wiki/%3Aen%3AUser%3AEntirety>
140 <http://en.wikipedia.org>

